

The role of lipid transfer proteins (LTPs) during the fertilization process in *Arabidopsis thaliana*

Untersuchungen zur Rolle von Lipidtransferproteinen (LTPs) während des Befruchtungsprozesses in *Arabidopsis thaliana*



DISSERTATION

Doctoral thesis for a doctoral degree at the Graduate School of Life Sciences

Julius-Maximilians-Universität Würzburg

Section: Integrative Biology

By

Khushbu Kumari

Born in Jamshedpur, India

Würzburg, 2019

Germany

The role of lipid transfer proteins (LTPs) during the fertilization process in *Arabidopsis thaliana*

Untersuchungen zur Rolle von Lipidtransferproteinen (LTPs) während des Befruchtungsprozesses in *Arabidopsis thaliana*



DISSERTATION

Doctoral thesis for a doctoral degree at the Graduate School of Life Sciences

Julius-Maximilians-Universität Würzburg

Section: Integrative Biology

By

Khushbu Kumari

Born in Jamshedpur, India

Würzburg, 2019

Germany

Date of submission:

Members of the promotion committee

Chairperson:

Primary referee: **Prof. Dr. Dirk Becker**

University Würzburg
Biozentre, Julius-von-Sachs-Institute for Biosciences
Department for Molecular Pflant-Pphysiologie and Biophysics - Botany I
Julius-von-Sachs-Platz 2
97082 Wuerzburg
Germany

Secondary referee: **Dr. Rosalia Deeken**

University Würzburg
Biozentre, Julius-von-Sachs-Institute for Biosciences
Department for Molecular Pflant-Pphysiologie and Biophysics - Botany I
Julius-von-Sachs-Platz 2
97082 Wuerzburg
Germany

Third referee: **Prof. Dr. Wolfgang Dröge-Laser**

University Würzburg
Lehrstuhl für Pharmazeutische Biologie
Julius-von-Sachs-Platz 2
97082 Wuerzburg
Germany

Date of public defence:

Date of Receipt of Certificates

Affidavit

I hereby confirm that my thesis entitled “**The role of lipid transfer proteins (LTPs) during the fertilization process in *Arabidopsis thaliana***” is the result of my own work. I did not receive any help or support from commercial consultants. All sources and / or materials applied are listed and specified in the thesis.

Furthermore, I confirm that this thesis has not yet been submitted as part of another examination process neither in identical nor in similar form.

Wurzburg, 30.07.2019

Place, Date

Signature

Eidesstattliche Erklärung

Hiermit erkläre ich an Eides statt, die Dissertation “

Untersuchungen zur Rolle von Lipidtransferproteinen (LTPs) während des Befruchtungsprozesses in *Arabidopsis thaliana*” eigenständig, d.h. insbesondere selbständig und ohne Hilfe eines kommerziellen Promotionsberaters, angefertigt und keine anderen als die von mir angegebenen Quellen und Hilfsmittel verwendet zu haben.

Ich erkläre außerdem, dass die Dissertation weder in gleicher noch in ähnlicher Form bereits in einem anderen Prüfungsverfahren vorgelegen hat.

Wurzburg, 30.07.2019

Ort, Datum

Unterschrift

Acknowledgement

I would like to extend my deepest gratitude to the many people who helped me during this journey of my doctoral studies. Foremost, I want to thank my Ph.D. supervisor **Prof. Dr. Dirk Becker** and **Prof. Dr. Rainer Hedrich** (Head of the Department, Botany1), for giving me the opportunity to pursue my doctoral thesis in his group. I appreciate all his contributions of time, ideas, and helpful discussions to make my Ph.D. experience productive and stimulating. His scientific teaching, supportive guidance and encouragement to explore novel ideas helped me not only in successfully completing my project but also in developing myself as a scientist.

I would like to thank the members of my thesis committee, **Dr. Rosalia Deeken** and **Prof. Wolfgang Dröge-Laser** for the critical and insightful discussions and feedback on my work, which have been instrumental in the development of this project. I would also like to thank **Prof. Christian Stigloher** and **Dr. Meng Zhao** for introducing me with electron microscopy. Importantly, I gratefully acknowledge the funding sources that made my Ph.D. work possible. The Graduate School of Life sciences (GSLs), University of Wuerzburg and DAAD fellowship for funding my Ph.D study and offering a well-structured PhD program. I would like to extend my sincere thanks to all the present and former members of the Graduate School of Life Sciences (**Dr. Gabriele Blum-Oehler, Sebastian Michel, Felizitas Berninger, Vikas Dalal, Katrin Lichosik**) for their administrative help and support.

I am especially grateful to the members of AG Becker (**Eva, Katha, Antonella** and **Christine**) for all the discussions, laughs and good times we had together. Special thanks to **Dr. Christine** for proofreading my thesis. I would like to thank all my colleagues in the department of Botany1 for their advice regarding the research and for providing an excellent fun working atmosphere. I further want to thank all the student that I was allowed to supervise during my PhD and for their supportive work: **Kevin, Alexander** and **Nils**. I owe a big thanks to my friends and guardian in Wuerzburg: my dearest friend and sister **Vini** for her endless support and mental encouragement and backing me up in the heavy moments, for her understanding and cheerful character, **Prathibha** and **Sohail** for all the troubleshoot discussions, laughs, lunches and great time we shared together, my other friends in Wuerzburg who made my PhD journey memorable (**Alok, Srikanth, Vishakha, Hemant, Janice, Anda, Rohini, Aparna, Ramya** and others). I also want to thank my closest friends **Shikha, Megha** and **Priyanka** for their support and encouragement. I can never forget the exciting ester vacation and other memorable moments I had with them. I owe a special thanks to my local guardian **Mrs. Ilonka Schneider** for her constant help and support throughout my stay in Wuerzburg and my mentor **Dr. Markus Zimmer** for his constant motivation and support.

I am indebted to my beloved family and friends in India. Especially my Mom, Dad, my In-laws, my sister (Lovely) and my brother (Akshay) for their unconditional love, encouragement and everlasting trust in me. I truly owe my success to my maa and papa.

Last but not least, I would like to express my deepest gratitude to my partner **Vicky** for his love, extreme patience during the years we've had to live separated, for the enormous encouragement and trust, without which this work would never have even been contemplated. He deserves my greatest acknowledgement for what he means to me. Thank you for your support and all your love.

————— *Thank you* —————

This Thesis is dedicated

To My Mom & Dad

Table of Contents

Page

| | |
|---|-----------|
| 1. ZUSAMMENFASSUNG / SUMMARY | 1 |
| 2. INTRODUCTION | 6 |
| 2.1. Sexual reproduction in angiosperms - double fertilization..... | 6 |
| 2.1.1. The long and demanding journey of the pollen tube-pollen pistil interaction..... | 7 |
| 2.1.2. Pollen tube growth and guidance – in search of target..... | 9 |
| 2.1.3. Pollen tube reception and termination..... | 17 |
| 2.2. Cystine-rich Proteins (CRPs) in Plant Reproduction Biology..... | 21 |
| 2.2.1. Cysteine-rich proteins in pollen-stigma recognition | 22 |
| 2.2.2. Cysteine-rich proteins in pollen tube growth and guidance | 22 |
| 2.2.3. Cysteine-rich proteins in seed development..... | 24 |
| 2.3. Plant lipid transfer proteins..... | 24 |
| 2.3.1. LTP biochemistry: Structure and lipid binding and transfer properties of nsLTPs. | 25 |
| 2.3.2. Targeting and sub-cellular localization of LTPs..... | 28 |
| 2.3.3. The proposed biological role of lipid transfer proteins | 30 |
| 2.3.4. Role of nsLTP in plant sexual reproduction and embryogenesis | 30 |
| 3. AIM OF THE STUDY | 33 |
| 4. MATERIALS AND METHODS | 34 |
| 4.1. Materials | 34 |
| 4.1.1. Plants | 34 |
| 4.1.2. Bacterial strains | 35 |
| 4.1.3. Vectors | 36 |
| 4.1.4. Primers | 36 |
| 4.1.5. Antibiotics | 40 |
| 4.2. Methods of manipulation with <i>E. coli</i> and <i>Agrobacteria</i>..... | 42 |
| 4.2.1. Preparation of chemically competent <i>E. coli</i> DH5 α cells | 42 |
| 4.2.2. Heat-shock transformation of chemically competent <i>E. coli</i> cells | 42 |
| 4.2.3. Preparation of electro-competent <i>Agrobacteria</i> | 43 |
| 4.2.4. Transformation of electro-competent <i>Agrobacteria</i> | 43 |
| 4.3. Plant Procedures..... | 43 |
| 4.3.1. Vapor-phase (gas) seeds sterilization protocol | 43 |
| 4.3.2. Plant growth conditions on soil and agar plates | 44 |
| 4.3.3. Floral dip transformation of <i>Arabidopsis thaliana</i> | 44 |
| 4.3.4. Antibiotic selection and screening for positive transformants | 45 |
| 4.3.5. Infiltration of <i>Nicotiana benthamiana</i> for transient expression via <i>Agrobacterium</i> . | 45 |
| 4.4. Pollination Experiments | 46 |
| 4.4.1. Emasculation of <i>Arabidopsis</i> flowers..... | 46 |

| | |
|---|-----------|
| 4.4.2. <i>In-vivo</i> reciprocal-cross pollination | 46 |
| 4.4.3. Aniline blue staining to visualize growing pollen tube <i>in-vivo</i> | 47 |
| 4.4.4. <i>In-vitro</i> pollen tube germination growth assays | 47 |
| 4.4.5. Seed set analysis..... | 48 |
| 4.5. Localization methods..... | 48 |
| 4.5.1. Histochemical β -glucuronidase (GUS) activity analysis..... | 48 |
| 4.5.2. Confocal Laser Scanning Microscopy (CSLM)..... | 49 |
| 4.5.3. Subcellular localization of LTP with Correlative Light and Electron Microscopy (CLEM)..... | 50 |
| 4.5.4. Technovit7100 embedding and sectioning for <i>Arabidopsis</i> flowers | 52 |
| 4.6. Molecular biology techniques | 54 |
| 4.6.1. Genomic DNA Isolation..... | 54 |
| 4.6.2. Polymerase chain reaction (PCR)..... | 54 |
| 4.6.3. Colony PCR..... | 56 |
| 4.6.4. Restriction digestion of the plasmid | 56 |
| 4.6.5. Agarose Gel Electrophoresis | 57 |
| 4.6.6. Isolation of Plasmid DNA | 57 |
| 4.6.7. RT-PCR analysis of specific transcript abundance..... | 58 |
| 4.6.8. Reverse transcription (cDNA synthesis)..... | 59 |
| 4.6.9. Quantitative real-time polymerase chain reaction (qRT-PCR) | 60 |
| 4.7. Cloning of reporter gene constructs using Gateway Cloning..... | 61 |
| 4.7.1. Generation of PromLTP::GUS construct | 63 |
| 4.7.2. Generation of PromLTP::LTP-YFP construct | 63 |
| 4.8. CRISPR Cas-9 Editing method | 63 |
| 4.8.1. Cloning into pHEE401-2sgRNA | 64 |
| 4.9. Sequencing..... | 66 |
| 4.9.1. Sanger sequencing..... | 66 |
| 4.9.2. Next generation sequencing | 66 |
| 5. RESULTS..... | 67 |
| 5.1. Expression analysis of nsLTPs in <i>Arabidopsis thaliana</i>: Bioinformatic analysis..... | 67 |
| 5.2. Lipid Transfer Proteins are induced upon pollination..... | 69 |
| 5.2.1. <i>LTPs</i> are induced upon pollination in <i>Arabidopsis thaliana</i> | 70 |
| 5.3. Tissue-specific expression patterns of <i>LTPs</i> in <i>Arabidopsis</i> flowers | 72 |
| 5.3.1. <i>LTP</i> expression patterns during vegetative <i>Arabidopsis</i> seedling growth | 74 |
| 5.4. Localization of <i>LTPs</i> during the ovule development in <i>Arabidopsis</i>..... | 77 |
| 5.5. Protein subcellular localization of <i>LTPs</i> | 79 |
| 5.5.1. Subcellular localization of 6 <i>LTP</i> protein from <i>Arabidopsis</i> | 79 |
| 5.5.2. Subcellular localization of <i>LTP2</i> , <i>LTP5</i> and <i>LTP6</i> | 80 |

| | |
|--|------------|
| 5.5.3. Subcellular localization of LTP3, LTP4 and LTP12 | 84 |
| 5.6. Mapping LTP protein localization to the cellular ultrastructure employing 'Correlative Light and Electron Microscopy | 88 |
| 5.7. Characterization of <i>LTP</i> T-DNA insertion mutant | 90 |
| 5.7.1. Localization of T-DNA insertions, primer design and identification of <i>ltp</i> knockout mutants..... | 90 |
| 5.7.2. Identification of <i>ltp</i> knockout mutants | 91 |
| 5.7.3. RT-PCR Analysis of <i>AtLTP</i> T-DNA insertion mutants | 91 |
| 5.8. Functional characterization of <i>ltp</i> knock-out mutants..... | 92 |
| 5.8.1. Analysis of pollen development, germination, tube growth and fertilization in <i>ltp</i> knock-out mutants..... | 92 |
| 5.9. No distinguishable phenotype for single <i>ltp2</i>, <i>ltp3</i>, <i>ltp5</i>, <i>ltp6</i> and <i>ltp12</i> knock-out mutants..... | 96 |
| 5.10. Generation of double knock out <i>ltp2ltp5</i> transgenic plants using the CRISPR- Cas9 gene editing technique..... | 97 |
| 5.10.1. Selection of sgRNA for LTP2 and LTP5 with no potential off-targets..... | 97 |
| 5.11. Experimental design and 2-sgRNA expression cassette construction | 99 |
| 5.12. Selection and screening of positive transformants..... | 100 |
| 5.12.1. Analysis of mutation in the T1 transgenic plants and their T2 progeny..... | 100 |
| 5.13. High-throughput sequencing evaluation of CRISPR/Cas9-induced mutagenesis in <i>AtLTP2</i> and <i>AtLTP5</i>. | 101 |
| 5.14. Phenotypic analysis of the <i>ltp2ltp5</i> double-ko mutants | 104 |
| 5.15. Characterization of mutant lines #P9-P2-P2 and #P9- P3-P3 | 104 |
| 5.16. Characterization of <i>ltp2ltp5</i> mutant lines #P31-P2 and #P31-P3..... | 106 |
| 5.17. <i>ltp2ltp5</i> double mutant defect occurs in pollen and impacts pollen morphology and growth | 107 |
| 5.18. Aberrant callose deposition in ovules of <i>ltp2ltp5</i> knock out mutants correlates with defective pollen tube guidance and reduced fertilization efficiency..... | 108 |
| 5.19. Loss of LTP2LTP5 causes a maternal effect seed abortion phenotype | 111 |
| 5.20. Callose deposition dynamics in <i>ltp2ltp5</i> and wild-type plants..... | 113 |
| 5.21. Deposition of callose in the synergid cell at the micropylar region | 114 |
| 6. DISCUSSION | 115 |
| 6.1. LTPs differential expression patterns in <i>A. thaliana</i> reproductive tissue | 115 |
| 6.2. Subcellular localization of LTPs..... | 116 |
| 6.3. Using CRISPR-Cas9 system gene-editing tool to create <i>ltp2ltp5</i> double knock- out mutants | 118 |
| 6.4. <i>ltp2ltp5</i> mutants exhibit a female gametophyte dependent fertilization phenotype | 120 |
| 6.5. Two female-derived <i>LTP2</i> and <i>LTP5</i> genes are critical to proper pollen tube guidance..... | 122 |
| 6.6. How does LTPs connect to the callose homeostasis?..... | 123 |

| | |
|-------------------------------------|------------|
| 7. REFERENCES | 132 |
| 8. APPENDIX | 152 |
| 8.1. Supplementary Data..... | 152 |
| 8.2. Vector maps | 154 |
| 8.3. List of Figures..... | 158 |
| 8.4. List of Tables..... | 159 |
| 8.5. Abbreviations | 161 |
| 8.6. Curriculum Vitae | 163 |

1. SUMMARY

Double fertilization is a defining characteristic of flowering plants (angiosperms). As the sperm cells of higher plants are non-motile, they need to be transported to the female gametophyte via the growing pollen tube. The pollen-tube journey through the female tissues represents a highly complex process. To provide for successful reproduction it demands intricate communication between the cells of the two haploid gametophytes - the polar growing pollen tube (carrying the two non-motile sperm cells) and the ovule (hosting the egg cell/synergid cells). The polar growth of the pollen tube towards the female gamete is guided by different signaling molecules, including sugars, amino acids and peptides. Some of these belong to the family of lipid transfer proteins (LTPs), which are secreted cysteine-rich peptides. Depending on the plant species several lines of evidence have also suggested potential roles for LTPs during pollen germination or pollen-tube guidance. Although *Arabidopsis thaliana* has 49 annotated genes for LTPs, several of which are involved in plant immunity and cell-to-cell communication, the role of most members of this family during fertilization is unknown.

The aim of this project was therefore to systematically identify LTPs which play a role in the fertilization process in *A. thaliana*, particularly during pollen tube guidance. To identify candidate proteins, the expression profile of LTPs in reproductive tissue was investigated. This was accomplished by *in-silico* bioinformatic analysis using different expression databases. Following confirmation of these results by qRT-PCR analysis, seven Type-I nsLTPs (*LTP1*, *LTP2*, *LTP3*, *LTP4*, *LTP5*, *LTP6* and *LTP12*) were found to be exclusively expressed in pistils. Except for *LTP12*, all other pistil expressed LTPs were transcriptionally induced upon pollination. Using reporter-based transcriptional and translational fusions the temporal and spatial expression patterns together with protein localizations for *LTP2*, *3*, *4*, *5*, *6*, and *12* were determined *in planta*. Stable transgenic plants carrying *PromLTP::GUS* constructs of the six different LTP candidates showed that most of LTPs were expressed in the stigma/stylar region and were induced upon pollination. With respect to protein localization on the cellular level, they split into two categories: *LTP2*, *LTP5* and *LTP6* were localized in the cell wall, while *LTP3*, *LTP4* and *LTP12* were specifically targeted to the plasma membrane.

For the functional characterization of the candidate LTPs, several T-DNA insertion mutant plant lines were investigated for phenotypes affecting the fertilization process. Pollen development and quality as well as their *in-vitro* germination rate did not differ between the different single *ltp* mutant lines and wildtype plants. Moreover, *in-vivo* cross pollination experiments revealed that tube growth and fertilization rate of the mutant plants were similar to wildtype plants. Altogether, no discernible phenotype was evident in other floral and vegetative parts between different single *ltp* mutant lines and wildtype plants. As there was no distinguishable phenotype

observed for single *ltp-ko* plants, double knock out plants of the two highly homologous genes LTP2 (expressed in the female stigma, style and transmitting tract) and LTP5 (expressed in the stigma, style, pollen pollen-tube and transmitting tract) were generated using the EPC-CRISPR-Cas9 genome editing technique. Two *ltp2ltp5* mutant transgenic-lines (#P31-P2 and #P31-P3) with frameshift mutations in both the genes could be established. Further experiments showed, that the CRISPR/Cas9-mediated knock-out of LTP2/LTP5 resulted in significantly reduced fertilization success. Cell biological analyses revealed that the *ltp2ltp5* double mutant was impaired in pollen tube guidance towards the ovules and that this phenotype correlated with aberrant callose depositions in the micropylar region during ovule development. Detailed analysis of *in-vivo* pollen-tube growth and reciprocal cross pollination assay suggested that, the severely compromised fertility was not caused by any defect in development of the pollen grains, but was due to the abnormal callose deposition in the embryo sac primarily concentrated at the synergid cell near the micropylar end. Aberrant callose deposition in *ltp2ltp5* ovules pose a complete blockage for the growing pollen tube to change its polarity to enter the funiculus indicating funicular and micropylar defects in pollen tube guidance causing fertilization failure.

Our finding suggests that female gametophyte expressed LTP2 and LTP5 play a crucial role in mediating pollen tube guidance process and ultimately having an effect on the fertilization success. In line with the existence of a N-terminal signal peptide, secreted LTPs might represent a well-suited mobile signal carrier in the plant's extracellular matrix. Previous reports suggested that, LTPs could act as chemoattractant peptide, imparting competence to the growing pollen tube, but the molecular mechanism is still obscure. The results obtained in this thesis further provide strong evidence, that LTP2/5 together regulate callose homeostasis and testable models are discussed. Future work is now required to elucidate the detailed molecular link between these LTPs and their potential interacting partners or receptors expressed in pollen and synergid cells, which should provide deeper insight into their functional role as regulatory molecules in the pollen tube guidance mechanism.

ZUSAMMENFASSUNG

Die ‚doppelte Befruchtung‘ ist ein charakteristisches Merkmal von Blütenpflanzen (Angiospermen). Da im Gegensatz zu vielen anderen Organismen die Spermien höherer Pflanzen nicht beweglich sind, müssen sie über den wachsenden Pollenschlauch zum weiblichen Gametophyten transportiert werden. Die je nach Pflanze durchaus lange Reise des Pollenschlauchs durch das weibliche Gewebe ist ein sehr komplexer Vorgang. Um eine erfolgreiche Reproduktion zu gewährleisten, ist eine fein abgestimmte Kommunikation zwischen den Zellen der beiden haploiden Gametophyten erforderlich - dem polar wachsenden Pollenschlauch (welcher die beiden nicht beweglichen Spermien trägt) und der Samenanlage (in der sich die Eizellen und Synergiden befinden). Das polare Wachstum des Pollenschlauchs in Richtung des weiblichen Gameten wird von verschiedenen Signalmolekülen gesteuert, darunter Zucker, Aminosäuren und Cystein-reiche Peptide (CRPs). Einige dieser Signalmoleküle gehören zur Familie der Lipidtransferproteine (LTPs), welche ebenfalls zur Klasse der CRPs gehören. Abhängig von der Pflanzenart deuten mehrere Hinweise auf eine mögliche Rolle von LTPs während der Pollenkeimung oder der Pollenschlauch-Navigation hin. Obwohl das Genom von *Arabidopsis thaliana* für mehr als 49 annotierte LTP-Gene kodiert, von denen einige an der ‚angeborenen Immunitätsreaktion‘ von Pflanzen sowie der Kommunikation von Zelle zu Zelle beteiligt sind, ist die physiologische Rolle der meisten Mitglieder dieser Familie während des Befruchtungsvorgangs bisher unbekannt.

Ziel dieses Projekts war es daher, systematisch solche LTPs zu identifizieren, die eine Rolle bei der Befruchtung von *A. thaliana* spielen, insbesondere bei der Navigation des Pollenschlauchs zur Eizelle. Um diese LTP Proteine zu identifizieren, wurde zunächst das Expressionsprofil von LTPs in reproduktiven Gewebe untersucht. Dies wurde durch bioinformatische ‚*in-silico*‘ Analyse unter Verwendung verschiedener Expressionsdatenbanken erreicht. Nach Bestätigung dieser Ergebnisse durch qRT-PCR-Analyse wurde festgestellt, dass sieben Typ-I-LTPs (LTP1, LTP2, LTP3, LTP4, LTP5, LTP6 und LTP12) präferentiell im Stempel exprimiert werden. Mit Ausnahme von LTP12 wurden darüber hinaus alle anderen Stempel-exprimierten LTPs nach Bestäubung auf transkriptioneller Ebene induziert. Unter Verwendung von Reporter-basierten Transkriptions- und Translationsfusionen wurden die zeitlichen und räumlichen Expressionsmuster zusammen mit Proteinlokalisationen für LTP2, 3, 4, 5, 6 und 12 ‚*in planta*‘ bestimmt. Stabile transgene Pflanzen, die PromLTP::GUS-Konstrukte der sechs verschiedenen LTP-Kandidaten exprimierten, zeigten, dass die meisten LTPs in der Stigma/Stylar-Region abundant waren und tatsächlich bei der Bestäubung induziert wurden. Die anschließende Proteinlokalisierung auf zellulärer Ebene klassifizierte diese LTPs in zwei Kategorien: LTP2,

LTP5 und LTP6 wurden in der Zellwand lokalisiert, während LTP3, LTP4 und LTP12 spezifisch an der Plasmamembran lokalisierten.

Zur funktionellen Charakterisierung der Kandidaten-LTPs wurden mehrere T-DNA-Insertionsmutanten auf Phänotypen hinsichtlich des Befruchtungsprozesses untersucht. Die Pollenentwicklung sowie die ‚*in-vitro*‘ Keimrate des Pollens unterschieden sich dabei nicht zwischen den verschiedenen LTP-Mutantenlinien und Wildtyp-Pflanzen. Darüber hinaus ergaben ‚*in-vivo*‘ Kreuzbestäubungsexperimente, dass das Pollenschlauchwachstum und die Befruchtungsrate der mutierten Pflanzen im Vergleich zu Wildtyp-Pflanzen ähnlich waren. Insgesamt war kein erkennbarer Phänotyp in der Blütenentwicklung oder der vegetativen Entwicklung zwischen verschiedenen LTP-Einzel-Mutanten und Wildtyp-Pflanzen erkennbar. Aufgrund möglicher funktioneller Redundanz, und der Tatsache, dass für einzelne LTP ‚knock-out‘ Pflanzen kein unterscheidbarer Phänotyp beobachtet wurde, wurden Verlustmutanten der beiden hoch homologen und ko-exprimierten Gene LTP2 und LTP5 unter Verwendung der EPC-CRISPR-Cas9-Genomeditiertechnik erzeugt. Zwei *ltp2ltp5*-mutierte transgene Linien (# P31-P2 und # P31-P3) mit In-Frame-Mutationen in beiden Genen konnten dabei etabliert werden. Weitere Experimente zeigten, dass das CRISPR/Cas9-vermittelte Ausschalten von LTP2 und LTP5 zu einem signifikant verringerten Befruchtungserfolg in diesen Linien führte. Zellbiologische Analysen ergaben, dass die *ltp2ltp5* Doppelmutante in der Pollenschlauch-Navigation zu den Ovulen hin beeinträchtigt war und dass dieser Phänotyp mit Kalloseablagerungen in der Region der Mikropyle während der Ovulen-Entwicklung in diesen Linien korrelierte. Eine detaillierte Analyse des ‚*in-vivo*‘ Wachstums der Pollenschläuche sowie eines wechselseitigen Bestäubungstests ergab, dass die stark beeinträchtigte Befruchtung nicht durch einen Entwicklungsdefekt im männlichen Gametophyten, dem Pollen, verursacht wurde. Stattdessen konnte die beeinträchtigte Befruchtung auf die abnormale Kalloseabscheidung im weiblichen Gametophyten, dem Embryosack, zurückgeführt werden. Interessanterweise, konzentrierte sich die Kalloseabscheidung in der *ltp2ltp5* Doppelmutante hauptsächlich im Bereich der Synergiden, am mikropylaren Ende des Embryosacks. Für den wachsenden Pollenschlauch stellen diese im Vergleich zum Wildtyp untypischen Kalloseablagerungen in *ltp2ltp5*-Mutanten in der Nähe der Eizellen möglicherweise eine Blockade für die Perzeption von Ovulen-Signalen dar. Dies behindert die erforderliche Richtungsänderung des polar gerichteten Wachstums und somit die Fähigkeit des Pollenschlauchs, entlang des Funikulus zu wachsen und in die Mikropyle eindringen zu können. Diese Beobachtung zeigt, dass funikuläre und mikropylare Defekte in der Pollenschlauch-Navigation den Befruchtungserfolg vermindern.

Die Ergebnisse dieser Dissertation legen nahe, dass der weibliche Gametophyt, in welchem LTP2 und LTP5 exprimiert werden, eine entscheidende Rolle bei der Regulation der

Pollenschlauch-Navigation spielt und letztendlich auch einen messbaren Einfluss auf den Befruchtungserfolg hat. Aufgrund der Existenz eines N-terminalen Signalpeptids und der damit verbundenen Sekretion in den Apoplasten könnten LTPs als Signalmoleküle in der extrazellulären Matrix der Pflanze fungieren. Frühere Arbeiten deuteten bereits an, dass LTPs als chemoattraktive Peptide wirken könnten und dem wachsenden Pollenschlauch die Kompetenz verleihen könnten, die Signale der Eizellen wahrzunehmen. Der zugrundeliegende molekulare Mechanismus ist jedoch noch immer unbekannt. Die in dieser Dissertation erzielten Ergebnisse liefern jedoch starke Hinweise darauf, dass LTP2/5 zusammen die Homöostase der Kallosebildung regulieren. Mögliche Modelle zur Aktivität von LTPs im Kontext der Regulation der Kallose-Homöostase werden vorgestellt und diskutiert. Zukünftige Arbeiten sind nun erforderlich, um die detaillierte molekulare Verbindung zwischen diesen LTPs und ihren potenziellen Interaktionspartnern oder Rezeptoren, die in Pollen- und Synergidzellen exprimiert werden, aufzuklären. Diese sollten einen tieferen Einblick in die funktionelle Rolle von LTP2 und LTP5 als regulatorische Moleküle für die Pollenschlauch-Navigation geben.

2. INTRODUCTION

2.1. Sexual reproduction in angiosperms - double fertilization

Reproduction is marked as a crucially important phase in the life cycle of all organisms. In angiosperms sexual reproduction is a very orchestrated process precisely controlled by both the male and female gametophyte. Darwin referred to the rapid success of flowering plants in evolution as an 'abominable mystery'. Fertilization is a process where haploid gametes fuse to initiate the development of new diploid organism. In contrast to animals, flowering plants have evolved on the basis of a unique fertilization mechanism called double fertilization, because it involves two pairs of male and female gametes. The gametes of flowering plants are not directly produced by meiosis. Instead, following meiosis and the generation of four haploid pollen cells, two subsequent consecutive mitotic cell divisions result in the formation of two sperm cells. These generative cells, together with a vegetative cell that drives pollen tube growth form a tricellular pollen grain – the male gametophyte. Moreover, the female gametophyte, the embryo sac, develops within the ovule deeply embedded in the pistil. During the meiotic division, one diploid megaspore mother cell divides into four haploid megaspores, three of them undergo programmed cell death. After three consecutive mitotic divisions of the functional megaspore, eight cells are produced. Following cell-differentiation, a seven celled mature embryo sac is developed, containing two female gametes (the haploid egg cell and the diploid central cell, which originated from a fusion event of two haploid central cells). In addition, the embryo sac harbors five accessory cells - two synergid cells located at the micropylar end, next to the egg cell and three antipodal cells.

During double fertilization, the otherwise immobile sperm cells are delivered by the pollen tube towards the receptive ovules by species-specific pollen tube guidance and attraction mechanisms. Recent studies have shown, that in *Arabidopsis thaliana* the female gametophyte secretes pollen-tube attractants named LURE and AMOR from the synergid cells (Okuda *et al.*, 2009; Kanaoka *et al.*, 2011), which bind to the tip region of the pollen tube (Okuda *et al.*, 2009; Okuda *et al.*, 2013) (Fig.1.1C). After pollen tube rupture, fertilization is accomplished by two-step sequence of events involving, fusion of one sperm cell with the egg cells to produce an embryo, while the second sperm cell fuses with the central cell developing an endosperm, together initiating the seed development.

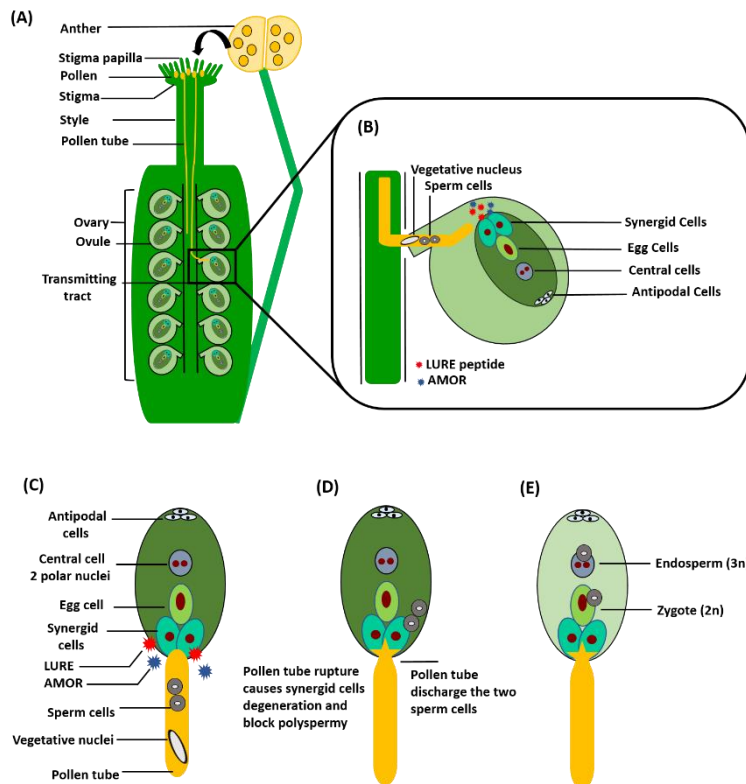


Fig. 1.1: Double fertilization mechanism in angiosperms. (A)

Following germination on the stigma, the compatible pollen grows through the transmitting tract of the pistil. (B) LURE and AMOR are secreted by the synergid cells attract the growing pollen tube towards the receptive ovule. (C) Pollen tube reception by a synergid cell. (D) Pollen tube burst, two sperm cells are discharged, and synergid cell degeneration. (E) One sperm cell fertilizes the egg cell giving rise to the zygote(2n) and the other sperm cell fuses with the central cell forming the endosperm (3n).

2.1.1. The long and demanding journey of the pollen tube: pollen pistil interaction

2.1.1.1. Pollen capture and adhesion

In angiosperm mating, the lack of mobility of individual plants is compensated by mobility of pollen grains which is either mediated by abiotic means, such as water or wind (anemophily), or by biotic pollinators such as birds or insects (entomophily). Whatever the vector, the first step ensuring reproductive success is the proper attachment of the pollen grain to the stigmatic papillae cells of the recipient plant, a process known as pollen capture. Pollen capture is dependent on the pollen exine, the outermost layer of the pollen grain. Biophysical and/or chemical interactions regulate the initial pollen capture between the polymers of the pollen exine and stigmatic papillae cells. After adhesion mediated capture, mobilization of pollen coat occurs, which initiates the formation of “foot” of contact on the stigma surface. The second-stage of foot formation requires protein–protein interactions, including the interaction between pollen coat proteins (PCPs) such as SLR-BINDING PROTEIN 1 and 2 (SLR-BP1 and SLR-BP2)) and the Brassica stigma-expressed gene S-locus–related glycoprotein (SLR1) (Shiba *et al.*, 2001; Takayama *et al.*, 2000). Plants of Brassicaceae family have a dry stigma which lacks surface secretion of liquid exudates. This feature represents an early selection mechanism for compatible pollen grains. The SLR1 mediated self-incompatibility response in Brassica allows

recognition and rejection of self-pollen by the stigmatic papillae. In contrast, the wet stigmata typical for Solanaceae, Liliaceae, and Rosaceae (in species such as *Lilium*, *Nicotiana* and *Petunia*) are covered with lipid-rich secretion fluid (HESLOP-HARRISON and SHIVANNA, 2017), facilitating pollen hydration efficiency but indiscriminately. A wet stigma non-selectively captures any pollen regardless of its origin. Species-specific recognition only occurs after pollen adhesion and hydration (Hiscock and Allen, 2008).

2.1.1.2. Pollen hydration, germination and penetration

Before anthesis the majority of pollen grains is metabolically quiescent and highly desiccated (15 to 35% water content) (HESLOP-HARRISON and SHIVANNA, 2017; Goto *et al.*, 2011). Pollen dehydration induces a metabolically latent state which helps the pollen to tolerate environmental stresses typically prevalent during the dispersal process. After capture and adhesion, the pollen must hydrate to initiate the process of pollen germination (Fig. 1.2). Water loss and phase transition are critical process in hydration of the pollen and previous reports suggested that pollen coat lipids are important for pollen grain hydration (Lush *et al.*, 1998; Wolters-Arts, 1998; Mayfield and Preuss, 2000; Mayfield *et al.*, 2001). Phosphatidylinositol-4-phosphate (PIP4) is crucial in this initial step, as reported by the fact that, PIP4 mutants exhibit slower hydration rates together with female sterility defects due to failed pollination (Chapman and Goring, 2011).

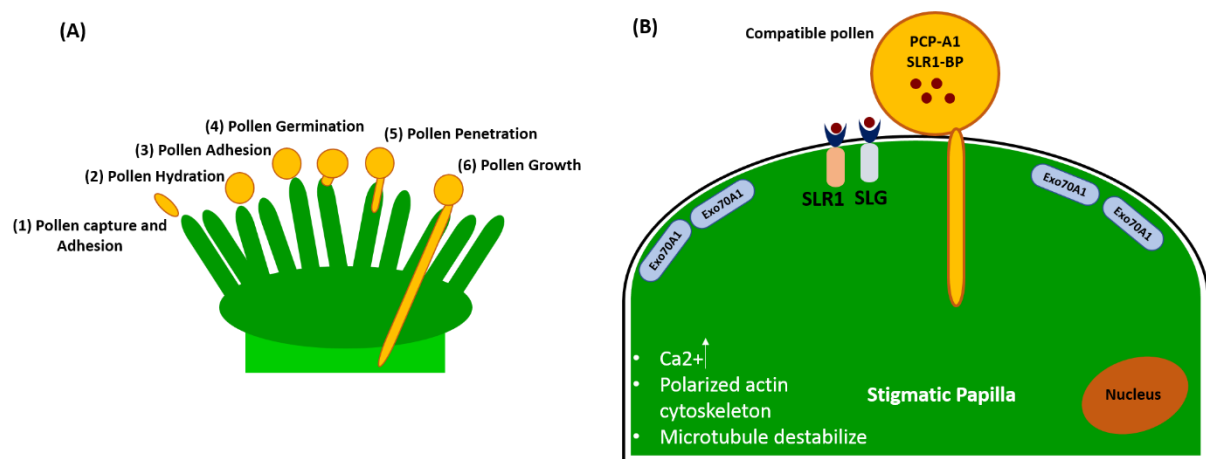


Fig. 1.2: Different phases of pollen-stigma interaction. (A) Schematic representation of pollen development and sequence of early events on the stigma cells, during Brassicaceae pollination. (B) Model of cellular signaling event in response to compatible pollination. The pollen PCP-A1 and SLR1-BP binds to stigma SLR1 and SLG proteins promotes pollen adhesion. The male ligand expressed on pollen coat, S cysteine-rich (SCR) binds to S-locus receptor kinase (SRK) present on the stigma cells. Exo70A1 is required for targeting secretory vesicle to the PM to facilitate water transfer for pollen hydration and releases enzymes required for papilla cell-wall loosening for pollen tube growth. Images in (A-B) are based on data published in (Samuel *et al.*, 2009).

Arabidopsis mutants with defects in long-chain lipid metabolism lack pollen oleosin-like proteins. As such, the male sterile *eceriferum* (*cer*) mutants (Preuss *et al.*, 1993; Hulskamp *et al.*, 1995) and *glycine-rich protein* (*grp*)17 mutant (Mayfield and Preuss, 2000) show a significant delay in the initiation of pollen hydration, in comparison to wild-type pollen. Exo70A1, a plasma membrane-localized stigmatic protein is involved in regulating Brassica self-compatibility at the pollen hydration stage. The stigma of the *Arabidopsis* Exo71 mutant is incapable of accepting compatible pollen. Exo70A1 takes part in the secretion pathway involved in the delivery of secretory vesicle loaded with aquaporins for increased water permeability, as well as unknown cell wall-modifying enzymes which facilitate the hydration and penetration of the pollen through the stigma (Samuel *et al.* 2009).

In general, pollen germination is the process by which the pollen hydrates on the stigma papilla and penetrates the cuticle of the epidermal papillae where it establishes a single polar tube growth site and moves inside and towards the base of the papillae. Hydration transforms a pollen grain from a nonpolar cell to a highly polarized cell. Pollen tubes grow by tip localized growth (Steer and Steer, 1989; Hepler *et al.*, 2001), which is regulated by cytoskeleton re-organization such as the polarization of actin filaments at the site of tube emergence (Tiwari and Polito, 1988; Heslop-Harrison and Heslop-Harrison, 1992) A repositioning of the large vegetative nucleus ensures that it enters the elongating tube before the generative cells (Heslop-Harrison *et al.*, 1986a; Heslop-Harrison and Heslop-Harrison, 1989; Lalanne and Twell, 2002). Oscillating, tip focused cytoplasmic gradients of chloride and calcium ions as well as protons are hallmarks of the polarized pollen tube growth process (Gutermuth *et al.*, 2018). A recent report demonstrated the role of arabinogalactan glycoproteins (AGPs) AGP-Ca²⁺ as the primary source of cytosolic Ca²⁺ regulating pollen tube growth and plasticity. AGPs present in the stigma papilla cells and in growing PTs have roles in pollen grain competency to initiate PT growth (Pereira *et al.*, 2016). A putative Protein O-Fucosyltransferase *FUCOSYLTRANSFERASE1* (*AtOFT1*) facilitates pollen tube penetration through the stigma-style interface through protein O-glycosylation events (Smith *et al.*, 2018). Recently, a novel pollen-specific membrane tension-gated mechanosensitive ion channel, MscS-like 8 (MSL8) was identified, which maintains optimal osmotic potential required during pollen hydration and germination process (Hamilton *et al.*, 2015; Hamilton and Haswell, 2016)

2.1.2. Pollen tube growth and guidance – in search of target

Once germinated, the next major task is to form pollen tube. In order to reach target cells deeply embedded in the ovule, the pollen tube has to conquer a distance of a few millimeters

in species such as *Arabidopsis* or up to 30 centimeters in maize. In *Arabidopsis* the pollen tube penetrates the stigmatic cells and elongates to grow directly towards the basal region of transmitting tract TT (Hiscock and Allen, 2008). In the TT, the growing pollen tube is exposed to chemotropic female guidance cues exerting a multistep control mechanism for pollen tube guidance, primarily at two major phases: pre-ovular guidance and ovular guidance. Gametophytic guidance subsequent to sporophytic guidance is further distinguished by funicular and micropylar guidance to the ovary (Higashiyama and Takeuchi, 2015).

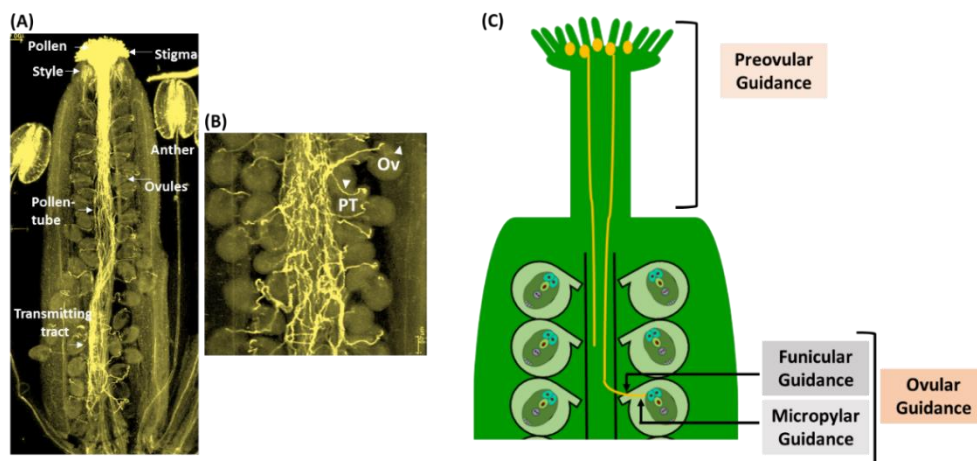


Fig. 1.3: Multiple guidance cues for pollen tubes. (A-B) Aniline blue staining of pollen tube in the wild-type *Arabidopsis* pistil. (B) Each ovule attracts exactly one pollen-tube. (C) Pollen tubes elongate within the pistil to find the target ovule through multiple steps primarily divided into sporophytic preovular guidance and gametophytic ovular guidance. The Ovular guidance is further categorized into funicular (guidance from the surface of the septum to the funiculus) and micropylar (guidance from the funiculus to the micropyle).

2.1.2.1. Preovular guidance

The long journey of the pollen tube through the female tissue represents a complex process relying on the intimate communication between the male and female gametophyte. In general, cell-to-cell communication mediated through wide range of biological and physical mechanisms, is a prerequisite for differentiation, growth and development in multicellular organisms. Cell-to-cell communication involves the perception of external signals by cell surface receptors. In plants, correct and coordinated cell-to-cell interaction is crucial for plant reproduction, growth, development, immune responses and the adaption to the external cues. The complexity of cell-to-cell communication is more crucial in plants, because plant cells are not migrating. They are enveloped in the rigid cell wall and confined to their relative positions surrounded by adjacent neighboring cells. Therefore, in plant cells positional information controls the specification of cellular identity (Berger *et al.*, 1998). Plant cells have evolved with

defense and surveillance system, capable to detect a broad range of endogenous as well as exogenous biotic and abiotic signals. A diverse array of membrane bound pattern recognition receptors (PRRs) which includes receptor-like kinases (RLKs) and receptor-like proteins (RLPs) contributes to this process (S.,-H., Shiu and Bleecker, 2003).

In contrast to animals, which rely on a limited number of PRRs like Toll-like receptors (TLRs), cytoplasmic NOD-like proteins (NLRs), G-protein coupled receptors and canonical tyrosine receptor kinases, plants employ sensor histidine kinases and have evolved a huge number of receptor-like kinases (RLKs) and receptor-like proteins (RLPs). Sequence analysis showed that there are over 600 proteins in *Arabidopsis* and over 1000 in rice, which belong to one of the biggest plant protein families, the RLK/Pelle family (Fritz-Laylin *et al.*, 2005; S., H., Shiu and Bleecker, 2003; Shiu *et al.*, 2004). Among 600 members of RLKs in *Arabidopsis*, 429 are transmembrane receptor-like proteins and 118 are receptor-like cytoplasmic kinases (RLCKs) (Shiu and Bleecker, 2001). With respect to the structural features of their ectodomains, plant RLKs are classified into different subgroups either possessing leucine-rich repeats (LRRs), lysine motifs (LysMs), lectin motifs, self-incompatibility locus (S-Locus), epidermal growth factor (EGF)-like domains and receptor-like cytoplasmic kinase (RLCK). The plant receptor-like kinases (RLKs) are structurally characterized by the presence of an extracellular ligand-binding domain, a single membrane-spanning domain and an intracellular cytoplasmic kinase domain. RLPs exhibiting a similar structural organization as RLKs, lack the cytoplasmic kinase domain. The ectodomain of RLKs and RPLs are highly diverse, providing means to recognize a wide spectrum of patterns, which upon binding cause conformational changes that trigger homodimerization (e.g.: Chitin Perception in *Arabidopsis*) (Miya *et al.*, 2007), heterodimerization (e.g.: Flagellin Perception in *Arabidopsis*) (Gómez-Gómez and Boller, 2000) and hetero multimerization (e.g.: Chitin Perception in Rice) (Kouzai *et al.*, 2014; Kaku *et al.*, 2006) between RLKs or RLK and RLP, respectively. Most of the known RLKs/RLPs are involved in plant growth and/or development, in plant defense but also reproduction and their ligands are as diverse as sugars, nucleotides or peptides. In case of cell-to-cell communication between the pollen tube and the female tissues CRPs appear to play a prominent role as ligands signaling through specific RLKs.

In the initial sporophytic phase of attraction, chemocyanins (small secreted proteins like CRPs), cell wall macromolecules of the TT like pectins and AGPs, gamma-aminobutyric acid (GABA), polysaccharides and glycolipids have been identified as the stylar attractant molecules. They are thought to facilitate and nourish PT development (Capron *et al.*, 2008). In the hollow style of Lily, the adherence of the pollen tube to the stylar matrix is mediated by a cysteine-rich protein called STIGMA/STYLAR CYSTEINE-RICH ADHESIN (SCA), which has been purified from the stylar exudate and shown to promote PT adhesion to an artificial stylar

matrix *in-vitro*, (Park *et al.*, 2000). In *Arabidopsis*, the SCA like lipid transfer protein LTP5 is expressed in the pollen as well as in the TT, and a putative gain-of-function mutant of LTP5 mainly affected the male gametophyte - the pollen. In this *ltp5* mutant PTs are characterized by impaired growth in both, in *in-vitro* pollen germination assays and in semi *in-vivo* cross pollination pollen tube growth assays (Chae *et al.*, 2009). In addition to these LTPs, *Arabidopsis plantacyanin* and Lily *chemocyanin* are also involved in PT guidance. Both peptides belong to the phycocyanin family of blue copper proteins. The *Arabidopsis* single-copy gene *plantacyanin* is highly expressed in inflorescence tissues, specifically in the stigma, the style, the ovary and the transmitting tract of the pistil. Plants overexpressing *plantacyanin* showed reduced seed set due to callose deposition on the pollen grain wall and degeneration of the anther endothecium which inhibits the proper maturation of pollen grain leading to anther dehiscence (Dong *et al.*, 2005). In tomato, CYSTEINE-RICH STIGMA SPECIFIC PROTEIN 1 (STIG1) interacts with a pollen receptor (LePRK2) and with phosphatidylinositol 3-phosphate (PI3P) as a signal peptide to promote PT growth (Tang *et al.*, 2004). Recently, it was reported that tomato POLLEN RECEPTOR-LIKE KINASE1 and 2, LePRK1/LePRK2 function through KPP (kinase partner protein), a Rop (Rho-like small GTPase from plant) guanine nucleotide exchange factor (RopGEF) and positively regulate pollen germination and pollen tube growth (Gui *et al.*, 2014; Zhang *et al.*, 2008). The LAT52 (LATE ANTHOR TOMATO 52) pollen-specific cysteine-rich extracellular protein interacts with the ectodomain of LePRK2 before pollen germination. While after pollen germination, a stigma-specific CRP, LeSTIG1, associates with LePRK1 and LePRK2, forming STIG1-LePRK1 or STIG1-LePRK2 complex and facilitates the pollen tube growth. Another paracrine ligand STIL, STYLE INTERACTOR FOR LePRKs also competes for the LePRK1 binding. The LePRK complex perceives STIL, which specifically promotes LePRK2 dephosphorylation and mediates pollen tube growth from the onset of germination. (W. Tang, Ezcurra, Muschietti, McCormick, Hepler, *et al.*, 2002; Tang *et al.*, 2004; Wengier *et al.*, 2010).

In *Nicotiana tabacum*, the arabinogalactan protein (AGP) TRANSMITTING-TRACT SPECIFIC (TTS), pistil extensin-like protein III (PELPIII) and a 120-kDa glycoprotein derived from the transmitting tissue, are involved in the stimulation of pollen tube growth and the attraction of pollen tubes *in vitro*. They further confer species-specific recognition of PTs in the S-RNase based self-incompatibility system. In *Arabidopsis*, the COBRA-LIKE 10 (COBL10), a GPI-anchored protein has been reported to regulate PT responses to female guidance cues (Li *et al.*, 2013). COBL10 is localized to the apical plasma membrane of the growing PT which probably acts as a cellular sensor for cell-cell communication. The *cobl10* mutant plants showed aberrant apical pectin and cellulose microfibril deposition, reduced pollen tube growth and defective directional sensing in the female transmitting tract (Li *et al.*, 2013).

2.1.2.2. Pollen-tube guidance

After navigating through the style, the pollen tube exit from the transmitting tract penetrating through the septum surface and enter the funiculus in search of the ovules. Pollen tube growth toward the ovules is precisely controlled by an ovular pollen tube guidance system which is divided into two phases: Funicular guidance, guidance from the surface of the placenta to the funiculus and micropylar guidance, guidance from the entrance of the micropyle to the female gametophyte. Some gametophytic mutants, such as *magatama* (*maa1*) and the helicase *maa3* (Shimizu and Okada, 2000), the SUMO E3 ubiquitin ligase *SIZ2-1* (Ling *et al.*, 2012), the nuclear protein *CENTRAL CELL GUIDANCE* (*CCG*) (Chen *et al.*, 2007), the disulfide-isomerase *PDIL2-1* (Wang *et al.*, 2008), the transcription factor *MYB98* (Kasahara *et al.*, 2005), gamete-expressed 3 (*GEX3*) Alandete-Saez, Ron, and McCormick 2008) and ccg-binding protein1 (*CBP1*; Li *et al.* 2015) show mistargeting of the pollen tube with PTs being targeted to the micropyle region, but not entering the synergids. The *Arabidopsis* *POLLEN ON PISTIL 2* (*POP2*) gene which encodes a GABA transaminase degrades GABA and contributes to the formation of a GABA gradient along the pistil. *Pop2* mutant pollen tubes exhibit an aberrant growth phenotype and are misguided due to increased levels of GABA throughout the ovule (Palanivelu *et al.*, 2003). The receptor for GABA has not been identified yet, but recently the activity of anion channels of the ALMT family have been shown to be regulated by GABA directly (Ramesh *et al.*, 2015; Sanchez, 2004). Further, in tobacco pollen protoplasts GABA binding to the plasma membrane was shown and electrophysiological studies in tobacco pollen grains and pollen tubes revealed that GABA modulates plasma membrane Ca^{2+} -permeable channels (Yu *et al.*, 2014). The resulting changes in Ca^{2+} oscillations by pistil produced GABA further activate the downstream response elements such as Calcium-Dependent Protein Kinases (CDPKs), thereby regulating PT growth and orientation (Yu and Sun, 2007). In addition to GABA and produced by the sporophytic ovule integument cells, the rare amino acid D-Serine is involved in pollen tube attraction by regulating PT cytosolic Ca^{2+} levels possibly via glutamate receptor like proteins (GLRs) (Michard *et al.*, 2011). Finally, nitric oxide (NO) is discussed as a possible regulator of pollen tube/ovule communication in line with the observation that *Atnos1* mutant plants which showed defective NO production, have reduced fertility (Prado *et al.*, 2008).

In-vitro studies of pollen tube growth have also highlighted the important role of ions and pH dynamics in the tip of the growing pollen tube, indicating the importance of active and spatially localized ion transporters. In *Arabidopsis thaliana* the two predicted pollen-expressed ER localized cation/proton exchangers (*CHX21* and *CHX23*), are essential for PT guidance. *chx21 chx23* double mutant pollen exhibit defective pollen tube guidance as the PTs failed to reorient

their growth towards the ovule and do not grow along the funiculus (Lu *et al.*, 2011). *CHX21* and *CHX23* are proposed to regulate the pH dynamics in the tip of growing pollen tube, and in turn, alter actin polymerization required for the reorientation of the pollen tube growth direction. (Lu *et al.*, 2011). Additionally, a pair of pollen expressed Mitogen activated protein kinases, namely (MPK3 and MPK6) were identified to mediate PT guidance in response to female cues. The *mpk3mpk6* double mutant pollen tubes showed impaired funicular guidance with defective navigation, where pollen tubes exhibited wandering phenotype without targeting any ovule (Guan *et al.*, 2014).

In addition, Receptor-like kinases (RLKs) plays a crucial role in maintaining the pollen-tube growth, guidance and homeostasis. A most recent study revealed, a peptide growth factor PSK (Phytosulfokine) that controls pollen tube growth and funicular polar tube guidance in *Arabidopsis*, too. PSK is perceived by the PSKR leucine-rich repeat receptor-like kinases (LRR-RLKs) and requires tyrosine sulfation by a tyrosyl protein sulfotransferase (TPST). Due to loss of funicular PT guidance, *pskr1-3 pskr2-1* and *tpst-1* knockout mutants showing a high number of unfertilized ovules and thus have reduced seed production. This finding suggested that PSK signaling is important to guide the PT from the transmitting tract to the embryo sac contributing to fertilization success (Stührwohldt *et al.*, 2015).

Micropylar guidance signals originate from the synergid cells embedded within the female gametophyte. Synergids are responsible for secreting guidance cues to attract the invading pollen tubes. This was shown in *Tourenia fournieri* by laser ablation assays of individual gametophytic cells in the embryo sac where embryos with ablated micropylar end showed impaired pollen tube attraction (Higashiyama *et al.*, 2001). Both the synergid cells contribute equally to attract the pollen tube and upon fertilization failure in the first attempt, they are still capable to receive a second pollen tube to recover fertilization and achieve double fertilization (Okuda *et al.*, 2009; Nagahara *et al.*, 2015). Both, *Arabidopsis* genetic (Kasahara *et al.*, 2005) and in-vitro studies with *Torenia* ovules have identified synergid cells as the specialized cells which secrete many peptides, including attractant molecules required for pollen tube guidance and reception (Higashiyama *et al.*, 2001). Most of the knowledge on embryo sac-derived pollen tube attractants is known from transcriptome analyses of isolated egg and synergid cells (Dresselhaus *et al.*, 1994; Márton *et al.*, 2005; Okuda *et al.*, 2009). The maize *Zea mays* *EGG APPARATUS 1* (*ZmEA1*) peptide which is expressed in egg and synergid cells of unfertilized female gametes represents an attractant peptide for micropylar guidance. EA1 RNAi plants produced significantly lower seeds compared to wild type due to defective pollen tube attraction mechanism (Márton *et al.*, 2005; Márton *et al.*, 2012). Contrary to *EA1*, *EAL1* is exclusively expressed in egg cells is involved in cell-to-cell communication to control antipodal cell fate (Krohn *et al.*, 2012). In *A. thaliana* and *T. fournieri*, Defensin-like (DEFL) cysteine-rich peptides

encoded by *LURE* genes are predominantly expressed in the synergid cells and are involved in pollen tube attraction at the micropyle. Two *LURE* genes from *T. fournieri* (*TfLURE1* and *TfLURE2*) and six duplicated *LURE* genes from *Arabidopsis* (*AtLURE1.1–AtLURE1.6*) have been identified. In semi in vivo assays, Gelatin beads containing recombinant *TfLUREs* at a very low concentration (40pM, corresponding to only ~1000 molecules) were sufficient to initiate pollen tube attraction in species-preferential manner (Goto *et al.*, 2011; Higashiyama, 2010). In *Arabidopsis* *AtLURE1* peptides are members of the CRP810 subfamily of CRPs. The expression of *AtLURE* peptide is controlled by the synergid-specific transcription factor MYB98. Heterologous expression of the *AtLURE1* gene in *T. fournieri* resulted in *Arabidopsis* pollen-tube attraction and penetration of egg apparatus, implying that *AtLURE1* can overcome the reproductive isolation barriers despite of the large evolutionary distance between *Arabidopsis* and *Torenia* (Takeuchi and Higashiyama, 2012). A recent study reported, the identification of novel Cysteine-rich XIUQIU peptides which act as non-species-specific pollen tube attractants. XIUQIU, a maternal-derived peptide is expressed in the filiform apparatus of the synergid cells and could equally attract the pollen tubes of different species in the *Arabidopsis* genus (e.g.: *A. Lyrata* and *A. halleri*). The hendecuple mutant of *XIUQIU1* to -4 in the *atlure1* null mutant background, showed reduced fertility and ovule abortion in siliques. Therefore, both *AtLURE1-PRK6* (Takeuchi and Higashiyama, 2016) and XIUQIU signaling pathway, contributes to the fertilization success and heterospecific fertilization (Zhong *et al.* 2019). The ovular methyl-glucuronosyl arabinogalactan (AMOR) renders the pollen tube fully competent to respond to the chemoattractant LUREs peptide at the micropylar end (Mizukami *et al.*, 2016; Jiao *et al.*, 2017).

These female-derived signals are perceived by the plasma-membrane localized RLKs in the pollen tube. The Higashiyama group identified tip-localized pollen-specific receptor-like kinases 6 (PRK6), with an extracellular leucine- rich repeat domain essential for sensing LURE 1 peptide. The *AtLURE1* peptide could also induce asymmetric re-localization of PRK6 before reorientation of the pollen tube growth. PRK6 interacts with other PRK family receptors like PRK1/PRK3/PRK8 and signals through the ROPGEF cascade, which activates the downstream signaling switch Rho GTPase of Plants (ROP1) required for pollen tube growth. Moreover, PRK6 was also shown to interact with cytosolic kinases LIP1 (lost in pollen tube guidance 1) and LIP2 involved in the LURE signaling cascade. Inactivation of LIP1 and LIP2 significantly reduce pollen tube attraction toward *AtLURE1* with impaired micropylar pollen tube guidance (Liu *et al.*, 2013). Both receptor-mediated phosphorylation of PRK receptor complex and Rop-GEF-based ROP activation acts as a major regulator controlling the dynamic of actin cytoskeleton, the cytosolic calcium gradient, and exocytosis in pollen tube tip growth and guidance mechanism. Another study described two pairs of pollen plasma-membrane-

localized receptor-like kinases, MDIS1 and MDIS2 (MALE DISCOVERER1/2), and MIK1 and MIK2 (MDIS1- INTERACTING RECEPTOR LIKE KINASE1/2) as LURE1 receptors. LURE1 induces the dimerization of MDIS1-MIK1 and transduce the signal into the cell by transphosphorylation, whereas *mdis1* and *mik1xmik2* mutant pollen displayed normal pollen tube growth but were less sensitive to the LURE1 guidance (T. Wang et al. 2016). Furthermore, *prk6* and *mdisxmik* mutants showed similar abnormal guidance defect, suggesting that, the perception mechanism of *At*LURE involves multiple RLKs contributing synergistically to robust pollen tube guidance and ensure the reproductive success.

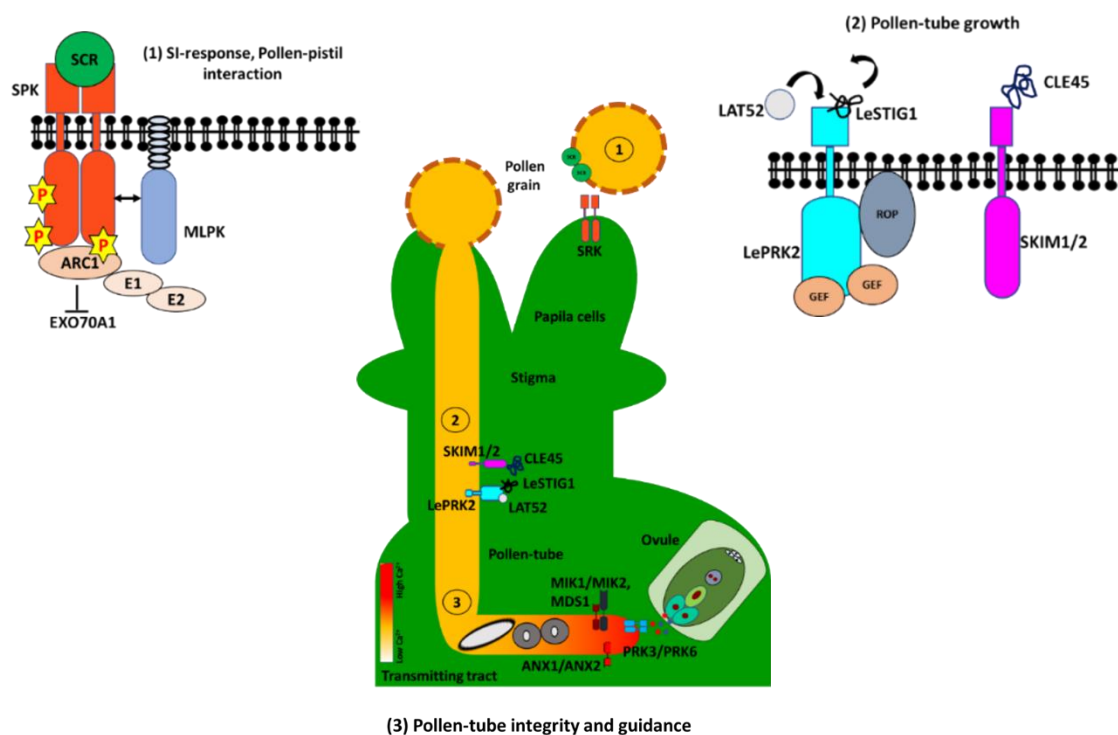


Fig. 1.4: Model of RLK signaling in different steps of pollen-pistil interaction. (1) The self-incompatibility response in the Brassicaceae. On self-pollination, pollen-derived S-locus cysteine rich ligand (SP11/SCR) binds to stigma-derived S-locus receptor kinase (SRK) and activates the SRK/MLPK complex. A phosphorylation cascade activates the ARC1 E3 ubiquitin which inactivates Exo70A1 causing pollen rejection (Stone et al. 2003), (Samuel et al., 2009). **(2) RLKs during pollen-tube growth.** A pollen-specific secreted protein LeLAT52 interacts with pollen-receptor kinase LePERK during the pollen-germination (Tang et al., 2002), (Zhang et al., 2008), whereas after germination the pollen-specific protein CLE45 interacts with the stigma receptor SKIM1/2. **(3) Pollen-tube integrity and guidance.** The pollen tube maintains its integrity through the action of RALF4/19, ANX1, and BUP51/2. The pollen tube bursts through the stigma due to the action of RALF34 and NADPH Oxidase. The pollen tube is guided by the action of LURE, MIK1/MIK2, and MDIS1. The pollen tube is also guided by the action of PRK3/PRK6, ANX1/ANX2, and MDS1. The pollen tube is also guided by the action of CNGC18, ROP, and LIP. The pollen tube is also guided by the action of ROP, LIP, and GEF.

LeLAT52 is replaced by stigma-secreted peptide LeSTIG1 involved in pollen-tube cell growth (Weihua Tang et al. 2004). **(3) RLKs involved in pollen-tube integrity and guidance mechanism.** Pollen expressed RLKs ANX1/2 and BUPS1/2 maintain pollen tube integrity and sperm release in RALF-dependent manner. During the pollen-tube growth, RALF4/19 interacts with BUPS1/ANX1 complex and regulate pollen-tube integrity, while once in reach of ovule, RALF34 takes over and causes rupture of the pollen tube (Ge et al., 2017). MDIS1-MIK and PRK6 receptor-complex are involved in sensing of LURE attractant peptide. Binding of LURE induces dimerization of MDIS1-MIK receptors and the autophosphorylation of kinase domain by MIK. PERK6 interacts with PRK3, LIP and pollen expressed ROPGEFs that regulate the calcium gradient, the dynamics of actin filaments and ROS production during pollen tube growth (Takeuchi and Higashiyama, 2016).

Both MDIS1-MIK and PRK6 receptor complex might have different preferences for multiple attractant peptides and regulating different aspects of pollen tube guidance mechanism. Another study identified, a new receptor-like kinases of the CrRLK1L subfamily, ERULUS (ERU), which is specifically expressed in pollen and root hairs as a tip-growth specific kinase, was shown to be involved in Ca^{2+} -dependent pollen-tube growth and guidance in Arabidopsis. ERU mediates pollen tube targeting to the ovules by regulating apical $[\text{Ca}^{2+}]_{\text{cyt}}$ oscillations in response to $[\text{Ca}^{2+}]_{\text{ext}}$. The *eru* loss-of-function mutation leads to aberrant PT targeting and reduced fertilization efficiency (Schoenaers *et al.*, 2017). Interestingly, in the root cells auxin-regulated ERULUS controls cell wall composition through pectin methylesterase activity and phosphorylation of FERONIA (FER) and AHA1/2 during root hair tip growth in Arabidopsis (Schoenaers *et al.*, 2018).

2.1.3. Pollen tube reception and termination

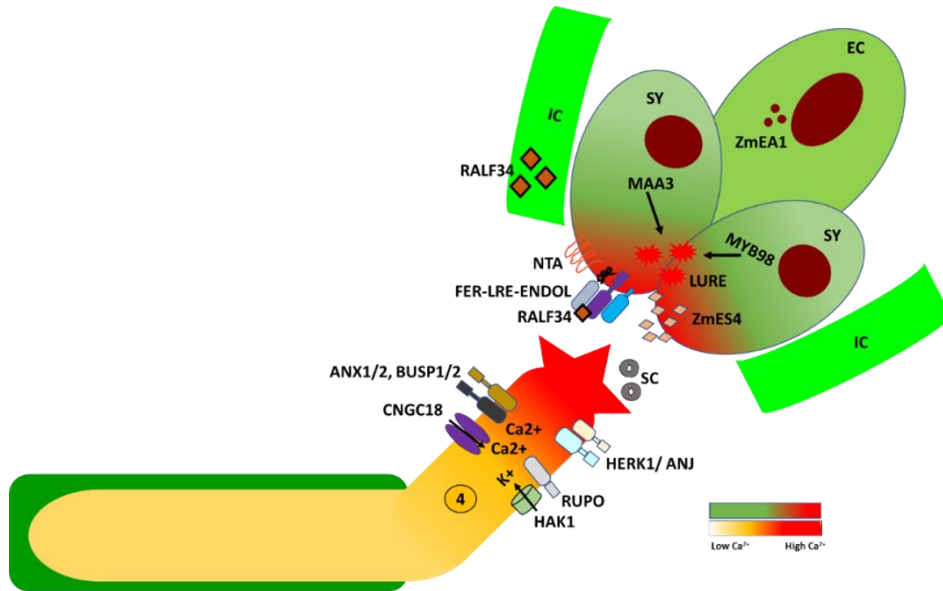
At the end of the journey, when the pollen tube reaches the target ovule, cell to cell communication mediated by receptor-like kinases (RLKs) are initiated in both the synergid cells and the tip of the pollen tube, leading to pollen tube growth arrest, programmed cell death of the synergid cells and pollen tube burst releasing the two sperm cells followed by gamete fusion. Several genes involved in regulating pollen tube termination have been identified (Kessler and Grossniklaus, 2011; Leydon *et al.*, 2014; Wolf and Höfte, 2014). FERONIA (FER) a plasma membrane-localized which belongs to the plant receptor-like kinases (RLKs) of the *Catharanthus roseus* RLK1-like (CrRLK1) subfamily is a key player in pollen tube termination by the synergid cells. The *FER* gene is ubiquitously expressed throughout the plant (except in mature pollen) and predominantly in the synergid membrane at the filiform apparatus. In *fer* mutants, the pollen tube fails to arrest its growth and continues to grow inside the female gametophyte (embryo sac) and further fails to rupture and to release the sperm cells. Recently, the rapid alkalization factor (RALF) peptide, a member of the CRP family, has

been identified as the ligand of FER in root cells to control cell elongation (Haruta *et al.*, 2014). However, it remains elusive whether FER also interacts with RALF-like peptides in the synergid cells during pollen tube reception. FER controls the NADPH oxidase-dependent ROS (reactive oxygen species) synthesis by synergid cells at the filiform apparatus. ROS-induced pollen tube rupture is dependent on Ca²⁺ channel activation and excess Ca²⁺ influx (Wolf and Höfte, 2014; Duan *et al.*, 2014). On the female side, other membrane localized signaling components like the glycosylphosphatidylinositol (GPI)-anchored protein LORELEI (LRE) (Capron *et al.*, 2008), the Mildew Resistance Locus O (MLO)-like protein NORTIA (NTA) (Jones *et al.*, 2017) and UDP-Glycosyltransferase TURAN (TUN) (Lindner *et al.*, 2012), have been identified as further potential candidates for direct interaction with pollen tube during PT reception. The UDP-glycosyltransferase *TURAN* and the putative dolichol kinase *EVAN*, two novel proteins expressed in the synergid cells, are involved in protein N-glycosylation in the endoplasmic reticulum and act in the FERONIA-mediated pollen tube reception pathway (Lindner *et al.*, 2015). Similar to *fer*, the *lre*, *nta* and *tun* mutants showed defective pollen tube reception and burst where the mutant ovule fails to receive the pollen tube since PT displayed overgrowth without rupturing. In maize, the cysteine-rich defensin-like peptide ZmES4 mediates rapid pollen tube burst by opening the potassium channel KZM1 in the PT (Amien *et al.*, 2010) and the pectin methylesterase inhibitor ZmPMEI1 appeared to destabilize the PT cell wall inducing pollen tube rupture (Woriedh *et al.*, 2013). Early nodulin-like proteins (ENODLs) are another class of phytocyanins glycosylphosphatidylinositol (GPI)-anchored proteins (GAP) required for pollen tube reception. Ovule-expressed ENODL14 and ENODL15 localize in the filiform apparatus of the synergid cells and similar to CRPs are involved in pollen-tube ovule communication. Similar to *fer* and *lre* mutants, the functional loss of ENDOLs in *en-RNAi* mutant ovules caused pollen tube overgrowth and discharge failure. In addition, ENDOLs directly interact with the ectodomain of FER, suggesting that ovule-specific ENDOLs might act as adaptors or cofactors associating with cell-to-cell communication major players like FERONIA (Hou *et al.*, 2016). While on the female side several factors involved in PT reception and burst have been identified, only a few players are known on the male side. CrRLK1L-1 receptor-like kinases and close homologs to *FER*, *ANXUR1* (*ANX1*) and *ANX2* together with BUPS1/BUPS2 (Zhu *et al.*, 2018) are specifically expressed in pollen and act synergistically to regulate cell wall integrity and stability of the growing pollen tube (Kessler *et al.*, 2015). The extracellular domains of *ANX1* and *ANX2* possess malectin-like domains predicted to bind carbohydrate moieties. Cysteine-rich peptides of the rapid alkalization factor (RALF) family have been identified as their ligand to mediate autocrine and paracrine receptor signaling, controlling pollen tube growth and rupture. The *anx1xanx2* double mutant pollen form bulges and burst eventually right after germination, whereas overexpression of *ANX1* in the pollen tube enhanced exocytosis, inducing an overaccumulation of cell wall material and impaired

pollen tube growth (Miyazaki *et al.*, 2009; Boisson-Dernier *et al.*, 2013). Two-pollen expressed functionally redundant, autocrine peptides, namely RALF4/19 interact with a BUPS–ANX complex maintaining pollen tube integrity. In the synergid cells (see below), at the interface of pollen tube female gametophyte contact, the female-derived paracrine ligand RALF34 competes with the pollen-tube-secreted RALF4/19 at the ANX/BUPS receptor-complex and triggers pollen tube burst and release of sperm cells (Boisson-Dernier *et al.*, 2013; Ge *et al.*, 2017; Mecchia *et al.*, 2017). In another study, analysis of *anx1 anx2* male sterility suppressor mutant, a plasma membrane-localized receptor-like cytoplasmic kinase MARIS (MRI) was identified as a positive regulator of ANX signaling pathway. Furthermore, mutation in MRI leads to premature burst of the pollen tube, whereas, the expression of MRI^{R240C} partially rescues the bursting phenotypes of *anx1 anx2* (Boisson-Dernier *et al.*, 2015).

ROS are downstream components of the CrRLK1L subfamily signaling pathway and the ANX-BUPS complex activates ROS production via the pollen-specific NADPH oxidases RbohH and RbohJ, which in turn modulate cell wall extensibility and activate Ca²⁺-permeable channels (Boisson-Dernier *et al.*, 2013). The ligand-bound CrRLK1Ls have been shown to interact with RAC/ROP guanine exchange factors (ROPGEFs) in order to activate RHO-GTPases which further stimulates ROS production and regulate Ca²⁺ dynamics and cell wall properties (Duan *et al.*, 2014). Thereby, these RLKs maintain a tip focused Ca²⁺ gradient, probably controlled by the CYCLIC NUCLEOTIDE GATED CHANNEL18 (CNGC18), which was the first calcium channel described to be involved in pollen tube guidance. Mutation of CNGC18 caused an abnormal calcium gradient causing guidance defect and severe male sterility (Gao *et al.*, 2016). In addition, sperm cell discharge is regulated by the activity of Ca²⁺ ATPases such as ACA9, which is expressed specifically in the pollen tube (Schjøtt *et al.*, 2004). Finally, and in line with the idea that CrRLK1L-type receptor-like protein kinases monitor cell wall integrity, it was reported that also mechanical stress plays a role in regulating pollen tube growth performance. A loss-of-function mutation in the pollen-expressed mechanosensitive channel *MSL8* leads to abortive pollen tube rupture upon germination (Hamilton *et al.*, 2015). Advancements in semi-in vitro live-cell imaging have enlightened the role [Ca²⁺]_{cyt} changes in synergid cells during pollen tube reception. These studies have further shown that Ca²⁺ signatures are observed throughout the male-female crosstalk as well as during the process of double-fertilization in angiosperms (Denninger *et al.*, 2014; Hamamura *et al.*, 2014). Two distinct types of Ca²⁺ oscillation were observed in the female gametophyte during the process of double fertilization: initial cytosolic Ca²⁺ oscillations due to the degeneration of synergid cells upon pollen tube discharge and a second Ca²⁺ spike during gamete fusion (Hamamura *et al.*, 2014). Coordination of Ca²⁺ dynamics during the intercellular crosstalk between PT and the receptive synergids clearly depends on the FER signaling pathway (Ngo *et al.*, 2014). During

gamete interaction in *Zea mays*, EC1-containing vesicles are secreted upon sperm cell arrival. In sperm cells, EC1 in turn triggers the redistribution of the fusogen *GENERATIVE CELL SPECIFIC 1/HAPLESS 2 (GCS1/HAP2)* from the endomembrane system to the sperm cell surface (Sprunck et al. 2012).



(4) Pollen-tube reception

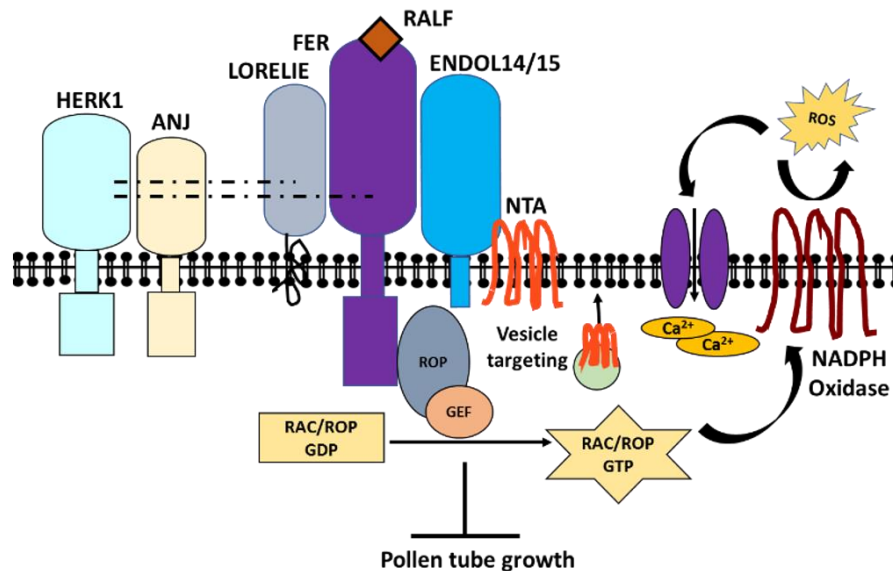


Fig. 1.5: Model of RLK signaling during pollen tube reception. FERONIA, a synergid-expressed, plasma-membrane receptor-like kinase mediates male-female interactions during pollen tube reception at the micropylar end of the target ovule. In the synergid cells, FER form complex with two GPI-anchored protein LORELI and ENDOL together with NTA. FER interacts with ROPGEFs and FER-RAC/ROP signaling complex activates the downstream effector NADPH oxidase leading to ROS production. ROS accumulation activates the opening of Ca^{2+} -channel leading to abrupt ion and water influx which causes pollen tube rupture (Duan et al. 2014).

GCS1/HAP2, encodes a sperm cell membrane protein crucial for gamete fusion. In *gcs/hap2* mutants, mutant sperm cells persist between the egg and central cells but did not fuse with the degenerated synergid cells, supporting GCS/HAP2 as a fusogen (von Besser *et al.*, 2006), (Mori *et al.*, 2006). Final cessation of ovular-pollen tube attraction process depends on gamete fusion, while both, the fertilization of the egg cell as well as the central cell control the cessation event independently. It involves ethylene signaling in the synergid cell and the Polycomb-group (PcG) proteins FERTILIZATION-INDEPENDENT ENDOSPERM (FIE), MEDEA (MEA), FERTILIZATION-INDEPENDENT SEED 2 (FIS2) in the central cell pathway which participates in the blockade of polytuby and the initiation of seed development (Maruyama *et al.*, 2013).

2.2. Cystine-rich Proteins (CRPs) in Plant Reproduction Biology

CRPs are characterized by their small size (less than 160 amino acids), having a secretory signal peptide at the N-terminal and a C-terminal cysteine-rich domain (reviewed in Marshall *et al.*, 2011). Cysteine-rich peptides (CRPs) are a group of signaling peptide discovered in plants that mediate many aspects of plant physiology and development ranging from pathogen defense, plant-bacterial symbiosis, stomata development and plant reproduction. Reported evidences demonstrate that CRPs acts at multiple stages of reproductive process including pollination, pollen tube guidance, attraction and seed development (Fig. 1.6).

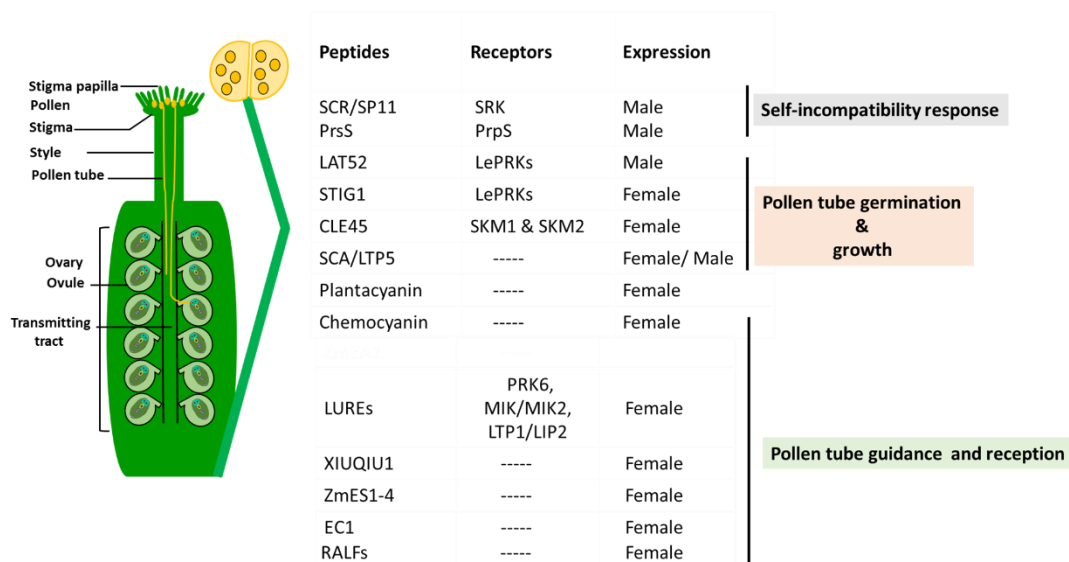


Fig. 1.6: Cystine-rich peptides (CRPs) and their putative role in plants reproduction. Classification of CRPs based on their expression pattern in male and female gametophyte. Both male and female derived CRPs are involved in multiple reproductive processes like pollen tube growth and guidance, fertilization, embryo maturation and seed development. Adapted from (Qu *et al.*, 2015).

High-throughput transcriptome analysis revealed that, among 756 CRP-encoding genes in *Arabidopsis*, 53% of the total number of 390 genes were classified as female gametophyte-specific genes, while 139 CRP genes (18%) were up-regulated in dry-pollen, accounting for 50% of all CRP gene being expressed in the male and female gametophyte of *Arabidopsis* (Simon and Dresselhaus, 2015; Costa *et al.*, 2014). Thus emphasizing their essential role in reproductive process, they are probably being involved in male-female gametophyte interaction, pollen tube growth and guidance, ovule maturation and seed development (Huang *et al.* 2015). CRPs represent a pool of highly polymorphic signaling peptides involved in species-specific functions during reproduction. CRP signaling during reproduction in plants has evolved from ancient defense mechanisms (Bircheneder and Dresselhaus, 2016).

2.2.1. Cysteine-rich proteins in pollen-stigma recognition

Many species of flowering plants have evolved with the process of Self-Incompatibility (SI) which is the first checkpoint encountered by male gametophyte while its reception at the stigma surface. SI is a pivotal mechanism for preventing self-fertilization and therefore maintain the genetic diversity. SI determinant sterility locus' (S-locus) were first identified in Brassica which were expressed in the stigma, pollen and anther. The S-locus cysteine-rich (SCR/SP11) gene encodes the male determinant. (Schopfer, Nasrallah, and Nasrallah 1999). SCR is a CRP expressed at the pollen coat which interacts with the stigmatic female determinant S-receptor kinase and leads to the phosphorylation of ARC1, an E3 ubiquitin ligase which inhibits Exo70A triggering pollen rejection as the self-incompatibility response (Stone *et al.*, 2003); Samuel *et al.* 2009). In *Papaver rhoeas*, the female determinant of SI the stigma S-determinant (PrsS) is a CRP that is secreted from stigmatic papillar cells encodes four conserved cysteine residues (Foote *et al.*, 1994a). Upon interaction with incompatible pollen S-determinant (PrpS), it activates the calcium ion channel to initiate calcium influx leading to PCD of the pollen tube (Wheeler *et al.*, 2010).

2.2.2. Cysteine-rich proteins in pollen tube growth and guidance

After pollen reception on the stigma cells, the compatible pollen grain hydrates and germinates a pollen tube. The growing pollen tubes adheres to the extracellular matrix and follow the guidance cues as they transverse towards the ovules to deliver the sperm cells. This directional journey requires intricate cell to cell communication between pollen and receptive female reproductive tissue (reviewed in Higashiyama & Takeuchi, 2015). Interestingly, many CRPs

have long been implicated in several steps of cell-to-cell communication (Jones-Rhoades et al., 2007; Higashiyama, 2010), such as pollen tube guidance - defensin-like proteins (Okuda et al., 2009) and pollen tube rupture- thionin-like proteins (Leydon et al., 2013). Lat52 a small pollen-specific cystine rich extracellular protein in *Lycopersicon esculentum* (tomato), was found essential for pollen hydration and germination *in vitro* and fertilization *in-vivo* (Muschiatti et al., 1994). Lat52 interacts with two leucine-rich repeat (LRR) receptor kinases 1 and 2 (*LePRK1* and *LePRK2*) localized in the extracellular domain of the pollen tube wall. This receptor-ligand interaction of Lat52- *LePRK1/ LePRK2* is crucial for pollen: pistil interaction as *LePRK1* interacts with Lat52 protein before germination, whereas *LePRK2* binds to Lat52 during pollen tube growth respectively (Tang et al., 2002). *LePRK1/LePRK2* also interact with pistil-specific CRP, *LeSTIG1*, therefore exhibiting multiple interaction with different ligands at different stages of pollen tube growth. *In-vitro* binding assay suggested that *LeSTIG1* abolishes the interaction of Lat52 and *LePRK2* implying that *LeSTIG1* acts as a positive regulator during pollen tube growth after germination on stigma (Tang et al., 2004). Adhesion is necessary for the successful delivery of the pollen tube to the ovary. In order to fertilize the egg cell embedded deep in the ovule, the pollen tube has to grow in the extracellular matrix (ECM) and to be guided alongside the transmitting tract (TT) by adhering to the TT epidermis (TTE) (Jauh et al., 1997). In *Lilium longiflorum*, an *in vitro* adhesion assay (Tang et al., 2004) suggested that a small, secreted CRP of (9 kDa) stigma/stylar cysteine-rich adhesin (SCA), which shares similarity with plant lipid transfer proteins (LTPs) facilitates pollen adhesion to the TTE (Mollet et al., 2000). SCA associated stylar pectin acts as an extracellular “glue” for the growing pollen tubes. Moreover, it has been reported that SCA which is localized in the extracellular matrix of stigma and style, enters the pollen tube tip via endocytic route, facilitating pollen tube tip growth (Chae et al., 2007). After the guided growth of the pollen tube through the transmitting tract, the next step is to guide the pollen tube toward the ovules. In *Arabidopsis*, MB98 a R2R3-type Myb transcription factor, regulates the activation of different attractant molecule in the synergid cells required for ovular/micropylar pollen tube guidance and filiform apparatus formation (Jones-Rhoades et al., 2007). Upon sperm cell arrival at the gamete fusion site, the egg cell secrete small cysteine-rich proteins of the EGG CELL 1 (EC1) which further activates the re-localization of HAP2/GCS1 to the sperm cell plasma membrane enabling the sperm cell to fuse with female gametes (Sprunck et al., 2012). In *Torenia fournieri*, laser ablation of the synergid cells identified defensin-like (DEFL) superfamily of CRPs, named as LUREs (specifically *TfLURE1* and *TfLURE2*) which are secreted from synergid cells and attract the pollen tubes (Higashiyama et al., 2001). Later studies on DEFL superfamily in *Arabidopsis*, identified two functional female attractant *AtLURE* proteins which interacts with the heterodimer male receptor MDIS1-MIK, thereby guiding the pollen tube to the micropylar opening (Wang et al., 2016). In *Zea mays*, defensin-like cysteine-rich proteins ZmES1-

4 secreted from synergid cells is required for pollen tube burst in maize, which is likely caused by activation of the potassium import channel KZM1 (Amien *et al.*, 2010). Similar to the LUREs, ZmES4 has been shown to exhibit species preferentiality.

2.2.3. Cysteine-rich proteins in seed development

Development of seed requires coordinated expression from both saprophytic and male/female gametophytic genes. After double-fertilization primarily matrigenic expression (derived from the maternally transmitted allele in the seed) plays a major role in embryo and endosperm development (Chaudhury *et al.*, 2001). From embryogenesis to the development of embryo and endosperm, numerous reported evidences have showed the importance of CRP in cell-cell communication and signaling. During the course of seed development, the embryo and the endosperm must also co-ordinate their growth with the surrounding maternal tissue which may include role of multiple CRPs in *Arabidopsis*. Recent studies using laser-capture microdissection (LCM) coupled to transcriptomic analysis of individual cells of the *Arabidopsis* female gametophyte has also identified CRPs expressed in the female gametophyte. In the maize kernel development, several CRPs have been characterized in the basal endosperm transfer layer (BETL) cells. One of the best characterized gene MATERNAL EXPRESSED GENE1 (MEG1) which is primarily expressed in the BETL cells and control the differentiation of BETL cell fate during early seed development (Costa *et al.*, 2012; Gutiérrez-Marcos *et al.*, 2004). Another peptide EMBRYO SURROUNDING FACTOR1 (ESF1), preferentially accumulates in central cell gamete and later in the embryo-surrounding endosperm cells during the plant embryogenesis. ESF1 peptide acts synergistically with the receptor-like kinase SHORT SUSPENSOR and positively regulates the suspensor elongation during early embryonic patterning (Costa *et al.*, 2012).

2.3. Plant lipid transfer proteins

Lipids and their derivatives are heterogeneously distributed in different cellular membranes and involved in various biological processes, including membrane biogenesis, inter/intra cellular signaling, cell differentiation and defense mechanisms. To maintain the integrity of the cell, the plasma membrane lipid bilayer forms a physical boundary, which regulate the exchange between the environment. Only a minority of the lipid moiety achieve their final intracellular distribution through vesicle- mediated transport. Instead, the majority of lipid trafficking in eukaryotes, is facilitated by an abundant group of lipid transfer proteins (LTPs),

that bind and transfer lipids between membranes. Plant non-specific lipid transfer proteins (nsLTPs) represent a ubiquitous prolamin family of protein identified in different plant species including monocots, dicots and gymnosperms (Kader, 1996), but they are apparently absent in charophyte green algae as well as in all other organisms. The prolamin superfamily also includes the cereal α -amylase/trypsin inhibitors, the 2S storage proteins, and the hybrid proline-rich proteins (Radauer and Breiteneder, 2007). The nsLTPs are primarily encoded by large multi-gene families with more than 40 members in the genomes of many flowering plants and 50 members in the bryophytes and ferns (Boutrot *et al.*, 2008; Monika M. Edstam *et al.*, 2011; Li *et al.*, 2014). Seemingly the non-seed plants have acquired a more limited set of nsLTP subfamilies or types compared to seed plants, indicating that the novel nsLTP type proteins have evolved during land plant evolution. Although the first LTPs were discovered almost 50 years ago, most of the progress toward their physiological roles has been made in the past few years.

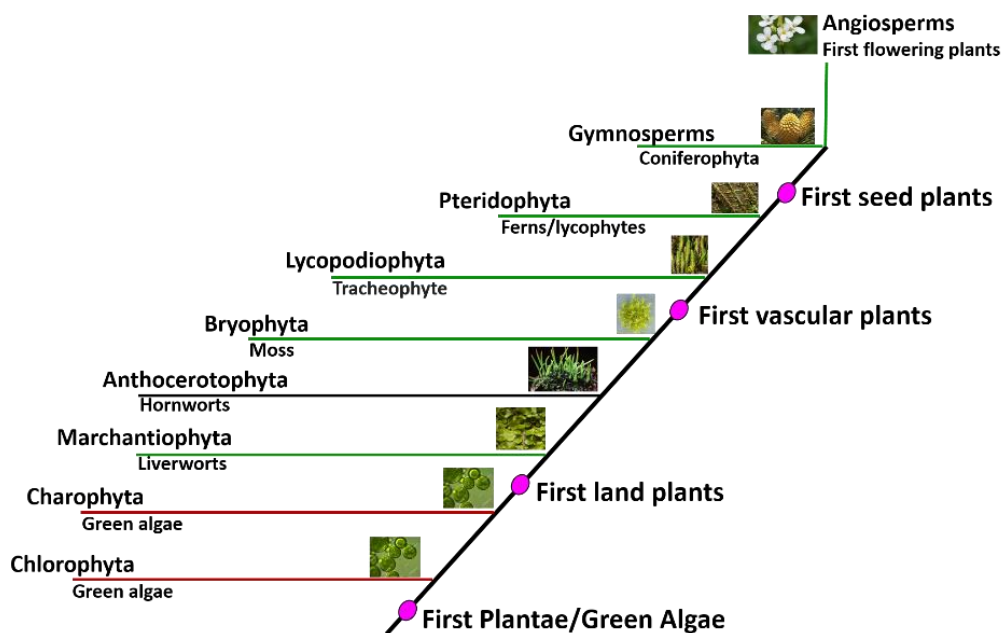


Fig. 1.7: Evolution and distribution of nsLTPs across different plant species. Lines of different colors represent occurrence of nsLTPs. Red branches in the cladogram indicate that no nsLTPs have been identified in green algae, and green branches denotes the presence of nsLTPs. Magenta dots mark the major divergence events in plant evolution. The figure was modified from (Edstam *et al.* 2011).

2.3.1. LTP biochemistry: Structure and lipid binding and transfer properties of nsLTPs.

The plant non-specific lipid transfer proteins (nsLTP) are basic proteins, are of low molecular weight of 9–10 kDa, are secreted, and represent soluble cysteine-rich proteins abundantly present in higher plants. nsLTPs are characterized by a globular α -helical structure (Kreis *et*

al., 1985; Shewry *et al.*, 2002) stabilized by four disulfide bridges formed by an eight-Cys motif (8CM) with the general form (CX_n-C-X_n-CC-X_n-CXC-X_n-C-X_n-C). A tunnel like hydrophobic cavity acts as ligand-binding site for a broad spectrum of lipids and hydrophobic molecules. The disulfide bonds provide stability and promote the folding of the protein into a compact structure which is highly stable towards heat, proteases and denaturants (Berecz *et al.*, 2010; Lindorff-Larsen and Winther, 2001). Almost all of the nsLTPs are synthesized with a N-terminal signal peptide indicating that they follow the secretory pathway, directing the protein to the extracellular, apoplasmic space - exterior to the plasma membrane. In discrete plant species, LTPs are encoded by several dozen paralogs. Based on comparative phylogenetic analysis, LTPs are categorized into at least nine different clades on the basis of their sequences, the presence/absence and location of an intron, the existence of a potential glycosylphosphatidylinositol modification site, as well as their conserved domain and cysteine residue pattern, and their molecular mass (Boutrot *et al.*, 2008; Monika M Edstam *et al.*, 2011). Many of the nsLTPs also encode glycosylphosphatidylinositol (GPI)-anchored proteins (Lee *et al.*, 2009; Debono *et al.*, 2009). The nsLTPs have been classified into types LTP1 and LTP2 based on the polypeptide length of the mature protein: LTP1s have about 90 amino acids and LTP2s have about 70 amino acids (Douliez *et al.*, 2000; Kalla *et al.*, 1994). The two families LTP1 and LTP2 are also characterized with different pairing of the disulfide bridges: in the LTP1s, the Cys residues 1–6, 2–3, 4–7, and 5–8 are paired (Pasquato *et al.* 2006), whereas in LTP2 family, due to interchange of fifth and the sixth Cys residues partners Cys 1–5, 2–3, 4–7, and 6–8 are paired respectively (Hoh *et al.* 2005). Proteins of the type I-LTPs are characterized by a long tunnel-like cavity, while type II-LTPs possess two adjacent hydrophobic cavities.

Non-specific lipid transfer protein facilitates the transport of lipid molecule across the membranes *in-vitro*, however their *in-vivo* biological role often still is not clear (Kader, 1996). The nsLTPs have an affinity towards wide variety of hydrophobic ligands like phospholipids, glycolipids, monoacylated and diacylated lipid molecules including fatty acids (Charvolin *et al.*, 1999), lysophosphatidylcholine (Sodano *et al.*, 1997), phosphatidyl-glycerol (Lerche *et al.*, 1997), prostaglandin B₂, hydroxylated fatty acid and fatty acyl CoA. The affinity of LTPs for a variety of heterogeneous lipid ligands has been confirmed by equilibrium titration experiments. However, the specificity and capacity of lipid binding varies from different nsLTP membranes depending on the size of the hydrophobic cavity and tertiary conformational fold. Some nsLTPs are capable of binding to multiple lipid molecules at a time (Charvolin *et al.*, 1999; Da Silva *et al.*, 2005), while other completely lack the internal lipid binding cavity whereas for other nsLTPs their binding and transport ability of lipids seems hindered by the

bulk side chain of aromatic amino acids present in the cavity (Cammue *et al.*, 1995; Tassin *et al.*, 1998).

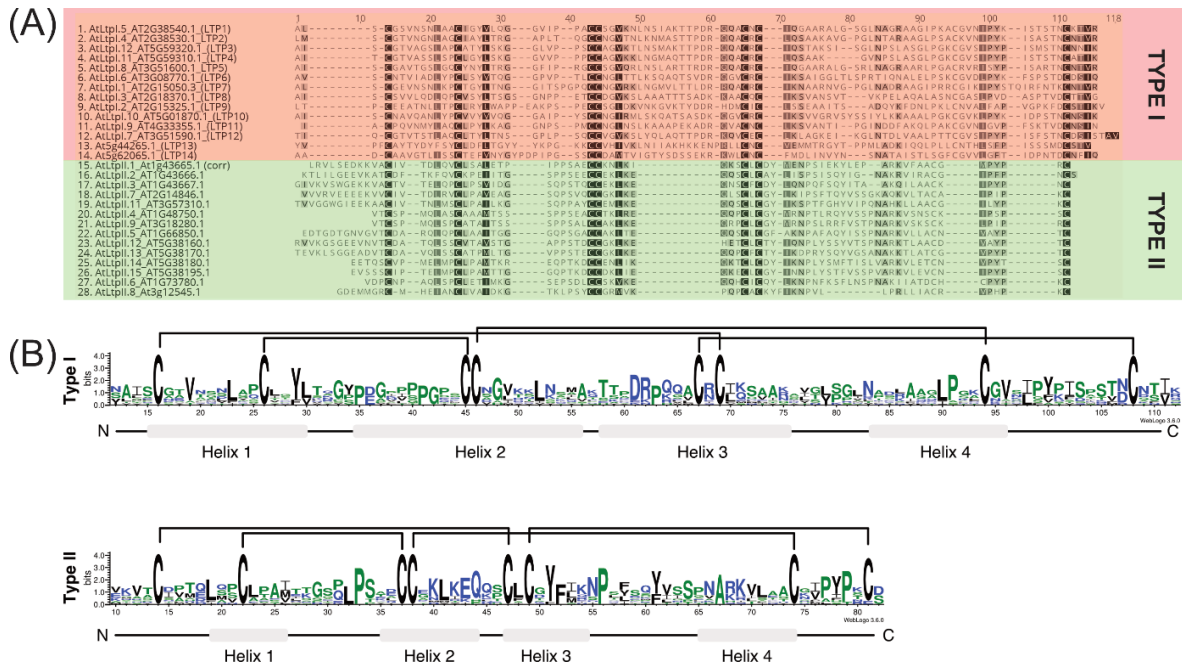


Fig. 1.8: Structural feature of plant nsLTPs: (A) Multiple sequence alignment nsLTP genes identified in the Arabidopsis thaliana genome as described in Boutrot *et al.* (2008). (B) Amino acid sequence of Type 1 and Type 2 nsLTP representing the 8-Cys patterns (primary structure) and four disulfide bridges denoted by the four linkages between cysteine residues. Black linkage depicts the location of four pairs of disulfide bonds indicated by connecting lines in type I and type II nsLTPs,

Reports where dissociation constants (K_d) for LTP-ligand interactions have been determined, suggest that LTPs have affinity towards their ligands in the micromolar range. The first LTPs were discovered and given the name by their ability to recapitulate lipid transfer in cell-free experiments using radiolabeled donor and acceptor liposome (Wirtz and Zilversmit, 1968; Helmkamp *et al.*, 1974) and another nsLTPs for its *in vitro* lipid binding or transfer ability between the membranes (Kader, 1996; Douliez *et al.*, 2000). But recent studies have suggested that nsLTPs do not only mediate a simple vectorial lipid transport in the cell but by different mode of action. Instead, a recent report in 2018 suggested that intracellular LTPs localizes to two organelles at the same time forming a confirmation like shuttle, tube or bridge building a link between the donor and the acceptor compartment and thereby transferring the lipids between the organelles (Wong *et al.*, 2019). LTPs can also act as lipid sensors altering the interaction with the binding partner and they can regulate the lipid content and plasticity in response to the membrane environment. Therefore, LTPs can control different cellular processes like lipid metabolism and homeostasis, signaling pathway and membrane trafficking (De Matteis *et al.*, 2007; Fairn and McMaster, 2008; Cockcroft, 1999). Further studies,

elucidating the precise mechanism on their mode of action and lipid homeostasis could broaden our understanding of LTP function.

2.3.2. Targeting and sub-cellular localization of LTPs

Lipid transfer proteins (LTPs) facilitate trafficking of lipids between organelles and membranes *in-vitro*. LTPs are abundantly expressed in the epidermal cells and secreted to the extracellular matrix (Thoma *et al.*, 1993). Numerous studies have shown that plant LTPs facilitate the vesicular transport of lipid moieties from the endoplasmic reticulum (ER) to plasma membrane (PM) and subsequently from the PM to the extracellular space. Various types of LTPs also transport lipids from ER to different organelles at the membrane contact sites (MCSs) in a non-vesicular manner (Holthuis and Menon, 2014; Helle *et al.*, 2013; Gatta and Levine, 2017) and shuttle across the cytosolic gaps. nsLTPs are synthesized with an N-terminal signal peptide and lacks ER retention signal H/KDEL, which direct them to the secretory pathway. With the increasing evidence that most of the plants LTPs are secreted to the extracellular space, it is unlikely that they are involved in mediating intracellular lipid transfer. However, few reports also support the proposed role of LTPs in intracellular lipid transfer. A recent study demonstrate that during seed germination, LTP *HaAP10* was localized in the apoplastic space, but relocates intra-cellularly by endocytosis during seed imbibition (Pagnussat *et al.*, 2012). Across diverse plant species including *Arabidopsis* (Maldonado *et al.*, 2002), tobacco (Dani *et al.*, 2005), barley (Mundy and Rogers, 1986), carrot and Medicago (Kusumawati *et al.*, 2008), it was shown that LTPs are primarily localized extracellularly. Some experimental evidence also suggests multiple subcellular- localization of nsLTP, both intracellularly in the cell-wall, plasma membrane, vesicles and in the extracellular space (Diz *et al.*, 2011; Tsuboi *et al.*, 1992; de O. Carvalho *et al.*, 2004), and this provides a new insight into the functional regulation of nsLTPs. Another class of proteins identified as, glycosylphosphatidylinositol-anchored lipid transfer proteins (LTPGs) is plasma-membrane associated proteins and are required for the export of wax to the cuticle through secretion pathway (Debono *et al.*, 2009). The apoplastic side of GPI-anchored LTPGs, receive polymer building blocks like suberin component from the plasma-membrane bound ABC transporter and then the cargo delivered the lipid to the subernization sites, such as casparian strips in the root cells or the seed coat (Edstam and Edqvist, 2014). Recent studies, in cotton, showed that the GhLTPG1 protein which is expressed in the elongating fiber and outer integument of cotton ovules, regulates the elongation of the cotton fiber through mediating the transport of phosphatidylinositol monophosphates (Deng *et al.*, 2016). It is still unclear, how the LTPs aid in the extracellular transport of the building blocks for lipid polymer synthesis. One hypothesis, suggest ABC transporter involved in lipid

transport, attempts to explain the mechanism behind the function of LTPs. Lipids can modulate ABC transporter structure, function and its dynamics. For example, during pollen wall formation, ABCG26, a member of ABC transporter family, plays a crucial role in the exine formation and pollen development, where ABCG26 transports sporopollenin precursors across the tapetum plasma-membrane to the locule of developing microspore walls. Loss-of-function mutant in *AtABCG26* showed reduced seed production due to failure in self-pollination caused by defective pollen due to impaired sporopollenin formation (Quilichini *et al.*, 2010). Conceivably, the ABC transporter facilitates the delivery of polymeric substrate to the GPI-anchored LTPs which are adheres to the extracellular apoplastic side of the plasma membrane. ABC transporters functions as flipase moving lipid-linked cargo from one LTPG to another LTP that may diffuse freely in the cell wall.

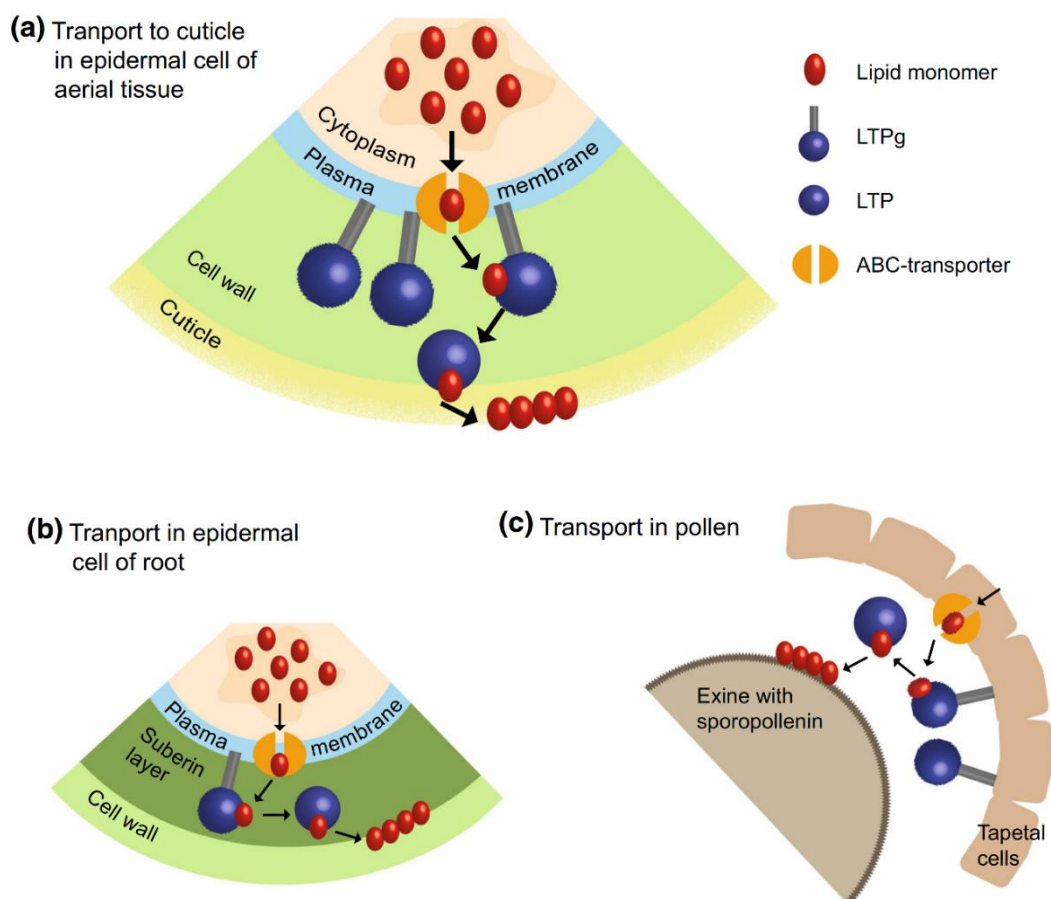


Fig. 1.9: A schematic illustration describing the proposed role of LTPs in (a) epidermal tissue (b) in the root cells (c) and in the pollen (Salminen *et al.*, 2016).

2.3.3. The proposed biological role of lipid transfer proteins

Based on the increasing knowledge regarding the structure, gene-expression, sub-cellular localization, their in-vitro activity of binding/transferring the heterogenous lipids and numerous studies over the last two decades, LTPs are likely to play an important role in diverse processes of plant physiology. The *Arabidopsis LTP* genes are also classified as pathogenesis-related (PR)-14 genes (Sels *et al.*, 2008). Although the precise function and mode of action is still obscure, several potential functions have been proposed for LTPs including adaption of plants to various environmental condition and resistance to biotic and abiotic stress, cutin formation, suberin synthesis and wax metabolism, embryogenesis, defense reactions against pathogens, symbiosis, sexual reproduction and as food allergen. But in this thesis, the potential role of nsLTPs in sexual reproduction and embryogenesis is discussed.

2.3.4. Role of nsLTP in plant sexual reproduction and embryogenesis

High expression of nsLTPs have been detected in distinct floral organ of a variety of plant species and thought to be associated with the reproduction process. LTPs are like SCA (stigma/stylar cysteine-rich adhesin) is expressed in stigma and stylar transmitting tract epidermis. In the stigma cells, SCA is involved in the pollen tube chemotropism, whereas in style it acts as a haptotactic (adhesion-mediated guidance) molecule in association with the pectin polysaccharide (Park and Lord, 2003; Dong *et al.*, 2005). Numerous lines of evidence suggest the expression of nsLTP in both male and female gametophytic tissue. Androecium specific expression of LTP gene was demonstrated by the anther -specific expression of type I and III nsLTPs (Boutrot *et al.*, 2008), *t42*, *Wda1* and *OsC6* in *O. sativa* (Imin *et al.*, 2006), (Zhang *et al.*, 2010a), two stamen-specific gene *tap1* and *fil1* in *Antirrhinum majus* (Nacken *et al.*, 1991), *MZm3-3* in *Zea mays* (Lauga *et al.*, 2000) and many more, primarily expressed at the early stage of pollen maturation and anther development. It has been suggested that nsLTPs are involved in the transport of lipid in the developing pollen wall required for the biosynthesis of the pollen exine. In *Capsicum annuum L.* (chili pepper), CaLTPcl was identified as novel-anther specific lipid transfer protein which was strictly expressed during the middle phase of anther development (stage 3-7 of flower development). Inhibition of CaLTPcl by virus-induced gene silencing method drastically affected pollen development causing lower germination rate, aberrant morphology, and retarded growth of the pollen-tube (Chen *et al.*, 2011). The rice OsLTPg25 (OsC6), which is abundantly expressed in the tapetal cells and localized to the extracellular space of the anther (Zhang *et al.*, 2010b; Zhang and Wilson, 2009), plays a crucial role in the development of orbicules and pollen exine during the post-

meiotic stages 9–11 phase of anther development. Silencing of *OsC6* reduces pollen fertility, causing pollen abortion and defective fertilization (Zhang *et al.*, 2010a). In *Arabidopsis* Type III LTPs showed abundant and highly restricted pattern of expression in the tapetum cells of developing anther of stages 7-9 of floral development (Smyth *et al.*, 1990). The RNAi silencing mutant showed impaired intine development but no fertility defect (Huang *et al.*, 2013). The glycosylphosphatidylinositol- anchored lipid transfer protein LTPGs *AtLTPG2*, *AtLTPG3*, *AtLTPG4*, *AtLTPG5* and *AtLTPG6* are all involved in the development of pollen and seed coat. The analyzed LTPG insertion lines showed reduced fertility with defect in pollen morphology and abnormal seed phenotypes, such as hair outgrowth in the seeds and distorted shape. Analysis of lipid composition in the mutants seed coat revealed significant reduction of ω -hydroxy fatty acid, indicating reduced subernization in the *ltpg* mutant seeds (Edstam and Edqvist, 2014).

In *Lilium longiflorum* female gametophyte (Chae *et al.*, 2007), abundant SCA (stigma/style Cys-rich adhesin) molecules similar to plant lipid transfer protein (LTP) are secreted from the pistil TTE and forms an adhesive matrix with pectin and provide chemotropic guidance to the pollen tube in search of target ovules. Using reverse genetic approach, it was shown that gain-of function mutant of LTP5 (*ltp5-1*) exhibited delayed pollen tube growth and fertilization defect. The *ltp5* gene was weakly expressed both in the male gametophyte (pollen) and in the female gametophyte (pistils TT) (Chae *et al.*, 2009). Also, diverse overlapping expression of LTP1, LTP2, LTP3, LTP4, LTP5, LTP6 and LTP12 were observed in *Arabidopsis* flower suggesting that each LTP gene play its own role in the pistil for pollen tube growth and guidance (Chae *et al.*, 2010; Chae and Lord, 2011). From *Prunus amygdalus*, three lipid transfer proteins (LTPI, LTPII and LTPIII) were highly expressed during the floral development and distinct accumulation of LTP mRNA was observed at the different stages of developing fruit, therefore indicating the importance of existence of different overlapping genes to ensure the presence of a certain amount of LTPs in all stages of developing flower (Suelves and Puigdomènech, 1997). Numerous lines of evidence with series of biochemical and genetic studies on cysteine-rich secreted peptides and LTPs (Alonso *et al.*, 2003; Chae *et al.*, 2009; Chae *et al.*, 2007), have revealed their vital role in adhesion-mediated pollen pistil interaction, pollen tube growth/guidance and endosperm development during double fertilization in angiosperm. nsLTPs also play a pivotal role in embryogenesis and endosperm development. LTP genes are specifically and predominantly expressed in the endosperm-transfer cells and have been identified in the developing maize kernels (BETL-1 and BETL-2) (Lopato *et al.*, 2014) and *OsPR9a* and *OsPR602* in rice (Li *et al.*, 2008). Another maternally regulated ETC-specific gene *MEG1* encoding a LTP gene, was expressed exclusively in the BETL cells of maize endosperm regulating the allocation of maternal nutrients to growing seeds (Gutiérrez-Marcos

et al., 2004), (Xiong *et al.*, 2014). *Endosperm1 (END1)* was identified as an ETC-specific nsLTP genes (Doan *et al.*, 1996) expressed in barley transfer cell domain of the endosperm coenocyte mediating the cellularization process with unknown mechanism. In wheat and barley *TaPR60*, a homologue of *END1* was involved in binding and transfer of lipid molecules as demonstrated by mimicking model of lipid binding. *TaPR60* is suggested to play a role in mediation of lipid delivery to or through a membrane (Kovalchuk *et al.*, 2009). The most probable roles of ETC-specific nsLTP-like protein in endosperm development are cell-wall ingrowth expansion, synthesis of the cellular membrane, and transfer of lipid molecules to the endosperm.

3. AIM OF THE STUDY

Secreted cysteine-rich peptides (CRPs) represent one of the major classes of signaling peptides in plants, and CRPs are over-represented in reproductive tissues. Some members of the non-specific lipid-transfer proteins (nsLTPs), a sub-class among the family of CRPs, are also supposed to play a role in fertilization processes. Although *Arabidopsis thaliana* possesses 49 *nsLTP* genes, the role of most members of this family is unknown. But there is evidence from experimental results of several plant species that LTPs might be important for pollen germination or pollen-tube guidance. Therefore, the aim of this work was to identify LTPs which are essential for fertilization in *Arabidopsis thaliana*.

To screen the potential LTP candidates, the first part of this work is dedicated to expression analysis using bioinformatic *in-silico* study as well as experimental methods like quantitative real time PCR. Subsequently, for those LTPs which were highly expressed in reproductive tissues, transgenic plants including reporter-based transcriptional and translational fusion constructs were generated to analyze their temporal and spatial expression patterns together with the localization of the corresponding proteins *in planta*.

The second part of this work aimed at the functional characterization of the candidate LTPs exclusively expressed in the pistils. To investigate the role of LTPs in this process, reverse genetics approaches (T-DNA insertion mutagenesis) and gene editing (CRISPR/Cas9) were used to create and characterize multiple *knock-out* mutant plants concerning different LTPs. Utilizing cell-biological and *in-vivo* pollination assays candidate LTPs were investigated for their possible role in pollen tube guidance mechanisms during the fertilization process.

4. MATERIALS AND METHODS

4.1. Materials

4.1.1. Plants

Arabidopsis thaliana lines with a T-DNA insertion in the gene coding for *LTP2* (AT2G38530), *LTP3* (AT5G59320), *LTP4* (AT5G59310), *LTP5* (AT3G51600), *LTP6* (AT3G08770) and *LTP12* (AT3G51590), were selected from the public T-DNA Express database established by the Salk Institute Genomic Analysis Laboratory accessible at the SIGnAL website <http://signal.salk.edu>. Seeds were obtained from the Nottingham Arabidopsis Stock Centre (SALK and SAIL lines in Columbia ecotype, (Sessions *et al.*, 2002; Alonso *et al.*, 2003) and Versailles INRA collection FLAG lines in Wassilewskija ecotype (Brunaud *et al.*, 2002), respectively. Information on T-DNA mutants used in this study are given in Table 1.1. Transgenic lines generated and/or used in this work are listed in Table 1.2.

Table 1.1: *Arabidopsis thaliana* T-DNA mutant lines used in this work

| Gene | AGI code | Accession | T-DNA mutants |
|--------------|-----------|-----------|--------------------|
| LTP2 | At2G38530 | Col-0 | GABI_639E08-022274 |
| LTP3 | AT5G59320 | Col-0 | SALK_095248C |
| LTP4 | AT5G59310 | Col-0 | GABI_194C08 (Set) |
| | | Col-0 | GABI_172E09 (Set) |
| LTP5 | At3g51600 | WS | FLAG_529A03 |
| | | Col-0 | SALK_104674 |
| LTP6 | AT3G08770 | Col-0 | SALK_120555 |
| LTP12 | AT3G51590 | Col-0 | GABI_905D04 |
| | | WS | FLAG_487D10 |

| Double mutants containing <i>ltp2</i> and <i>ltp5</i> alleles | | |
|---|-------|-----------|
| <i>ltp2ltp5</i> (P31-P2) | Col-0 | This work |
| <i>ltp2ltp5</i> (P31-P3) | Col-0 | This work |
| <i>ltp2ltp5</i> (P9-P2-P2) | Col-0 | This work |
| <i>ltp2ltp5</i> (P9-P3-P3) | Col-0 | This work |

Table 1.2: Transgenic *Arabidopsis thaliana* lines used in this work

| Transgene | Background | Vector | Selection marker | Reference |
|------------------|------------|-------------|--------------------|-------------------------------|
| prom LTP2:LTP2 | Col-0 | pGWB540 | Hyg ^R | This work |
| prom LTP3:LTP3 | Col-0 | pGWB540 | Hyg ^R | This work |
| prom LTP4:LTP4 | Col-0 | pGWB540 | Hyg ^R | This work |
| prom LTP5:LTP5 | Col-0 | pGWB540 | Hyg ^R | This work |
| prom LTP6:LTP6 | Col-0 | pGWB540 | Hyg ^R | This work |
| prom LTP12:LTP12 | Col-0 | pGWB540 | Hyg ^R | This work |
| 35S:LTP2-mcherry | Col-0 | pCambia3300 | Basta ^R | (Deeken <i>et al.</i> , 2016) |
| promLTP2::GUS | WS | pmDC164 | Hyg ^R | This work |
| promLTP3::GUS | Col-0 | pmDC164 | Hyg ^R | This work |
| promLTP4::GUS | Col-0 | pmDC164 | Hyg ^R | This work |
| promLTP5::GUS | Col-0 | pmDC164 | Hyg ^R | This work |
| promLTP6::GUS | Col-0 | pmDC164 | Hyg ^R | This work |
| promLTP12::GUS | Col-0 | pmDC164 | Hyg ^R | This work |

4.1.2. Bacterial strains

Escherichia coli

For all the cloning approaches chemically competent *Escherichia coli* MRF+ cells ($\Delta(mcrA)$ 183; $\Delta(mcrCBhsdSMRmrr)$;173 *endA1 supE44 thi-1 recA1 gyrA96 relA1 lac* [F';proAB lacIq Δ M15 Tn10 (*Tetr*)] were used.

Agrobacterium tumefaciens

The *A. tumefaciens* strain GV3101 (Koncz and Schell, 1986) was used for stable transformation of *A. thaliana* plants. For transient expression in the *Nicotiana Benthamiana* leaves, antisilencing agrobacterium strain GV3101 19K was used.

4.1.3. Vectors

The following Table 1.3 lists the vectors used during this work and it includes further description and their antibiotic resistances.

Table 1.3: List of the vectors used in this study

| Vector | Description | Selection marker in bacteria and plant | References |
|------------|---|--|---------------------------------|
| pDONOR207 | Gateway Entry clone | Kan | (NAKAGAWA <i>et al.</i> , 2007) |
| pGWB540 | Gateway Destination vector (no promoter, C-Fusion EYFP), binary vector for <i>A.tumerfacien</i> -mediated transformation of plants. | Spec, Hyg ^R | NAKAGAWA <i>et al.</i> , 2007) |
| pmDC164 | Gateway Destination vector for GUS fusion, binary vector for <i>A.tumerfacien</i> - mediated transformation of plants. | Kan, Hyg ^R | |
| pCBC-DT1T2 | CRISPR/Cas9 two sgRNA expression cassettes | Kan | (Xing <i>et al.</i> , 2014) |
| pHEE401 | EPC-controlled CRISPR/Cas9 binary vector, binary vector for <i>A.tumerfacien</i> mediated transformation of plants. | Kan, Hyg ^R | Xing <i>et al.</i> , 2014) |

4.1.4. Primers

All the primers used for T-DNA genotyping was designed using the iSECT primer designing tool and obtained from SIGMA-Aldrich (Germany) (Table 1.4, 1.5). For qPCR expression analysis, the primers were designed using GeneiousR-7.0.6 and obtained from TIB MOLBIOL Syntheselabor GmbH (Berlin, Germany) (Table 1.6). The lyophilized oligonucleotides were diluted to a stock-concentration of 100 µM with ultrapure water. For standard usage, aliquots with a working concentration of 10 µM were prepared by dilution with ddH₂O. Oligonucleotides were stored at -20°C.

Table 1.4: List of gene-specific primer used for genotyping T-DNA insertion mutants

| Gene/AGI code | T-DNA insertion mutant | LP Primer | RP Primer | Product Size RP-LP | Product Size RP-LB |
|-----------------------------|------------------------------------|---|--|--------------------|--------------------|
| LTP2/ AT2G38530 | GK_639E08-022274 | TCTCCAAATGT TTGTTCAAGC | ATTCAAAGAAC GTTGTTTGGC | 1066 | 539-839 |
| LTP3/ AT5G59320 | SALK_095248C | TCGATGCATA ATCAAATCGT G | GTTCAAACACA ATGGCTTTCG | 1025 | 434-734 |
| LTP4/ AT5G59310 | GK_194C08 (Set) GK_172E09 (Set) | TTTTTACGTAT GAGTGC GTT G GTAAAAATCTT CCTGCAGGGC | TGGTCTTTGTAC ATTCTGAAA ACT G TAAGCATCTGC ATGCTTGTTG | 1057 1051 | 496-796 434-734 |
| LTP5/ AT3G51600 | FLAG_529A03 SALK_104674 | TTGAGGGATC CAAGACAAAT C CTTATTTTGTA CCAGCGAGGC | CATCCAAAAGC AGAACGTGAC TTGTGTACGGA CTGTGGAGAAG | 1109 1097 | 434-734 433-733 |
| LTP6/AT3G08770 | SALK_120555 | AACTAGCAAA CCAATGCCCT C | TTTTTCCTTTTG TCGACGTTG | 1097 | 439-739 |
| LTP12/ AT3G51590 | GK_905D04 FLAG_487D10 | TTAGTTTCTTT TCAATCGCCG ACATGCCTCA TTGTCCTTAC G | GCTGGCAAGTT TGATTAGTCG GATCCTTGCTA ATGGCAACTG | 1160 1086 | 504-804 458-758 |

Table 1.5: T-DNA primer/Locus specific primer list used for genotyping T-DNA insertion mutants

| Gene/AGI code | T-DNA insertion mutant | T-DNA primer/Locus specific primers |
|------------------------|--|-------------------------------------|
| LTP2/ At2G38530 | GABI_639E08-022274 | 8474 – SD32 |
| LTP3/ AT5G59320 | SALK_095248C | LB1.2 - RP |
| LTP4/ AT5G59310 | GABI_194C08 (Set) GABI_172E09 (Set) | 8474 – 39yf 8474 – ML4 |
| LTP5/ AT3G51600 | FLAG_529A03 | RP - Tag3 / Rb4 |

| Gene/AGI code | T-DNA insertion mutant | T-DNA primer/Locus specific primers |
|-----------------------------|----------------------------|-------------------------------------|
| | SALK_104674 | LB1.2 - RP |
| LTP6/AT3G08770 | SALK_120555 | LB1.2 - RP |
| LTP12/ AT3G51590 | GABI_905D04 FLAG_487D10 | 8474 – SD35 |

Table 1.6: List of primer pair used for qPCR

| Gene | Primer direction | 5' to 3' sequence | T _m , °C | Fragment length, bp |
|---|------------------|--|---------------------|---------------------|
| ACT2 / At3g18780 ACT8/ At1g49240 | Fwd Rev | ACTGAGCACAATGTTAC GGTGATGGTGTGTCT | 55 | 435 |
| LTP1/ At2G38540 | Fwd Rev | CTCAGTTAACAGCAACTT GTTGAGACCAGAGCCTA | 56 | 173 |
| LTP2/ At2G38530 | Fwd Rev | CGGCGTTACTAACCTTA AGGAATATTGACTTTGCAT | 55 | 186 |
| LTP3/ AT5G59320 | Fwd Rev | GTGGGTTGGTGCCACCTTCA TCACTTGATGTTGTTGCAGT | 57 | 218 |
| LTP4/ AT5G59310 | Fwd Rev | CATGTCTAGGCTACCTAT GGCTAGACTTGGATTAAC | 56 | 155 |
| LTP5/ At3g51600 | Fwd Rev | ATGGAGGGACTCTTGAA CAACACCCTCTAGGAAT | 58 | 161 |
| LTP6/AT3G08770 | Fwd Rev | TCACAACACTCAAGAGTC GCTGAACTTGTAAAGGA | 55 | 161 |
| LTP12/ AT3G51590 | Fwd Rev | TCACAACACTCAAGAGTC GCTGAACTTGTAAAGGA | 54 | 160 |

Table 1.7: List of primers used for amplifying LTP promoters

| Gene | Primer direction | 5' to 3' sequence | T _m , °C |
|------------------------|------------------|---|---------------------|
| LTP2/ At2G38530 | Fwd Rev | AACAAGCAACAAGCCCG AACAAGCAACAAGCCCG | 58 |
| LTP3/ AT5G59320 | Fwd Rev | TGACTACACAAACCTCTACC TGTGTTTGAACCTCTTTTTGG | 60 |
| LTP4/ AT5G59310 | Fwd Rev | GTGGTTCAATTTGAGACGCG TGTGTTTGCTCTTCTTTTTGG | 54 |
| LTP5/ At3g51600 | Fwd Rev | TTTTGGTAATTAATCGTAAG ATCTTAATTTTTTTTTTCTC | 58 |

| | | | |
|-----------------------------|-----|----------------------------|----|
| LTP6/AT3G08770 | Fwd | AAGCTAATTAGTTGCATACATATTG | 56 |
| | Rev | GTTACTTTCTGTTTTTTTTTTTTTTG | |
| LTP12/ AT3G51590 | Fwd | TTGGATGCATCCTATTC | 55 |
| | Rev | TTTTGTTTTTTATTGCTTTTAC | |

Table 1.8: List of primers used for amplifying promLTP::LTP

| Gene | Primer direction | 5' to 3' sequence | T _m , °C |
|-------------------------|------------------|---------------------------|---------------------|
| LTP2/ At2G38530 | Fwd | GCAACAAGCCCGATTTCGGC | 58 |
| | Rev | CCTCACGCTGCATTCACATAC | |
| LTP3/ AT5G59320 | Fwd | TGACTACACAAACCTCTACC | 56 |
| | Rev | CTTGATGCTGCAACAATCC | |
| LTP4/ AT5G59310 | Fwd | GTGGTTCAATTTGAGACGCG | 60 |
| | Rev | CTTGATGCTGCAACAATACAAAC | |
| LTP5/ At3g51600 | Fwd | CCAGGAAAAAAGGCAGATTTATG | 58 |
| | Rev | CCTGACGCTGCAACCAAC | |
| LTP6/AT3G08770 | Fwd | AAGCTAATTAGTTGCATACATATTG | 56 |
| | Rev | AGATTTTCTGCTTGTCTCACTG | |
| LTP12/ AT3G51590 | Fwd | TTGGATGCATCCTATTCCTTCTTC | 58 |
| | Rev | CACGGCAGTCGATATACTGC | |

Table 1.9: List of primers used for amplifying LTP cDNA

| Gene | Primer direction | 5' to 3' sequence | T _m , °C |
|-------------------------|------------------|-----------------------------------|---------------------|
| LTP2/ At2G38530 | Fwd | GGCTTAAUATGGCTGGAGTGATGAAGTTGG | 58 |
| | Rev | GGTTTAAUCCCTCACGGTGTTGCAGTTGGTGC | |
| LTP3/ AT5G59320 | Fwd | GGCTTAAUATGGCTTTTCGCTTTGAGGTTTC | 56 |
| | Rev | GGTTTAAUCCCTTGATGTTGTTGCAGTTAGTGC | |
| LTP4/ AT5G59310 | Fwd | GGCTTAAUATGGCTTTTCGCTTTGAGGTTTC | 60 |
| | Rev | GGTTTAAUCCCTTGATGGTGGCGCAGTTGGTGC | |
| LTP5/ At3g51600 | Fwd | GGCTTAAUATGGAGGGACTCTTGAAGTTGTC | 58 |
| | Rev | GGTTTAAUCCCTGACGGTGTTACAGTTGGTTC | |
| LTP6/AT3G08770 | Fwd | GGCTTAAUATGAGATCTCTCTTATTAGCCGTG | 56 |
| | Rev | GGTTTAAUCCCTGGATACTGTTCGAGTCAGTG | |
| LTP12/ AT3G51590 | Fwd | GGCTTAAU ATGGCGTTTACTCCGAAGATCATC | 58 |
| | Rev | GGTTTAAUCCACGGCAGTCGATATACTGTCCG | |

Table 1.10: List of primers used for generating LTP2sgRNA and LTP5sgRNA

| Target 1: LTP2 | FORWARD PRIMERS (Target1- LTP2) | T _m , °C | Fragment size |
|-------------------------|--|---------------------|---------------|
| LTP2_153/fw_DT1- BsF | ATATATGGTCTCGATTGC GAGGTGCTCCACTTACCCA GTT | 53 | 645bp |
| LTP2_153/fw_DT1- F0 | TGCGAGGTGCTCCACTTACCCA GTTTTAGAGCTAGAAATAGC | 54 | |
| Target 2: LTP5 | REVERSE PRIMERS (Target1- LTP5) | T _m , °C | Fragment size |
| LTP5_154/fw_DT2- R0 | AACCTAGGAATGAAACCGCCTC CAATCTCTTAGTCTGACTCTAC | 55 | 635bp |
| LTP5_154/fw_DT2- BsR | ATTATTGGTCTCGAAAC TCTAGGAATGAAACCGCCTC CAA | 54 | |

Table 1.11: List of primers used for sequencing

| Primer | Sequences |
|---------------------|----------------------------|
| YFP_FP | GACTTCAAGGAGGACGGCAA |
| YFP_RP | TCTCGTTGGGGTCTTTGCTC |
| CRISPR- LTP2_153/fw | GGGTCTACATTAATGAGTACAG |
| CRISPR- LTP2_153/rv | CGCTGCATTCACATACAAATTAA |
| CRISPR- LTP5_154/fw | GATAAGAGAAGAGAAAGCAATGC |
| CRISPR- LTP5_154/rv | GCAACCAACCAATACATCAATC |
| U6-26p-F | TGTCCCAGGATTAGAATGATTAGGC |
| U6-29p-R | AGCCCTCTTCTTTTCGATCCATCAAC |
| U6-26p-F | TGTCCCAGGATTAGAATGATTAGGC |
| U6-29p-F | TTAATCCAACTACTGCAGCCTGAC |

4.1.5. Antibiotics

All the antibiotics used in this work are summarized in the Table1.12. Aqueous solutions were filter sterilized (pore size of 0.2 µm). Stock solutions were stored at -20°C.

Table 1.12: List of antibiotics

| Antibiotic | Stock conc. | Final conc | Solvent |
|-------------------------|--------------------|-------------------|--------------------|
| Ampicillin (Amp) | 100 mg/ml | 100 µg/ml | ddH ₂ O |
| Gentamycin (Gent) | 50 mg/ml | 50 µg/ml | ddH ₂ O |
| Kanamycin (Kan) | 50 mg/ml | 50 µg/ml | ddH ₂ O |
| Rifampicin (Rif) | 20 mg/ml | 20 µg/ml | methanol |
| Hygromycin (Hyg) | 50 mg/ml | 50 µg/ml | ddH ₂ O |
| Spectinomycin (Spec) | 50 mg/ml | 100 µg/ml | ddH ₂ O |

4.2. Methods of manipulation with *E. coli* and *Agrobacteria*

4.2.1. Preparation of chemically competent *E. coli* DH5 α cells

To prepare competent cells, firstly single colony of *E. coli* DH5 α strain was inoculated in 10 ml of Ψ -broth media and grown at 37°C overnight in 100 ml flask. *E. coli* was grown overnight in LB medium and subsequently inoculated 500 ml LB medium with antibiotics if needed. The cells were grown at 37°C at 140 rpm to an OD600 of 0.7 (mid-log phase). The culture was cooled on ice for 20 min. The culture, containers and solutions were kept as close to 0°C as possible in the subsequent steps. The cells were harvested by spinning down at 4000 x g for 15 min at 4°C. The supernatant was discarded, and the obtained pellet was resuspended in the cold TfB1, with incubation on ice for 90 mins. The cells were centrifuged at for 5000 x g for 15 min at 4°C. The obtained supernatant was discarded, and the pellet was finally resuspended in TfB2 media. The cell suspension was separated into aliquots (40 μ l per aliquot), frozen in liquid nitrogen, and stored at -80°C. All media for preparation of chemically competent *E. coli* cells were prepared according to protocols listed below:

| Ψ -broth media for 1 L | TfB1 for 100 ml | TfB2 for 20 ml |
|--|--|--|
| Bacto tryptone: 20 g | RbCl ₂ (100 mM): 1.21 g | RbCl ₂ (10 mM) |
| Yeast extract: 5 g | MnCl ₂ *4H ₂ O (50 mM): 0.99 g | CaCl ₂ *2H ₂ O (75 mM) |
| MgSO ₄ *7H ₂ O (0.4%): 4 g | KOAc (Potassiumacetate) (30 mM): 0.3 g | glycerol 100% (15% v/v) |
| | CaCl ₂ *2H ₂ O (10 mM): 0.15 g | MOPS (10 mM) |
| | Glycerol 100% (15% v/v): 15 ml | |

4.2.2. Heat-shock transformation of chemically competent *E. coli* cells

E. coli transformations were conducted using competent *E. coli* strain DH5-alpha. For transformation, 50 μ l of competent cells were thawed on ice and mixed with 100 ng of the experimental DNA or 5 μ l of ligation mixture. Tubes were swirled gently and incubated on ice for 30 min. After incubation, cells were heat-shocked in a 42°C water bath for 30-60 sec and then immediately transferred on ice for 2 min. Then, 450 μ l of the SOC medium was added to the cells and incubated at 37°C for 1h with shaking at 350rpm. For positive selection, 50-75 μ l of transformation mixtures were plated on LB agar plates containing the appropriate antibiotic and incubated at 37°C for overnight.

4.2.3. Preparation of electro-competent *Agrobacteria*

For competent cell preparation, the agrobacterial pre-culture was incubated overnight in 5 ml of YEP media with vigorous shaking at 200-250 rpm and 28°C. Overnight incubation for large culture was needed to reach mid-log phase. Afterwards, pre-culture was mixed with 400ml of YEP media and grown at 28°C (10-12 h) until $OD_{600} = 1$. All further centrifugation steps were performed at 4000 rpm for 15 min and at 4°C. Centrifuge tubes, falcon tubes, ddH₂O and 10% glycerin were pre-cooled on ice. The obtained pellet was resuspended in 200 ml of cold dd H₂O and centrifuged. Additionally, the pellet was washed with cold dd H₂O in a final volume of 50-100 ml and centrifuged again. Finally, the bacterial pellet was washed in 10 ml of 10% glycerol, centrifuged and subsequently resuspended in equal volume of 10% glycerol. Small volumes (50µl) of cell aliquots were frozen in liquid nitrogen and stored at -80°C.

4.2.4. Transformation of electro-competent *Agrobacteria*

Binary vector containing desired insert were transformed into *A. tumefaciens* strain GV3101. For *Agrobacterium* transformation, 50 µl of competent cells were placed on ice, gently mixed with 50ng of DNA vector (5 µl) and incubated for 2 min. After incubation, the mixture was transferred into pre-cooled electroporation cuvette (2 mm gap). Electroshock was performed at 25 µF, 400 Ω, 2.5 kV on Bio-Rad electroporator. 500ul of SOC medium was immediately added to transformed cells and incubated at 28°C with shaking for 1h. After 1hr of incubation the cells were centrifuged at 14000 rpm for 3min. 350ul of supernatant was discarded and pellet was resuspended in the remaining supernatant. Finally, 50 µl µl of the bacterial culture was placed on selection plates with appropriate antibiotics and incubated at 28°C for 2 days. Following incubation, colonies appearing on plates were picked with the help of tooth prick and streaked on a fresh YEP agar plate. The cells were allowed to grow overnight at 28 °C. A colony PCR was set up to screen the positive clones using insert-specific primers.

4.3. Plant Procedures

4.3.1. Vapor-phase (gas) seeds sterilization protocol

For seed sterilization, 300-500 seeds were transferred into 2ml microcentrifuge eppendorf tubes. A glass vessel for sterilization, typically a desiccator jar, was kept under fume hood. Tubes containing the seeds were placed on a rack and inside of a desiccator next to a beaker

with 100 mL of sodium hypochlorite. Immediately prior to sealing the jar, 6 ml of concentrated HCl were added to the bleach carefully. Seal jar and chlorine gas sterilization was allowed to proceed for 2-3hrs. After treatment, the chlorine gas was evaporated from the Eppendorf tubes for 1-2 hours under sterile bench.

| Required Chemicals | |
|-------------------------|-----------|
| Na-hypochlorite | 12% (v/v) |
| Hydrochloric acid (HCl) | 37% (v/v) |

4.3.2. Plant growth conditions on soil and agar plates

Arabidopsis thaliana seeds of the ecotype Columbia-0 (Col-0) were obtained from the Nottingham *Arabidopsis* Stock Centre (NASC). Seeds were sown on soil (Solarite), kept for two days at 4°C in the dark to induce stratification, and then grown under controlled long-day photoperiod 16/8hrs conditions in a climate chamber (Percival cabinet). Plants were illuminated for 16 hours with a light intensity of 120 $\mu\text{mol s}^{-1} \text{m}^{-2}$ using fluorescent lamps from Osram (L58W / 77 FLUORA; Munich, Germany) and Philips (TLD 58W / 840; Hamburg, Germany). The temperature was constantly maintained at 22°C and 16°C during the light and dark period, respectively. The relative humidity was maintained at 60%. After stratification (two days at 4°C). All *Arabidopsis thaliana* mutants were grown under identical environmental conditions as WT plants. Surface sterilized *Arabidopsis* seeds were sown in half strength Murashige and Skoog medium, complemented with 0.8% agar. Agar plates were kept for 2 days at 4°C in the dark, to induce stratification, and subsequently they were transferred to a growth chamber at 22°C under a long day photoperiod (16h light/8h dark), with irradiance of 120 $\mu\text{mol s}^{-1} \text{m}^{-2}$ and 60% relative humidity. For GUS histochemical staining, seedlings were collected 10 days after germination. *Nicotiana benthamiana* plants were grown from seeds on soil in a greenhouse with 16 hours of light at 28°C (16 h) / 25°C (8 h).

4.3.3. Floral dip transformation of *Arabidopsis thaliana*

Arabidopsis stable transformed plants were generated by *Agrobacterium* mediated transformation of *A. thaliana* ecotype Col-0 as per floral dip method (Clough and Bent 1998). The plants were grown in the controlled condition as described in section 3.3.2. After bolting, the apical region was nipped to induce lateral branching via loss of apical dominance. Twenty-five to thirty-day old plants showing profuse flowering with >50% of inflorescence was selected. The *Agrobacterium* were regrown overnight in liquid YEP medium with required antibiotic with vigorous shaking at 200-250 rpm and 28°C. Next day, the cells were centrifuged at 3000rpm for 20 mins at 4°C. The supernatant was discarded, and the pellet was resuspended in the

infiltration medium (5.0% sucrose, 0.05% Silwet L-77). The concentration of the infiltration medium was adjusted until the OD 600 was between 0.8-1. The pots containing the plants were inverted and aerial parts of the plants were dipped in bacterial cell suspension for about 20-30 sec. Afterward, the plants were covered with plastic bags to maintain humidity and kept in dark. After 16-18 hrs of incubation, plastic bags were removed and then the plants were grown in the climate chamber until they completed their lifecycle. After attaining maturity, seeds were collected and stored under cool and dry condition.

4.3.4. Antibiotic selection and screening for positive transformants

The seeds collected from putative *A. thaliana* Col-0 T1 transgenic plants were surface sterilized as mentioned in section 3.3.1. The sterilized seeds were plated on MS medium containing Hygromycin B (40mg/L) and stratified in dark at 4 °C for 2 days. Following a stratification period of 2 d at 4°C in the dark, seedlings were incubated for 8 h at 22°C in white light, followed by incubation at 22°C in the dark for 4 days. The plants were allowed to grow until positive transformants could be distinguished as long green hypocotyl from non-transformants. When green seedlings (T1) reached 3-4 leaf stage, they were transferred to pots (11 cm diameter) containing 1:1:1 mixture of soilrite, vermiculite and perlite. The seedlings were grown in a growth chamber under same conditions as mentioned earlier (section 3.3.2).

4.3.5. Infiltration of *Nicotiana benthamiana* for transient expression via *Agrobacterium*

For transient expression, 1.5-2-month-old *Nicotiana benthamiana* plants were used for agrobacterial infiltration. Binary construct GV3101 containing desirable constructs and antisilencing 19K agrobacterial strains were taken from a fresh plate and grown overnight in 10 ml of YEP medium containing antibiotics at 28°C, 200 rpm. Following incubation, *Agrobacterium* cells were harvested by centrifugation of culture at 4,000 rpm for 10 min at 20°C. Subsequently, the supernatant was discarded, and the bacterial pellet was washed with distilled water followed by centrifugation of culture at 4,000 rpm for 10 min at 20°C. Finally, the bacterial pellet was resuspended in the 5ml of Agromix buffer (10 mM MgCl₂, 10 mM MES pH= 5.6 and 150uM Acetosyringone) and incubated for 2 h at 30°C in a dark. After incubation the culture were diluted to 1:100 and OD600 nm was measured. Afterwards bacterial suspensions were mixed with Agromix buffer until the final OD600nm=1. For co-infiltration equal volumes of the specific *A. tumefaciens* strains were mixed with 1ml of anti-silencing 19K strain. The bacteria were slowly injected into the abaxial side of the leaf using 1ml syringe. The plants

were grown under greenhouse conditions and checked for the transient expression 4 days post infiltration.

4.4. Pollination Experiments

Numerous hand-pollination/crosses were employed to visualize the *in-vivo* growth of pollen tube. The list below summarizes each of them.

4.4.1. Emasculation of *Arabidopsis* flowers

To compare the expression of different LTPs in the pollinated and non-pollinated pistils. Closed buds of stage 12 (Smyth *et al.*, 1990) (Fig. 3.1) were used to prepare the pistil for non-pollinated and hand-pollinated pistils. The petals and the androecium were gently removed using the fine forceps without hurting the pistils. The emasculated pistil was marked with a piece of thread around its stem. The isolated pistils were left to grow for 1 day and then harvested for non-pollinated sample. Some of the emasculated pistils were pollinated with fresh pollen grains. Hand-pollinated pistils were collected 24 hours after pollination (24HAP) and immediately frozen in liquid nitrogen for RNA isolation. To minimize biological variation, three replicates were collected for each experiment containing 30-40 pistils per replicate.

4.4.2. *In-vivo* reciprocal-cross pollination

To study the growth of pollen tube *in-vivo* various cross pollination experiment was performed utilizing, T-DNA knock-out and wild-type plants. Closed buds of stage 12 (Smyth *et al.*, 1990) (Fig. 3.1) were used to prepare the pistil. The isolated pistils were left to grow for 1 day. Fresh pollen at flower stage 13-15 of the respective *Arabidopsis* species, was fully applied to the stigma of the emasculated buds. 14-hrs post pollination, the pollinated pistil was harvested to perform aniline blue staining. As a control, wild-type pistils were hand pollinated with wild-type pollens. For the fertilization study, half of the pollinated flowers were further grown in the growth chamber for 8 to 10 days. Siliques were dissected or decolorized at maturity to examine seed set.

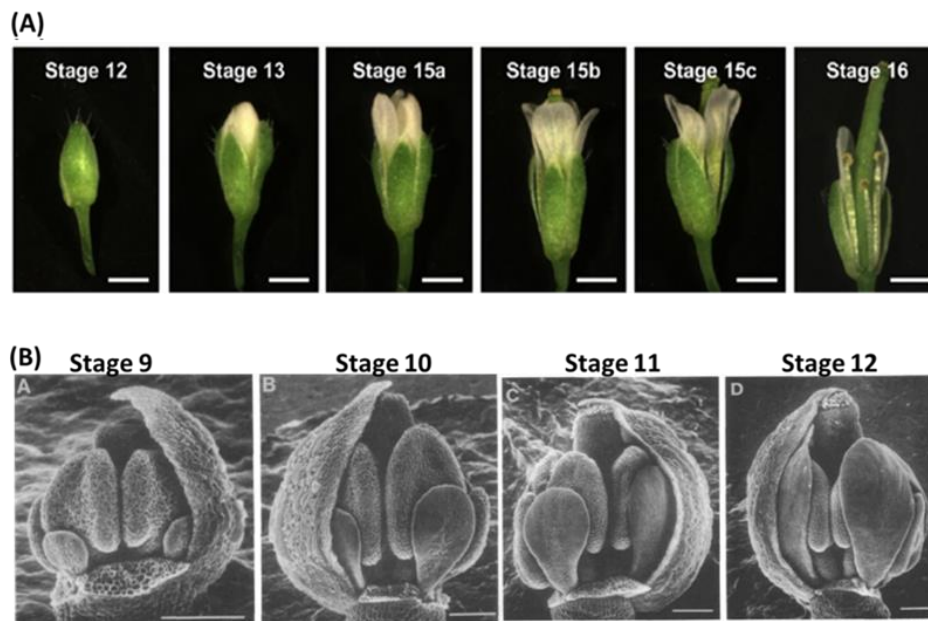


Fig. 3.1: Different developmental stage of flower development. Adopted from (Cai and Lashbrook, 2008; Smyth et al., 1990).

4.4.3. Aniline blue staining to visualize growing pollen tube *in-vivo*

For Aniline blue staining, both hand pollinated flowers and naturally pollinated flowers at stages 12-15 (Smyth *et al.*, 1990) were removed from the stem and fixed in 3:1 Ethanol: Acetic Acid solution for 12-24hrs. After fixation the samples were washed 3 times with 70% EtOH and incubated in 8M-NaOH alkaline solution 12hrs. After incubation in 8M NaOH solution, the samples were washed 3 times with 50mM K-Phosphate buffer, pH=7.4 and then stained with aniline blue dye for overnight at RT. After adding aniline blue dye to the samples, they are kept in dark and not exposed to light. The stained samples were transferred into 50mM K-Phosphate buffer, (pH=7.4). For visualizing the samples in LSM, a drop of glycerol solution (Glycerol in 50mM K-Phosphate buffer, pH=7.4) was used. It was added to the glass slide together with the pistils, and a cover slip was carefully placed from the end of pistil with avoiding bubble contamination. Pistils were observed under a fluorescence microscope at 350-400nm.

4.4.4. *In-vitro* pollen tube germination growth assays

All *in-vitro* pollen tube experiments were performed as described by (Boavida and McCormick, 2007). Flowers from *Arabidopsis thaliana* plants two weeks after bolting were used as source of pollen. Pollen grains were germinated on a solid germination medium as describe in Table 2.1. The *A. thaliana* flowers were removed with a pair of tweezers, and the pollen grain was

tapped on PGM and incubated for 6 hours in black box at room temperature for germination. After 6hrs, images of pollen tubes were acquired using a digital microscope (VHX-100; Keyence).

Table 2.1: *Arabidopsis* pollen germination media

| Pollen germination medium |
|--|
| 1 mM CaCl ₂ 2H ₂ O |
| 0.01% (w/v) H ₃ BO ₃ |
| 1 mM CaCl ₂ |
| 1 mM MgSO ₄ 7H ₂ O |
| 18% (w/v) sucrose |
| low melting agar pH 7.5 |

4.4.5. Seed set analysis

Siliques from the primary inflorescences of wild type and T-DNA knock-out plants were selected from top to bottom and bleached in 70% ethanol for 48-72 hours. The ethanol-bleached siliques were then imaged using the dissecting microscope and the number of seeds was counted based on the pictures.

4.5. Localization methods

4.5.1. Histochemical β -glucuronidase (GUS) activity analysis

In order to study the tissue-specific expression of LTP2, LTP3, LTP4, LTP5, LTP6 and LTP12 in the different part of the flowers, the individual LTP promoter was fused to the gene which encodes for β -Glucuronidase (GUS) (pmdc164-LTPProm::GUS). GUS is commonly used as a reporter gene as the according enzyme can cleave the chromogenic substrate X-gluc (5-bromo-4-chloro-3-indolyl β -D-glucuronic acid, resulting in the production of a blue indigo colour/precipitate (Jefferson *et al.*, 1987). Plant cells themselves do not contain any endogenous GUS activity, so the production of a blue color when stained with X-gluc in particular cells indicates the activity of the promoter that drives the transcription of the gusA-chimeric gene in that particular cell.

For the localization study, flowers of different developmental stages (closed bud, mature flower, siliques) and 10-days old seedling was used for analyzing *PromLTP::GUS* activity. The samples were harvested and vacuumed in GUS staining solution (Table.3.1) for 5 minutes at 100mbar, followed by incubation at 37°C for 2hr 30min. Afterwards the chlorophyll from stained tissues was removed by incubation in 70% (v/v) ethanol at room temperature overnight. The

samples were then examined by means of a digital microscope (Keyence, Osaka, Japan). Subsequently, the samples were stored in darkness until further use. Three independent homozygous transgenic plants were used for the LTP-GUS analysis.

Table 3.1: GUS staining solution

| GUS-Staining Buffer |
|--|
| 150 mm sodium phosphate buffer, pH 7 |
| 10 mm EDTA |
| 0.5 mg mL ⁻¹ 5-bromo-4-chloro-3-indolyl β-d-glucuronic acid [Duchefa] |
| 0.1% [v/v] Triton X-100 |
| 0.5 mm potassium ferricyanide |
| 0.5 mm potassium ferrocyanide |

4.5.2. Confocal Laser Scanning Microscopy (CLSM)

CLSM was utilized to visualize the localization pattern of C-terminal fusions of LTP2, LTP3, LTP4, LTP5, LTP6 and LTP12 protein with the yellow fluorescent mVenus reporter protein. After transferring them to *Agrobacteria*, those were subsequently infiltrated into leaves of *Nicotiana benthamina* together with the plasma membrane marker *35S::DsRED-REMORIN* (Bozkurt *et al.*, 2014) and cell wall marker *35S::LTP1-mCherry* (Deeken *et al.*, 2016). 4 days after infiltration with *Agrobacteria*, samples were prepared for the CLSM. The fluorescent signals from YFP and RFP were analyzed using the. A small area of the infiltrated leaf was cut out and the abaxial surface was observed for fluorescent signals using the 40x water immersion objective of the confocal laser scanning microscope (CLSM; TCS SP5 2; Leica Microsystems Nussloch GmbH, Nussloch, Germany). For the detection of fluorescent signals from YFP and RFP, different the excitation and emission wavelengths were used as described below.

| Fluorescence Protein | Excitation Wavelength | Emission Wavelength |
|-----------------------------|------------------------------|----------------------------|
| mVenus | 514 nm | 530–555 nm |
| DsRED | 561 nm | 560-600 nm |
| mCherry | 561 nm | 580–615 nm |

To visualize the localization of LTP protein in the ovule development of stable transgenic *Arabidopsis* plants, T2 seeds from hygromycin-resistant plants were used for YFP expression analysis. Ovules and developing seeds of transgenic plants were cleared in the fixed using (4% PFA in PBS) and cleared in ClearSee solution {Xylitol Powder (final 10% w/v), Sodium deoxycholate (final 5% w/v), Urea (final 25% w/v), mix ingredients in H₂O dest} for overnight and were visualized using confocal laser scanning microscopy. Excitation at 514 nm and

emission wavelengths of 525–555 nm were collected for YFP fluorescence. Colocalization - analysis was done using colocalization plugin (JACoP, Just Another Co-localization Plugin JaCOP from ImageJ) from ImageJ (BOLTE and CORDELIÈRES, 2006). JACoP tool was used to analyse the Pearson and Manders correlation coefficients from 4 randomly selected ROI in each group of colocalization image pair.

4.5.3. Subcellular localization of LTP with Correlative Light and Electron Microscopy (CLEM)

To determine the precise sub-cellular localization of LTP2/LTP5 protein at their ultrastructure level within the cell, CLEM technique was employed.

High-Pressure Freezing

The *N. benthamiana* leaves were infiltrated with *Agrobacteria* containing 35S::LTP2-YFP and 35S::LTP5-YFP constructs. 4 days post infiltration, small leaf discs were punched out of the area with higher expression and was subjected to high-pressure freezing. Fresh samples were placed in the platelet and the recess was overfilled with hexadecane, the cryoprotectant. The samples were then frozen with a cooling rate of >20,000 K/s and a pressure of > 2100 bar with EM HPM100 machine (Leica Microsystems) and later stored in liquid nitrogen.

Freeze substitution and embedding into LR-White resin

After cryofixation the frozen crystalline and non-crystalline water in the samples is replaced with an organic solvent, usually acetone plus fixatives, a process known as freeze substitution (Kang, 2010). For this, the EM AFS2 freeze substitution system (Leica Microsystems) was used and the protocol was adapted from a previously published method (Weimer, 2006) as described in the Table 3.2.

Table 3.2: Protocol for freeze substitution and LR-white embedding

| | |
|----|---|
| 1. | Freeze substitution at –90°C for 80hrs |
| 2. | Gradual warming to –45°C in the course of 11hrs period |
| 3. | Samples are washed 3 time with acetone in the course of 3hrs |
| 4. | Washing with anhydrous acetone at room temperature (three changes of acetone) and gradual warming to 4°C over a period of 16hrs |
| 5. | Dehydration / Resin Infiltration 50% EtOH/50% water - 15 min 70% EtOH/30% water - 15 min * |

| | | |
|--|--------------------------------|-----------|
| | 80% EtOH/20% Water | 10 min |
| | 2:1 LR White resin to 70% EtOH | 1 hour** |
| | 100% LR White resin | 1 hour |
| | 100% LR White resin | overnight |
| | 100% LR White resin | 30 min |
| | 100% LR White resin | 30 min |

After complete resin infiltration, the samples were carefully transferred to the center of the gelatin capsules with a glass pipet. The resin LR White (London Resin Company Ltd.) is a hydrophilic embedding medium and does not polymerize in the presence of oxygen, so the embedding capsules was tightly locked. The gelatin capsule was filled up to the rim with LR White, add a small paper strip with sample name was placed inside the capsule before locking it. The samples were polymerized under UV light at 4°C for 48-72 hrs.

Mounting, Trimming and Ultramicrotomy

After polymerization, the LR-embedded tobacco leaf-disc samples, were trimmed using a sharp blade under a dissecting light microscopy, until a trapezoid block face was achieved. The ultra-thin section of 200nm was cut with histo Jumbo diamond knife from DiATOME (Hatfield, USA) using the ultramicrotome Leica EM UC7 (Leica Microsystems). The ultra-tin sections were checked for the region of interest by fast staining with methylene blue dye. The desired sections were carefully transferred on the poly-L-lysine coated slides (Polysine, Thermo Fisher), and subsequently dried for at least 30min at 50°C to allow sections to irreversibly adhere to the glass surface. Sections on dried slides were later used for immunolabeling.

Immunolabelling and Light Microscopy

Slides with serial sections were stained by using Immunolabelling procedure as described before (Markert *et al.*, 2017), (Micheva and Smith, 2007) (see Table 3.3). The immunostaining procedure was performed in dark and humid chamber at RT. The stained samples were checked for YFP-signal, under light microscopy using a 40x objective.

Table 3.3: Protocol for immunolabelling

| | |
|-------------------------|--|
| Blocking | The LR-embedded section was blocked with blocking solution (0.1% BSA and 0.05% Tween 20 in 50 mM Tris buffer, pH 7.6) for 10mins. |
| Primary antibody | After blocking, the sections were incubated with polyclonal chicken anti-GFP diluted 1:200 in the blocking solution, for 1hr at RT. After 1hr incubation with primary antibody, the sections were carefully washed five times in 5 min intervals with Tris buffer. |

| | |
|---------------------------|---|
| Secondary antibody | After the wash, monoclonal secondary antibody chicken anti-goat IgG was applied on the section for 30mins at RT in dark. After 30 mins incubation with primary antibody, the sections were washed five times in 5 min intervals with Tris buffer and finally, once with ddH ₂ O to remove salt. The sections were mounted in the Mowiol and stored at 4°C until further use. |
|---------------------------|---|

Contrasting and carbon coating

After immunostaining, the sections were contrasted and subjected to carbon coating to reduce the charging and make the samples electrically conductive, for good results with the scanning electron microscopy (SEM) imaging. As the microscopic slides were too big for the SEM, the desired portion of the slide was cut with a diamond pen, before doing the contrasting procedure. For contrasting, the samples were incubated in 2.5% uranyl acetate in ethanol for 15 min, then in 50% Reynolds' lead citrate in water for 10 min according to standard protocol(ref). After contrasting, the cut glass pieces were mounted to SEM specimen holders and surrounded with a contact adhesive, silver paint, to reduce charging. Then the samples were carbon coated using Carbon coater Med 010 (Balzers Union).

Scanning Electron Microscopy (SEM)

To image the ultrastructure of the leaf sample, a scanning electron microscope (JSM-7500F JEOL, Japan) with a LBE detector (for backscattered electron imaging at extremely low acceleration voltages) was used. The light microscopic images with fluoresce signal was used as a reference to find the region of interest. SEM images were acquired with an acceleration voltage of 5 kV, a probe current of 0.3 nA, and a working distance of 6e8 mm.

Image Processing and Correlation of Light Microscopy and Scanning Electron Microscopy Images.

To correlate the fluorescence and the SEM image, open source vector graphics editor Inkscape (version 0.91;<http://www.inkscape.org>) and image editor GIMP (<http://www.gimp.org>) were used.

4.5.4. Technovit7100 embedding and sectioning for *Arabidopsis* flowers

The mature flower from *Arabidopsis* wild-type and *ltp2ltp5* mutant plants, were emasculated and isolated pistil was fixed using FAA solution (see Table 3.4) at room temperature for 2-3hrs until the tissue sinks to the bottom of the vial. After fixation, the fixed tissue was subsequently dehydrated with different EtOH concentration (see Table 3.5). The dehydrated tissue was cleared in different concentration of infiltration solution and ethanol solutions (see Table 3.6).

Afterward, the 100% Technovit solution was replaced with infiltration solution (100% Technovit “basis solution + Härter I) and incubated for overnight at RT. The infiltrated tissue was transferred to polymerization resin (Infiltration solution + Härter II) and carefully placed inside the gelatin capsule and incubated for overnight at RT. After polymerization, the Technovit-embedded flower samples were trimmed using a sharp blade under a dissecting light microscopy. The cross section of 2-4µm was cut with glass knife using the ultramicrotome Leica EM UC7 (Leica Microsystems). The semi-thin sections were stained for 30 mins in 0.1% aniline blue in 0.1 M K₃PO₄ at RT. Slides were overlaid with a coverslip and sealed with 1-2 drops of aniline blue. The stained sections were observed within 1hr to detect callose deposition using confocal laser scanning microscopy.

Table 3.4: Fixation FAA solution

| Chemicals | %in Mix | for 100ml |
|-------------------------|---------|-----------|
| Ethanol 95% | 50% | 52.6ml |
| Glacial Acetic Acid 37% | 5.0% | 5ml |
| Formaldehyde | 3.7% | 10 ml |
| Water | 41.3% | 32.4 ml |

Table 3. 5: Dehydration

| EtOH% | Incubation time |
|-------|-----------------|
| 50% | 30mins x3 |
| 60% | 30mins |
| 70% | 30mins |
| 85% | 30mins |
| 95% | 30mins |
| 95% | overnight at RT |
| 100% | 1hr |
| 100% | 30mins x 2 |

Table 3.6: Resin Infiltration

| Technovit%+ EtOH% | Incubation time |
|--|-----------------|
| 25% Technovit “basis” Solution:75% ethanol | 2hrs |
| 50% Technovit “basis” Solution:50% ethanol | 2hrs |
| 75% Technovit “basis” Solution:25% ethanol | 2hrs |
| 100% Technovit “basis” Solution | 24hrs |

4.6. Molecular biology techniques

4.6.1. Genomic DNA Isolation

Arabidopsis leaves (5 –10 mg) were harvested in 2 ml Eppendorf centrifuge tubes containing about 2 ceramic beads, and frozen in liquid nitrogen quickly. The tubes were quickly transferred to a tissue homogenizer and thoroughly shaken to homogenize the leaves. 300 µl of extraction buffer (200mM TRIS pH:7.5, 250mM NaCl, 25mM EDTA, 0.5% SDS) was added and mixed by vortexing. The samples were spinned down at 14,000g for 8 mins. 300ul supernatant was added to 300ul of Isopropanol and mixed by short vortexing. The mixture was centrifuged, and supernatant was discarded, the obtained pellet was washed with 70%EtOH for 5 mins. After washing the pellet with EtOH the samples were kept at 37°C for 25mins. After drying the pellet was dissolved in 25ul of water and stored at -20°C.

4.6.2. Polymerase chain reaction (PCR)

PCR based genotyping analysis for the GABI-KAT/SALK/FLAG T-DNA insertion mutants.

The T-DNA insertion mutant lines were analyzed by PCR genotyping using combinations of the gene-specific primers LP/RP and T-DNA left border (LB) primer (see Table 1.4 and 1.5). Gene-specific primers gave rise to PCR products in WT but not in the homozygous mutant, because the elongation time is suitable for WT fragments (usually about 1 kb) but is too short for fragments containing a T-DNA insertion. In contrast, the primer pair of LB and RP led to PCR products in the homozygous mutants but not in WT, as the LB primer sequence exists in the T-DNA mutant only. The heterozygous mutant which contains a T-DNA in one of the alleles had PCR products from both primer pairs. The primers were designed using the iSECT primer designing tool. For GABI-KAT T-DNA insertional mutant combination of gene-specific primer (LP/RP) and T-DNA primer/locus-specific primers were used to screen the homozygous knockout mutant. Components for a single genotyping reaction are PCR conditions are described in Table 4.2 and Table 4.3.

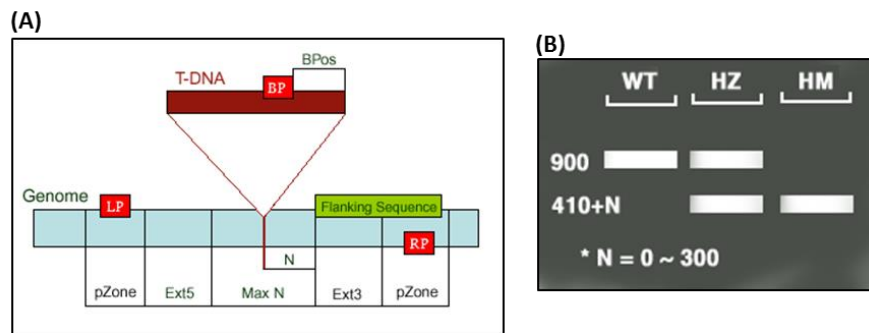


Fig. 3. 2: Illustrates a guide to identifying T-DNA insertion localization and map. N-Difference of the actual insertion site and the flanking sequence position, usually 0 – 300 bases. MaxN- Maximum difference of the actual insertion site and the sequence, default 300 bps. Ext5, Ext3-regions between the MaxN to pZone, reserved not for picking up primers. LP, RP – Left, Right genomic primer. BP TDNA border primer LB – the left T-DNA border primer. Bpos – The distance from BP to the insertion site. LB – Left border primer of the T-DNA insertion: (LBb1.3 and Lba1) (B) Guide for the PCR genotyping and gel analysis of the insertion lines for the identification of wild type (WT), heterozygous (HT) and homozygous (HM) lines provided by the SALK institute genomic analysis laboratory (SIGnAL) (<http://signal.salk.edu/tdnaprimers.2.html>).

Table 4.1: Primer pair to screen different T-DNA insertion mutant

| T-DNA | Set of primers used for genotyping |
|----------------|--|
| SALK T-DNA | (LBb1.3+LP+RP) |
| GABI-Kat T-DNA | (LP+RP), (T-DNA primer + Locus-specific primer) T-DNA primer: 8474 Locus-specific primer: 39yf, ML44, BA37, SD35, SD32 |
| FLAG T-DNA | (LP+RP+Tag3/Rb4) |

Table 4.2: PCR reaction mix

| Component | Volume (µl) |
|-------------------------|-------------|
| 10X Phusion buffer | 5 µl |
| 100 mM dNTP Mix | 0.5 µl |
| 100 µM Forward Primer | 0.5 µl |
| 100 µM Reverse Primer | 0.5 µl |
| Genomic DNA | 1 µl |
| Phusion Hifi polymerase | 0.5 µl |
| PCR-grade water | Up to 25 µl |

Table 4.3: Settings used in thermocycler for genotyping

| Steps | Temperature | Time | Cycles |
|-------|-------------|--------|--------|
| 1 | 95°C | 2 min | 37 |
| 2 | 95°C | 30 sec | |
| 3 | 59°C | 30 sec | |
| 4 | 72°C | 90 sec | |
| 5 | 72°C | 5min | |
| 6 | 4°C | | Hold |

Amplification of PCR products for cloning

The PCR amplification was done using Phusion polymerase and reaction was performed according to the manufacture protocol. Components of the PCR reaction and conditions are described in Table 4.2 and 4.4.

Table 4.4: Settings used in thermocycler for gradient PCR amplification

| Steps | Temperature | Time | Cycles |
|-------|-------------|------------|--------|
| 1 | 98°C | 2 min | 1 |
| 2 | 98°C | 30 sec | 30 |
| 3 | 50-60°C | 30 sec | |
| 4 | 72°C | 1000bp/min | |
| 5 | 72°C | 5min | |
| 6 | 4°C | | Hold |

4.6.3. Colony PCR

In order to identify the transformed colonies containing recombinant plasmids colony PCR was carried out. Gene specific primers were employed to screen bacterial colonies for identification of recombinant transformants and presence of inserts of expected size. The obtained colonies were picked from the plate and resuspended in 50 µl of sterile distilled water. The cell suspensions were incubated at 100 °C for 1 min. One µl of the cell suspension was used to carry out PCR. The reaction mix comprised of 1 µl of the cell suspension, 1X reaction buffer, 0.2 mM dNTPs, 0.5 µM each primer, and 1 U Phusion Polymerase. The PCR was conducted in thermocycler (Eppendorf, Germany) as described in Table 4.4.

4.6.4. Restriction digestion of the plasmid

To perform single or double digestion of the plasmid, several different restriction enzymes were employed using the same basic reaction mixture. Each digestion reaction was incubated at specific temperature and time specified by the manufacturer for each enzyme. The following components were used for restriction enzyme digest reactions:

| Components | Volume |
|--------------------------|------------------|
| DNA | up to 1µg |
| 10X NE Buffer | 2 µl |
| Restriction Enzymes (HF) | 1 µl |
| Nuclease-free water | Made up to 20 µl |
| Total 20 µl | 20 µl |

4.6.5. Agarose Gel Electrophoresis

During gel electrophoresis, an electrical field is used to move the negatively charged DNA through an agarose gel matrix towards a positive electrode to separate DNA by size (e.g., length in base pairs). 0.8% -2% agarose gels were prepared depending on the size of the DNA. All the samples were mixed with 5x DNA loading buffer (bromophenol blue, 0.25% (w/v); xylene cyanol, 0.05% (w/v); EDTA, 0.1 M; glycerin 50% (w/v) in deionized water). Depending of the size of the DNA fragment, different concentrations of agarose powder was melted in 1X TAE buffer (50X: 242g Tris-base, 100% acetic acid- 57.1ml, 100ml of 0.5M sodium EDTA) and cooled down. To visualize the DNA fragments, the DNA dye GelGreen™ (Biotium, <http://www.biotium.com>) was added to the gel with a final concentration of 0.05 ‰ (v/v). Besides the samples, 5µl of the suitable DNA-ladder (Lambda PstI Marker, Gibco/ Invitrogen, Life Technologies, Carlsbad, CA, USA), were applied to the pockets and the agarose gel was run for 45-60 minutes at 120V. The gel was photographed under UV light of a wavelength of 260-360 nm, using the gel imager.

4.6.6. Isolation of Plasmid DNA

To get appropriate material for plasmid isolation, 3 - 4 mL of LB-medium containing antibiotics were inoculated with a fraction of the bacterial colony from the plate using a sterile pipette tip. Antibiotics were added to the final concentrations as described in section 3.1.5. The cultures were grown overnight at 37°C. Plasmid DNA was isolated using the Plasmid Plus DNA Purification Mini Spin Column Kit (Genaxxon BioScience GmbH, Ulm). Overnight cultures were harvested by centrifugation at 14,000 rpm for 3 minutes, the supernatant was discarded, and plasmid isolation was performed according to the manufacture's procedure as described in Table 4.5. Finally, the plasmid concentrations were determined using a spectrophotometer Nanodrop (Thermo Scientific- 2000 c- UV-VIS spectrophotometer).

Table 4.5: Protocol for isolation of plasmid DNA

| | |
|--|---|
| Resuspension of the bacterial pellet | The obtained cell pellet was thoroughly resuspended in 250µL Resuspension Buffer by pipetting or vortexing. NOTE: Incomplete resuspension may result in considerable decrease of yield. The resuspended cell pellet was then transferred to a sterile 1.5mL Eppendorf microcentrifuge tube. |
| Lysis of the bacterial cells | 250µL of the lysis buffer was added to the resuspended cells and was mixed carefully by inverting the tube 4 to 6 times. |
| Neutralization of the bacterial cells | 350µL of neutralization buffer was added to the lysed samples and carefully mixed inverting the |

| | |
|-----------------------------------|--|
| | tube several times. The samples were transfer to the purification min-column and centrifuged at 14,00rcf for 10 mins. |
| Washing | The supernatant was discarded, and the column was washed twice using the 600 μ L wash buffer and was subjected to centrifugation at 14,00rcf for 3 mins. |
| Elution of the plasmid DNA | The obtained flow-through was discarded and the column was transferred to a sterile 1.5mL Eppendorf microcentrifuge tube. 25 μ L of ddH ₂ O was added at the center of the column and was incubated for 15 mins at RT. After 15mins of incubation the column was centrifuged at 14,00rcf for 1 min. |

4.6.7. RT-PCR analysis of specific transcript abundance

Isolation of total RNA and RT-PCR analyses were performed as described by (Szyroki *et al.*, 2001). The gene-specific primers which were used to amplify first-strand cDNAs are described in Table 1.6. Transcripts of the *A. thaliana Actin2* (AT3G18780) and *Actin8* (AT1G49240) gene were used as reference (An *et al.*, 1996) for normalization.

Isolation of RNA from emasculated pistils and mature flower

Mature flowers and emasculated pistils were used for RNA extraction and cDNA synthesis. The plants were grown in a long-day photoperiod 16/8hrs conditions in a climate chamber (Percival cabinet) with maintained irradiance of 120 μ mol s⁻¹ m⁻², temperature at 23°C and 60% relative humidity. All plant tissues collected were placed immediately in liquid N₂ and stored at -80°C until RNA was extracted. To extract RNA, RNeasy kit from QIAGEN was used according to manufacturer's instructions with minor modifications (see Table 4.6).

Table 4.6: Protocol for isolation of RNA

| | |
|--|---|
| Homogenization | Frozen plant material was homogenized into fine powder using Tissue lyzer II system (Qiagen) at a high frequency (30 Hz) for 3 minutes using ceramic milling balls. |
| Cell Lysis | 350 μ L of (RA1+10 μ L of tris(2-carboxyethyl) phosphine (TCEP) was added to homogenized sample and was vortexed vigorously to suspend the sample in the buffer. Samples were then centrifuged at 11000 x g for 1 minute. |
| Filtrate lysate | Supernatant was transferred into NucleoSpin Filter column (Violet ring) and was centrifuged at 11000 x g for 1 minute. The flow through from the filter was transferred into a clean 1.5 mL tube and equal volume of 70% ethanol was added followed by vigorous shaking on vortex for 20 seconds. |
| RNA binding | The lysate is transferred into the RNA binding column NucleoSpin RNA Plant Column (light blue ring) followed by centrifugation at 11,000 x g for 30 seconds. |
| Washing and drying of the silica membrane | 1st Wash: 200 μ L of buffer RAW2, 30 seconds, 11,000 x g. Flow through was discarded. 2nd Wash: 600 μ L of buffer RAW3, 30 seconds, 11,000 x g. Flow through was discarded. |

| | |
|--------------------|--|
| | 3rd Wash: 250µL of buffer RAW3, 30 seconds, 11,000 x g. Flow through was discarded. |
| RNA Elution | 20-30 µL of RNase free water (provided by the manufacturer) was added into the dried RNA binding column and placed at room temperature for 1 minute. Afterwards, RNA was collected into the clean 1.5 mL tubes (provided with the kit) by centrifuging at 11,000 x g for 1 minute. Quality of the RNA was measured by using nanodrop (Thermo Scientific- 2000 c- UV-VIS spectrophotometer). A quality score of ~2.0 was used for optical density at 260/280 and 260/230 absorbance ratios. |

4.6.8. Reverse transcription (cDNA synthesis)

cDNA (complementary DNA) synthesis from mRNA was performed according to the protocol described in (Biemelt *et al.*, 2004). To remove the residual genomic DNA, the samples were first treated with DNase I enzyme. The DNase1 digestion reaction was performed as described below.

| Components | Volume |
|---|---------------------------|
| Total RNA | Up to 1µg |
| 10x DNase Buffer (Thermo Scientific) | 2 µl |
| DNase I (Thermo Scientific, 1U/µl) | 1µl |
| RNase Inhibitor (Thermo Scientific, Ribolock 40 U/µl) | 0.5 µl |
| Nuclease-free H ₂ O | To a total volume of 20µl |
| Incubated at 37°C for 45 minutes in the incubator provided by Eppendorf (Thermomixer 5436). | |

After DNase1 digestion, for better precipitation of the residual RNA, mixture of isopropanol (70 µL) (AppliChem GmbH, Germany), 10 µL glycogen (20mg/mL) (Thermo Fisher Scientific Inc., Waltham, Massachusetts, USA), 10 µL of 5 mM ammonium acetate and water to a total volume of 150 µL was added to the sample. The samples were centrifuged at 14000 rpm (Eppendorf- 5810 R) and stored for 24hrs at -20 °C. Next day, the samples were centrifuged (45 minutes at 4°C and 14000 rpm, Eppendorf Centrifuge 5430R). After centrifugation, the supernatant was removed carefully without disturbing the pellet. 500 µL of 70% ethanol (from Carl Roth GmbH) was added into each sample and centrifuged again at 14000 rpm and at 4 °C for 20 minutes. Without disturbing the pellet, supernatant was discarded followed by pellet drying at 37 °C for 30 minutes. The dry RNA pellet was finally dissolved in 7 µl DEPC-H₂O. After poly(A)-mRNA extraction, an RNA-dependent DNA polymerase Moloney Murine Leukemia Virus Reverse Transcriptase (M-MLV RT) was utilized to generate cDNA complementary to mRNA. cDNA synthesis was performed using 1µg of RNA template. 6 µl of total RNA was added to a mixture of 0.4 µl Oligo-dT-Primer, 0.6 µl 10 µM dNTPs and 2 µl 5x M-MLV Reverse Transcriptase Buffer (Promega). Total RNA was denatured at at 70°C for

2mins and quickly cooled on ice. After few seconds, 0.4 μ l MMLV-RT reverse transcriptase (100 U/ μ l, Promega, Mannheim, Deutschland) was added to the sample and cDNA was finally synthesized at 42°C with a 1 h period of incubation. MMLV-RT generated double-strand cDNA was used for either qRT-PCR reaction directly or stored at -80°C.

4.6.9. Quantitative real-time polymerase chain reaction (qRT-PCR)

Quantitative polymerase chain reaction (Q-PCR) is a method for quantifying cDNA in real-time, and is very useful for investigating gene expression. qRT-PCR was performed using the Light Cycler (Roche, USA). Each reaction mixture (20 μ L) contained 10 μ L of SYBR-Green (ABsolute QPCR SYBR green capillary mix, Thermo Scientific), 6 μ L of nuclease-free water, 1 μ L of each primer and 2 μ L of diluted cDNA. The qRT-PCR reaction conditions are described in Table 4.7. All reactions were repeated in triplicate. Actin 2 and actin 8 (ACT2/8; At3g18780/At1g49240) were used as internal standards. Transcripts of a gene of interest were determined by using standard curve for the gene of interest and normalized to the reference internal standard. The starting materials for the standard series were PCR products purified according to the manufacturer's instructions using the DNA purification kit (Quiagen, Hilden, Germany). Specificity of the PCR product was additionally analyzed by melting point analysis. Additionally, separation in agarose gel was checked. The concentration of the purified PCR product was determined spectrophotometrically (Nanodrop 200c, Thermo Fisher Scientific). The purified PCR product is serially diluted in a 1:10 dilution (10; 1; 0.1; 0.01 fg/ μ l) with tRNA-water (Sigma-Aldrich Chemie GmbH, Steinheim, Germany). All cDNAs used for real-time PCR were diluted to 1:20 with tRNA water to avoid cDNA binding to the wall of the reaction vessel. The internal standards and test samples were measured together in the same reaction for each gene of interest. In addition, one non-template control (NTC) as well as one positive control were also added in every run. The relative expression was determined using standards the C_t value, threshold cycle, i.e. the cycle in which amplification increases exponentially. The data was analyzed in order to calculate the expression levels of the genes in the different tissues. Therefore, the emitted fluorescence was used to first calculate the number of molecules (using formula 1) and then the number of molecules per 10,000 actin molecules (using formula 2). The equation uses the correlation that a DNA fragment of 1000 bp has an average weight of 910 femtograms (Giulietti *et al.*, 2001). The expressed number of molecules was calculated for each gene. Afterwards the number of transcripts per 10,000 actin molecules was calculated to be able to compare the relative expression levels of the genes of interest.

$$\text{Formula 1: } \textit{number of molecules} = \frac{910}{\textit{length of fragment [kb]}} \cdot \textit{fluorescence [fg]}$$

$$\text{Formula 2: } \textit{rel. transcription} = \frac{\textit{molecules gene of interest}}{\textit{molecules NtActin}} \cdot 10,000$$

Table 4.7: Settings used in thermocycler for qPCR

| Steps | Temperature | Time | Cycles |
|-------|-------------|--------|--------|
| 1 | 95°C | 10 min | 1 |
| 2 | 95°C | 15 sec | 40 |
| 3 | 50-60°C | 20 sec | |
| 4 | 72°C | 5 sec | |
| 5 | 79°C | 5 sec | |
| 6 | 95°C | 20 sec | Hold |

4.7. Cloning of reporter gene constructs using Gateway Cloning

The Gateway® Technology is a universal cloning method based on the site-specific recombination properties of the bacteriophage lambda (Landy, 1989) that provides a rapid and highly efficient way to transfer a gene of interest into multiple vector systems. There are two simple steps to generate expression vectors: the first is the construction of an entry clone by transferring a blunt-end PCR fragment into a pENTR vector; secondly, LR recombination reaction between an entry clone and destination vector needs to be performed to generate an expression vector. Gateway cloning was performed as described before (Raissig et al., 2013) and gene-specific primers containing the first 12 base pairs of the attB sites.

Entry vectors

The genes of interest were amplified using high fidelity Phusion DNA polymerase (New England Biolabs) and gene specific primers with attB sites. The qualified PCR products were cloned into entry vector pDONOR207. The BP recombination reaction was performed using an attB-flanked DNA fragment and an attP-containing donor vector to generate an entry clone according to the manufacturer's protocol. The following components (see Table 5.1) were used in the BP reaction mixture.

Table 5.1: Set-up for BP recombination reaction

| Component | Volume |
|--|----------|
| attB-PCR product (40-100 fmol) | 1-10 µl |
| pDONR™ vector (supercoiled, 150 ng/µl) | 2 µl |
| 5X BP Clonase™ reaction buffer | 4 µl |
| TE Buffer, pH 8.0 | to 16 µl |

After gently mixing the reaction was incubated at 25°C for 1 hour and subsequently transformed into electrocompetent *E. coli* cells (see section 3.2.2). The gentamycin resistant colonies were checked by colony PCR to ensure that the gene of interest was cloned into the vector and avoid false positive colonies which contained empty vectors. After purification from a 5 ml pre-culture, the putative plasmids were digested by suitable restriction endonucleases which cut both the gene of interest and the vector sequence. If the restriction analysis showed a correct size and direction of insertion, sanger sequencing was performed using gene specific forward and reverse primer. After inserted sequence was confirmed, the entry vector was ready for performing the LR recombination reaction.

Expression vectors

The Gateway® LR recombination reaction (Invitrogen) was performed between an attL-containing entry clone and an attR-containing destination vector to generate an expression clone. The LR (attL x attR) reaction is catalyzed by Gateway LR Clonase™ II enzyme mix. The recombination between the entry clone containing attL flanked gene and the destination vector generates the expression clone containing the gene flanked by attB sequences, and a by-product. The destination vector contains a different selection marker compared to the entry clone, so that one can distinguish between the desired product and others. The Gateway Destination vectors are binary vector which contain additional other selection markers which will function in the transformed organisms, such as plants. For the LR reaction the components were mixed as described in the Table 5.2.

Table 5.2: Set up for LR recombination reaction

| Component | Volume |
|--|----------|
| attB-PCR product (40-100 fmol) | 1-10 µl |
| pDONR™ vector (supercoiled, 150 ng/µl) | 2 µl |
| 5X LR Clonase™ reaction buffer | 4 µl |
| TE Buffer, pH 8.0 | to 16 µl |

The LR Clonase II enzyme mix (2µl) was added and the reaction was carried out at 25 °C for 1 hour. To terminate the reaction, 1 µl of Proteinase K solution was added and the mixture was incubated at 37 °C for 10 min. Electrocompetent *E. coli DH5α* cells were transformed with LR reaction products by adding 1 µl of mixture to 40 µl of bacterial cells followed by the electrotransformation protocol described in section 3.2.2. Transformants were selected on LB plates with suitable antibiotics. The plasmids of expression clones were confirmed by restriction analysis and Sanger sequencing before transforming into Col-0 *Arabidopsis*.

4.7.1. Generation of PromLTP::GUS constructs

For plants expressing GUS reporter, the promoter of six different LTP gene (LTP2, LTP3, LTP4, LTP5, LTP6 and LTP12) was cloned and fused to the gus reporter gene. A 2,000-bp fragment from the region upstream of the selected LTPs were amplified with primers as listed in Table 1.7. The amplified 2,000-bp promoter fragment was inserted into the entry vector pDONOR207 using the BP Clonase enzyme. The resulting entry clone was transferred into the binary destination vector pmDC164 using LR clonase enzyme. The resulting *PromLTP::GUS* contains a 2-kb promoter fragment upstream of the start codon which was transcriptionally fused to the N-terminus β -glucuronidase (*GUS*). The plasmid with the final construct *PromLTP::GUS* was transformed into *Agrobacterium tumefaciens* strain GV3101 (including rifampicin and gentamicin resistance) and transformed into *A. thaliana* as previously described in section 3.3.4.

4.7.2. Generation of PromLTP::LTP-YFP constructs

For reporter plants expressing fusion products of YFP with the 6 different LTP genes (LTP2, LTP3, LTP4, LTP5, LTP6 and LTP12) under the control of their native the promoter region and the corresponding gene including the introns were amplified with the primer pair listed in Table 1.8. The amplified 3000-bp fragment was inserted into the entry vector pDONOR207 using the BP Clonase enzyme. The resulting entry clone was transferred into the binary destination vector pGWB540 using LR clonase enzyme. The cloned pGWB540 construct contains C-terminus EYFP. The final vector *promLTP:LTP::YFP* was transformed to *Agrobacterium tumefaciens* strains GV3101 (Rifampicin and gentamicin resistant) and transformed into *A. thaliana* as described in section 3.3.4.

4.8. CRISPR Cas-9 Editing method

Generation of *ltp2ltp5* double knock out *Arabidopsis* plants using the CRISPR-Cas9 technique

Selection of guide RNA

Single guide RNA (sgRNA) was generated within the first exonic region of LTP2 and LTP5 using (<http://www.genome.arizona.edu/crispr/CRISPRsearch.html>). The single guide RNA was selected with zero off target. For F/F0 primers, the 19-nt N was replaced with 19-nt target sequence in front of PAM (NGG). For R/R0 primers, the 19-nt N was replaced with reverse complement sequence of 19-nt target sequence in front of PAM (NGG) (see Table 6.1). The

schematic diagram in (Fig. 3.3) represent the assembly of DT1T2-PCR with Targets 1 and 2 for dicots.

Table 6.1: Primers design for two target DT1T2-PCR

| |
|---|
| sgRNA for LTP2, Target 1: 153/fw- GAGGTGCTCCACTTACCCA AGG |
| sgRNA for LTP5, Target 2: 154/Fw: GAGGCGGTTTCATTCCTAGA GGG |
| For 2 sgRNAs DT1T2-PCR |
| DT1-BsF ATATATGGTCTCGATTGNNNNNNNNNNNNNNNNNNNNNGTT |
| DT1-F0 TGNNNNNNNNNNNNNNNNNNNNGTTTTAGAGCTAGAAATAGC |
| DT2-R0 AACNNNNNNNNNNNNNNNNNNNNNCAATCTCTTAGTCGACTCTAC |
| DT2-BsR ATTATTGGTCTCGAAACNNNNNNNNNNNNNNNNNNNNNCAA |

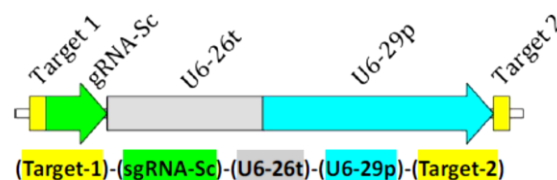


Fig. 3.3: Assembly of DTIT2-PCR. For the assembly of two sgRNA (Target1:LTP2 and Target2: LTP5) expression cassettes, we used DT1-BsF/DT1-F0/DT2-R0/DT2-BsR four-primer mixture with DT1-F0/DT2-R0 diluted to 20 times of DT1-BsF or DT2-BsR, resulting in DT1T2-PCR (Wang et al., 2015).

4.8.1. Cloning into pHEE401-2sgRNA

A 23-bp sequence in the first exon of LTP2 and LTP5 was chosen as the guide RNA for gene editing. This sequence was not conserved in the *Arabidopsis* LTPs and no off-target sites were found when this sequence followed by the four protospacer adjacent motif (PAM) sequences (GGG, AGG, TGG or CGG) was used as query in a nucleotide BLAST analysis of the *Arabidopsis* genome. Two single guide RNAs (sgRNAs) were used to target LTP2 and LTP5 gene, respectively. pCBC-DT1T2 vector and designed DT1 and DT2 primer set were used to amplify a single PCR fragment flanked by two sgRNA targets and two *BsaI* sites were incorporated by primers. After sequencing, the chimeric sgRNA, the PCR product was digested with *BsaI* and ligated with the *BsaI*-linearized binary vectors pHEE401E vector by performing golden gate reaction. The schematic diagram in (Fig. 3.4) represent the assembly of 2 sgRNA in the expression vector pHEE401E. The positive transformants was confirmed by colony PCR using U6-26p-FP and U6-29p-RP primers, and later confirmed by sanger sequencing using the primers U6-26p-FP and U6-29p-FP.

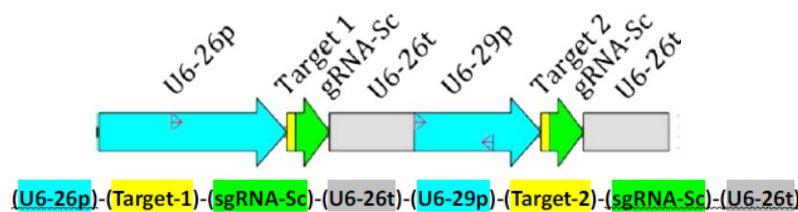


Fig. 3. 4: Schematic representation of two sgRNA expression cassette (DT1DT2-PCR + pHEE401)

Table 6.2: Set up for creating two sgRNA construct pCBC-DT1T2

| Component | Volume | Cycling conditions |
|-----------------------------------|------------|---|
| 10x KOD plus Buffer | 5 μ l | 1. One cycle: 94 °C, 2 min. 2. 30 cycles: 94 °C, 15 sec; 60 °C, 30 sec; 68 °C, 1 min. 3. One cycle: 68 °C, 5 min |
| MgSO ₄ (25mM) | 3 μ l | |
| dNTPs (2mM, Toyobo) | 4 μ l | |
| KOD plus (Toyobo) | 1 μ l | |
| pCBC-DT1T2 (diluted to 200 times) | 1 μ l | |
| DT1-BsF (20 μ M) | 1 μ l | |
| DT1-F0 (1 μ M) | 1 μ l | |
| DT2-R0 (1 μ M) | 1 μ l | |
| DT2-BsR (20 μ M) | 1 μ l | |
| ddH ₂ O | 32 μ l | |
| Total volume | 50 μ l | |

Golden Gate Reaction

| Component | Volume | Cycling conditions |
|---|-------------|--|
| Purified PCR fragments (~100 ng/ μ l) | 2 μ l | 5 hours at 37°C 5 min at 50°C 10 min at 80°C |
| pHEE401 (~100 ng/ μ l) | 2 μ l | |
| 10x T4 DNA Ligase Buffer (NEB) | 1.5 μ l | |
| 10x BSA | 1.5 μ l | |
| Bsal (NEB) | 1 μ l | |
| T4 DNA Ligase (HC, NEB) | 1 μ l | |
| ddH ₂ O | 6 μ l | |
| Total volume | 15 μ l | |

The final CRISPR/Cas9 binary vector pHEEE401E which includes an egg cell specific promoter (*EC1.2*), was used for the transformation of Col-0 wildtype plants. Hygromycin resistance plants of the T1 generation were tested for the insertion of the sgRNA-Cas9-T-DNA by PCR with primers LTP2-sgRNA-153 Fw and LTP5-sgRNA-154 Fw, respectively. Targeted gene mutations were detected by sequencing of these PCR products. Plants with an identified LTP2 and LTP5 double mutation were allowed to self-fertilize and homozygous plants in the T2 generation were detected by sequencing of LTP2 and LTP5 PCR products.

4.9. Sequencing

4.9.1. Sanger sequencing

All amplified PCR products and plasmids were verified by Sanger sequencing at Eurofins GATC Biotech, Cologne (www.eurofinsgenomics.eu). For this purpose, 5µl plasmid DNA solutions with a concentration between 80 to-120 ng/µl) were mixed with 5µl (5 µM) of gene-specific or sequencing primer in 1.5mL Eppendorf microcentrifuge tube and was sent to GATC for further analysis. The determined DNA sequences were then analyzed with the help of Geneious-R7 analysis program ([/www.geneious.com](http://www.geneious.com)).

4.9.2. Next generation sequencing

Based on sanger sequencing, four different double mutant transgenic lines (#P9-P2-P2, #P9-P3-P3, #P31-P2 and #P31-P3) were chosen for constructing next generation sequencing libraries following the manufacture's protocol (NEB Next Ultra II DNA kit). Sequencing was carried out 2x 150 nt HO NextSeq500 (1-2 Mio reads for all samples together) in Core Unit SysMed, IMIB, University of Wuerzburg. Data processing and statistical analysis was performed using CRISPresso computational tool (<http://crispresso.rocks/>).

5. RESULTS

5.1. Expression analysis of nsLTPs in *Arabidopsis thaliana*: Bioinformatic analysis

Plant non-specific lipid transfer proteins (*nsLTPs*) are characterized by low molecular weight (usually 6.5 to 10.5 kDa), a basic isoelectric point (pI; ranging usually from 8.5 to 12) and the occurrence of an eight-cysteine motif backbone (8 CM, C-X_n-C-X_n-CC-X_n-CXC-X_n-C-X_n-C). They are encoded by multigene family, with redundant property and possess physiological functions that remain largely unclear. Previous studies suggested that SCA (stigma/stylar Cys-rich adhesin) like *LTPs*, possess a function during plant fertilization (J., C., Mollet *et al.*, 2000). Likewise, CRPs are possibly associated with male-female interaction during fertilization such as pollen tube guidance, pollen tube reception, gamete fusion and are also involved in embryo-endosperm-seed communication (Huang *et al.*, 2015). To gain insight into the function of these enigmatic proteins a combination of expression profiling and bioinformatic analyses was performed to predict tissue-specific expression patterns that may be important for their function in the plant fertilization process.

Our first objective was to screen those candidate *LTPs* which are expressed in the male and female gametophyte of *Arabidopsis thaliana*. Toward this objective, we referred to the publication of Boutrot *et al.* (2008) which presented a genome-wide analysis of rice and *Arabidopsis* (*nsLtp*) gene families and focused our *in-silico* analysis on Type I and Type III *nsLTPs*. Members of the type I and III class of *nsLTP* are reported to express in reproductive tissue like stigma, pollen and seed, indicating their functional involvement in the fertilization process, primarily regulating pollen-pistil interactions, as well as endosperm and seed development (Wang *et al.*, 2012; Foster *et al.*, 1992). Using different public available microarray gene expression databases like (Genevisible from Geneinvestigator), Aramemnon, TAIR and *Arabidopsis* eFP Browser, we identified the expression profiles of Type I and Type III *nsLTPs* in reproductive tissues (male and female gametophyte) of *A. thaliana* (see Table 7.1).

| <i>nsLTP</i> | AGI Code | TAIR | BAR ePF | Genevisible |
|--------------|-----------|--------------------|----------------|-----------------|
| LTP1 | AT2G38540 | po, sy, st, sg | st | fl |
| LTP2 | AT2G38530 | pe, po, se, sg, em | se, sil | st |
| LTP3 | AT5G59320 | po, ov, st, se, sd | pe, st, sp, sd | ov, pi |
| LTP4 | AT5G59310 | em, po, st, sy | sd, sil, se | ped, se, sy, se |
| LTP5 | AT3G51600 | pe, em, st, sy | pe, em, st, sy | pe |
| LTP6 | AT3G08770 | em, po, ov, sy, st | po, sil, st | ov, pi, ca |
| LTP12 | AT3G51590 | an, st, sd | st, sd | po, an, at, spc |

| <i>nsLTP</i> | AGI Code | TAIR | BAR ePF | Genevisible |
|-----------------|-------------|--------------------|-----------------|----------------|
| PR-14 | AT4G08530 | pe, st | po, st | po |
| Pu-LTP (AtATA7) | AT4G28395 | po | po | spc, po |
| (PR-14) | AT5G01870 | se, st | po | em, ov |
| Pu-LTP | AT5G59330 | em, se | --- | sg, ca, ov |
| Pu-LTP | At1g48750.1 | po, st, em | st, sil, em | sg |
| Pu-LTP | At1g66850.1 | sd, se, st | st, sd | st, po |
| Pu-LTP | AT5G38160 | pt | sil, sd | end |
| Pu-LTP | At5g38170.1 | spc | sil, sd | em, end |
| Pu-LTP | At5g38180.1 | --- | sil, sd | em, end |
| Pu-LTP | At5g38195.1 | pr | sil, sd | em, end |
| Pu-LTP | At5g07230.1 | fl, sd | fl, sd | po, spc |
| Pu-LTP | At5g52160.1 | --- | fl | Po, end |
| Pu-LTP | At5g62080.1 | em, sd, st | fl | sg, st, po, fl |
| Pu-LTP (AtDIR1) | At5g48485.1 | po, sd, st, em, fl | po, st, sd, sil | pi, ov, pe |
| Pu-LTP (AtEND2) | At5g56480.1 | em, cc | po, sd, sil | ov, po, end |

Table 7.1: Comparative analysis of tissue-specific expression of nsLTPs using different gene expression databases. sg-stigma, sy-style, st-stamen, fu-funiculus, ov-ovules, po-pollen, an-anthers, pi-pistil, pt-pollen tube, pe-petals, se-sepals, sd-seeds, em-embryo sac, end-endosperm, fl- different floral developmental stages, spc-sperm cells, sil-siliques, an-anther, pe-petal, pr-primary root, ca-carpel. Pu-LTP: Putative LTP. TAIR, BAR ePF and Genevisible expression database were used for the comparative analysis. LTPs lacking information about their expression pattern in the databases were excluded from the analysis.

Upon critical analysis of the expression profiles from different databases, we narrowed down the number of candidates to seven members of Type I *nsLTPs* which were selected for further studies. The seven selected members from Type I *nsLTPs* were *LTP1* (AT2G38540), *LTP2* (AT2G38530), *LTP3* (AT5G59320), *LTP4* (AT5G59310), *LTP5* (AT3G51600), *LTP6* (AT3G08770) and *LTP12* (AT3G51590). In addition to the bioinformatic analysis, a survey of the literature suggested a dynamic overlapping expression profile in various tissues for the selected *LTPs*. The publication (Chae *et al.*, 2009) reported that *LTP1* (AT2G38540) and *LTP2* (AT2G38530) are expressed in stigma and style while *LTP4* (AT5G59310), *LTP5* (AT3G51600), *LTP6* (AT3G08770) and *LTP12* (AT3G51590) are expressed in the style region of the pistil. For *LTP5* (AT3G51600), expression was shown in pollen and the transmitting tract. *LTP3* (AT5G59320) and *LTP6* (AT3G08770) showed significant expression levels in ovules.

Taken together, the seven selected *LTPs* were either expressed in female gametophyte or male gametophyte, with most of them highly expressed in the styler region of the pistil. Furthermore, we checked the pistil specific expression of the candidate *LTPs* using GENEVESTIGATOR expression-data analysis tools (<https://genevestigator.com/gv/>). This analysis revealed high expression levels for all seven candidate *LTPs* in the stigma/style region of the pistil (Fig.4.1), which is suggestive for possible roles for these *LTP* genes in the female gametophyte function for pollen tube guidance mechanism in the transmitting tract and embryo-seed development.

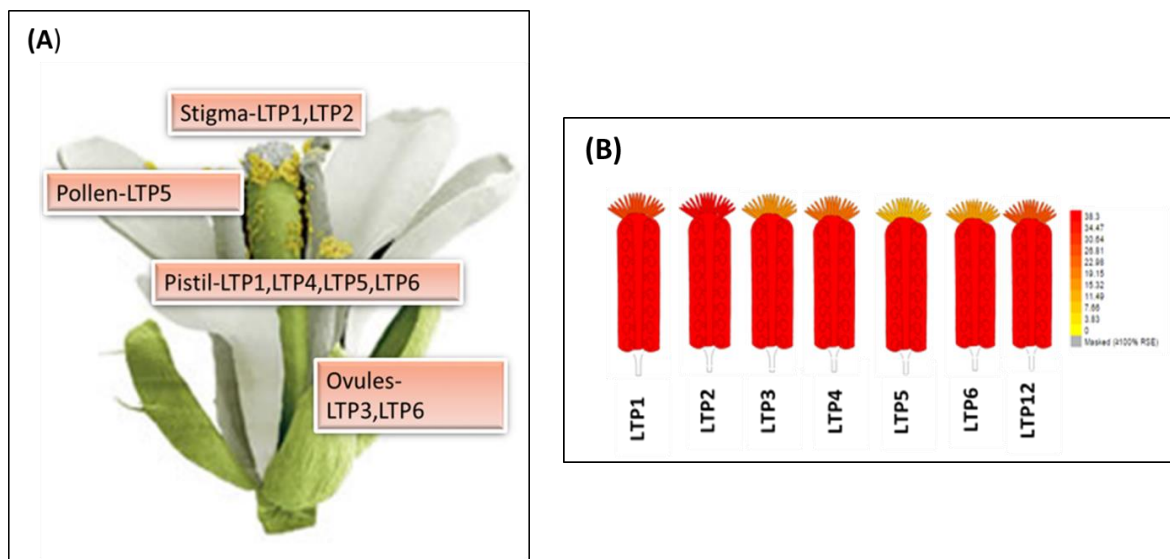


Fig. 4.1: A comprehensive analysis of LTP in *Arabidopsis* flower. (A) Schematic diagram representing the tissue-specific expression of individual LTPs in the different part of floral tissue. The representative diagram was prepared on the basis of *in-silico* gene expression analysis. **(B)** *Arabidopsis thaliana* gynoecium showing specific expression of 6 individual LTP. Expression Heat map was generated using Genevisible from Geneinvestigator.

5.2. Lipid Transfer Proteins are induced upon pollination

To follow the temporal expression of nsLTPs, flowering *Arabidopsis* plants were used to prepare pistils. Closed buds of stage 12 (Smyth *et al.*, 1990) were dissected carefully using sharp forceps to remove the androecium, petals and sepals. The naked pistils were allowed to grow for one day under controlled long day conditions. After one day, the grown pistils were hand pollinated with fresh pollen and after 24hrs the pollinated pistils were harvested. For the non-pollinated samples, the emasculated pistils were harvested one day after preparation from the closed buds (Fig. 4.2).

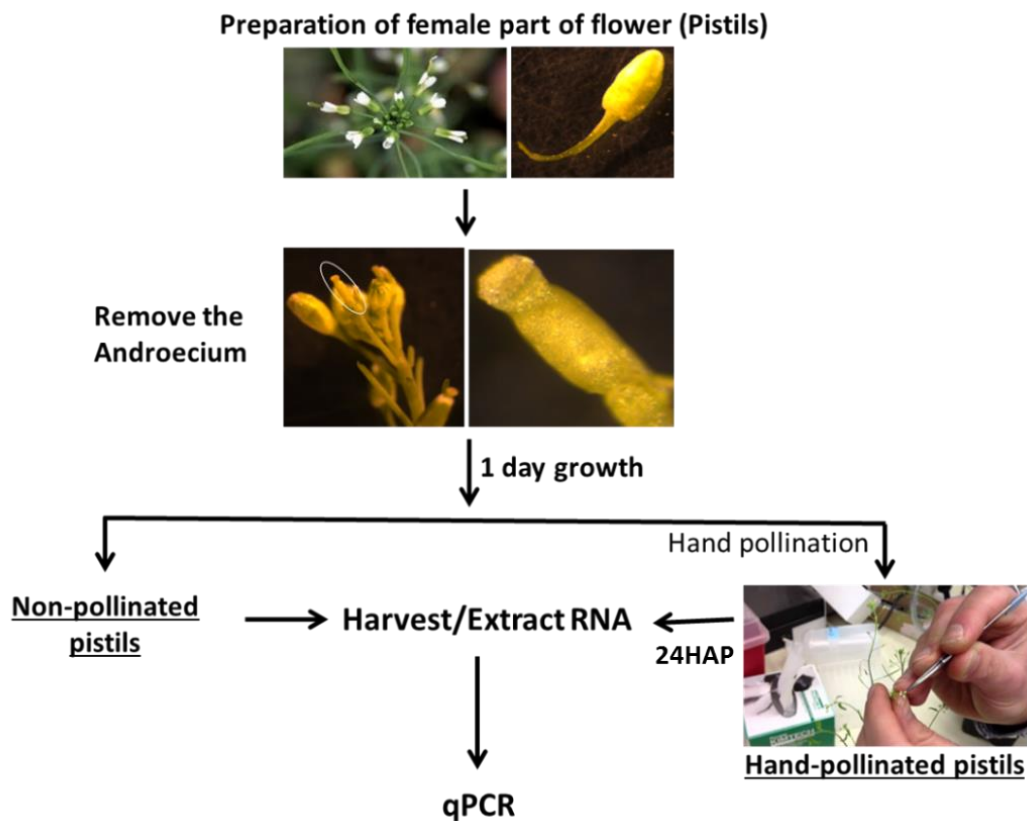


Fig. 4.2: Schematic representation depicting sample preparation and harvest of the pollinated and non-pollinated pistils from the flowers of *Arabidopsis thaliana*.

5.2.1. *LTPs* are induced upon pollination in *Arabidopsis thaliana*

In compatible pollination, pollen hydration, germination and penetration of the stigma by pollen tubes are all influenced by the exudate on wet stigma and by the pollen coat secretions in species with dry stigma (Verhoeven *et al.*, 2005). The exudate consists of a complex mixture consisting mainly of lipids, proteins and saccharides (Konar and Linskens, 1966; Cresti *et al.*, 2006). High-throughput RNA-seq analysis of ovules before and after fertilization revealed that hundreds of CRP genes were up-regulated within hours or a few days after pollination, representing a major cluster of genes specifically expressed in the female gametophyte during fertilization, pollen-tube growth, ovule maturation and early seed development in *Arabidopsis* (Huang, Dresselhaus, Gu and L., J., Qu, 2015; Ingram and Gutierrez-Marcos, 2015; Costa *et al.*, 2014). Therefore, we aimed to check the expression of selected *LTPs* (*LTP1*, *LTP2*, *LTP3*, *LTP4*, *LTP5*, *LTP6* and *LTP12*) comparing pollinated and non-pollinated pistil samples. Using qPCR, we observed that all *LTPs* were highly expressed in pistils. For pollinated pistils there was a significant increase in the expression of *LTP1*, *LTP2*, *LTP3*, *LTP4*, *LTP5* and *LTP6* in comparison to the non-pollinated pistils (Fig. 4.3) while *LTP12* represented an exception and

was downregulated. These results suggested that many of the *LTPs* may play a regulatory role during pollination.

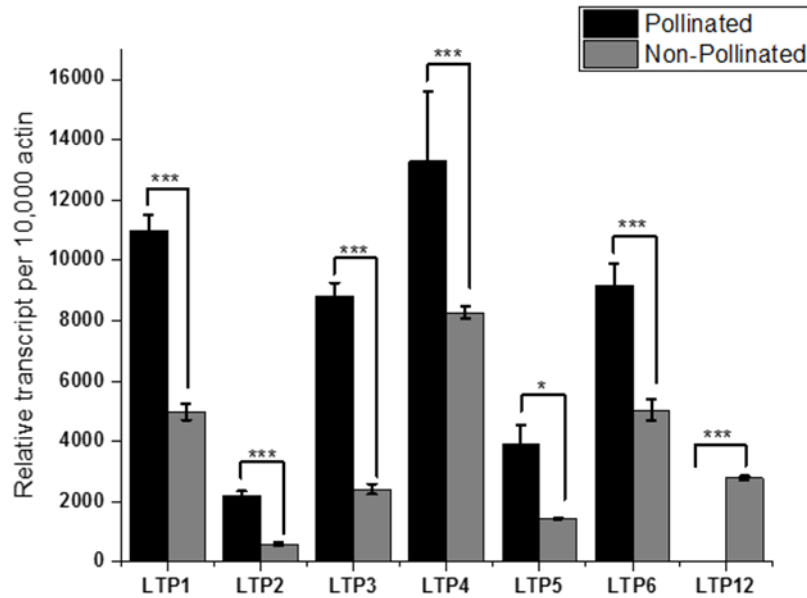
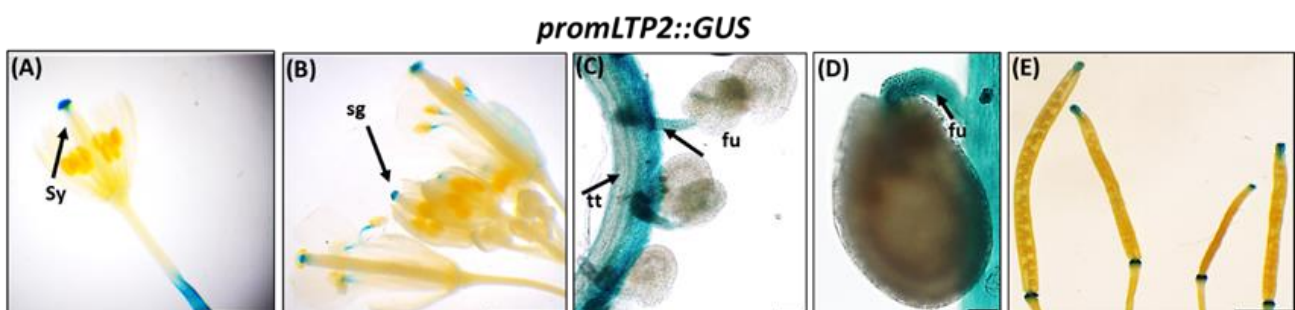


Fig. 4.3: Transcriptional regulation of *LTPs* upon pollination. *LTPs* (*LTP1*, *LTP2*, *LTP3*, *LTP4*, *LTP5*, *LTP6* and *LTP12*) gene expression relative to *AtACT2/AtACT8* gene analyzed by qRT-PCR comparing pollinated (black bars) and non-pollinated (grey bars) pistils of *Arabidopsis* (WT, Col-0). Three independent biological replicates were used for each treatment. Error bars represent standard deviations. Asterisks indicate significance *** $P < 0.001$; ** $P < 0.01$; * $P < 0.05$; differences in pollinated pistils compared to non-pollinated pistils.

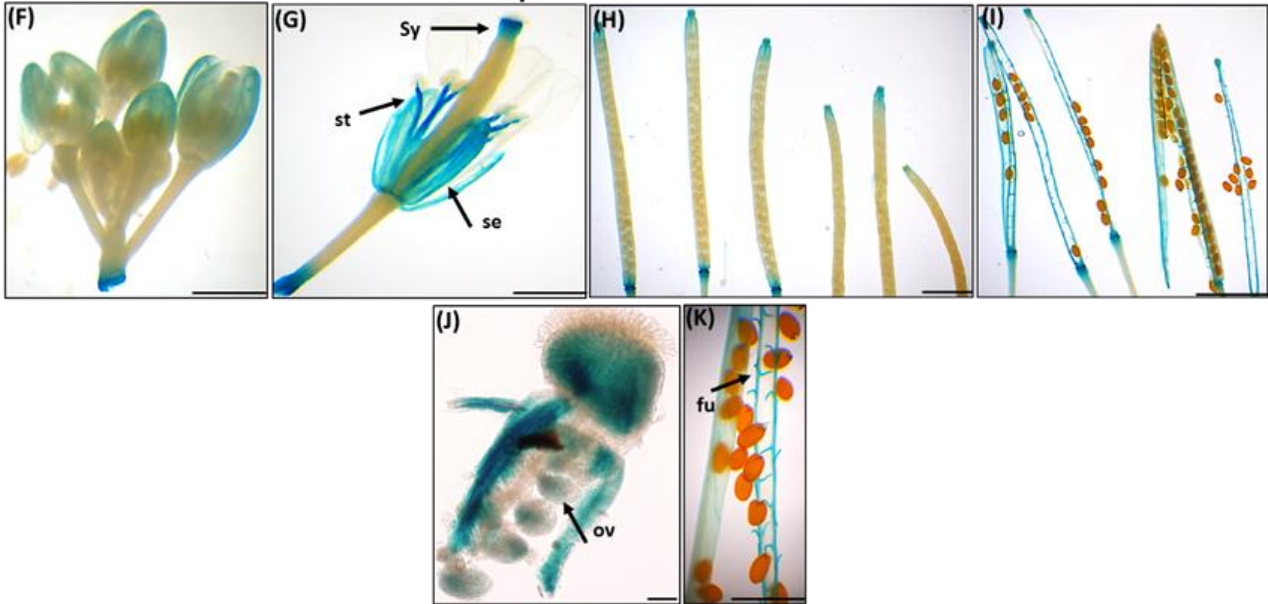
5.3. Tissue-specific expression patterns of *LTPs* in *Arabidopsis* flowers

To study the tissue-specific expression of *LTP2*, *LTP3*, *LTP4*, *LTP5*, *LTP6* and *LTP12*, their respective promoter regions (2000bp) were used to create a transcriptional fusion construct with the *uidA* (*GUS*) reporter gene. Stable *Arabidopsis* transformants were obtained using *A. tumefaciens*-mediated transformation and selection on MS plates with hygromycin. Subsequently, several stable transformed *Arabidopsis PromLTP::GUS* transgenic lines obtained at the T2 generation were further analyzed for tissue-specific gene expression in developing seedlings, flowers and in vegetative tissues.

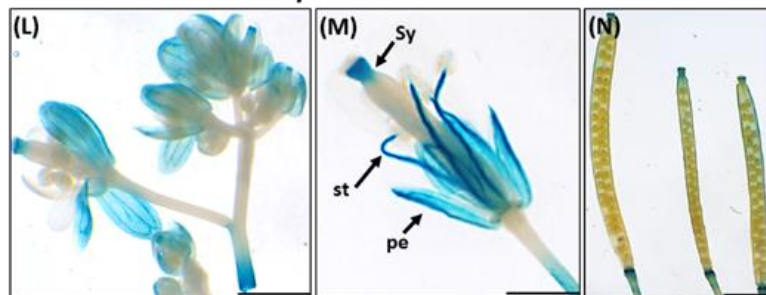
GUS expression driven by the *LTP2* promoter was detected in style, stigma, funiculus, transmitting tract and receptacle of the mature silique (Fig.4.4 A-E). However, *LTP3* expression was found in the style, anther filaments, sepals, ovules and in funiculus (Fig.4.4 F-K). *LTP4* was expressed in style, sepals and in the mature siliques (Fig.4.4 L-N), while *LTP5* was expressed in almost all floral tissues. Its expression was also found in the stigmas of young buds and mature flowers, style, anther, anther filaments, funiculus and low expression in pollen, pollen tube, ovules and transmitting tract (Fig.4.4 O-U). It should be noted, that the weak expression of *LTP5* in pollen and pollen tube developed after 3 days of *GUS* reaction (Fig.4.4 R). For *LTP6*, gene expression was found in style, anther filaments and sepals (Fig.4.4 V-X). *LTP12* was expressed in sepals, style and anther filaments (Fig.4.4 Y-Z). Taken together, the results obtained from *GUS* reporter analysis indicated a redundant overlapping pattern of expression for the selected *LTP* genes in various parts of floral tissue with a certain level of diversity. Almost all the selected *LTPs* showed high levels of expression in the pistil specifically in the style. In the siliques, *LTP2*, *LTP3* and *LTP5* were expressed in the funiculus, which has a function in guiding the pollen tube to reach the micropyle during the fertilization process.



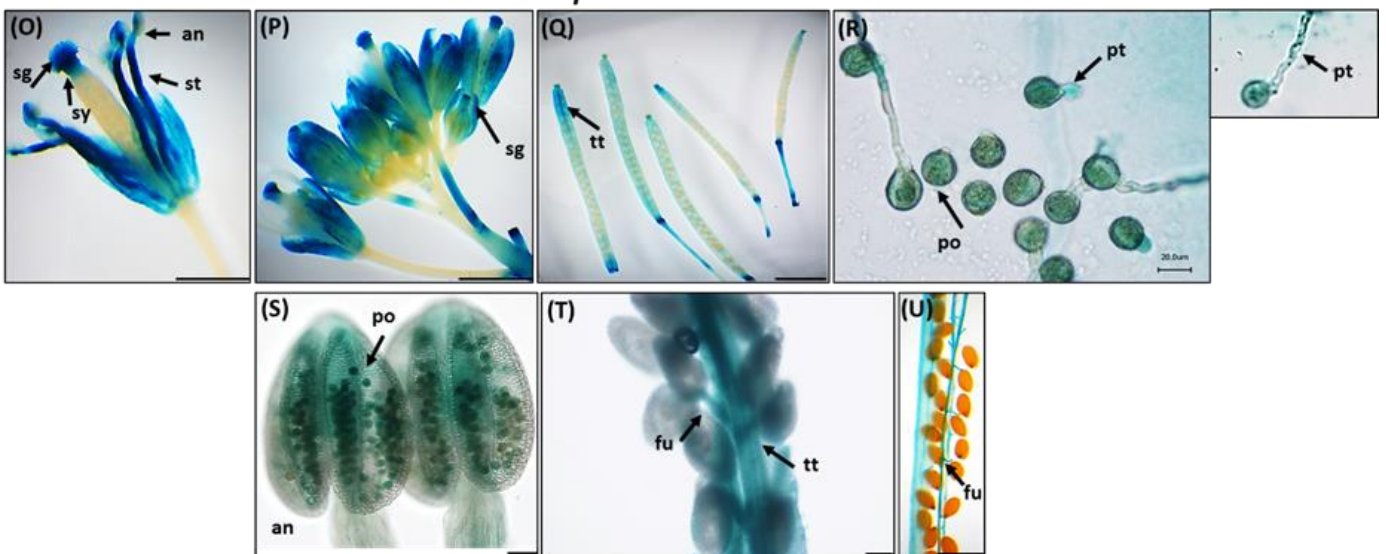
promLTP3::GUS



promLTP4::GUS



promLTP5::GUS



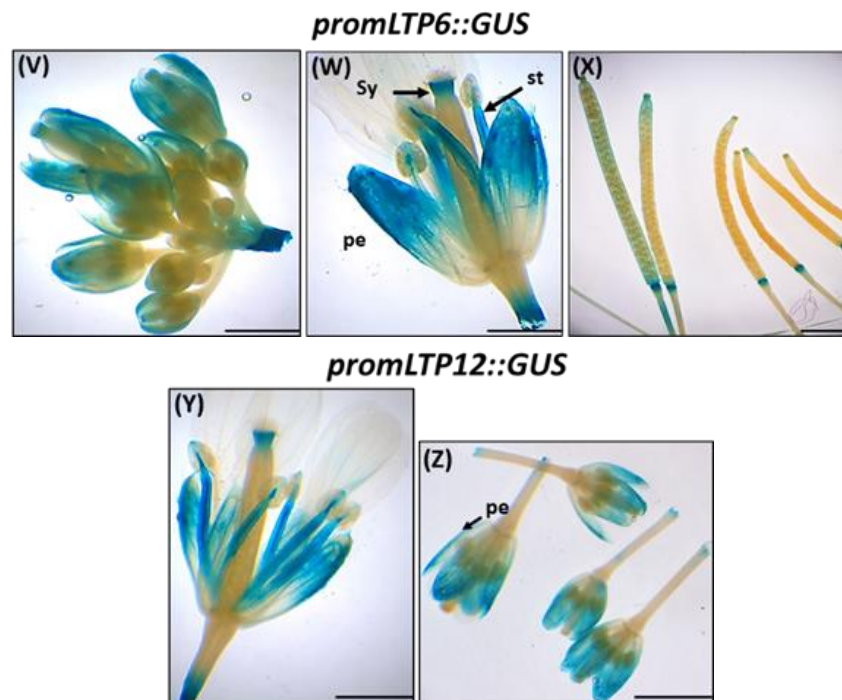


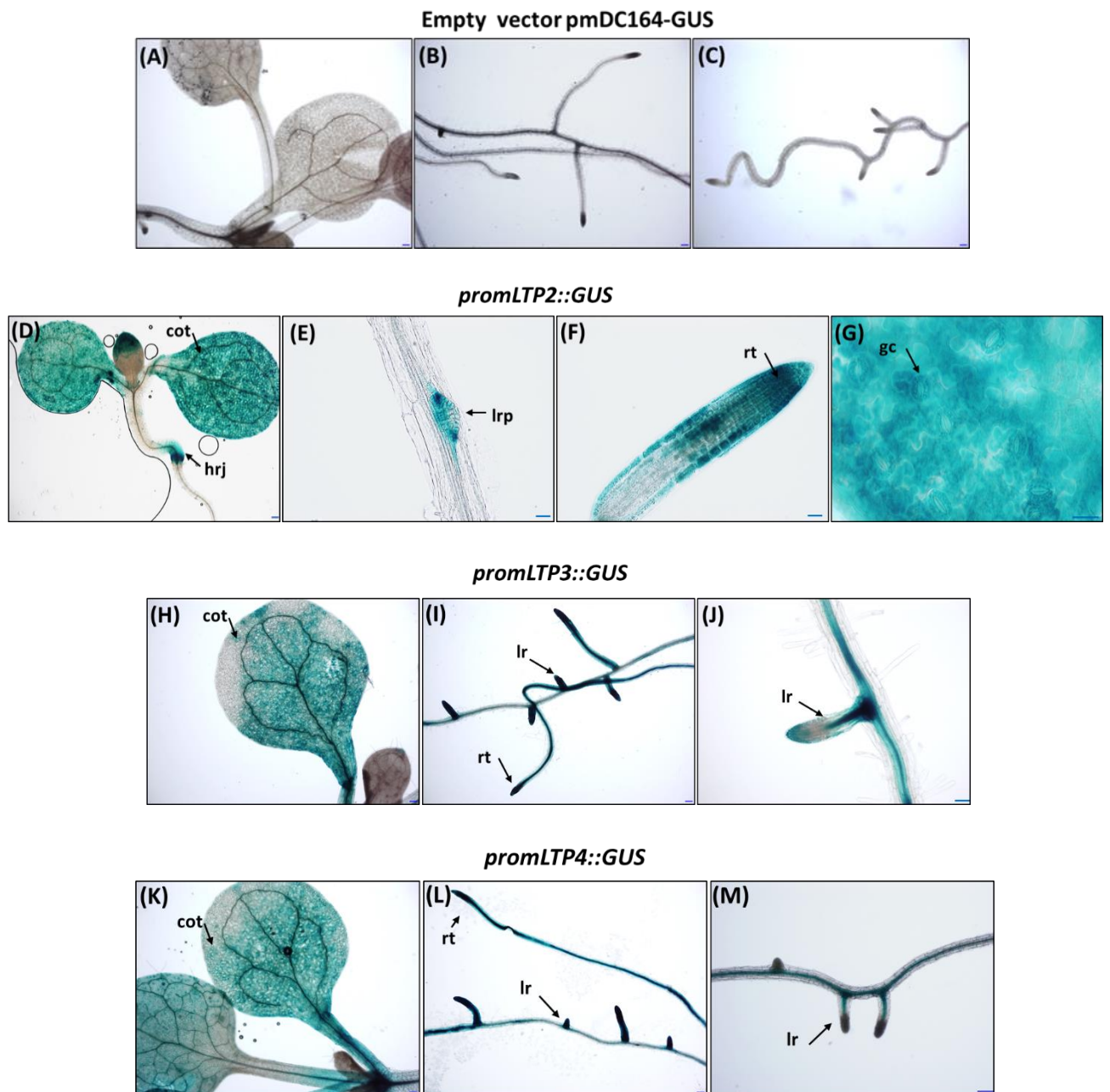
Fig. 4.4: GUS expression of 6 LTPs in the floral and reproductive tissue of *A. thaliana*. (A-E) LTP2 gene expression in the style, stigma, funiculus, transmitting tract, petiole and immature siliques. (F-K) LTP3 gene expression in the style, sepals, anther filaments, ovules, funiculus, mature and immature siliques. (L-N) LTP4 gene expression in the style, anther filament, sepals, petals, petioles and immature siliques. (O-U) LTP5 gene expression in the pollen, pollen tube, anther, anther filament, funiculus, stigma, style, transmitting tract, mature and immature siliques. (V-X) LTP6 gene expression in the style, anther filaments, petals, petioles and mature and immature siliques. (Y-Z) LTP12 gene expression in the style, anther filaments, petals and mature siliques. Plants were grown under long-day condition (16hrs light/ 8hrs Dark). GUS signals were developed for 2:30 hrs. **sg**-sigma, **sy**-style, **st**-stamen, **fu**-funiculus, **tt**-transmitting tract, **ov**-ovules, **po**-pollen, **an**-anthers, **pt**-pollen tube, **pe**-petals, **se**-sepals. Scale: 2mm, (C, D, E, K, T, U: 50 μ m), (S :20 μ m)

5.3.1. Expression patterns of LTPs during vegetative seedling growth in *Arabidopsis thaliana*

To understand the transcription patterns of *LTP2*, *LTP3*, *LTP4*, *LTP5*, *LTP6* and *LTP12* genes during vegetative growth, homozygous *PromLTP::GUS Arabidopsis* seedlings were grown in MS-agar plates under normal plant growth conditions and stained for GUS enzymatic activity at 10 days after germination.

LTP2 expression was present in the cotyledons, the hypocotyl-root junctions (Fig. 4.5D), initiation site of lateral root primordias (Fig. 4.5E), the root tips and in guard cells (Fig. 4.5 F, G). For *LTP3* and *LTP4*, a high level of gene-expression was found in the apical meristem

region, the primary root tips and lateral root initiation sites (Fig. 4.5 H-J, Fig. 4.5 K-M). *LTP5* expression was similar to that of *LTP2* in the cotyledons, the hypocotyl-root junctions, the primary root tips, lateral root primordias and in guard cells (Fig. 4.5 N-Q). Finally, *LTP6* and *LTP12* expression was also observed in cotyledons and lateral root initiation sites but it was not found in the root tips (Fig. 4.5 R-S, Fig. 4.5 T-U). However, no GUS signal (Fig. 4.5 A-C) was found in the seedlings transformed with pmDC164-GUS empty vector (the control). In the developing root system, for all examined nsLTP genes, GUS staining was present throughout most of the root tissue with overlapping expression pattern.



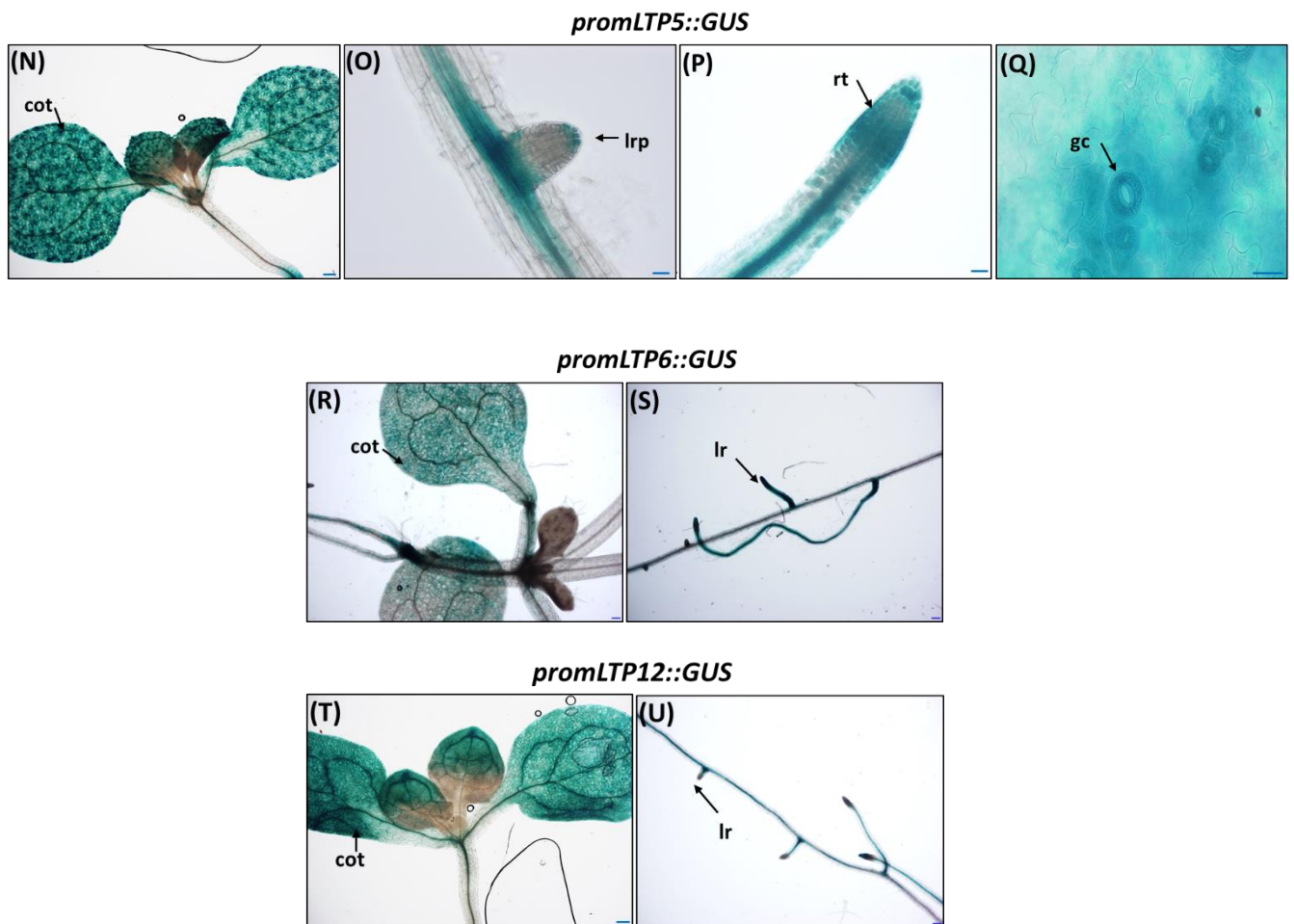
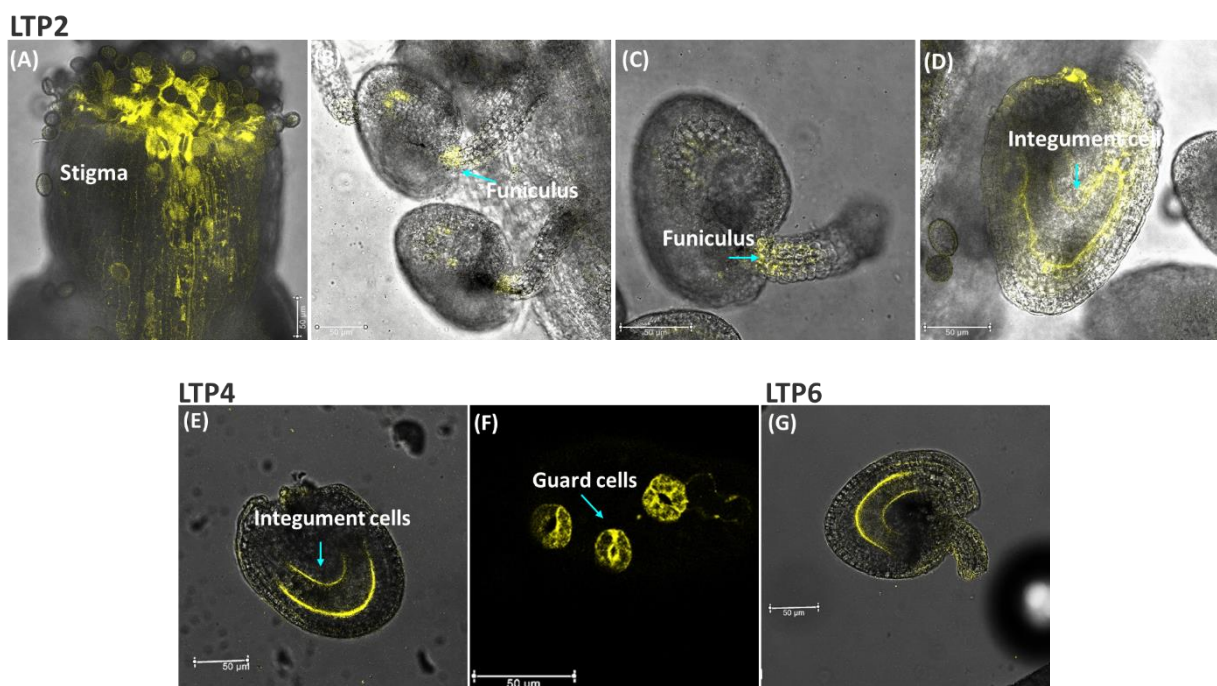


Fig. 4.5: GUS expression of LTP2, LTP3, LTP4, LTP5, LTP6 and LTP12 in 10 days old *Arabidopsis* seedling. Histochemical localization of GUS activity in PromLTP::GUS plants. (A-C) control, (D-G) GUS activity under LTP2 promoter was observed in the cotyledon, emerging lateral root primordia, primary root tip, vascular bundles and in the guard cells. (H-J) PromLTP3::GUS and (K-M) PromLTP4::GUS expression was observed in the cotyledon, root tip emerging and mature lateral root. (N-Q) PromLTP5::GUS expression was localized in the cotyledon, emerging lateral root primordia, primary root tip and in the guard cells. (R-S) PromLTP6::GUS and (T-U) PromLTP12::GUS expression was also detected in the cotyledon and lateral root. Plants were grown under long-day condition (16hrs light/ 8hrs Dark). GUS signals were developed for 2:30 hrs. cot: cotyledons, hrj: hypocotyl-root junction, lrp: lateral root primordia, rt: root tip, gc: guard cells, lr: lateral root. Scale: 50 μ m, (G, Q): 20 μ m).

5.4. Localization of LTPs during the ovule development in *Arabidopsis thaliana*

To determine LTP expression at the protein level, we utilized the fluorescent tagging of full-length proteins to generate translational LTP fusions. For this purpose, C-terminal YFP fusion constructs (*ProLTP:LTP-YFP*) were generated to establish stable transgenic *Arabidopsis* plants expressing the LTP-YFP fusion under control of the respective LTP promoter. Plants homozygous for the transgene from T2 generation were used to study the LTP protein localization. Using confocal imaging, fusions for LTP2 were detected faintly in the stigma, funiculus and integument cells of *Arabidopsis* ovules (Fig. 4.6 A-D). LTP3 showed a wide spectrum of expression in the embryos, integument cells and funiculus of the ovules (Fig. 4.6 H-J). A strong fluorescent signal was also detected in the outer integument cells of the seed coats (Fig. 6M). At seedling stage LTP3 expression was detected in the endodermis and lateral root primordias (Fig. 4.6 K, L). LTP4 (Fig. 4.6E) LTP5 (Fig. 4.6N) and LTP6 (Fig. 4.6G) were also detected in the integument cells of *Arabidopsis* ovules. In addition, weak YFP fluorescence was observed in *ProLTP:LTP5-YFP* pollen (Fig. 4.6O) and at the seedling stage LTP5 expression was also detected in the root tips (Fig. 4.6P) and root hairs (Fig. 4.6Q).



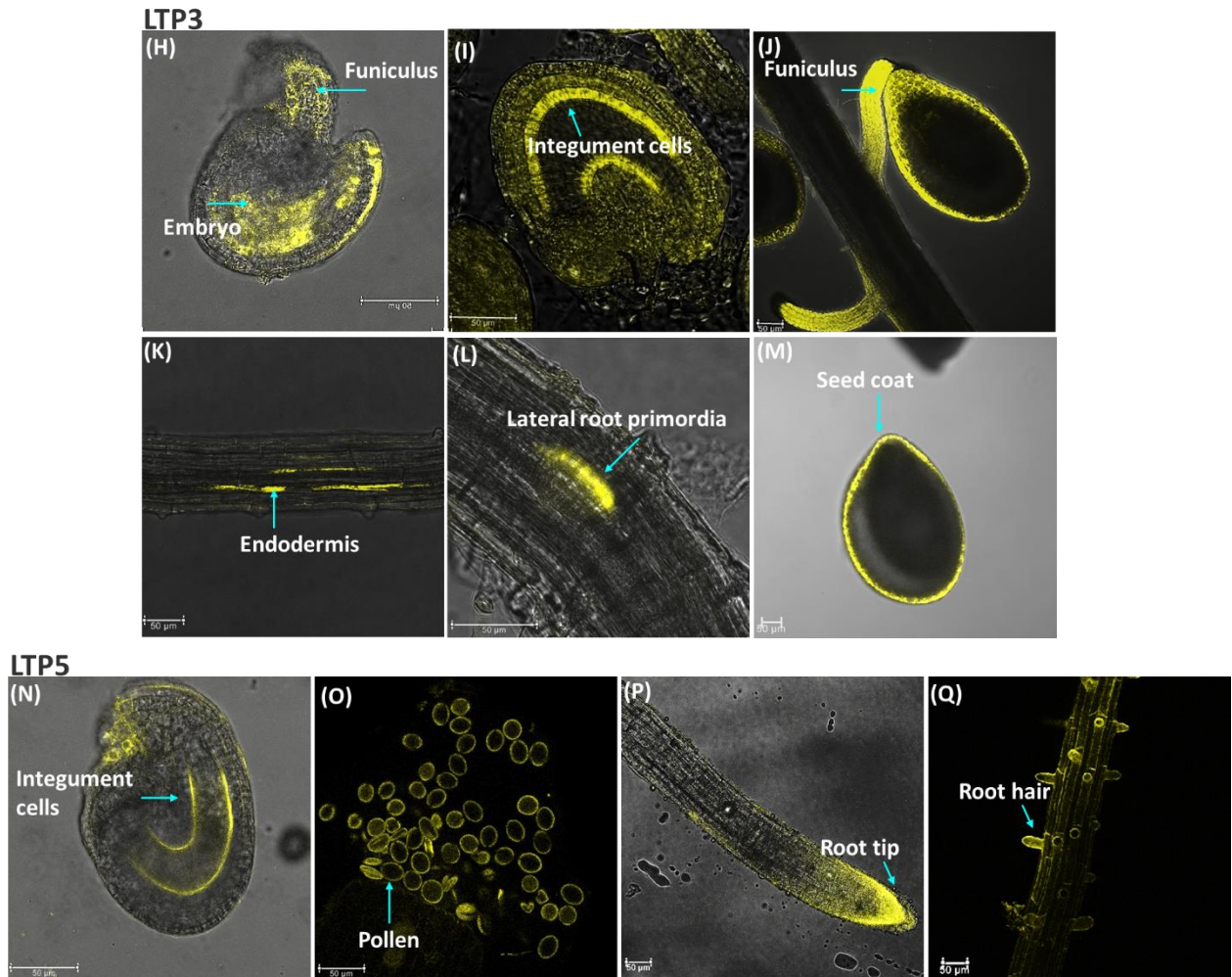


Fig. 4.6: Sub-cellular localization of LTP2, LTP3, LTP4, LTP5 and LTP6 protein in *Arabidopsis* ovule and seedling. (A-D) Low-expression of ProLTP2:LTP2-YFP in the stigma, funiculus and integument cells of ovules. **(E, F)** ProLTP4:LTP4-YFP expression was detected in the integument cells and guard cells. **(G)** ProLTP6:LTP6-YFP was expressed in integument cells of ovules. **(H-M)** ProLTP3:LTP3-YFP expression was localized in the embryo, integument cells, funiculus, endodermis, lateral root primordia and in the seed coat. **(N-Q)** ProLTP5:LTP5-YFP was expressed in integument cells, pollen, root tip and root hair, Scale=50µm.

5.5. Protein subcellular localization of LTPs

5.5.1. Subcellular localization of 6 LTP protein from *Arabidopsis*

In-silico predictions by several analysis programs suggest that lipid transfer proteins harbor an N-terminal signal peptide, which would target LTP proteins to the extracellular compartment of the cell. In order to get a better resolution regarding the localization of LTP proteins at the sub-cellular level, we performed *Agrobacteria* mediated transient expression of LTP-YFP fusion proteins in *Nicotiana benthamiana*. To overcome the artifact due to the overexpression of transgene under the constitutive promoter CaMV 35S, we also analyzed the localization pattern of some of the LTPs using the endogenous native promoter. LTP2, LTP5 and LTP12 (Fig. 4.7A) cloned under constitutive promoter CaMV 35S (Fig. 4.7B) and LTP3, LTP4 and LTP6 cloned under their native promoters were used for the subcellular localization study using transient *Agrobacterium*-mediated gene expression.

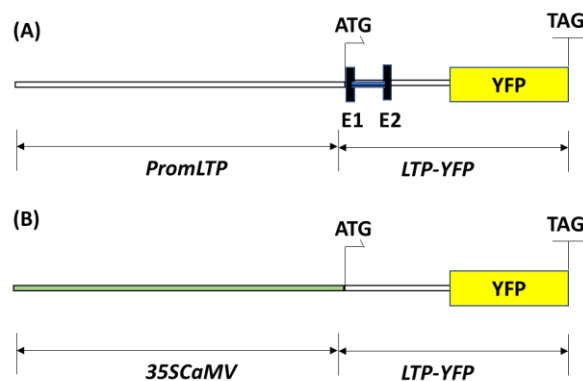


Fig. 4.7: Schematic representation of fusion constructs (A) Diagram of *ProLTP:LTP-YFP* in which the YFP is placed toward the C-terminal portion of the LTP protein and the LTP-YFP is expressed under the LTP promoter (*ProLTP*, open rectangle). Filled black rectangles and blue rectangle refer to exons and introns respectively, in the LTP gene. E1, exon1; E2, exon2; ATG and TAG, the start and stop codons, respectively in LTP. **(B)** Diagram of *35S::LTP-YFP*, full-length LTP cDNA was cloned under the constitutive 35SCaMV promoter sequence. Filled green rectangle refer to 35SCaMV promoter.

For localization studies, *promLTP::LTP-YFP* and *35S::LTP-YFP* constructs were co-infiltrated with either the cell wall marker *35S::LTP1-mCherry* (Deeken *et al.*, 2016) or the plasma membrane marker *35S::DsRED-REMORIN1.3* (Bozkurt *et al.*, 2014), into *Nicotiana benthamiana* leaves. Due to the inadequate resolution of the microscope, a clear distinction between plasma membrane and cell wall was not possible. Transiently expressed LTP-YFP fusion proteins in epidermal cells were examined by confocal laser scanning microscopy. In order to allow for a better resolution of plasma membrane and cell wall fluorescence, additional plasmolysis experiments were performed and finally, LTPs were grouped based on their localization patterns.

5.5.2. Subcellular localization of LTP2, LTP5 and LTP6

To determine the subcellular localization of LTP2, LTP5 and LTP6, respective *LTP::YFP* constructs were transiently expressed in *Nicotiana benthamiana* epidermal cells. To facilitate the assessment of its localization an apoplastic marker (*LTP1::mCherry*) (Fig. 4.8 - Fig. 4.10 D-E) and plasma membrane marker (*DsRED::REM*) (Fig. 4.8 - Fig. 4.10 F-G) were co-infiltrated. Epidermal cells infiltrated with *LTP2::YFP*, *LTP5::YFP* and *LTP6::YFP* showed similar patterns of expression in fluorescence associated with the cell periphery, at the nucleus, in the tubular ER networks as well as in granular bodies associated with tubular ER. Co-expression of *LTP2::YFP*, *LTP5::YFP* and *LTP6::YFP* with the apoplastic marker *LTP1::mCherry* clearly showed that the YFP signal was localized in the cell periphery and co-localizes with the mCherry signal (Fig.4.8-Fig. 4.10 D). To overcome the difficulty of appropriate resolution, plasmolysis was induced by adding 0.5M KNO_3 to the leaf tissue, allowing the distinction between the peripheral fluorescence of the LTP-YFP fusion protein and the cell-wall marker *LTP1::mCherry*. Upon plasmolysis, both YFP and mCherry fluorescence were perfectly co-localized in the apoplast as *LTP2::YFP*, *LTP5::YFP* and *LTP6::YFP* appeared in the apoplastic space in the plasmolyzed cells, indicating that LTP2, LTP5 and LTP6 are indeed localized to the apoplast (Fig. 4.8 - Fig. 4.10 E, H).

Similar further co-expression experiments were performed with *LTP2::YFP*, *LTP5::YFP*, *LTP6::YFP* and the plasma membrane marker *DsRED::REM*. In this case, YFP fluorescence also co-localized with the DsRED signal in the plasma membrane (Fig. 4.8 – Fig. 4.10 F) and upon plasmolysis the signal was found in the Hechtian strands (Fig. 4.8 - Fig. 4.10 F). To determine a possible co-localization of LTP2, LTP5 and LTP6 with both, the apoplastic marker *LTP1::mCherry* and the plasma membrane marker *DsRED::REM*, Pearson coefficients were calculated for plasmolyzed and non-plasmolyzed cells. In selected areas, for each LTP in combination with either *LTP1::mCherry* or *DsRED::REM*, the Pearson coefficients were approximately 0.9 (Fig. 4.8 – Fig. 4.10 I). Thus, the present data suggests a dual sub-cellular localization of LTP2, LTP5 and LTP6 at the plasma membrane as well as extracellularly, in the apoplastic space.

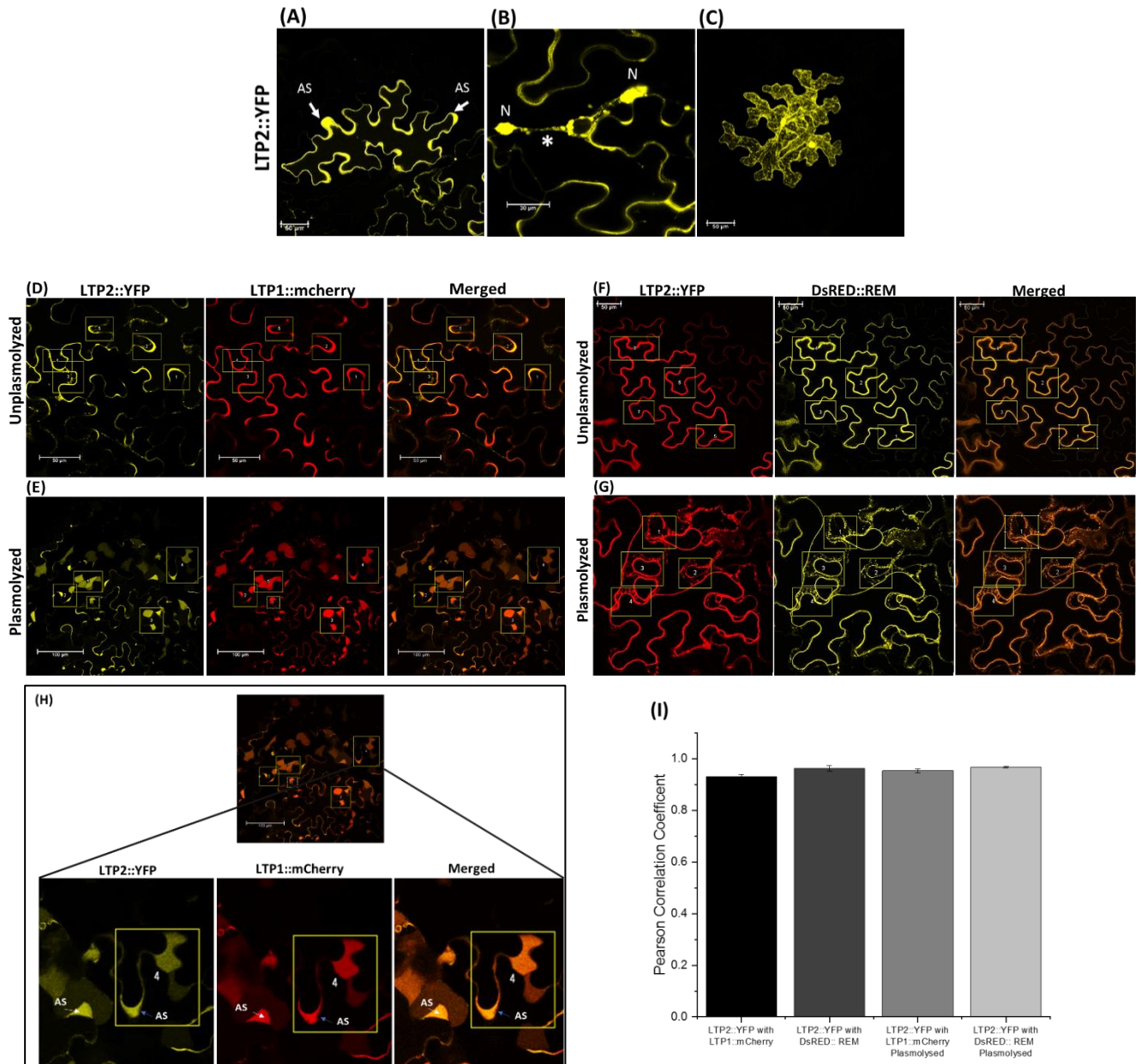


Fig. 4.8: Sub-cellular localization of LTP2 fused to YFP in *N. benthamiana* epidermal cells imaged 4 days post infiltration. (A) LTP2::YFP localizes to cell wall, **(B)** in apoplastic space (AS, indicated by bold arrow) **(C)** in ER network. **(D)** Co-expression of the two-fusion proteins LTP2::YFP and cell wall marker LTP1::mCherry. **(E)** Plasmolysis after co-infiltration of LTP2::YFP and cell wall marker LTP1::mCherry **(F)** Coexpression of the two fusion proteins LTP2::YFP and plasma membrane marker DsRED::REM. **(G)** Plasmolysis after co-infiltration of LTP2::YFP and plasma membrane marker DsRED::REM. **(H)** Zoom-in image depicting co-localization of LTP2::YFP with LTP1::mCherry in the apoplastic space (AS) of the plasmolyzed cell. **(I)** The average Pearson correlation coefficients \pm SEM calculated from 4 randomly selected ROI in each group, $n=3$. Each selected ROI is marked in yellow box and labelled, respectively. mCherry (Excitation: 561 nm, Emission: 580–615 nm; mVenus (Excitation: 514 nm, Emission: 530–555 nm); DsRED (Excitation: 561 nm, Emission: 560–600 nm). Cells were plasmolyzed with 0.5M KNO_3 and documented after 5mins of incubation. The image (C) was reconstructed by superposition of series of confocal optical sections. Scale: 50 μ m.

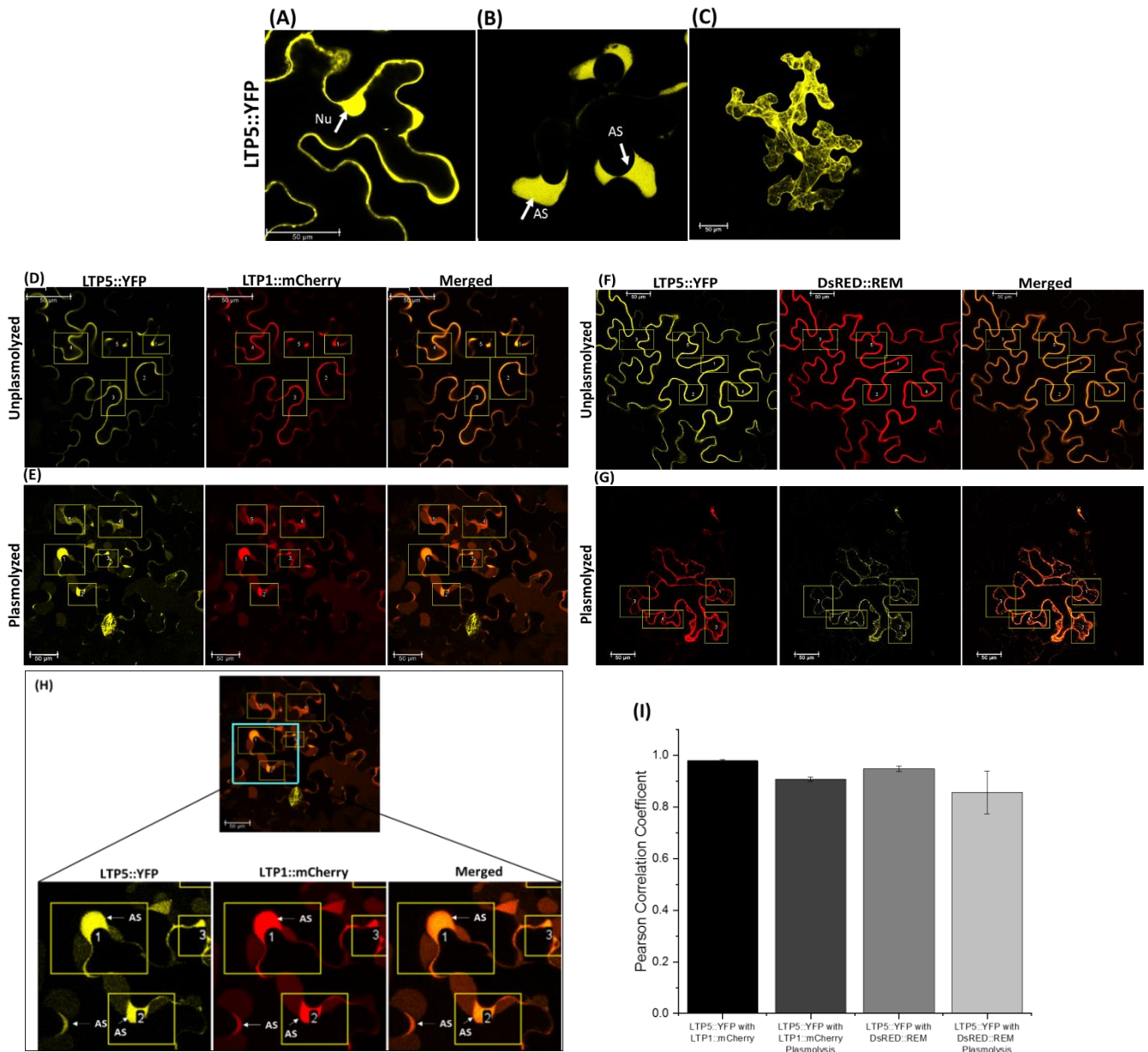


Fig. 4. 9: Sub-cellular localization of LTP5 fused to YFP in *N. benthamiana* epidermal cells imaged 4 days post infiltration. (A) LTP5::YFP localizes to cytoplasm, cell periphery and nucleus (indicated by bold arrow), (B) apoplast region (marked as AS), (C) in ER network. (D) Co-expression of the two-fusion proteins LTP5::YFP and cell wall marker LTP1::mCherry. (E) Plasmolysis after co-infiltration of LTP5::YFP and cell wall marker LTP1::mCherry.(F) Coexpression of the two fusion proteins LTP5::YFP and plasma membrane marker DsRED::REM. (G) Plasmolysis after co-infiltration of LTP5::YFP and plasma membrane marker DsRED::REM. (H) Zoom-in image depicting co-localization of LTP5::YFP with LTP1::mCherry in the apoplastic space (AS) of the plasmolyzed cell. (I) The average Pearson correlation coefficients \pm SEM calculated from 4 randomly selected ROI in each group, n=3. Each selected ROI is marked in yellow box and labelled, respectively. mCherry (Excitation: 561 nm, Emission: 580–615 nm; mVenus (Excitation: 514 nm, Emission: 530–555 nm); DsRED (Excitation: 561 nm, Emission: 560-600 nm). Cells were plasmolyzed with 0.5M KNO_3 and documented after 5mins of incubation. The image (C) is reconstructed by superposition of series of confocal optical sections.

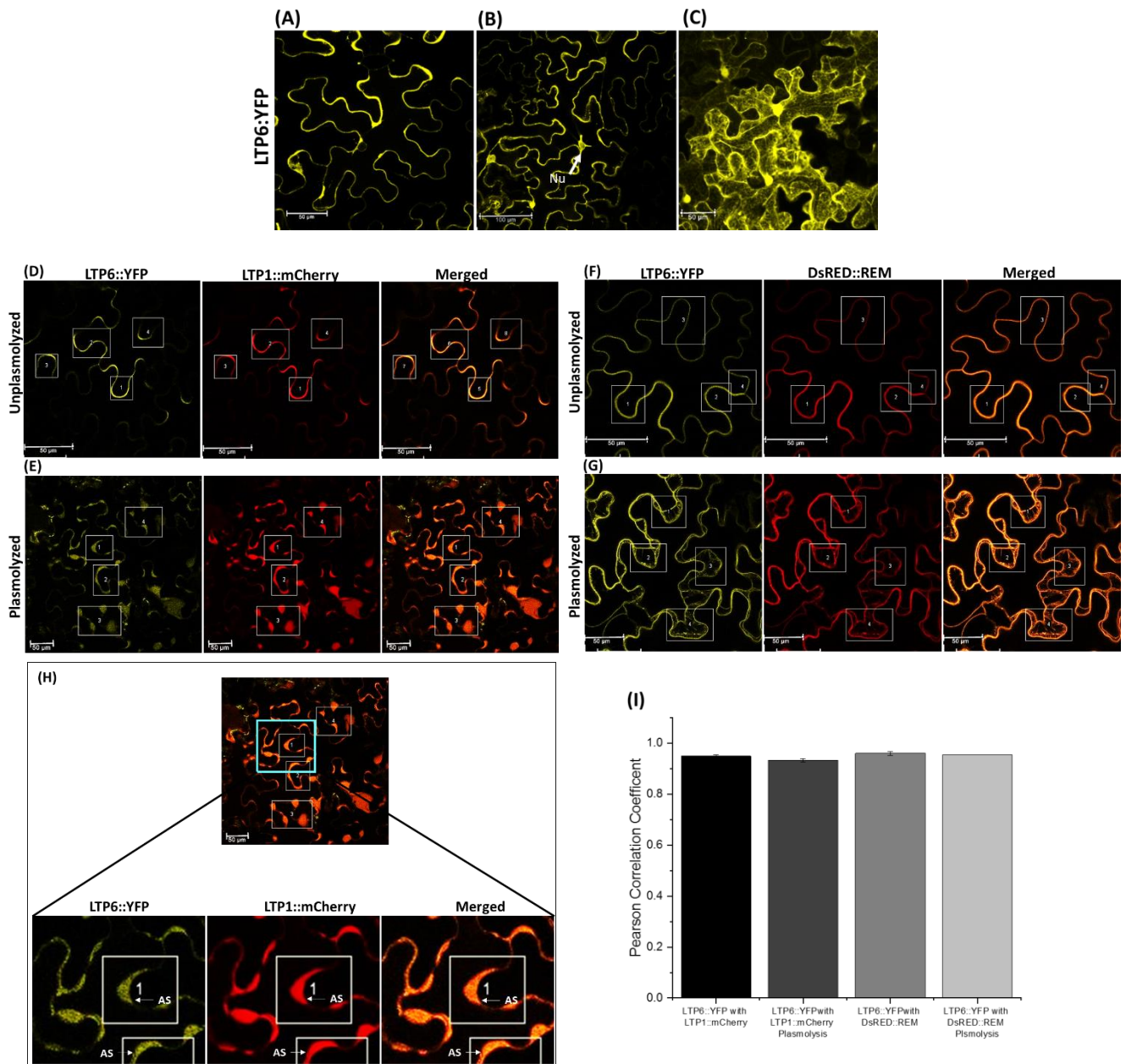


Fig. 4.10: Sub-cellular localization of LTP6 fused to YFP in *N. benthamiana* epidermal cells imaged 4 days post infiltration. (A-B) LTP6::YFP localizes to cytoplasm, cell periphery and nucleus (indicated by bold arrow), **(C)** in ER network. **(D)** Co-expression of the two-fusion proteins LTP6::YFP and cell wall marker LTP1::mCherry. **(E)** Plasmolysis after co-infiltration of LTP6::YFP and cell wall marker LTP1::mCherry. **(F)** Coexpression of the two-fusion proteins LTP6::YFP and plasma membrane marker DsRED::REM. **(G)** Plasmolysis after co-infiltration of LTP6::YFP and plasma membrane marker DsRED::REM. **(H)** Zoom-in image depicting co-localization of LTP5::YFP with LTP1::mCherry in the apoplastic space (AS) of the plasmolyzed cell. **(I)** The average Pearson correlation coefficients \pm SEM calculated from 4 randomly selected ROI in each group, $n=3$. Each selected ROI is marked in yellow box and labelled, respectively. mCherry (Excitation: 561 nm, Emission: 580–615 nm; mVenus (Excitation: 514 nm, Emission: 530–555 nm); DsRED (Excitation: 561 nm, Emission: 560–600 nm). Cells were plasmolyzed with 0.5M KNO₃ and documented after 5mins of incubation. The image (C) was reconstructed by superposition of series of confocal optical sections.

5.5.3. Subcellular localization of LTP3, LTP4 and LTP12

Similar co-infiltration experiments with an apoplastic marker (LTP1::mCherry) (Fig. 4.11 - Fig. 4.13 D-E) and plasma membrane marker (DsRED::REM) (Fig. 4.11 - Fig. 4.13 F-G), were performed for LTP3, LTP4 and LTP12. Epidermal cells transformed with LTP3::YFP, LTP4::YFP and LTP12::constructs showed comparable expression patterns in the fluorescence associated at the cell periphery, in the nucleus, in the tubular ER networks and in granular bodies associated with tubular ER. LTP3::YFP, LTP4::YFP and LTP12::YFP did not exhibit co-localization with the cell-wall marker LTP1::mCherry, but showed a good overlap when co-expressed with the plasma-membrane marker DsRED-REM. To further investigate the specificity of subcellular localization, plasmolysis was induced by adding 0.5M KNO₃ to the leaf tissue.

Under plasmolysis conditions, LTP3::YFP was progressively loosened from the cell-walls and was primarily associated with the shrinking plasma membranes (PM) and Hechtian strands (HS) along with the plasmolyzed cells. At the same time, co-expressed LTP1-mcherry diffused into the apoplastic space (AS) delimited by the plasma membrane as observed in (Fig. 4.11- Fig. 4.13 E, H). The Pearson correlation coefficient for LTP3/LTP1 co-localization in non-plasmolyzed and KNO₃ plasmolyzed cells were as low as (0,7+0,08) and (0,4+0,02), respectively. Likewise, for LTP4::YFP and LTP12::YFP upon plasmolysis, the YFP signal was abundant along the shrinking plasma membrane (Fig. 4.11 - Fig. 4.13 H), while again the LTP1-mcherry fluorescence was maintained in the cell wall (Fig.11- Fig.13 H). The LTP4/LTP1 Pearson correlation coefficients for non-plasmolyzed and KNO₃ plasmolyzed cells were 0,7+0,03 and 0,4+0,01, respectively. Likewise, for LTP12/LTP1 the average Pearson correlation coefficients for non-plasmolyzed and KNO₃ plasmolyzed cells were as low as 0,6+0,09 and 0,2+0,01, respectively. These observations suggest that LTP3::YFP, LTP4::YFP and LTP12::YFP do not localize to the apoplast. This finding was supported upon co-expression assay of LTP3::YFP, LTP4::YFP and LTP12::YFP and the plasma membrane marker DsRED::REM. YFP fluorescence co-localized with the DsRED signal in the plasma membrane (Fig. 4.11 - Fig. 4.13 E) and upon plasmolysis the signal was also found in the Hechtian strands along with the plasmolyzed cells (Fig. 4.11 - Fig. 4.13 F, G). The Pearson correlation coefficients between LTP3::YFP, LTP4::YFP, LTP12::YFP and the plasma membrane marker DsRED-REM in both the non-plasmolyzed and plasmolyzed cells showed significantly higher average values (0,9) in comparison to those samples co-infiltrated with the cell-wall marker LTP1::mCherry (Fig. 4.11 - Fig. 4.13 I). These results clearly indicated that LTP3, LTP4 and LTP12 are specifically targeted to the plasma membrane.

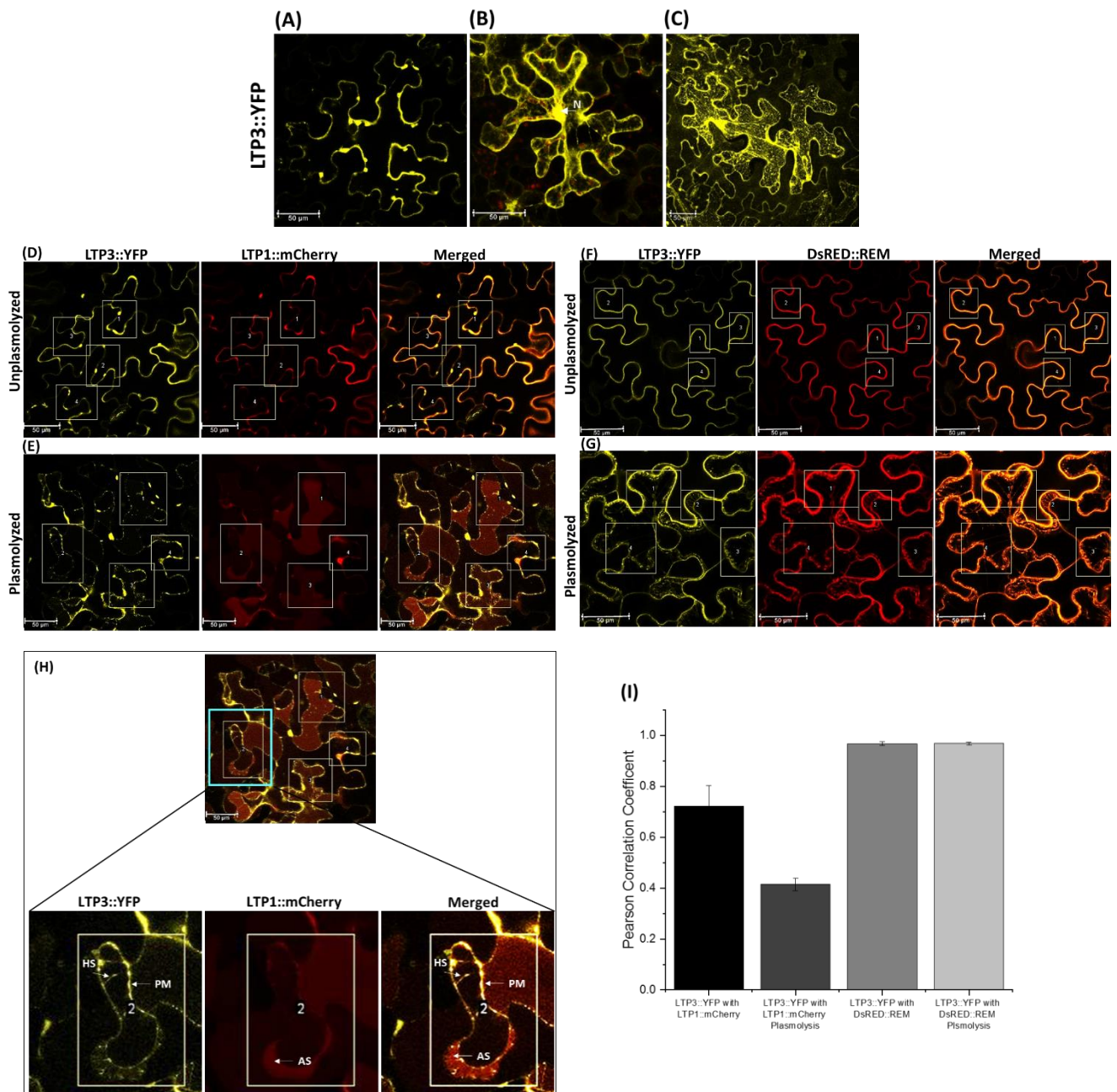


Fig. 4.11: Sub-cellular localization of LTP3 fused to YFP in *N. benthamiana* epidermal cells imaged 4 days post infiltration. (A) LTP3::YFP localizes to the cytoplasm, cell periphery and nucleus (indicated by bold arrow), **(B)** apoplast region (marked as AS), **(C)** in ER network. **(D)** Coexpression and **(E)** Plasmolysis of the two fusion proteins LTP3::YFP and cell wall marker LTP1::mCherry. **(F)** Co-expression and **(G)** Plasmolysis of the two fusion proteins LTP3::YFP and plasma membrane marker DsRED::REM. **(H)** Zoom-in image depicting co-localization of LTP3::YFP with DsRED::REM in the retracting plasma membrane and Hechtian strand, while LTP1::mCherry retained in the apoplastic space (AS) of the plasmolyzed cell. **(I)** The average Pearson correlation coefficients \pm SEM calculated from 4 randomly selected ROI in each group, $n=3$. Each selected ROI is marked with yellow box and labelled, respectively. mCherry (Excitation: 561 nm, Emission: 580–615 nm; mVenus (Excitation: 514 nm, Emission: 530–555 nm); DsRED (Excitation: 561 nm, Emission: 560–600 nm). Cells were plasmolyzed with 0.5M KNO₃ and documented after 5mins of incubation. The image **(C)** is reconstructed by superposition of series of confocal optical sections.

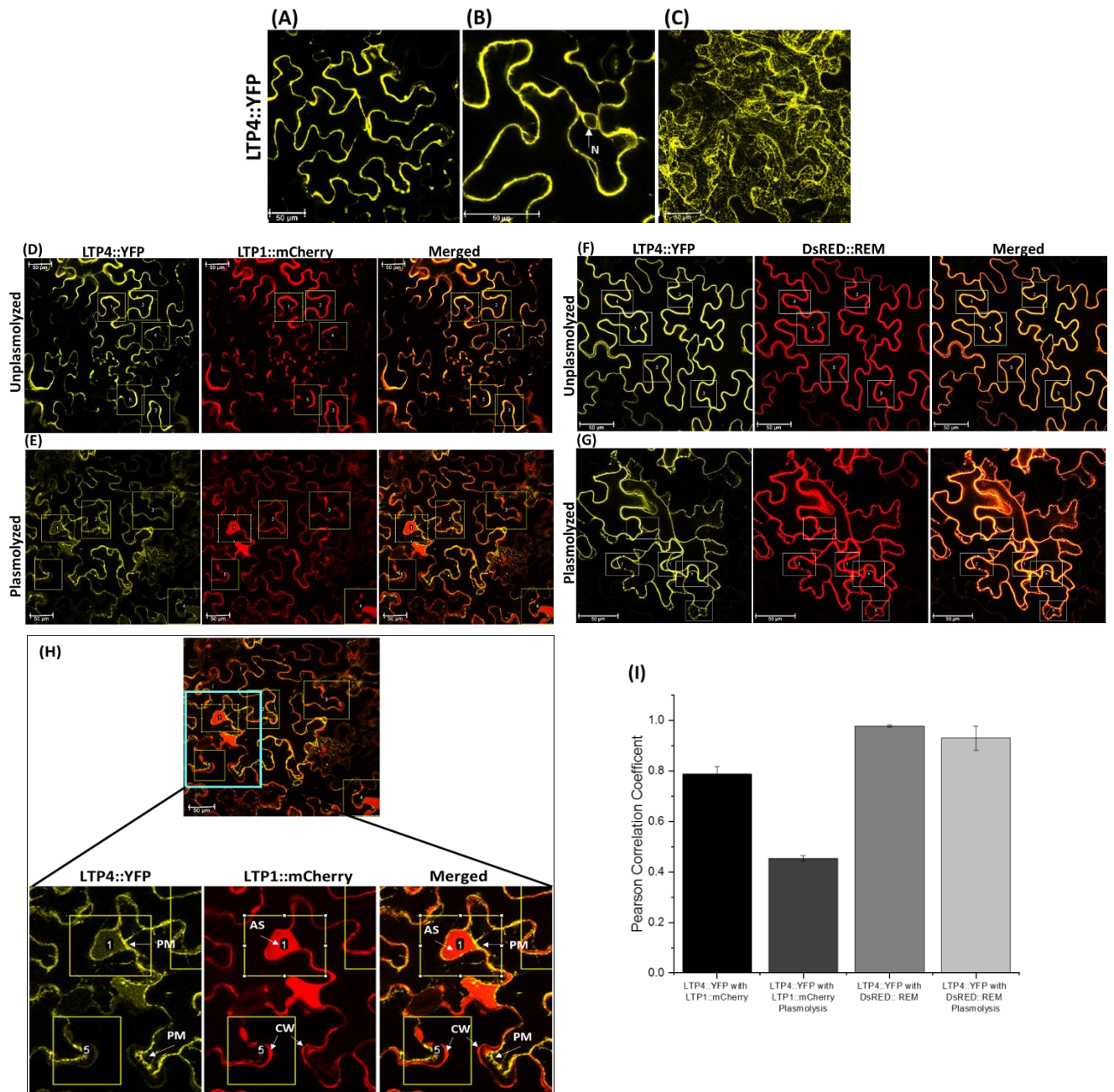


Fig. 4.12: Sub-cellular localization of LTP4 fused to YFP in *N. benthamiana* epidermal cells imaged 4 days post infiltration. (A) LTP4::YFP localizes to the cytoplasm, cell periphery and nucleus (indicated by bold arrow), **(B)** apoplast region (marked as AS), **(C)** in ER network. **(D)** Co-expression and **(E)** Plasmolysis of the two fusion proteins LTP4::YFP and cell wall marker LTP1::mCherry. **(F)** Coexpression and **(G)** Plasmolysis of the two fusion proteins LTP4::YFP and plasma membrane marker DsRED::REM. **(H)** Zoom-in image depicting co-localization of LTP4::YFP with DsRED::REM in the retracting plasma membrane (PM) and Hechtian strand (HS), while LTP1::mCherry retained in the cell wall (CW) of the plasmolyzed cell. **(I)** The average Pearson correlation coefficients \pm SEM calculated from 4 randomly selected ROI in each group, $n=3$. Each selected ROI is marked with yellow box and labelled, respectively. mCherry (Excitation: 561 nm, Emission: 580–615 nm; mVenus (Excitation: 514 nm, Emission: 530–555 nm); DsRED (Excitation: 561 nm, Emission: 560–600 nm). Cells were plasmolyzed with 0.5M KNO_3 and documented after 5mins of incubation. The image **(C)** is reconstructed by superposition of series of confocal optical sections.

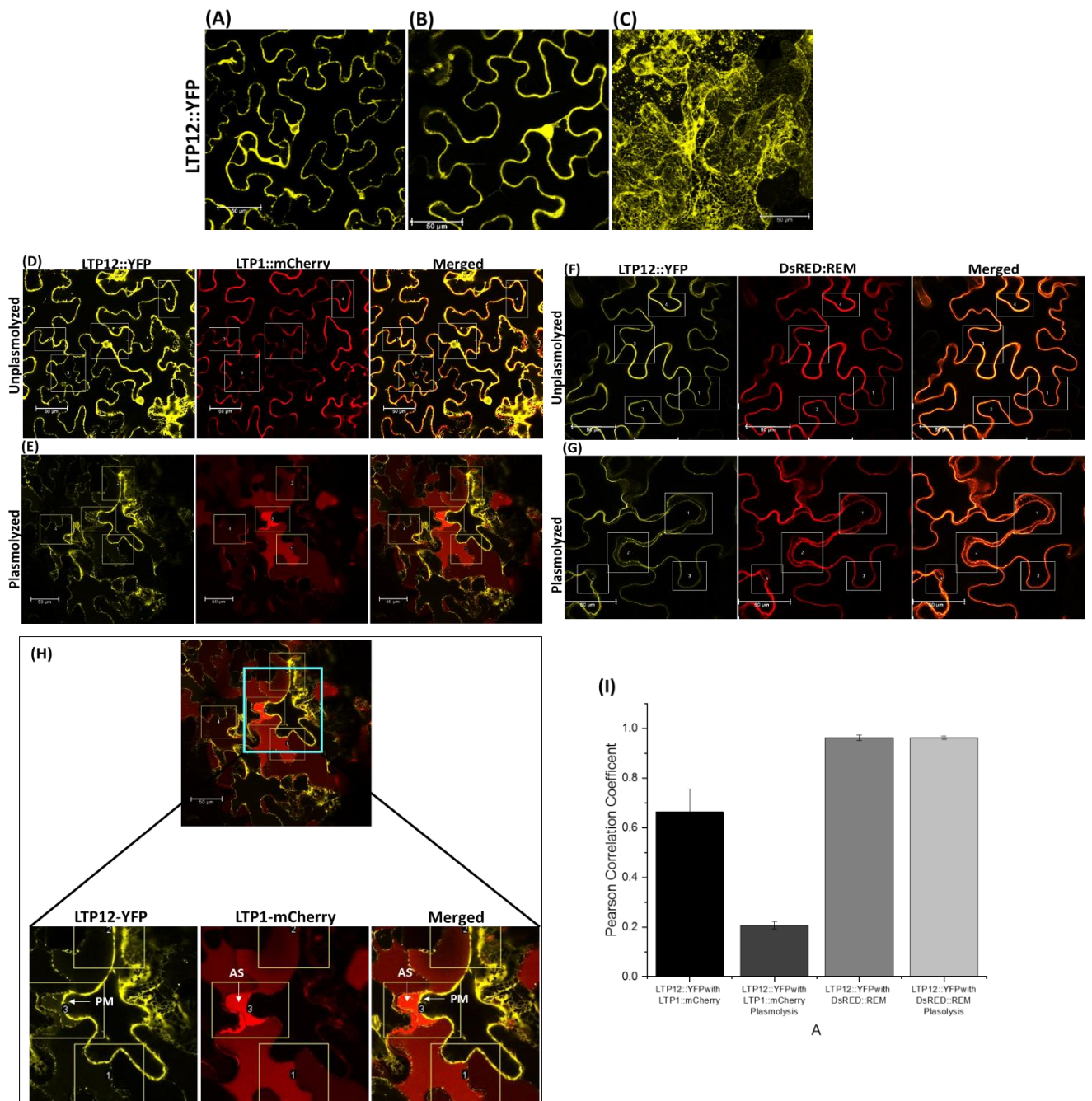


Fig. 4.13: Sub-cellular localization of LTP12 fused to YFP in *N. benthamiana* epidermal cells imaged 4 days post infiltration. (A) LTP12::YFP localizes to cell periphery and **(B)** nucleus **(C)** in ER network. **(D)** Coexpression and **(E)** Plasmolysis of the two fusion proteins LTP12::YFP and cell wall marker LTP1::mCherry. **(F)** Co-expression and **(G)** Plasmolysis of the two fusion proteins LTP12::YFP and plasma membrane marker DsRED::REM. **(H)** Zoom-in image depicting co-localization of LTP12::YFP with DsRED::REM in the retracts plasma membrane (PM) while LTP1::mCherry is in the apoplast-space (AS) of the plasmolyzed cell. **(I)** The average Pearson correlation coefficients \pm SEM calculated from 4 randomly selected ROI in each group, $n=3$. Each selected ROI is marked with yellow box and labelled, respectively. mCherry (Excitation: 561 nm, Emission: 580–615 nm; mVenus (Excitation: 514 nm, Emission: 530–555 nm); DsRED (Excitation: 561 nm, Emission: 560–600 nm). Cells were plasmolyzed with 0.5M KNO_3 and documented after 5mins of incubation. The image **(C)** is reconstructed by superposition of series of confocal optical sections.

5.6. Mapping LTP protein localization to the cellular ultrastructure employing 'Correlative Light and Electron Microscopy'

To increase the resolution for sub-cellular localization studies of the LTP2/LTP5 proteins down to the ultrastructure level, we decided to employ the CLEM technique. Correlative Light and Electron Microscopy (CLEM) is the combination of fluorescence microscopy (FM) with high-resolution electron microscopy (EM). CLEM utilizes the Array Tomography technique in which ultrathin sections of 100nm are subjected to immunofluorescence staining followed by Scanning Electron Microscopy (SEM) imaging on exactly the same cells, in order to obtain a correlated view of the specimen ultrastructure and its specific fluorescence signal.

Following immunostaining of ultrathin sections using a FITC-conjugated GFP antibody, green fluorescence was detected by epi-fluorescence microscopy. Subsequent SEM imaging revealed specific LTP5 abundance in the cell walls. In some cases, also non-specific GFP-fluorescence of infiltrated bacterial colonies was detected suggesting that GFP can be expressed in *Agrobacterium* under the control of the constitutive 35S promoter (Finer and Finer, 2000). Ultrathin sections of epidermal cells expressing 35S::LTP5-YFP showed good structural preservation (Fig. 4.14 A, B, C, D) and SEM imaging allowed localization of the cytoplasm, the nucleus, the vacuole, plastids and Golgi apparatus, as well as the cell-wall and the plasma membrane (Fig.15 D). In areas free of *Agrobacteria*, a specific LTP5-YFP signal in the cell-periphery primarily appeared to be localized in the cell wall as observed in CLEM images (Fig. 4.14 H, I, J).

Taken together, our initial efforts demonstrate that Correlative Light and Electron Microscopy (CLEM) can be utilized to study the sub-cellular localization of LTP proteins at the ultrastructural level. Future studies using different sub-cellular markers will have to prove the localization of additional LTPs.

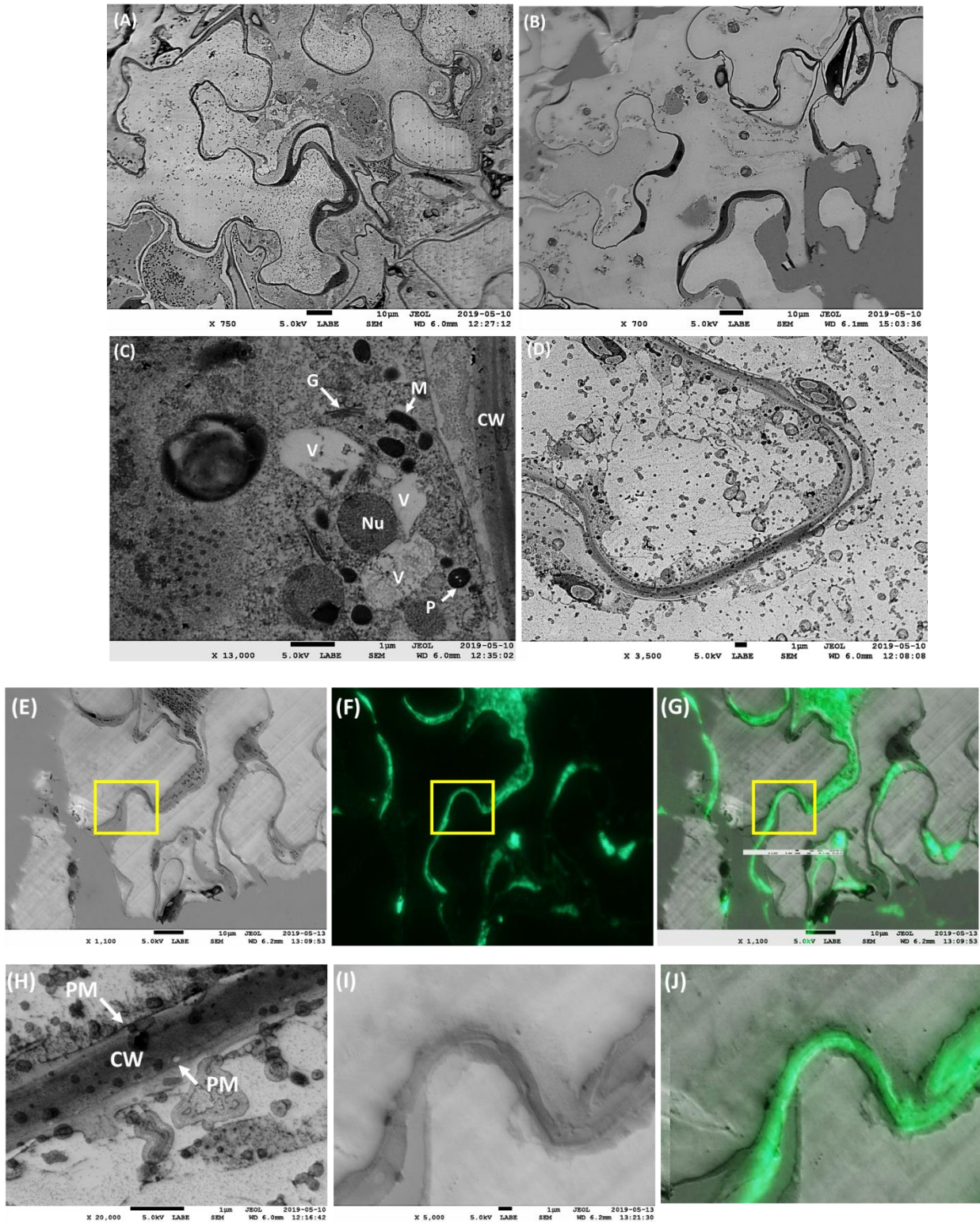


Fig. 4.14: CLEM of 35S::LTP5-YFP in *N. benthamiana* agro-infiltrated epidermal cells embedded in LR White. (A, B, C) A ultra-thin section of epidermal cells showing preserved jigsaw puzzle shaped cells. **(D, H)** A scanning electron micrograph of the cytoplasm of a plant cell. M = mitochondrion; V = vacuole; G = Golgi apparatus ; CW = cell wall; P = plastid; Nu=nucleus, PM= Plasma membrane. **(E-J)** CLEM of 35S::LTP5-YFP. **(E)** SEM image of ultrathin section, **(F)** YFP staining, **(G)** Merged image of **(E)** and **(F)**. **(I)** Zoomed in SEM image and **(J)** CLEM image of boxed area showing specific YFP fluorescence along the cell wall.

5.7. Characterization of *LTP* T-DNA insertion mutants

5.7.1. Localization of T-DNA insertions, primer design and identification of *ltp* knockout mutants

Based on our *In-silico* and qPCR analysis it was found that out of 49 nsLTPs in *A. thaliana* seven members of the LTP-Type1 sub-family are expressed in floral tissues namely LTP1 (AT2G38540), LTP2 (AT2G38530), LTP3 (AT5G59320), LTP4 (AT5G59310), LTP5 (AT3G51600), LTP6 (AT3G08770) and LTP12 (AT3G51590) which were chosen for further molecular studies.

To study the biological function of genes several ways to create loss-of-function mutations have been developed. Among them one powerful method is via T-DNA insertional mutagenesis, which occurs within particular genetic elements, including 5' and 3' untranslated regions (UTRs), exons, introns, and predicted promoter regions (Alonso *et al.*, 2003). For our studies several T-DNA tagged *ltp* mutant alleles for the selected six LTP were chosen from the Nottingham Arabidopsis Stock Centre (NASC) and INRA Versailles T-DNA collection (Fig. 4.15). Homozygous mutant lines were identified by PCR using gene-specific primers LP and RP, as well as a T-DNA left border (LB) primers.

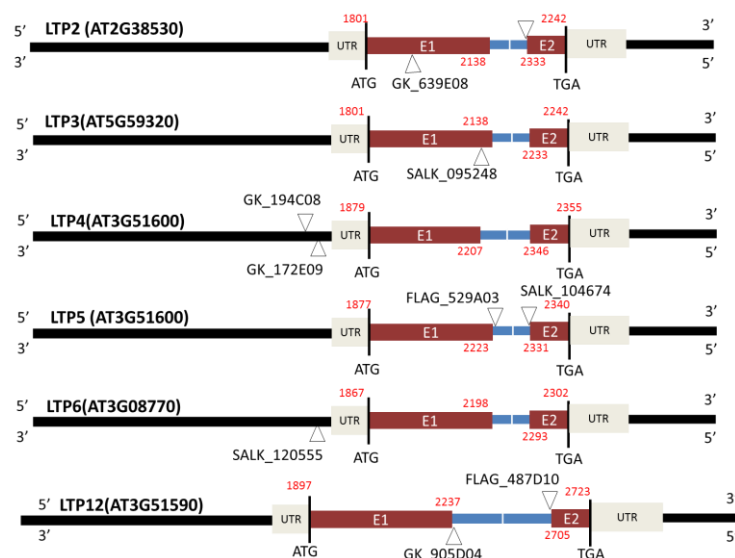


Fig. 4.15: Schematic diagram of T-DNA insertions in the LTP2 (GK_639E08), LTP3 (SALK_095248) and LTP4 (GK_194C08, GK_172E09), LTP5 (SALK_104674, FLAG_529A03), LTP6 (SALK_120555), LTP12 (GK_905D04, FLAG_487D10) lines. The alleles of At2g38530 (LTP2), AT5g59320 (LTP3), AT5g59310 (LTP4), At3g51600 (LTP5), AT3g08770 (LTP6), AT3g51590 (LTP12) were shown in exon-intron structure. The red bar marked as E1 and E2 represent exon1 and exon2 represent exons, black filled rectangles represent promoter region, sky blue bar between the exons represent the intron region, a grey box represent the 5' and 3' untranslated regions and white bold arrowhead marks the position of T-DNA insertion.

5.7.2. Identification of *ltp* knockout mutants

In order to identify homozygous T-DNA insertion mutants, we performed three primer PCR using gene specific primers and T-DNA locus specific primers (See supplementary Fig. S1).

5.7.3. RT-PCR Analysis of *AtLTP* T-DNA insertion mutants

Further confirmation was attained at mRNA transcript level by performing qRT-PCR. RNA was extracted from the flowers of homozygous screened *ltp* knockout mutants and wild-type *Arabidopsis* plants. RT-PCR analysis using *Arabidopsis* LTP gene-specific primers sets (see Table 1.6) showed that LTP2(GABI_639E08), LTP3(SALK_095428C), LTP5(FLAG_529A03) LTP6(SALK_120555), and LTP12(FLAG_487D10) were loss-of-function mutants i.e. transcript was no longer detectable. On the other hand, LTP4(GABI_194C08, GABI_172E03) and LTP5(SALK_104674) T-DNA insertion mutants were not the true knockouts of gene expression (see Fig. 4.16) as they exhibited detectable LTP transcript levels.

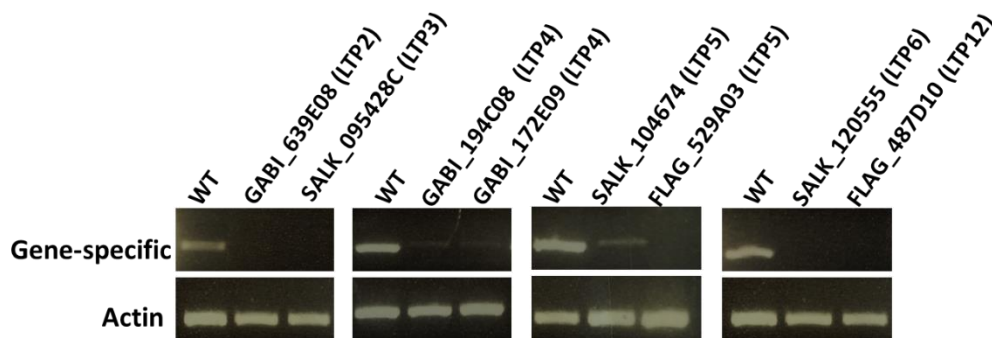


Fig. 4.16: q-PCR gene expression analysis of *AtLTPs* T-DNA insertion mutants. Homozygous T-DNA alleles for LTPs, screened by PCR-based genotyping, were evaluated for gene expression by RT-PCR analysis using the gene-specific primer sets (Table 1.6) and actin (ACT2/8) as a control. PCRs amplification were performed in 35 cycles for both LTPs and the actin control.

5.8. Functional characterization of *ltp* knock-out mutant

5.8.1. Analysis of pollen development, germination, tube growth and fertilization in *ltp* knock-out mutants

A combination of *in-vivo* cross pollination and *In-vitro* pollen tube growth assay for loss-of function mutants of LTP2 (GABI_639E08), LTP3 (SALK_095428C), LTP5 (FST_529A03) LTP6 (SALK_120555) and LTP12 (FLAG_487D10) was performed to understand the effect of these LTPs for the *Arabidopsis* fertilization process. LTP4 (GABI_194C08, GABI_172E03) was not included in this study because it was not a loss of function mutant.

5.8.1.1. *In-vivo* cross pollination of *ltp2-ko* to wild-type plants

In-silico and GUS analysis data suggested wide expression of LTP2 in the various reproductive tissues of *Arabidopsis thaliana*. LTP2 was detected in style, stigma, funiculus, transmitting tract and receptacle of the mature silique. To study the effect of *ltp2* on the fertilization process and to observe pollen tube guidance, we performed self and reciprocal cross-pollination assays between wild-type and *ltp2* plants using *ltp2* pollen as donors and wild-type pistil as acceptors and vice-versa. Closed buds of stage 12 (Smyth *et al.*, 1990) were emasculated a day before each cross-pollination experiment. After 12-14hrs, when the growing pollen tubes arrived at the base of the ovaries (Kandasamy *et al.*, 1994), hand-pollinated pistils were fixed and pollen tube growth was examined by aniline blue staining.

When the wildtype pistil was pollinated with wildtype or *ltp2* pollen, both pollen tubes grew normally to the base of the pistil 12hrs after hand pollination. In contrast to wildtype pistil, however, retarded pollen tube growth was observed after 12hrs when pistils of the *ltp2 mutant* were used as the acceptor (n=15). This suggested a defect in pollen tube guidance of the female *ltp2* gametophyte. Except for the shorter length of the *ltp2* pollen tubes, there was no other noticeable difference in the morphology of the pollen tubes compared to wild types. The shorter length of *ltp2-ko* pollen tube was not a factor of hand-pollination in these experiments because the stigma surface was completely saturated with the donor pollen in each instance. As shown in (Fig.4.17 A-D), the *ltp2-ko* pollen tubes were able to germinate and grow on stigmatic cells similar to the wild type. Also, *in-vitro* pollen germination assays showed reproducible germination and normal growth of *ltp2-ko* pollen as observed for wild-types. Therefore, it is unlikely that the *ltp2* mutation affects the ability of pollen germination on female stigmatic tissue, but rather suggests, it might affect the later stage of pollen growth and guidance process.

Moreover, a reduced seed set was observed for the reciprocal cross when *ltp2-ko* pistils were used as the acceptor and wild-type pollen as the donor ($n= 30 \pm 5.9$) (Fig. 4.17D). Again, no morphological abnormality in other floral and vegetative parts was observed for the *ltp2* mutant. This may be due to the expression of redundant LTPs, like LTP1 which is homologous to LTP2 or related pathways which can compensate for the gene disruption. Surprisingly, the average number of seeds per siliques from self-pollinated *ltp2* ($n=40 \pm 2.5$) plants were equivalent to those of self-pollinated wild-type plants ($n= 46 \pm 3$) (Fig. 4.17E). The variation in the seed set for hand pollinated and self-pollinated plants could be due to the fact that LTP2 is induced upon wounding (Deeken *et al.*, 2016) while emasculating the pistils. Altogether the *in-vivo/in-vitro* pollen-tube growth studies showed that wild-type and *ltp2* mutant pollen tubes grow slowly through the transmitting tract of the *ltp2* pistil, with no significant difference in the seed count in comparison to the wild-type plants which suggests that, although delayed, pollen-tubes were capable of growing to the base of the gynoecium and could fertilize the *ltp2* ovules normally.

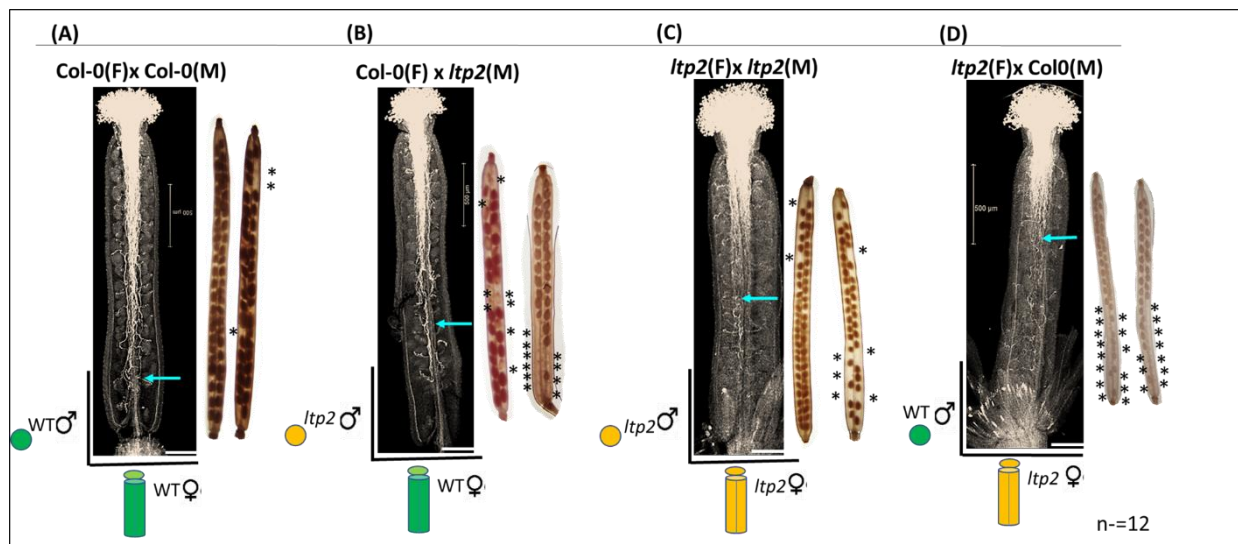


Fig. 4.17: Characterization of *Itp2-ko* plants.

(A-D) *In-vivo* cross pollination of *Itp2-ko* to wild-type plants. Flower bud at stage 12 (Smyth et al., 1990) were dissected a day before each cross-pollination (n = 12 per cross). After 12hrs, the hand-pollinated pistils were fixed, and pollen-tube growth was examined via aniline-blue staining. Arrow indicates the maximum length of the visible pollen tube growing toward the base of the pistil. (E) The remaining pollinated pistils were allowed to develop into mature silique and examined after 8 days of pollination. SP: Self-pollinated, HP: Hand-Pollinated. (F) The *in-vitro* germination and tube elongation of *Itp2-ko* mutant pollen grains showed no significant difference to the wild type. Scale bar: 100µm.

5.8.1.2. *In-vivo* cross pollination of *Itp3-ko* to wild-type plants

The *LTP3* gene was shown to be expressed in the style, the anther filaments, sepals, ovules and the funiculus of the *Arabidopsis* flowers. To study the effect of *Itp3* on the fertilization process and pollen tube guidance, as shown for *LTP2*, we performed self and reciprocal cross-pollination assay between wild-type and *Itp3* plants. In the reciprocal cross-pollination experiment, no difference was observed in the *Itp3-ko* plant in comparison to the wild-type plant (Fig. 4.18 A-D). Wild-type pollen showed active growth through the *Itp3-ko* pistil and vice-versa. *In-vitro* pollen germination and pollen tube growth showed no morphological defect in comparison to the wild-tube pollen (Fig. 4.18 E, F). No distinguishable abnormality in other floral and vegetative parts was observed for the *Itp3-ko* plants.

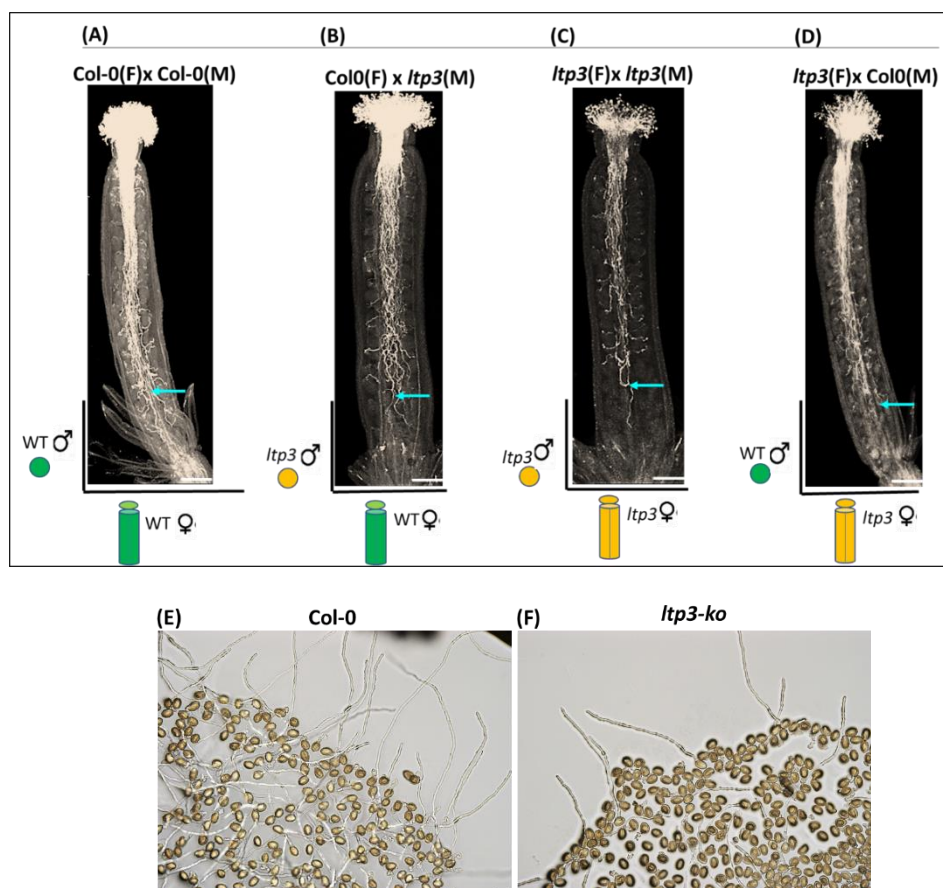


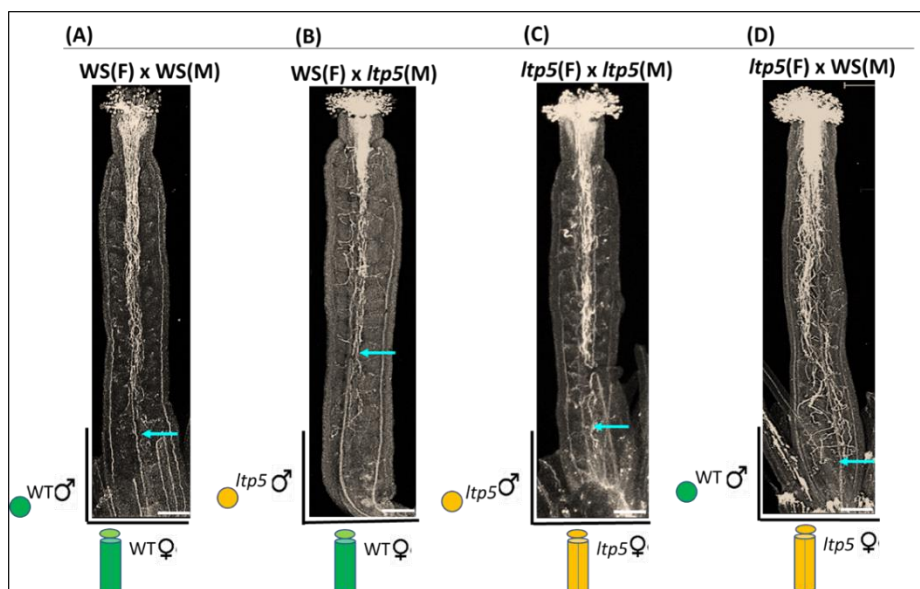
Fig. 4.18: Characterization of *ltp3-ko* plants

(A-D) *In-vivo* cross pollination of *ltp3-ko* to wild-type plants. Flower bud at stage 12 (Smyth et al., 1990) were dissected a day before each cross-pollination (n = 12 per cross). After 12hrs, the hand-pollinated pistils were fixed, and pollen-tube growth was examined via aniline-blue staining. **(E-F)** *In-vitro* pollen germination assay showed no significant difference to the wild-type. Scale bar: 100um.

5.8.1.3. *In-vivo* cross pollination of *ltp5-ko* to wild-type plants

The *LTP5* gene is expressed in various parts of the inflorescence. Our GUS-expression data showed that *LTP5* is expressed in stigma and style, the anther and anther filament and the funiculus. Additionally, a weak expression was observed in pollen, pollen tubes, the ovules and the transmitting tract. It has been reported previously that a gain of function mutant (*ltp5-ko*, SALK_104674) exhibits severe defects in pollination and seed formation (Chae et al., 2009). Since the reported T-DNA insertion line was a gain-of function mutant with the presence of an aberrant *LTP5*-transcript, we investigated a true loss-of-function T-DNA insertion mutant (FLAG_529A03).

To clarify if this loss-of-function mutant has a similar defect as gain-of-function *ltp5* mutant, we again performed reciprocal cross-pollination assays and examined pollen development, germination and pollen tube length. In the reciprocal cross-pollination, both wild-type and mutant pollen showed active pollen-tube growth 12hrs after pollination (Fig. 4.19 A-D). Moreover, *in-vitro* pollen germination assays showed normal germination and pollen tube growth in the *ltp5-ko* plants (Fig. 4.19 E, F). No discernible phenotype was evident in other floral and vegetative parts of the *ltp5-ko* plant.



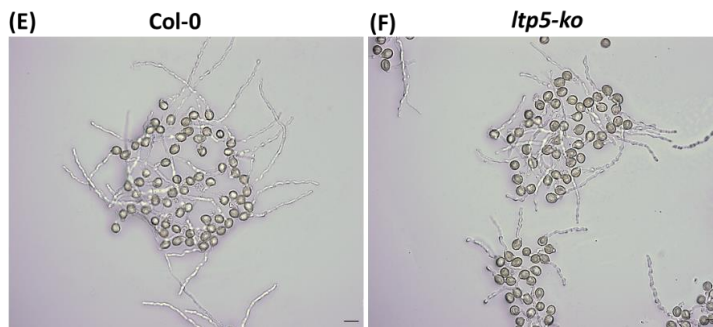


Fig. 4.19: Characterization of *ltp5-ko* plants.

(A-D) *In-vivo* cross pollination of *ltp5-ko* to wild-type plants. Flower bud at stage 12 (Smyth et al., 1990) were dissected a day before each cross-pollination (n = 12 per cross). After 12hrs, the hand-pollinated pistils were fixed, and pollen-tube growth was examined via aniline-blue staining. **(E-F)** *In-vitro* pollen germination assay showed no significant difference to the wild-type. Scale bar: 100 μ m

5.9. No distinguishable phenotype for single *ltp2*, *ltp3*, *ltp5*, *ltp6* and *ltp12* knock-out mutant.

Further analyses of the single *ltp2*, *ltp3*, *ltp5*, *ltp6* and *ltp12* mutants did not reveal any obvious developmental and fertilization defects like (pollen germination, *in-vivo* pollen tube growth, seed count and silique length) under our experimental conditions. These single *ltp* mutants did not differ phenotypically from wild-type plants. Furthermore, overlapping expression patterns together with possible functional redundancy of these Cys-rich proteins may often mask the phenotypes when only one family member is successfully disrupted. Therefore, to address this issue, we decided to use the CRISPR-Cas9 gene-editing technique to create multiple knock-outs of related LTPs.

5.10. Generation of double knock out *lpt2/lpt5* transgenic plants using the CRISPR-Cas9 gene editing technique

A combination of *in-vivo* cross pollination and *in-vitro* pollen tube growth assays for all the six LTP T-DNA insertion mutants provided the first hint for the LTP candidate with a role in the pollen tube growth and guidance process. However, no obvious fertilization defect in terms of fertilization efficiency, seed set, or silique development was observed for single LTP loss-of-function mutants, probably due to functional redundancy of highly similar LTPs.

To circumvent the problem of functional redundancy, the CRISPR-Cas9 system was established and used to create multiple knockouts (KO) simultaneously for the selected LTP genes. LTP2 is highly expressed in female stigma and style while LTP5 is expressed in the stigma, style, pollen and pollen tubes. In addition, according to phylogenetic analyses, LTP2 and LTP5 are highly homologous and belong to the same clade within the type-I LTPs (Boutrot *et al.*, 2008). Therefore, among the six LTPs, LTP2 and LTP5 were chosen as potential candidates to be knocked out simultaneously using the CRISPR-Cas9 technique.

5.10.1. Selection of sgRNA for LTP2 and LTP5 with no potential off-targets

5.10.1.1. Off-target prediction

The success of the CRISPR/Cas9 genome editing technique depends on the choice and quality of the guide RNA sequence. The specificity of CRISPR/Cas9 approaches has been a major concern mainly due to the high frequency off-target mutagenesis induced by CRISPR/Cas9. Avoiding off-target activity of Cas9, i.e. cleaving at other unwanted sites in the genome, is the crucial step in designing guide RNAs. We used the CRISPOR web-based algorithm (<http://crispor.tefor.net/>) to design the single-guide RNA for LTP2 and LTP5. Single guide RNAs (sgRNAs) were generated within the first exons of LTP2 and LTP5 exhibiting a high specificity score and a zero off-target score (Fig. 4.20 A, B). To examine the specificity of the mutagenesis, we searched the *Arabidopsis* genome for potential off-targets. To evaluate off-target prediction accuracy, CRISPOR utilizes cumulative data from eight recently published studies that detect and quantify the off-target cleavage sites (Tsai *et al.*, 2015; Cho *et al.*, 2014; Ran *et al.*, 2015). In addition, to confirm no off-targets for the selected sgRNAs we also used different algorithms like Cas-OFFinder (<http://www.rgenome.net/cas-offinder/>), CHOP-CHOP (<http://chopchop.cbu.uib.no/>), e-CRISPR (<http://www.e-crisp.org/E-CRISP/>) and CC-TOP (<https://crispr.cos.uni-heidelberg.de/>) to check for the specificity of the designed sgRNAs. All the different algorithms tested predicted zero off-target for the sgRNAs selected for LTP2 and LTP5 (Fig. 4.20C).

(A)

| | |
|--------------------------|----------------------------------|
| sgRNA for LTP2, Target 1 | 153/fw: CGAGGTGCTCCACTTACCCA AGG |
| sgRNA for LTP5, Target 2 | 154/fw: GAGGCGGTTTCATTCTAGAGGG |

(B)

LTP2_ Exon1

ATGGCTGGAGTGATGAAGTTGGCATGCATGGTCTTGGCTTGCATGATTGTGGCCGGTCCCAATCACAGCGAACCGCTTATGAGT
TGTGGCACCGTCAACGGCAACCTGGCAGGGTGCATTGCCTACTTGACC **CGAGGTGCTCCACTTACCCA** AAGGGTGCAGCAACGGC
GTTACTAACCTTAAAAACATGGCCAGTACAAACCCAGACCGTACGCAAGCTTGGCGTTGCCTTCAATCTGCCGCTAAAGCCGTT
GGTCCCGTCTCAACACTGCCCGTGCAGCTGGACTTCTAGGCGATGCAAAAGTCAATATTCCTTACAAAATCAGCGCCAGCACC
AACTGCAACAC

LTP5_ Exon1

ATGGAGGGACTCTGAAGTTGTCAACTTGGTGATTGTGTGCATGTTAGTGACCCTCCATGGCGTCCGAGGAGCAATCTCG
TGGCGGCGAGTACCCGGCAGCTTAGGTCAATGCTATAACTACTTGACC **GAGGCGGTTTCATTCTAGAGGG** GTTGTGCTCTGGC
GTTTCAGAGGCTCAACAGCTTGGCTCGTACCACCCGTGACCGCAACAAGCTTGTGTTGTATCCAGGGAGCAGCGAGAGCCTTG
GGTCTCGACTTAACGCTGGTCTGCTGCTCCTGGTCTTGGCGTGTAGGATCTTACCCCATCAGTGCCAGAAC
AACTGTAACAC

(C)

CRISPOR

Download as Excel tables: [Guides](#) / [Off-targets](#) / [Saturating mutagenesis assistant](#)

| Position/ Strand | Guide Sequence + PAM + Restriction Enzymes <input type="checkbox"/> Only G- <input type="checkbox"/> Only GG- <input type="checkbox"/> Only A- <input type="checkbox"/> <input type="checkbox"/> | MIT Specificity Score | CFD Spec. score | Predicted Efficiency <input type="checkbox"/> Show all scores Doench '16 Mor-Mateos | Outcome Out-of-Frame | Off-targets for 0-1-2-3-4 mismatches + next to PAM | Genome Browser links to matches sorted by CFD off-target score <input type="checkbox"/> exons only <input type="checkbox"/> chrom 2 only |
|---------------------|--|-----------------------------|-----------------------|--|-------------------------|---|--|
| 153 / fw | CGAGGTGCTCCACTTACCCA AGG Enzymes: <i>EcoI</i> , <i>BseDI</i> Cloning / PCR primers | 100 | 100 | 61 | 43 | 70 | 0-0-0-0-0 0-0-0-0-0 0 off-targets |

Download as Excel tables: [Guides](#) / [Off-targets](#) / [Saturating mutagenesis assistant](#)

| Position/ Strand | Guide Sequence + PAM + Restriction Enzymes <input type="checkbox"/> Only G- <input type="checkbox"/> Only GG- <input type="checkbox"/> Only A- <input type="checkbox"/> <input type="checkbox"/> | MIT Specificity Score | CFD Spec. score | Predicted Efficiency <input type="checkbox"/> Show all scores Doench '16 Mor-Mateos | Outcome Out-of-Frame | Off-targets for 0-1-2-3-4 mismatches + next to PAM | Genome Browser links to matches sorted by CFD off-target score <input type="checkbox"/> exons only <input type="checkbox"/> chrom 2 only |
|---------------------|--|-----------------------------|-----------------------|--|-------------------------|---|--|
| 154 / fw | GAGGCGGTTTCATTCTAGAGGG Enzymes: <i>MaeI</i> Cloning / PCR primers | 100 | 100 | 62 | 82 | 58 | 0-0-0-0-0 0-0-0-0-0 0 off-targets |

**Cas-OFFinder -
CRISPR RGEN Tools**

| Target | Chromosome | Position | Direction | Mismatches | Bulge Size |
|--|------------|----------|-----------|------------|------------|
| crRNA: GAGGCGGTTTCATTCTAGAGGG DNA: GAGGCGGTTTCATTCTAGAGGG | chr3 | 19138968 | - | 0 | 0 |
| crRNA: CGAGGTGCTCCACTTACCCAAGG DNA: CGAGGTGCTCCACTTACCCAAGG | chr2 | 16128612 | + | 0 | 0 |

CHOP-CHOP

| Target sequence | Genomic location | Exon | Strand | GC (%) | Self-complementarity | Off-targets | | | | Efficiency |
|-------------------------|------------------|------|--------|--------|----------------------|-------------|---|---|---|------------|
| | | | | | | 0 | 1 | 2 | 3 | |
| CGAGGTGCTCCACTTACCCAAGG | Chr2:16128613 | 1 | + | 60 | 0 | 0 | 0 | 0 | 0 | 0.68 |
| GAGGCGGTTTCATTCTAGAGGG | Chr3:19138969 | 1 | - | 50 | 1 | 0 | 0 | 0 | 0 | 0.55 |

E-CRISPR

| Name | Nucleotide sequence | SAE-Score | Target | Matchstring | Number of Hits |
|----------|-------------------------------------|-----------|----------------|----------------------------------|----------------|
| LTP2_3_0 | GAGGTGCTCCACTTACCCA CCCA NGG | | AT2G38530:LTP2 | Matchstring Info | 1 |
| LTP5_3_0 | GAGGCGGTTTCATTCTAGAGGG CTAGA NGG | | AT3G51600:LTP5 | Matchstring Info | 1 |

**CCTop -
CRISPR/Cas9**

T6 out of 43
[Previous](#) [Next](#)
Sequence: CGAGGTGCTCCACTTACCCAAGG
Efficacy score by CRISPRater: **0.82 HIGH**
Oligo pair with 5' extension fwd: TAGGCGAGGTGCTCCACTTACCCA rev: AAACCTGGGTAAGTGGAGCACCTCG
Oligo pair with 5' substitution fwd: TAGGCGAGGTGCTCCACTTACCCA rev: AAACCTGGGTAAGTGGAGCACCT

| Coordinates | strand | MM | target_seq | PAM | distance | gene name | gene id |
|------------------------|--------|----|-------------------------|-----|----------|-----------|-----------|
| chr2:16128613-16128635 | + | 0 | CGAGGTGC [TCCACTTACCCA] | AGG | 0 | E LTP2 | AT2G38530 |

T8 out of 40
[Previous](#) [Next](#)
Sequence: GAGGCGGTTTCATTCTAGAGGG
Efficacy score by CRISPRater: **0.66 MEDIUM**
Oligo pair with 5' extension fwd: TAGGCGGTTTCATTCTAGAGGG rev: AAACCTAGGAAATGAAACCGCCT
Oligo pair with 5' substitution fwd: TAGGCGGTTTCATTCTAGAGGG rev: AAACCTAGGAAATGAAACCGCCT

| Coordinates | strand | MM | target_seq | PAM | distance | gene name | gene id |
|------------------------|--------|----|---------------------------|-----|----------|-----------|-----------|
| chr3:19138969-19138991 | - | 0 | GAGGCGGT [TTCATTCTAGAGGG] | GGG | 0 | E LTP5 | AT3G51600 |

Fig. 4.20: Evaluation of potential off-target using different algorithm. (A) single-guide RNA for LTP2 and LTP5. **(B)** gRNA target region shown in LTP2 and LTP5 exon **(C)** Different *in-silico* algorithm like CRISPOR, Cas-OFFinder, CHOP-CHOP, e-CRISPR and CC-TOP were used to check for the potential off-target for the selected sgRNA for LTP2 and LTP5.

5.11. Experimental design and 2-sgRNA expression cassette construction

In order to introduce the sgRNAs into *Arabidopsis*, we used the recently published germ-line egg cell-specific promoter-controlled CRISPR/Cas9 system allowing targeted mutation of two *Arabidopsis* genes- LTP2 and LTP5 simultaneously (Fig. 4.21A) (Wang *et al.*, 2015). To create the double-sgRNA-CRISPR expression cassette, we used the pCBC-DT1DT2 plasmid as an entry vector. We designed primers for the two target genes LTP2 and LTP5 and obtained a single PCR product flanked with two sgRNA fragments and two *BsaI* sites incorporated by the primers. The purified PCR product was subjected to a golden-gate reaction with the CRISPR/Cas9 binary vector pHEE401 harboring the *Cas9* gene driven by the *Arabidopsis* egg-cell specific promoter EC1.2p and the LTP2/LTP5 sgRNAs driven by the Pol-III promoter U6-26p and U6-29p, respectively (Fig. 4.21B). We confirmed the positive clone via Sanger sequencing using U6-26p-F and U6-29p-F primers. A positive clone was used to transform *Agrobacteria* for subsequent generation of homozygous stable CRISPR transgenic *Arabidopsis* plants.

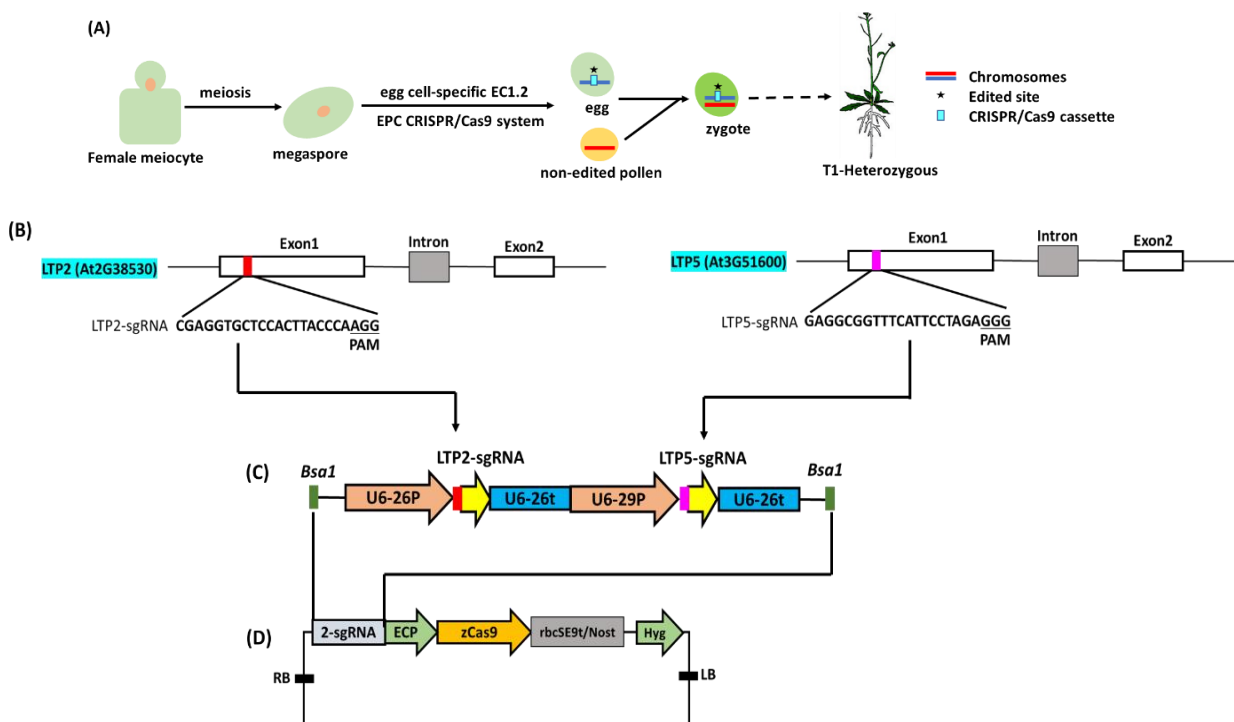


Fig. 4.21: Generation of *ltp2ltp5* knockout lines by CRISPR/Cas9-mediated mutagenesis. (A) The working model for the egg-cell specific promoter-driving Cas9 system. The editing system only performs its activity in female gamete, leading to heterozygous plants in the T1 generation. Target site design and EPC CRISPR/Cas9 vector construction (B) Schematic description of target sites in the LTP2 and LTP5 genomic (C, D) Diagrams illustrating the assembly procedure of CRISPR/Cas9 system. CRISPR/Cas9 binary vectors, each harboring Cas9 driven by the egg-cell specific promoter ECP and two sgRNA genes driven by Pol-III promoters U6-26p and U6-29p, respectively. RB/LB, T-DNA right/left border; *rbcS-E9t*, *rbcS* E9 terminator; *Nost*, nos gene terminator; 2-sgRs, two sgRNA expression cassettes; *zCas9*, *Zea*

mays codon-optimized Cas9; Hyg, hygromycin-resistance gene. For the sgRNAs, the red and magenta part represents 20-bp target sequences for LTP2 and LTP5 and the yellow arrowhead represents 76-bp sgRNA scaffold. **(C)** The expression module containing designed sgRNA sequence was inserted into destination vector EPC-pHEE401 through Golden Gate reaction.

5.12. Selection and screening of positive transformants

5.12.1. Analysis of mutation in the T1 transgenic plants and their T2 progeny

The EPC CRISPR/Cas9 pHEE401 binary vector harbors Cas9 driven by the egg cell specific EC1.2 promoter, providing the Cas9 system to function in T1 egg cells, T2 one-cell stage embryos, and T2 early embryos. According to the publication of Wang *et al.* (2015), the specific expression of Cas9 in the egg cell can also lead to the creation of T1 plants with no clear phenotype, which might be heterozygotes or mosaics rather than wild types. In the next generation, the T1 plants with no clear phenotype should be able to give rise to homozygous or bi-allelic mutant T2 plants (Wang *et al.*, 2015). Based on the above information, we screened approximately 60 plants in the T1 generation, among which two plants (#PI-9 and #PI-31), were likely single mutant for LTP5, based on sequence analysis of the region surrounding the target site. The analyses were conducted by examining their sequencing chromatograms. Mutant plants (#PI-9 and #PI-31) demonstrated a phenotype similar to *ltp5* gain of function mutant as reported in (Chae *et al.*, 2009).

The T2 progeny from self-fertilized T1 parent plants (#PI-9 and #PI-31) were further examined for the double mutation. In the T2 generation, more than 50% (10/20) of their progeny were likely to be double mutant T2 plants. We sequenced the *ltp2ltp5* double mutant in the T2 progeny (10 T2 plant per line) to confirm the mutation. Furthermore, we propagated the *ltp2ltp5* double mutant plants from T2 progeny to T3 generation and rechecked for the stability of mutation in the next generation.

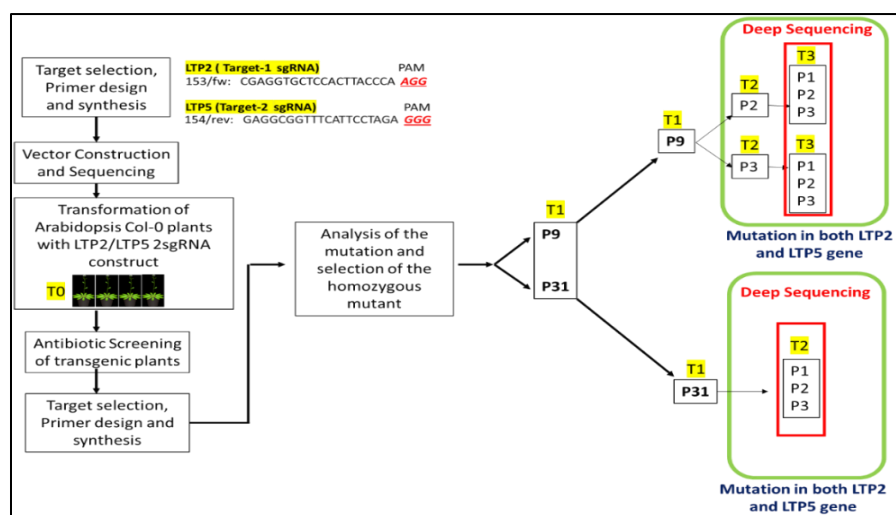


Fig. 4.22: CRISPR workflow. Schematic overview for generating *ltp2ltp5* homozygous mutants in the T2 and T3 generation.

We screened four double knock-out mutants (#P9-P2-P2, #P9-P3-P3, #P31-P2 and #P31-P3) with different degrees of mutations in the two target genes. As shown in Fig. 4.23, for LTP2 the majority of indel mutation were +1bp insertions and -1bp/-8bp/-18bp deletions, whereas for LTP5 the frequency of indel mutation was rather stable with a +1bp insertion or -33bp deletion.

| LTP2 | |
|-----------------|---|
| WT | AGGGTGCATTGCCTACTTGACC CGAGGTGCTCCACTTACCCAAGG GTGCTGCAACGGC |
| P9-P2-P2 | AGGGTGCATTGCCTACTTG----- ACCCAAGG GTGCTGCAACGGC |
| P9-P3-P3 | AGGGTGCATTGCCTACTTGACC CGAGGTGCT ----- CCAAGG GTGCTGCAACGGC |
| P31-P2 | AGGGTGCATTGCCTACTTGACC CGAGGTGCTCCACTTAC - CAAGG GTGCTGCAACGGC |
| P31-P3 | AGGGTGCATTGCCTACTTGACC CGAGGTGCTCCACTTACCC AAGG GTGCTGCAACGG |
| LTP5 | |
| WT | AGGTCAATGCTATAACTACTTGACCC GAGGCGGTTTCATTCTAGAGGG TGTTGCTCTG |
| P9-P2-P2 | AGGTCAATGC----- AGAGGG TGTTGCTCTGGC |
| P9-P3-P3 | AGGTCAATGC----- AGAGGG TGTTGCTCTGG |
| P31-P2 | AGGTCAATGCTATAACTACTTGACCC GAGGCGGTTTCATTCT TAGAGGG TGTTGCTCTGG |
| P31-P3 | AGGTCAATGCTATAACTACTTGACCC GAGGCGGTTTCATTCT TAGAGGG TGTTGCTCTGG |

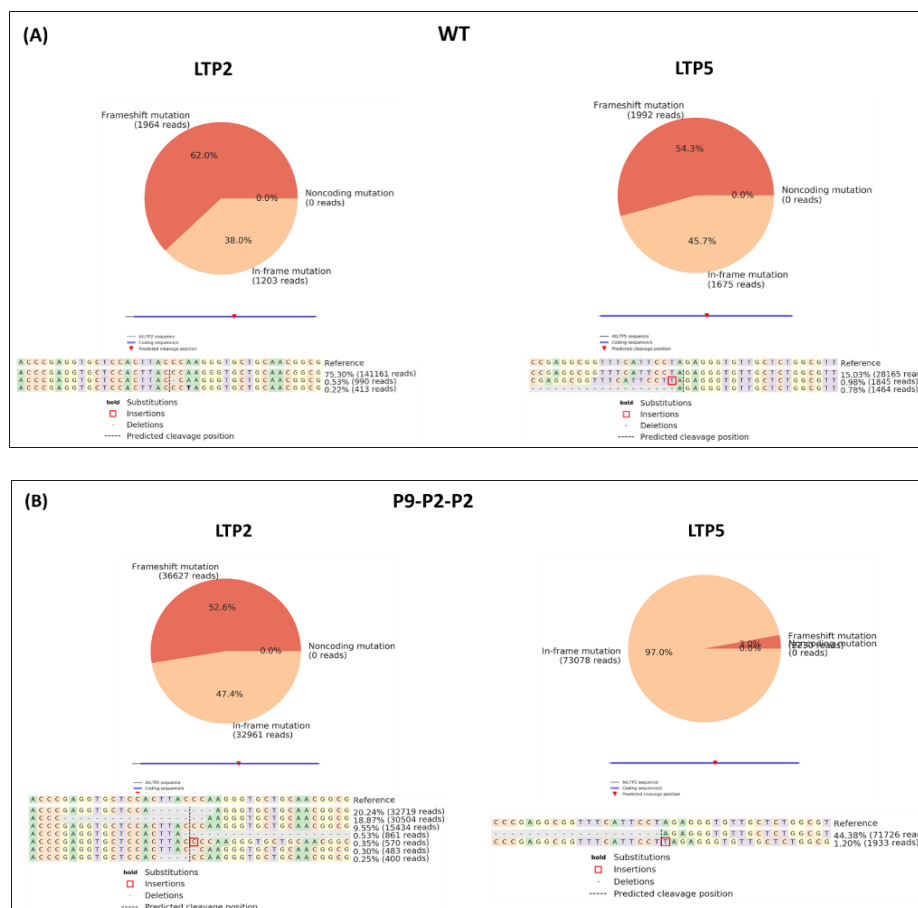
Fig. 4.23: Alignment of T3 homozygous double mutants obtained via EPC CRISPR/cas9 mutagenesis. The targeted region was amplified by PCR and sequenced using standard Sanger sequencing. The sgRNA^{AtLTP2} and sgRNA^{AtLTP5} sequence are highlighted in yellow and the PAM sequence in green. Deletions are indicated by dots and insertions are highlighted in red.

5.13. High-throughput sequencing evaluation of CRISPR/Cas9-induced mutagenesis in *AtLTP2* and *AtLTP5*.

Based on the Sanger sequencing results, four mutant lines (#P9-P2-P4, #P9-P3-P3, #P31-P2 and #P31-P3) were further analyzed using next-generation, high-throughput sequencing to examine the mutation distribution at the genome scale and to test the mutation efficacy of the CRISPR/Cas9 system. The PCR products, encompassing the designed LTP2/LTP5 mutation region of the selected mutant plants, were purified for next generation sequencing. More than 2,00,000 reads were obtained for each of the mutants analyzed. The analysis of the sequencing results was performed using the CRISPresso computation tool (<http://crispresso.rocks/>). Reads were then mapped to the reference wild-type *LTP2/LTP5* genomic sequence and the proportion of mutagenesis caused by CRISPR/Cas9 system was

calculated. Thereby, we could show that the mutation efficiency in all four mutant lines were in the range of 60 to 100% for both genomic sites, *AtLTP2* and *AtLTP5*. From our analysis, we identified line #P31-P2 to exhibit the highest mutation rates. This line showed 99.8% and 99.9% frameshift mutations in LTP2 and LTP5, respectively (Fig. 4.24D). Another mutant line, #P31-P3 also showed >85% mutation rates for both genes (Fig. 4.24E). On the other hand, the mutation frequency in line #P9-P2-P2 was 52.6% for a frameshift mutation in LTP2 and 97% for an in-frame mutation in LTP5 (Fig.4.24B), whereas line #P9-P3-P3 exhibited a frameshift mutation (99,9%) for LTP2 together with an in-frame mutation (98,3%) in LTP5 (Fig. 4.24C). We included all the four double mutant lines (#P9-P2-P2, #P9-P3-P3, #P31-P2 and #P31-P3) for further analyses in order to make a comparison between in-frame mutants and frame-shift mutants.

Taken together, these results demonstrated that the EPC-mediated CRISPR/Cas9 genome editing system is an effective strategy to rapidly generate mutated *Arabidopsis* plants in the first generation by specifically expressing Cas9 in egg cells and one cell stage embryos under egg cell-specific EC1.2 promoters. This system enables the generation homozygous or biallelic T1 mutants for multiple target genes. However, further studies will have to determine what percentage of Cas9-free T2 plants contain the edited mutations.



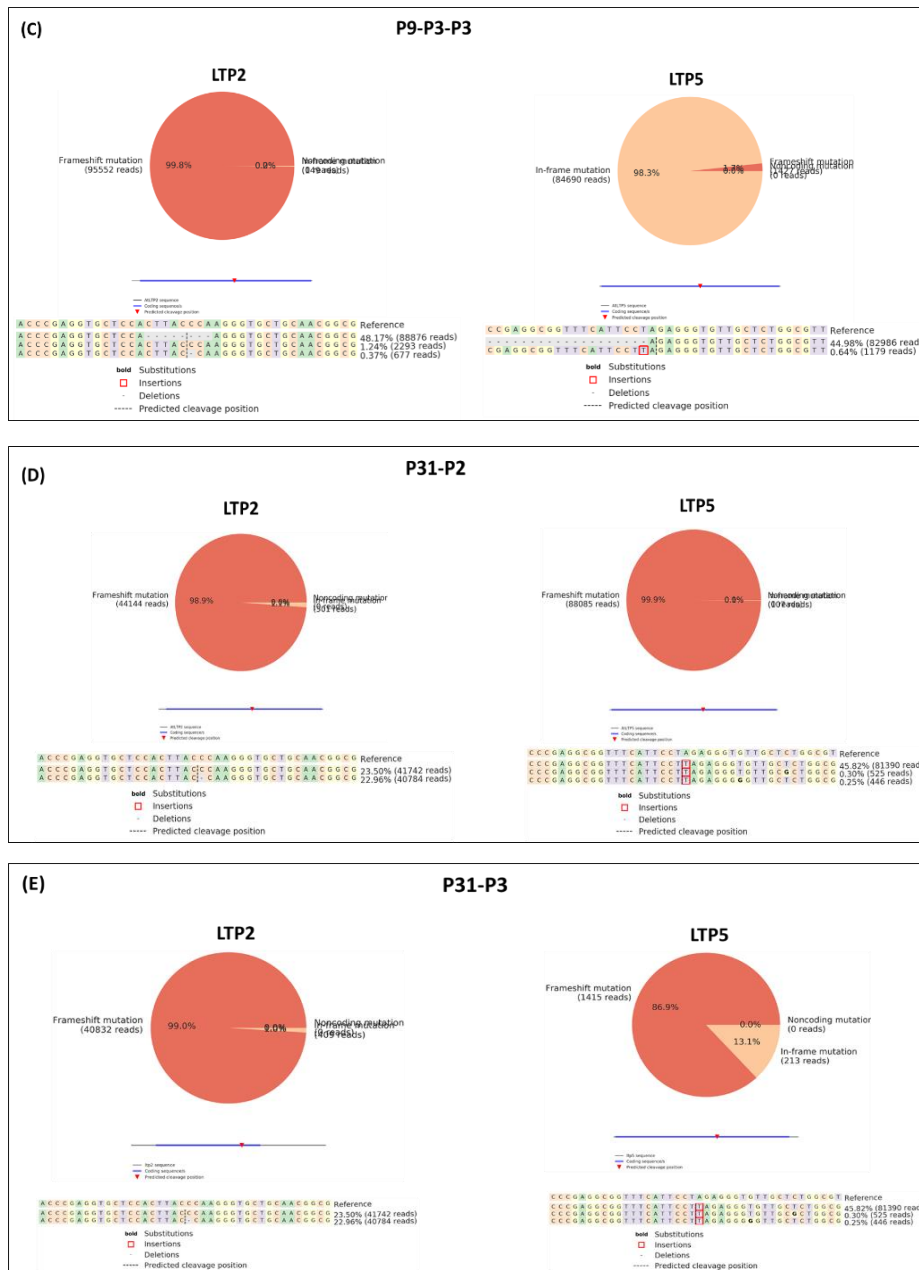


Fig. 4.24: Analysis of mutagenesis profile from deep sequencing data using CRISPResso2 analysis tool. (A) WT, (B) #P9-P2-P2, (C) #P9-P3-P3, (D) #P31-P2, (E) #P31-P3 Quantification of editing frequency as determined by the percentage and number of sequences reads showing frameshift and in-frame mutations. Frameshift and in-frame mutations include any mutations that partially or fully overlap coding sequences, with any non-overlapping mutations classified as noncoding. Unmodified reference reads are excluded from the plot, and all HDR reads are included in this plot. Allele Plot of AtLTP2 and AtLTP5 for each CRISPR mutants. Visualization of the distribution of identified alleles around each cleavage site. Nucleotides are indicated by unique colors (A = green; C = red; G = yellow; T = purple). Substitutions are shown in bold font. Red rectangles highlight inserted sequences. Horizontal dashed lines indicate deleted sequences. The vertical dash line indicates the predicted cleavage site.

5.14. Phenotypic analysis of the *ltp2ltp5* double-ko mutants

Mutant phenotypes are essential for the identification of the *in-vivo* role of a gene product at the cellular or organismal levels. To date, the function of LTP family members have been genetically investigated, revealing a wide range of biological roles primarily related to the plant immune response and defense mechanisms (García-Olmedo *et al.*, 1995). Of the 49 members of non-specific LTPs, only the LTP5 gain-of-function mutant has been reported to be involved in plant fertilization (Chae *et al.*, 2009). While none of the *ltp2/ltp5* single knockout mutants exhibited a fertilization phenotype, we next characterized the different double knock-out mutants of *ltp2ltp5* to investigate if the loss of function of two genes has any effect on the fertilization process and pollen tube guidance mechanism in *Arabidopsis*. For this purpose, we performed different *in-vivo* cross pollination and *in-vitro* pollen tube growth assays in combination with seed count analysis.

5.15. Characterization of mutant lines #P9-P2-P2 and #P9- P3-P3

Mutation spectrum of the CRISPR/Cas9 edited LTP2 and LTP5 gene

Since the designed gRNAs were positioned in the coding region, EPC-CRISPR/Cas9 based indel mutations often caused a frameshift, resulting in a non-sense mutation with a premature stop codon. Only the large deletion in some of the mutants of *ltp2ltp5* resulted in an in-frame mutation. In mutant #P9-P2-P2 there was in-frame mutation due to the deletion of 18bp in LTP2 and 33bp in LTP5 genomic region, respectively (Fig. 4.25 A, B). The in-frame mutation did not alter the cystine motifs which are essential for the proper folding of LTP protein providing the correct configuration to function. While in mutant #P9-P3-P3 there was frameshift mutation for LTP2 gene but in-frame mutation for LTP5 as depicted in (Fig. 4.25 A, B). Therefore, mutant #P9-P3-P3 was a loss-of function for LTP2 which did not differ phenotypically from wild-type plants. We also examined the pollen germination/viability *in-vitro* (Fig. 4.25C) and analyzed the *in-vivo* pollen tube growth in a fully developed flower by doing aniline blue-staining (Fig. 4.25D).

The *in-vitro* pollen germination and tube elongation of #P9-P2-P2 and #P9-P3-P3 pollen grains showed no significant difference to the wild type. The aniline blue staining of stage 12 naturally self-pollinated flowers from #P9-P2-P2 and #P9- P3-P3 showed normal pollen tube growth similar to control wild-type plants. The seed count from #P9-P2-P2 and #P9- P3-P3 were also comparable to those of the wildtype plants. Therefore, both the mutant lines #P9-P2-P2 and #P9-P3-P3 showed no obvious distinguishable phenotype to the wild-type plants.

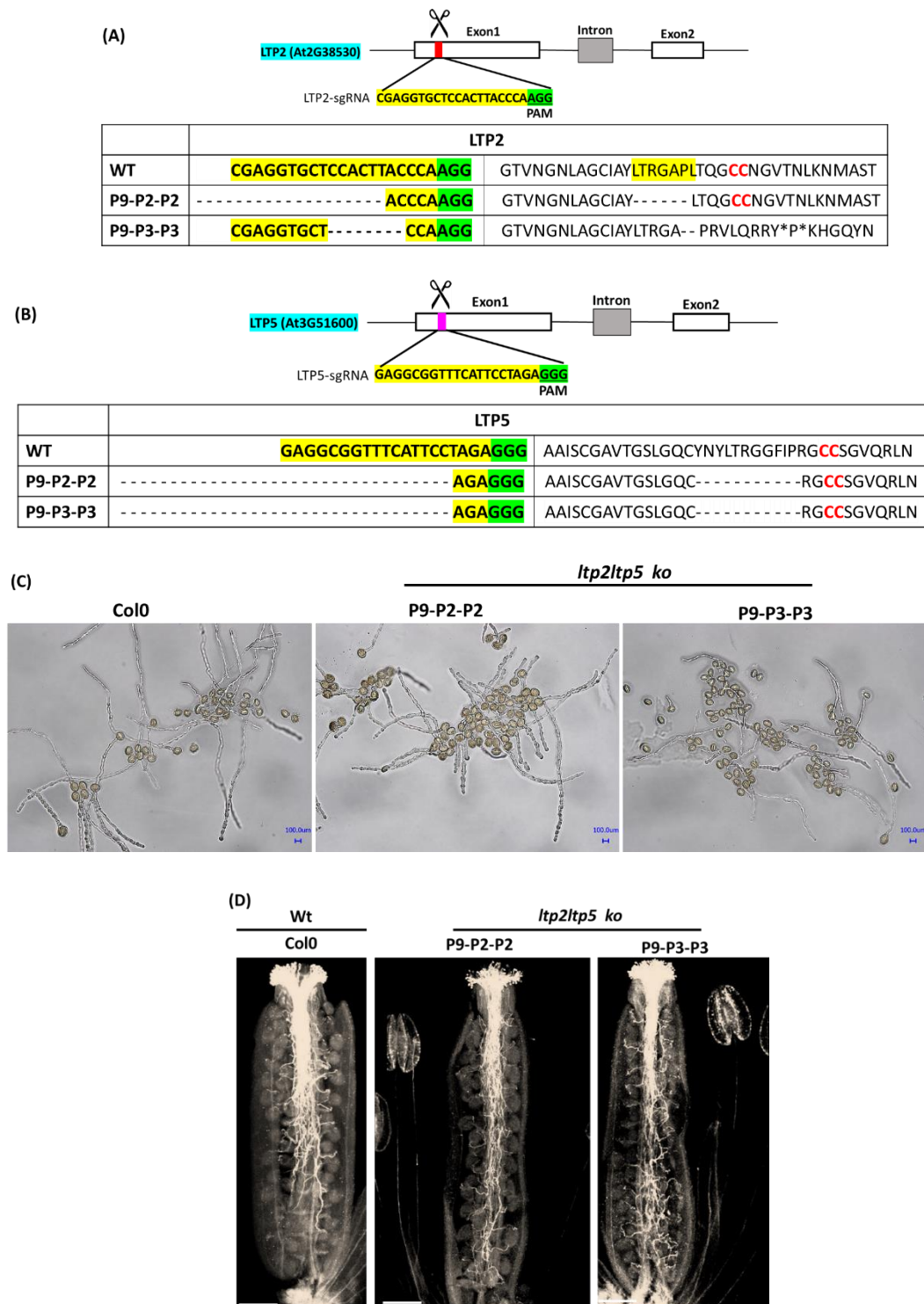


Fig. 4.25: Genotypic and phenotypic analyses of *ltp2ltp5*-ko mutant lines #P9-P2-P3 and #P9-P3-P3. (A, B) The targeted site in the AtLTP2 genomic region. The sgRNA^{AtLTP2} is located in the first exon (132 bp downstream of the start codon), while sgRNA^{AtLTP5} is located in the first exon (133 bp downstream of the start codon). The sgRNA^{AtLTP2} and sgRNA^{AtLTP5} sequence are highlighted in yellow and PAM in green. The black scissor indicates the targeted position. Sanger sequencing results of *ltp2ltp5*-ko mutants generated by the EPC CRISPR/Cas9 pHEE401 system in T2 generation. Deletion are indicated by dots. (C) The in-vitro and (D) *in-vivo* pollen germination and tube elongation of mutant lines #P9-P2-P3 and #P9-P3-P3 pollen grains showed no significant difference to the wild type. Scale bar: 100um.

5.16. Characterization of *ltp2/ltp5* mutant lines #P31-P2 and #P31-P3

Among the four *ltp2/ltp5* mutants, there was no distinguishable phenotype for the transgenic lines #P9-P2-P2 and # P9-P3-P3 in comparison to the wild-type plants. Moreover, transgenic lines #P31-P2 and #P31-P3 showed aberrant callose deposition with misguided pollen tubes and severe defects in the seed formations.

In mutant #P31-P2, a deletion of single cytosine nucleotide occurred 2bp before the PAM sequence of gRNA designed for LTP2 gene. Due to the single nucleotide deletion there was a frameshift in the exonic sequences of LTP2, which changes the two-cysteine residue (Cys-54 and Cys-55) into alanine (Fig. 4.26A). For mutant #P31-P3, there was an insertion of single cytosine nucleotide, which results in premature termination of translation with the synthesis of 30aa peptide of LTP2. While for LTP5 gene, both the mutant lines #P31-P2 and #P31-P3 had an insertion of single thymidine before the PAM sequence of target LTP5 guide RNA. This insertion caused the frameshift mutation disrupting the reading frame of mRNA by introducing a premature stop codon (Fig. 4.26B). However, due to the frameshifts indel mutation and premature stop codons, it is most likely that the mRNAs are either degraded by nonsense-mediated decay (NMD) or truncated incomplete proteins are synthesized which are non-functional. The frameshift indel mutations in both the target genes LTP2 and LTP5 lead to the generation of double loss-of-function *ltp2/ltp5* mutants.

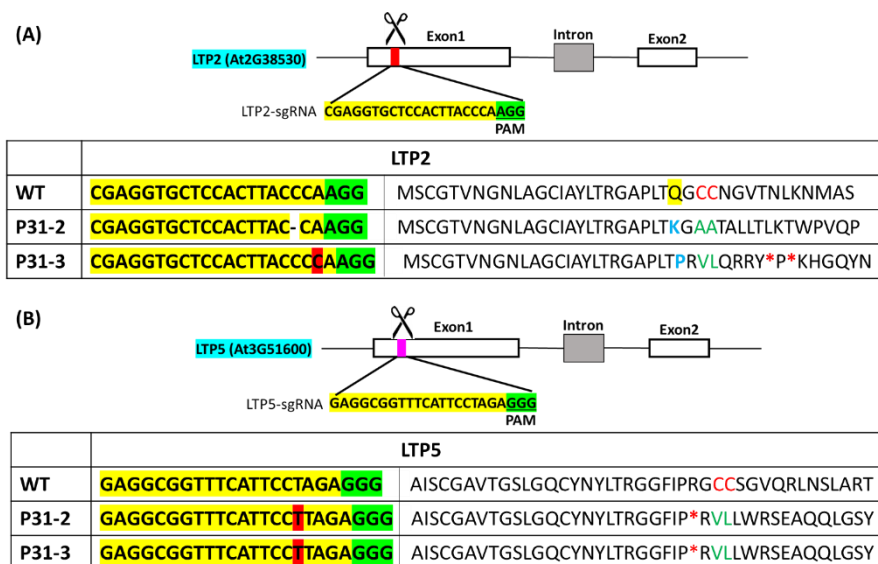


Fig. 4.26: Characterization of the EPC-CRISPR/Cas9 edited mutants #P31-P1, #P31-P2. (A, B) The targeted site in the AtLTP2 and AtLTP5 genomic region. The sgRNA^{AtLTP2} is located in the first exon (132 bp downstream of the start codon), while sgRNA^{AtLTP5} is located in the first exon (133 bp downstream of the start codon). The sgRNA^{AtLTP2} and sgRNA^{AtLTP5} sequence are highlighted in yellow and PAM in green. Deletion are indicated by dots and insertions are highlighted in red. Asterisk denotes pre-mature stop codon due to the mutation in the reading frame.

5.17. *ltp2ltp5* double mutant defect occurs in pollen and impacts pollen morphology and growth

Plants lacking functional LTP2/LTP5 proteins exhibit a severe defect in pollen morphology and viability. Although some pollen grains appeared normal, a significant number of abnormal and collapsed pollen grains were detected in the *ltp2ltp5* mutant lines #P31-P2 and #P31-P3 (Fig. 4.27 B,C). To study how *ltp2ltp5* mutation affects the male gametophytic function, we further examined the germination of *ltp2ltp5* pollen *in-vitro*. 45.54% and 35.6% of the viable pollen grains of #P31-P2 and #P31-P3 germinated *in-vitro*, compared to that 70.45% of the pollen grains from wild type plants germinated under the same growth conditions (Fig. 4.27D). This indicates that the *ltp2ltp5* mutants displays significantly reduced pollen germination rate *in-vitro* due to aborted pollen grains.

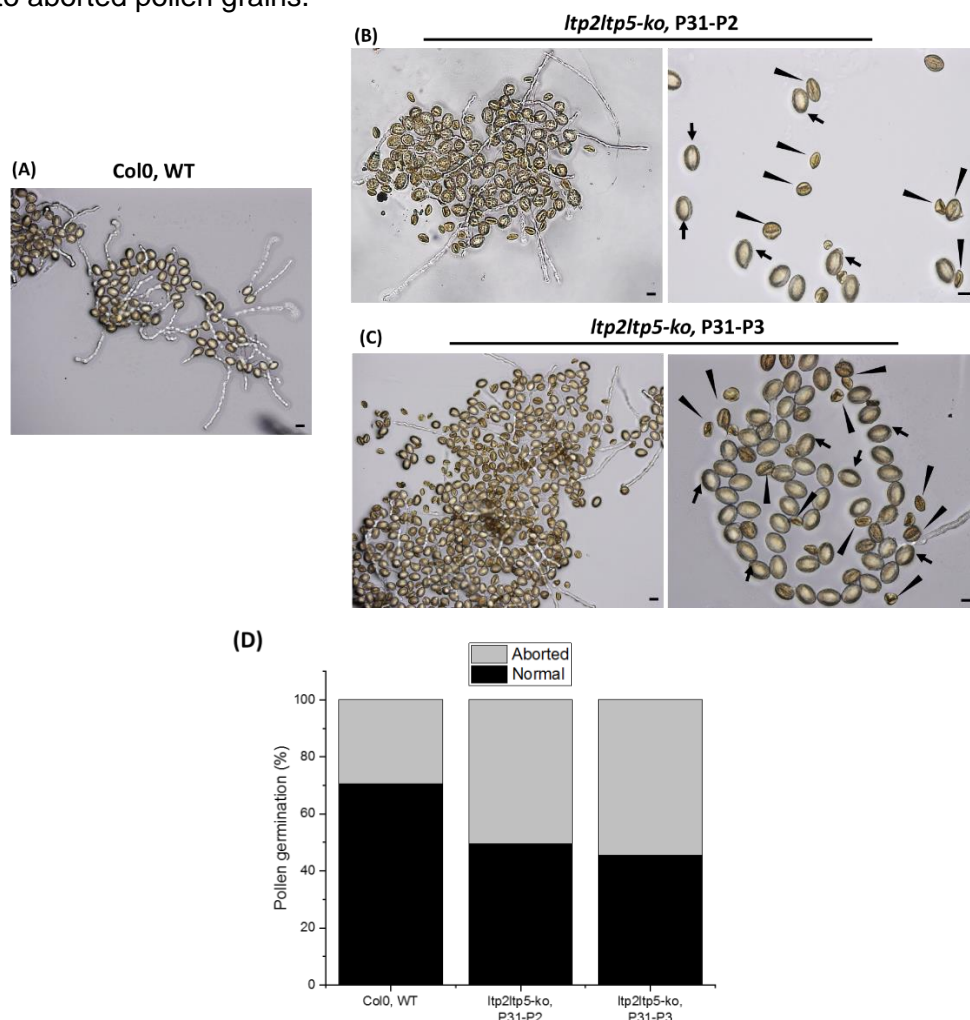


Fig. 4.27: Loss of function mutant *ltp2ltp5* confers aberrant pollen grain morphology and germination. In-vitro pollen tube growth assay. (A) Col-0 (B) *ltp2ltp5-ko* #P31-P2 (C) *ltp2ltp5-ko* #P31-P3 pollen tubes were grown on the solid medium for 6 hrs. There are two types of pollen grains: aborted (shrunken, indicated by arrow) and normal (arrowhead). (D) *In-vitro* germination efficiency for the wild-type and *ltp2ltp5-ko*.

5.18. Aberrant callose deposition in ovules of *ltp2ltp5* knock out mutants correlates with defective pollen tube guidance and reduced fertilization efficiency

Flowers from the *ltp2ltp5* mutant lines #P31-P2 and #P31-P3 were female sterile and produced significantly lower number of seeds in comparison to the wild-type plants. To further investigate whether the sterility is caused by pollen-pistil interaction, the *in-vivo* pollen tube growth in *ltp2ltp5* pistil from self-pollinated mature flowers of stage 14-15 (Smyth, Bowman and Meyerowitz 1990) was observed carefully. Aniline-blue was used to stain the callose plugs in the pollen tube cell wall to allow the detection of any abnormal morphology and growth defects of the pollen tube while growing through the pistil. The *ltp2ltp5* double knockout pollens were competent in germination and tube growth *in-vivo* (Fig. 4.28A), but many pollen tubes failed to turn at the micropyle, as shown in (Fig. 4.29 C-H). Moreover, for many cases, among the untargeted *ltp2ltp5* ovules, we often observed massive callose accumulation. In the mature *ltp2ltp5* ovules, callose accumulation was observed at the position where in wild-type ovules an embryo sac is formed (Fig. 4.28A). Many ovules had no pollen tubes in the vicinity indicating funicular and micropylar defects in pollen tube guidance, whereas *ltp2ltp5* double mutant pollen has lost the competence to shift its directional growth at the micropyle (Fig. 4.29C-H). In contrast to that, in some cases, wild-type ovules attracted multiple pollen tube suggesting defect in pollen tube guidance (Fig. 4.29 I-M).

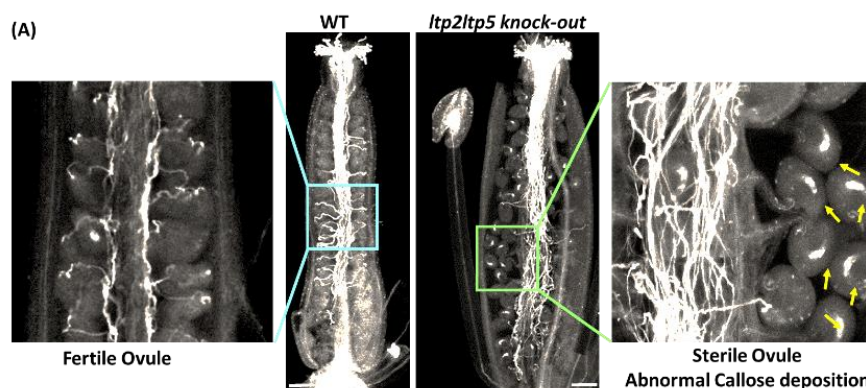


Fig. 4.28: Aberrant callose deposition in *ltp2ltp5-ko* mutants #P31-P2 and #P31-P3. (A) Compared to the wild type, several self-pollinated ovules of *ltp2ltp5-ko* mutant showed massive abnormal deposition of callose (indicated by yellow arrow) around the nucellus region of the embryo sac. Scale: 100µm.

Contrary to wild type, *ltp2ltp5* double knockout mutants (#P31-P2 and #P31-P3) self-pollination revealed clear abnormalities to pollen tube growth morphology and defect in the guidance mechanism. The pollen tubes showing abnormal pollen tubes attraction and pollen tube reception in *ltp2ltp5* mutant pistils include three types: (1) failure to attract pollen tube towards the micropyle of mutant ovules with callose deposition (2) inability of pollen tube to burst and release the sperm cell (3) multiple pollen tube targeting causing fertilization failure.

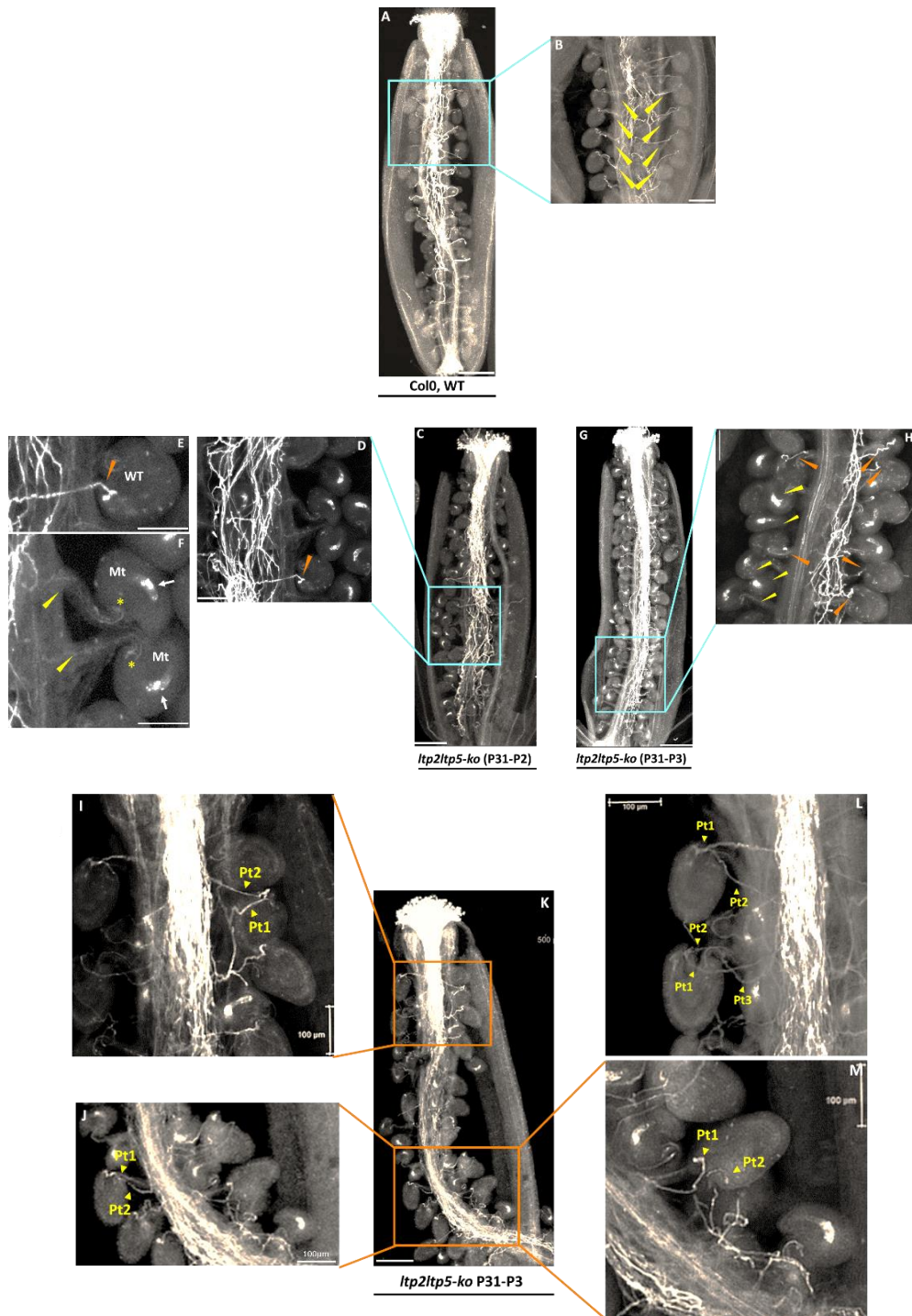


Fig. 4.29: Defective pollen tube guidance and decreased ovule-targeting ability observed in the *Itp2ltp5* mutant lines #P31-P2 and #P31-P3. Confocal fluorescence microscopy images of self-pollinated *Itp2ltp5* mutant pistils emasculated from stage 12 mature flower. Staining of callose walls with aniline-blue. **(A,B)** The pollen tube was attracted normally to the wild-type ovules in the self-pollinated wild-type pistil (indicated by yellow arrowhead). In self-pollinated *Itp2ltp5* mutants **(C-F)** (#P31-P2) and **(G-H)** (#P31-P3) mutant ovules (Mt) failed to attract pollen tubes to its micropyle (indicated by yellow arrowhead) in comparison to Wt ovules (indicated by orange arrowhead). Pollen tubes only grow towards the ovules where callose is degraded or absent. **(I-M)** The wild-type ovules were detected with multiple pollen tube targeting by a single micropyle. Scale: 100 μ m.

In *Itp2ltp5* mutant plants, we observed a remarkably reduced seed set due to aborted ovules (41% in #P31-P2 and 52% in #P31-P3, respectively) (Fig. 4.30 A, C) and smaller siliques in

comparison to the wild-type plants (Fig. 4.30 B, D). Taken together, our results demonstrate that in *ltp2ltp5* double knockout plants, abnormal callose accumulation in the embryo sac resulted in pollen-tube misguidance causing ovule abortion and fertilization defects.

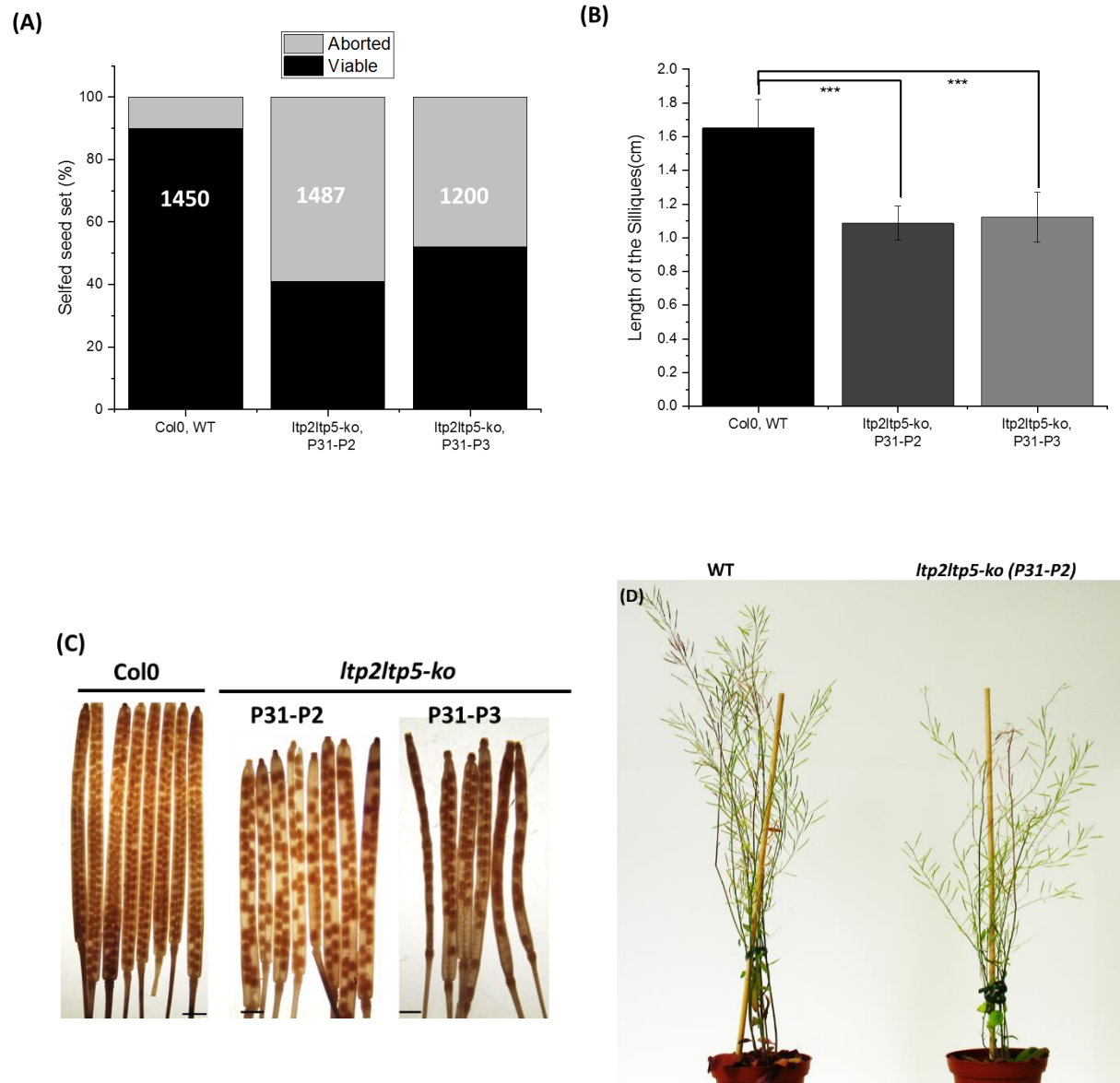


Fig. 4.30: The *ltp2ltp5* mutants #P31-P2 and #P31-P3 are semi-sterile and showed reduce seed set due to defect in the female gametophyte. (A) The reduced seed set defect in *ltp2ltp5* mutant #P31-P2 and #P31-P3 in comparison to the wild-type. Total number of seeds analyzed are in the center of each column. **(B)** Sizes of mature siliques from self-pollinated plants were analyzed. Data are shown as mean \pm SD. **(C)** Siliques of the wild type are filled with seeds, whereas *ltp2ltp5* mutant siliques show severe seed abortion. Mature siliques were de-stained with 100% ethanol to examine seed sets ($n = 60$). Bars = 1 mm. For (B) the error bars and asterisks indicate values that differ significantly from those of the wild-type plant (*, $P < 0.05$; **, $P < 0.01$; and ***, $P < 0.001$, calculated using Student's t test). **(D)** Photographs of 6-weeks old wild-type Col-0 and *ltp2ltp5* mutant #P31-P2 plant.

5.19. Loss of LTP2LTP5 causes a maternal effect seed abortion phenotype

Our previous results supported female gametophytic defect, but the phenotype is also manifested in the male gametophyte, we therefore tried to understand to what extent the two gametophytes contribute to the invading pollen tube and the fertilization efficiency. Toward this objective, reciprocal crosses between wild-type and *ltp2ltp5* mutant #P31-P2 and #P31-P3 plants were performed as described below (Fig. 4.31) and pistils were analyzed 24 HAP.

When wild-type pistils were pollinated with wild-type or *ltp2ltp5* mutant pollen, neither the callose deposition nor any defective pollen guidance phenotype were observed (Fig. 4.31 E, F). In contrast, pollinated *ltp2ltp5* pistils always showed massive deposition of callose in the ovules, and defective pollen tube targeting towards the ovules regardless of whether the pollen was derived from wild-type or *ltp2ltp5* plants (Fig. 4.31 B, C). These data suggested that most of the deformation occurs close to the ovule or at the micropyle. This suggests that pollen tube guidance in *ltp2ltp5* mutants is relatively affected at certain phases of the pollen tube growth through the pistils and the mutation predominantly affects the pistil.

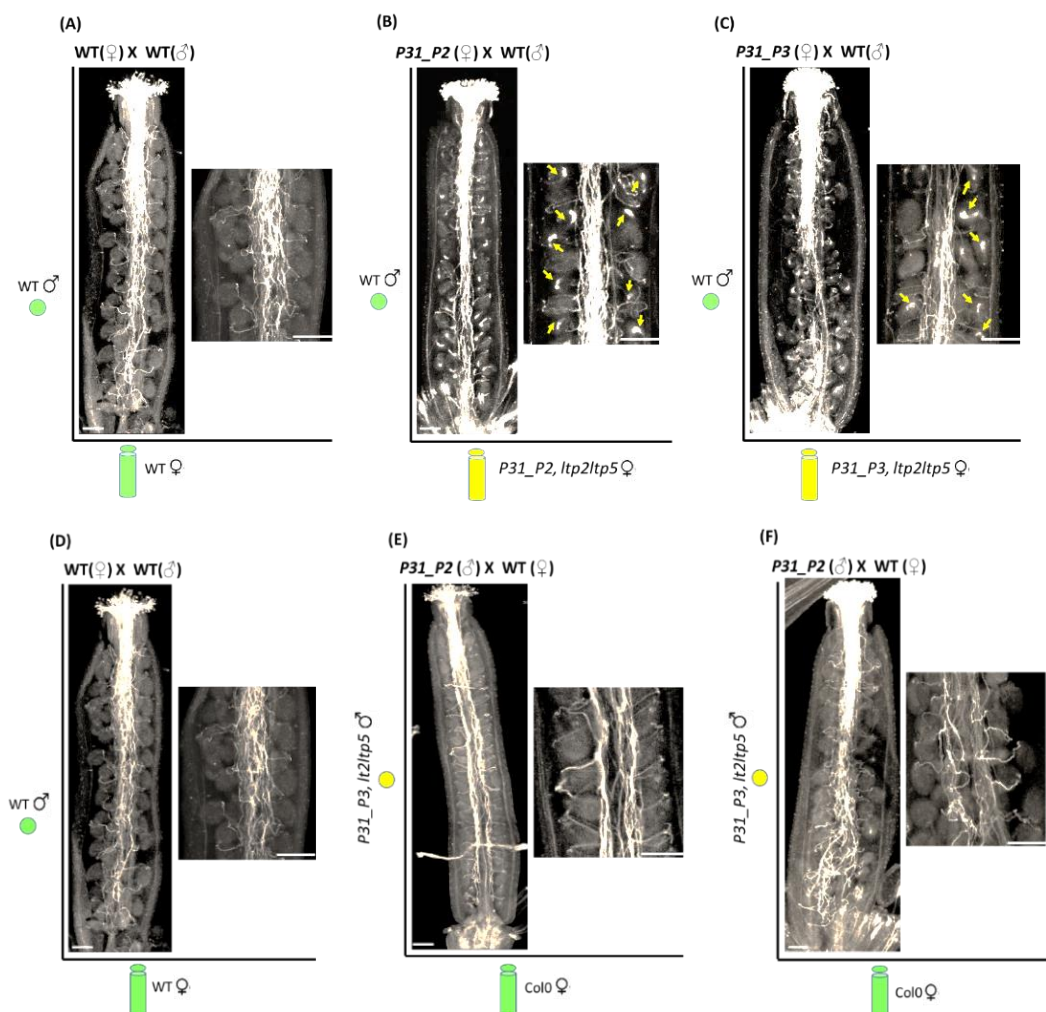


Fig. 4.31: Detection of abnormal pollen tube guidance in self and cross-pollination between *ltp2ltp5* and Wt plants. *In-vivo* reciprocal cross-pollination of *ltp2ltp5* (#P31-P2 and #P31-P3) to the wild-type plants (**A, D**) Wild-type pollen as donor and wild-type pistils as acceptor (**B, C**) Wild-type pollen as donor and #P31-P2, #P31-P3 pistils as acceptor. Callose deposition in the mutant ovules are indicated by arrowhead. (**E, F**) #P31-P2, #P31-P3 pollen as donor and as wild-type pistils acceptor. No callose deposition was observed in the wild-type ovules when pollinated with mutant pollen, indicated by asterisk. Aniline-blue staining after 24HAP shows *in-vivo* pollen tube growth (n=10). Scale: 100µm.

5.20. Callose deposition dynamics in *ltp2ltp5* and wild-type plants

Callose (β -1,3-glucan polymer) plays an essential role in female reproductive development. During the early ovule development, at the megasporogenesis stage, the megaspore mother cell accumulates callose in the cell walls during meiotic divisions. As reported by (Webb *et al.*, 1994) and (Kay Schneitz†,*, Martin Hülskamp‡, 1997), callose is present in all ovules at the onset of cytokinesis and tetrad after meiosis. It appears in the sporocyte wall at the early stage of meiotic prophase I and disappears at the tetrad stage of ovule development. After meiosis, callose degrades during the process of embryo sac development which begins the transition from megasporogenesis to megagametogenesis (Newbiggin and Read, 2009). Our fluorescence microscopy data revealed massive callose deposition in the *ltp2ltp5* fertilized ovules in comparison to the wild-type flowers.

In order to determine the callose depositions more precisely, ovules were dissected at different developmental stages and stained with aniline blue to visualize callose in the developing ovules as shown in the (Fig. 4.32). Fluorescent callose around megaspores is visible for both wild-type and *ltp2ltp5* ovules (Fig. 4.32 A, E). At later stages of megagametogenesis (stages 3-V, eight-nuclei embryo sac and 3-VI, mature embryo sac) (Schneitz *et al.*, 1995), no callose was visible in the WT ovules (Fig. 4.32 C, D). In contrast, in the *ltp2ltp5* mutant ovules at stages 3-V and 3-VI, stronger fluorescence was observed in the majority of the ovules (Fig. 4.32 F, G). Callose gradually degraded during the process of embryo sac development and almost disappeared upon embryo-sac maturation as observed in the ovules of self-fertilized wild-type plants (Fig. 4.32D), but the presence of callose was still visible after pollination in *ltp2ltp5* self-fertilized plants (Fig. 4.32H). High levels of callose remained in the nucellus region of embryo sac during the late development of female-sterile *ltp2ltp5* ovules in comparison to wild-type.

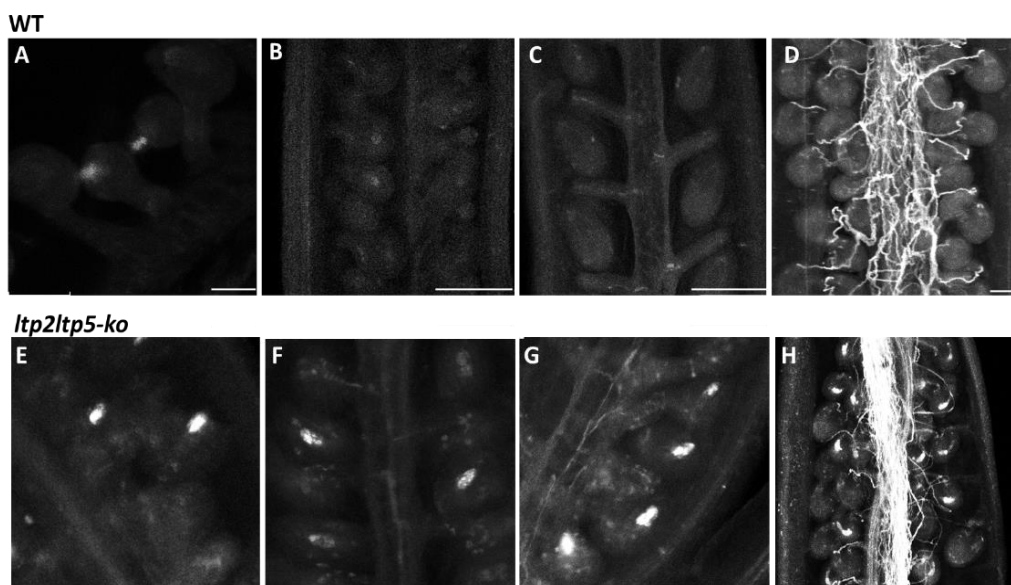


Fig. 4.32: Analysis of callose deposition pattern in wild-type and *ltp2ltp5* mutant ovules. (A, B, C, D) Wild-type ovules during megasporogenesis and megagametogenesis. **(A)** Visible callose staining around the megaspores. **(B)** Stage 3-II (two-nuclear embryo sac), faint callose is visible in the young developing ovules. **(C)** No visible callose deposition at stage 3-V (eight-nuclei embryo sac). **(D)** No visible callose at postfertilization stage (4-VI), mature fertilized flower. **(E, F, G, H)** Ovule development of *ltp2ltp5* mutant. **(E)** Visible callose deposition in the megaspores. **(F)** Ovule showed fluorescent callose at stage 3-II (two-nuclear embryo sac). **(G)** Stage 3-V (eight-nuclei embryo sac), increased amount of callose deposition in the ovules. **(H)** After fertilization, callose deposit still persist in the ovules. Scale: 100µm.

5.21. Deposition of callose in the synergid cells at the micropylar region

To locate the exact position of callose deposition in the ovules, callose staining was performed on the 2µm semi-thin sections of ovules from matured flowers (stage-14) embedded in Technovit-7100 resin. Fluorescence microscopy revealed almost no callose deposition in the embryo sacs during the course of ovule maturation in wildtype plants, and callose began to degrade and only thinned callose walls were visible in the mature embryos (Fig. 4.33 A-E). In contrast, callose deposition in the *ltp2ltp5* mutant lines (#P31-P2 and #P31-P3) concentrated around the synergid primarily deposited at the micropylar end with the development of the embryo sac (Fig. 4.33 G-L). There was clear callose accumulation in the mature embryo sacs of *ltp2ltp5* mutant plants.

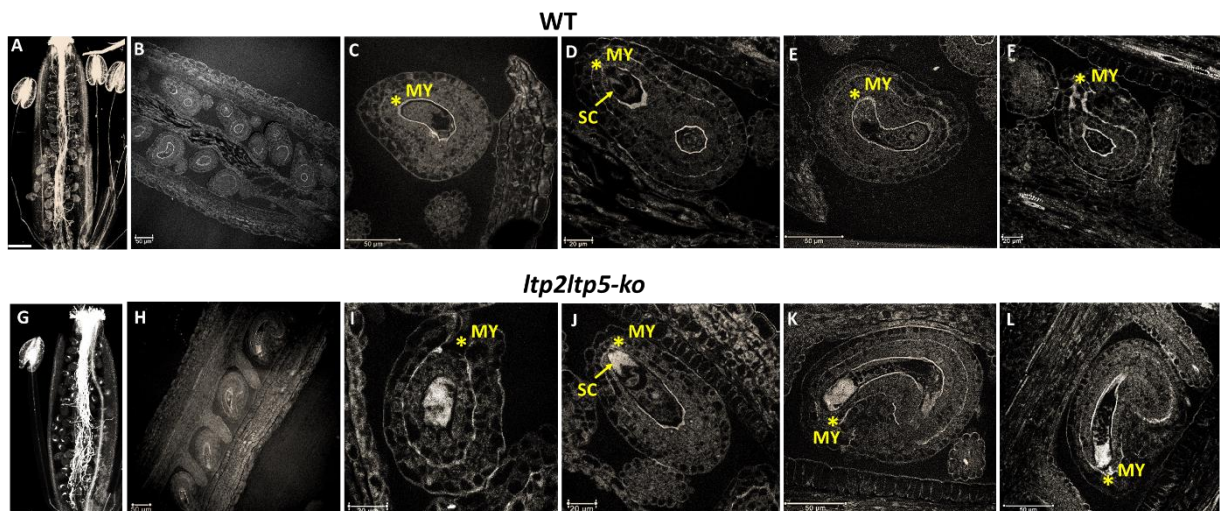


Fig. 4.33: Callose deposition during embryo sac development in wild-type and *ltp2ltp5* plants of *Arabidopsis thaliana*. (A-E) Wild-type **(G-L)** *ltp2ltp5* ovules undergoing embryo sac maturation. Scale: 50µm. MY: Micropylar end, SC: Synergid cells.

6. DISCUSSION

Based on bioinformatic analyses that provided evidence for the expression of various LTPs in reproductive tissues, this work focused on the elucidation of their putative role in the fertilization process of *Arabidopsis thaliana*. Our qPCR expression analyses confirmed the *in-silico* studies and further showed the up-regulation of six members of Type-I nsLTP genes in pollinated pistils in comparison to non-pollinated pistils isolated from closed buds. This observation suggests that the pollination event is recognized by the female tissue and strengthens the hypothesis that LTPs regulate the pollen tube journey through the female tissues and/or towards the ovules. During sexual reproduction in angiosperms, pollen performance, i.e. the success of pollination, is indeed greatly influenced by the female tissue. Since LTPs harbor a signal peptide they are able to localize in the extracellular matrix (ECM) (Yeats and Rose, 2008). LTPs expressed in the stigma and style, such as LTP2 and LTP5 may thus already play a role in pollen adhesion. Those LTPs may function in the formation of an adhesive pectin matrix facilitating the directional growth of the pollen tube during the pollination, a function similar to SCA (Stigma/Style Cysteine-rich Adhesin) in lily (Park *et al.*, 2000; Park and Lord, 2003). Numerous lines of evidence suggest that cysteine-rich peptides play a pivotal role in plant reproduction - inducing pollination (Schopfer *et al.*, 1999), pollen tube guidance (Muschiatti *et al.*, 1994; Tang *et al.*, 2004; Chae *et al.*, 2009), attraction and gamete fusion (Okuda *et al.*, 2009; Amien *et al.*, 2010). Thus, like those secreted cysteine-rich peptides, in general, LTPs in particular, might function in multiple signaling events during the pollen-pistil interactions, initiating at the stigma during pollination and ending at the micropyle with pollen tube reception.

6.1. LTPs differential expression patterns in *A. thaliana* reproductive tissue

GUS-reporter aided localization and expression analysis of six members of *Type-I nsLTP* genes (*LTP1*, *LTP2*, *LTP3*, *LTP4*, *LTP5*, *LTP6* and *LTP12*) displayed distinct but also overlapping gene expression patterns during seedling growth (see Result, Fig. 4.4, 4.5) as well as during flower development (Fig. 4.4). In the *Arabidopsis* flower, only *LTP2* and *LTP5* were expressed in the stigma during the young bud stage of the mature flowers. The spatial-temporal expression of *LTP2* and *LTP5* genes in the stigma cells suggests their plausible role in the synthesis and secretion of the stigmatic exudate to facilitate pollen adhesion and hydration. Moreover, in the stylar region of the pistil where the pollen tube grows to reach the ovules, *LTP2*, *LTP3*, *LTP4*, *LTP5*, *LTP6* and *LTP12* exhibited overlapping expression patterns, suggestive for their function in providing competency during the pollen tube growth and guidance into the transmitting tract (TT). Furthermore, the presence of *LTP2*, *LTP3* and

LTP5 in the primary female reproductive tissues – the funiculus, the ovules and the transmitting tract, strengthens the putative role of LTPs during pollen tube growth and ovular guidance. This observation is in line with several studies in *Arabidopsis*, showing that *LTPs* are expressed in the pistil and TT where pollen tubes grow (Thoma *et al.*, 1993; Arondel *et al.*, 2000; Tung *et al.*, 2005). To date however, except for a *LTP5* gain-of function mutant, no-other nsLTP has been functionally characterized with respect to its function in pollen tube guidance. Notably, the majority of peptides reported to be involved in the communication and signaling process during fertilization and seed development are secreted, extracellular CRPs. A molecular survey of several reproductive tissues (like pollen and ovary) in *Zea mays*, revealed the prominent expression of genes coding for different CRP groups, like DEFLs and RALFs, possibly contributing to the reproduction process in maize (Li *et al.*, 2014). Alike many other CRPs, *LTPs* are suggested to be secreted to the apoplast to exert their possible function in pollen adhesion, directional growth and guidance of pollen tube and seed development. The subcellular localization of *LTPs*, however, has only been analyzed for a few members of this big protein family.

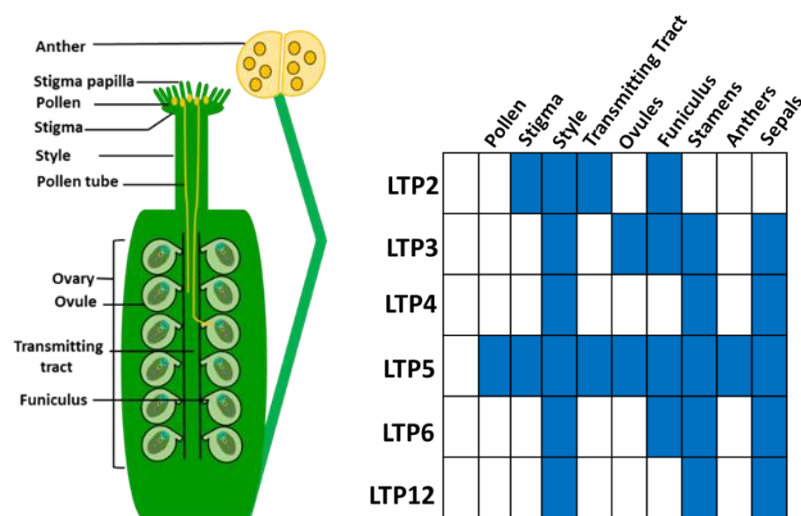


Fig. 5.1: A schematic representation of the reproductive structures and tissues of *A. thaliana* and the distribution of the six Type-I nsLTPs based on *PromLTP::GUS* expression

6.2. Subcellular localization of LTPs

Plant lipid transfer proteins are synthesized in plant cells as preproteins containing a N-terminal hydrophobic signal sequence, which should guide protein localization predominantly to the extracellular space. To test this prediction, we performed subcellular-localization studies for the six selected LTPs, using a transient expression assay in *Nicotiana benthamiana* pavement cells. In contrast to *in-silico* predictions, these studies revealed two distinct types of localization

patterns: AtLTP2, AtLTP5 and AtLTP6 were found to localize at the plasma-membrane as well as in cell wall compartments whereas, AtLTP3, AtLTP4 and AtLTP12 were detected exclusively in the plasma-membrane. In contrast to LTPg type G LTPs (Lee *et al.*, 2009), AtLTP3, AtLTP4 and AtLTP12 proteins do not harbor a glycosylphosphatidyl anchor (GPI anchor) nor a transmembrane domain. Therefore, the association of these LTPs, as a peripheral protein, with the plasma membrane would probably rely on ionic-protein-lipid interaction and hydrophobic stability. On a similar line, there was a report on rice, where it was shown that rice nsLTP110 binds to the proteinaceous molecule or domain on the plasma membrane, possibly mediating as ligand-receptor complex and activating the downstream response (Wang *et al.* 2009). It was further suggested that in line with the relatively high abundance of LTPs with redundant functions, some of the LTPs can be characterized as “cytosolic lipid holders” rather than “inter-membrane lipid carriers (Hanada, 2018). Besides an extracellular localization, some LTPs, were also reported to be targeted to intracellular organelles; like LTPs from castorbean seeds which were found in glyoxysomes (Tsuboi *et al.*, 1992), and another LTP from cowpea (*Vigna unguiculata*) seeds was localized in protein storage vacuoles and in lipid-containing vesicles (de O. Carvalho *et al.*, 2004). A recent report further correlated the dynamic distribution and trafficking of apoplastic LTPG, in response to change in cell shape and curvature during cell growth and differentiation. Localization of LTPG to its functional site changes from plasma membrane to apoplast at different stages of development in developing leaf and hypocotyl cells of *A. thaliana* (Ambrose *et al.*, 2013). There are also reports which suggest that synthesis and localization of those LTPs which belong to the family of pathogenesis-related proteins (PRPs), is triggered and re-directed upon exposure to various types biotic and abiotic stress (Masuta *et al.*, 1991). Taken together, this might explain the broad localization pattern for LTPs, primarily in the apoplast, plasma membrane and in ER networks. It should be noted further that ectopically expressing LTPs using the *Agrobacterium* infiltration method, can induce dynamic changes in the gene expression pattern in the host cell, possibly affecting the expression and localization of the test protein. The high protein production levels driven by a strong, constitutive promoter such as the cauliflower mosaic virus promoter (CaMV 35S) can invariably result in artifacts that may bias conclusion on the true subcellular localization. The overexpression of transgene under the progressive promoter CaMV 35S can also cause gene silencing often repressing the expression of transgene and thereby causing variability in the protein localization (Dehio and Schell, 1994), (Wassenegger and Pélissier, 1998). To rule out this possibility, we also expressed some of the LTPs like LTP3, LTP4 and LTP6 under their own native promoters in *N. benthamiana* cells. The transient expression showed that LTP3 and LTP4 was localized in plasma membrane, whereas LTP6 was detected in the cell-wall. Finally, *N. benthamiana* pavement cells might not provide the proper host cell type for some LTPs considering their specific expression profile

and the possibility that proper localization of any LTP protein might require specific interaction partners. To this end, it would be ideal to study the localization pattern of LTPs using stable transgenic plants expressing the translational YFP fusion under control of their native promoters.

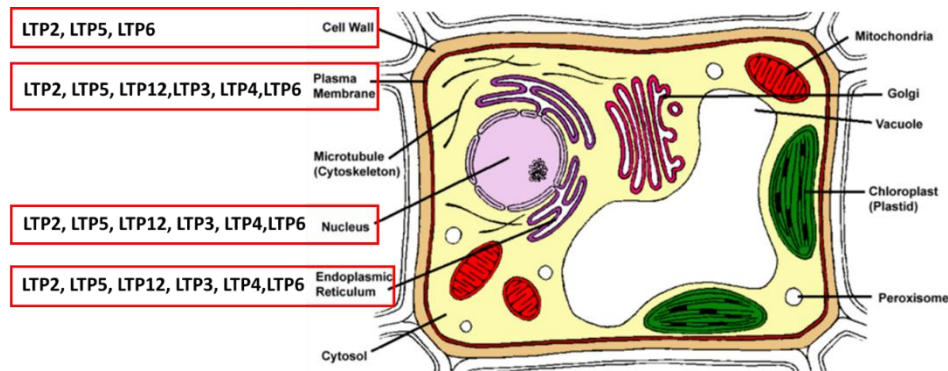


Fig. 5.2: Schematic diagram representing the subcellular localization of six Type-I nsLTP based on the transient expression in *Nicotiana Benthalian*.

6.3. Using CRISPR-Cas9 system gene-editing tool to create *ltp2/ltp5* double knock-out mutant

Possibly due to existing functional redundancy of LTP proteins, no single *ltp* knock-out mutant investigated in this study exhibited any obvious vegetative or reproductive phenotype, suggesting that LTPs might act in concert to exert their function. We therefore decided to generate double knock-out LTP mutants for LTP2 and LTP5. This pair was chosen, because both, LTP2 and LTP5, are expressed in the stigma, style, the transmitting tract and funiculus of the female gametophyte. In addition, and according to phylogenetic analyses, LTP2 and LTP5 are highly similar and group into the sub-clade of *Arabidopsis* type I LTPs. Since the corresponding single T-DNA mutants are in different genetic backgrounds (LTP2 in Col0 and LTP5 in WS), instead of crossings, we decided to employ the CRISPR-Cas9 gene editing technique to create a double knock-out. The CRISPR/Cas9 system is a multi-purpose technique which has been widely used in various species to generate targeted mutations for functional studies. To generate transgenic *Arabidopsis* lines, we used a vector system providing for germline egg cell-specific promoter (*EC1.2*; EPC) driven Cas9 expression. rather than using the constitutive Cauliflower mosaic virus (CaMV) 35S or ubiquitin promoter, which have been reported to produce mosaic-like mutations in the T1 generation (Feng *et al.*, 2013)

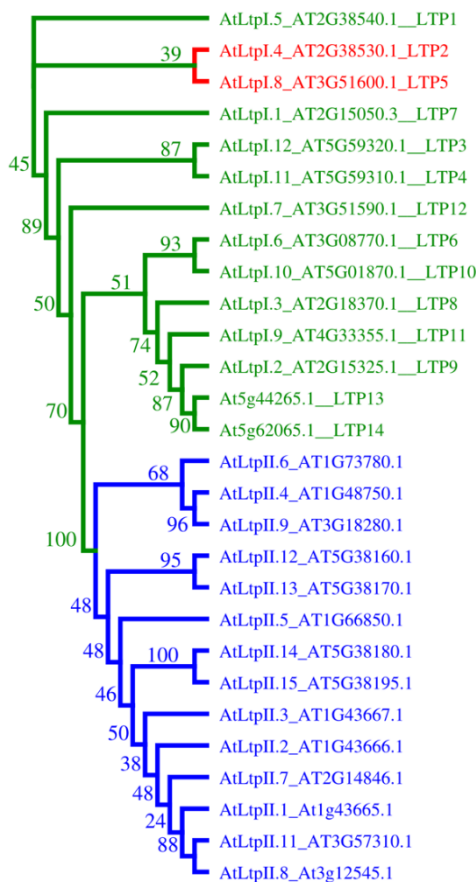


Fig.5.3: Phylogenetic analysis of *Arabidopsis thaliana* type I and type II LTPs: A phylogenetic analysis of *Arabidopsis* LTPs shows that type-I and type-II LTP proteins separate into distinct clades. Within the type-I clade the highly homologous LTP2 and LTP5 (60% identity, 85% similarity) share a common branch in the tree. Protein alignment was performed on sequences with the signal-peptide removed using MAFFT. Phylogenetic distances were calculated with IQ-Tree using standard parameters with 1000 bootstrap alignments

Another drawback for the CaMV 35S system is that variously non-heritable mutations can be created in many somatic cells (Feng *et al.*, 2013; Mao *et al.*, 2013). Thus, the rationale behind using EPC controlled CRISPR/Cas9 system was to obtain the genome-edited mutation exclusively in gametes. This has been shown to produce non-mosaic T1 mutants for multiple target genes with high efficiency within a short span of time. Using the EPC CRISPR/Cas9 pHEE401 binary vector, we were able to generate numerous mutants for both LTP2 and LTP5 already in the T1 generation. However, it appeared that upon self-fertilization of the T1 plants, CRISPR/Cas9 mediated genome-editing of the respective target sites continued and *ltp2ltp5* double knock-out mutants were obtained in the T2 and T3 generations. In our mutant analysis we screened our T2 and T3 plants based on sanger sequencing, and the homozygous plants for both the genes were further confirmed by deep sequencing. Finally, the selected mutants, #P31-P1 and #P31-P2 were proven stable in the next generation, without any new modifications at the target sites. These studies show that CRISPR/Cas9 is present and active in egg cells of every new generation, which would impede verification of LTP function/phenotypes via complementation or genetic allelic tests. Therefore, it would be desirable to isolate Cas9-free heritable CRISPR mutants in one of the *ltp2ltp5* mutants, which

would ensure the stable transmission of the identified mutations to the next generations in mendelian fashion. Screening of Cas9-free mutant lines is currently ongoing but could not be finalized within the time frame of this thesis. On the other hand, several reports suggest using an improved CRISPR/Cas9 system such as the MSC (meiocyte-specific CRISPR/Cas9) system. This construct can edit the targeted gene in question and the introduced Cas9 gene simultaneously, thus maintaining stable mutated alleles for further functional studies (Xu *et al.*, 2018).

6.4. *ltp2ltp5* mutants exhibit a female gametophyte dependent fertilization phenotype

In support of the hypothesis that LTPs might act in concert to exert their physiological function, we observed that the *ltp2ltp5* mutant produced shorter siliques and less seeds compared to either single mutants or wild types. Cross-pollination experiments together with cell-biology studies revealed that in the *ltp2ltp5* mutant pollen tubes rarely found their way to the ovules. Data from *ltp2ltp5* self-pollination and cross-pollination experiments between the *ltp2ltp5* mutant and wild-type plants are suggestive for the action of LTP2 and LTP5 in pollen tube guidance *in-vivo*. The observation that both wild-type and mutant pollen failed to fertilize the ovules in *ltp2ltp5* pistils, while mutant pollen could fertilize the wild-type ovules indicates a possible role of LTP that orchestrates the perception and final re-orientation of pollen tube and penetration into the micropyle. These results also explain the reduced seed set observed in the *ltp2ltp5* mutant and it indicates that the mutation affects the female gametophyte. In the search for the causal relationship between the observed fertilization phenotype and LTP function our cell biology studies together with aniline-blue based callose staining revealed that the mutations in LTP2 and LTP5 genes caused aberrant callose depositions in ovules of the *ltp2ltp5* mutant. Our result showed that in contrast to wildtype ovules, a massive callose accumulation was apparent in the embryo sac of *ltp2ltp5* mutants around the synergid cells at the micropylar end. In *ltp2ltp5* plants the percentage of callosized ovules was higher in comparison to the non-callosized ovules. Ovule sterility due to aberrant callose deposition impedes fertilization contributing to abortion and lower seed set. The β -1,3-glucan polymer callose plays an essential role in female reproductive development. Typically, during the early ovule development, at the megasporogenesis stage, callose acts as a temporary isolation barrier, preventing the meiocyte from cohesion/fusion. Later, its dissolution results in the release of free microspores. Thus, after meiosis, callose is degraded over the time course of embryo sac development which begins the transition from megasporogenesis to megagametogenesis (Newbigin and Read, 2009). Despite these findings, knowledge of the role of callose deposition in embryo sac development is limited. A similar phenotype of

abnormal callose deposition associated with a fertilization defect was also reported for the multi-pistil mutant (*mp1*) in *Medicago sativa* (Zhou *et al.*, 2016), the floral homeotic gene mutant *STERILE APETALA (SAP)* (Byzova *et al.*, 1999), as well as in the *Arabidopsis* female sterile mutants *bell1*, *short integuments (sin1)*, *47H4*, and *54D12* (Hulskamp *et al.* 1995). Several mutants that affect female gametophyte development in *Arabidopsis* have been described, though the majority of these mutants display aberrations in sporophytic as well as gametophytic tissues of the ovule. The sporophytic and megagametogenesis-defective (*smd*) mutants primarily showed defects in the diploid and haploid tissues of the ovule, while the megasporogenesis-defective (*msd*) mutant group encompasses mutation confined to spore development. Another class of mutants defective in ovule development is designated as embryo sac-defective (*emd*) mutants, specifically affecting megaspore/embryo sac development within the nucellus (Schneitz *et al.*, 1997). A recent report also suggested that mutations in *TURAN (TUN)* and *EVAN (EVM)*, two important members of the PT reception pathway mediated by the FERONIA (FER) receptor-like kinase (RLK), displayed pollen tube overgrowth and increased callose accumulation at the filiform apparatus. However, the callose accumulation at the micropylar region of *tun* and *evn* ovules did not mediate the failure in PT reception (Lindner *et al.*, 2015), which is contrary to our result in this study. The receptor like kinase FERONIA forms a complex with the GPI-anchored protein LORELEI (LRE) and secretory nodulin-like proteins (ENODLs) to mediate pollen tube reception. Recently in 2016, Yingnan and his colleague showed that loss of function mutations in *ENs* causes pollen tube burst and failure in pollen tube reception due to pollen tube overgrowth and abnormal callose accumulation in the embryo sac (Hou *et al.*, 2016). But in our study, the *ltp2ltp5* mutant ovules showed a total blockage of pollen tube growth into the embryo sac. We observed sustained presence of callose in the *ltp2ltp5* ovules starting from megaspore formation until embryo sac maturation, whereas in wild-type ovules the initially observed callose disappears upon embryo sac maturation. The massive accumulation of callose in the *ltp2ltp5* ovules could also result in functional megaspore dysplasia, leading to embryo abortion. The position of callosized ovules within the ovary was random in our study, indicating that sterility does not depend on the position of proximal vs distal ovules, which could be caused by inefficient metabolite and nutrient transport.

It should be noted that in wild-type plants, a sharp, but tiny callose barrier lines the boundary of the mature embryo sac and the engulfing integuments. Very thin tissue sectioning revealed that this boundary apparently opens towards the micropyle in wild-type ovules but is clogged with a callose plug in the *ltp2xtp5* mutants. Taken together, our result clearly demonstrates a novel role of LTPs in the homeostasis of complex barrier polymers in the form of callose which controls the plant fertilization process via a yet unknown mechanism.

6.5. Two female derived *LTP2* and *LTP5* genes are critical to proper pollen tube guidance

Pollen tube growth and guidance during plant sexual reproduction is broadly divided into six stages: (1) stigma penetration (2) pollen tube growth in style and transmitting tract (3) pollen tube -exit from the transmitting tract (4) funicular guidance (5) micropylar guidance and ovule targeting (6) pollen tube reception and gamete fusion (Johnson and Lord, 2006). Using aniline blue staining to examine *in-vivo* pollen tube growth, we showed that *ltp2ltp5* double mutant pollen grains were able to germinate and grow a tube invading the transmitting tract in the style. This is suggestive for a normal early sporophytic growth phase and guidance. Similar to wild type pollen, the double mutant pollen tube was capable of growing to the basal part of the transmitting tract but failed to change direction at the funiculus and exit the transmitting tract. This phenotype in funicular guidance is reminiscent to an *Arabidopsis* mutant, lacking the two pollen-tube expressed K⁺ transporters CHX21 and CHX23. *Chx21* and *chx23* pollen tubes grew normally through the transmitting tract but failed to shift their polarity to grow towards the funiculus (Lu *et al.*, 2011). Due to massive callose deposition around the nucellus, primarily at the micropylar region in the *ltp2ltp5* mutant ovules, pollen tubes obviously failed to sense/or respond to the funicular and micropylar guidance cues. The aberrant deposited callose may hence hinder the diffusion of pollen tube attractants from the synergid that guide the pollen tubes into the embryo sac, eventually resulting in female sterility in *ltp2ltp5* plants. Using intact pistils in these experiments we cannot clearly distinguish whether the observed guidance defect resulted from an impairment of the growing pollen tube to exit the septum of the transmitting tract or the inability to shift its direction and to turn toward the funiculus. Further studies using semi *in-vivo* assays should be performed using excised styles (where the barrier to exit the TT is abolished) together with isolated ovules placed in front of the pollen tubes to distinguish between a funicular or micropylar guidance defect. The AMOR controlled priming process of the pollen tube during its early growth phase is also considered a critical process, rendering the pollen tube competent to perceive ovular guidance cues (Higashiyama *et al.*, 1998), (Palanivelu and Preuss, 2006). Secreted stigma-stylar small cysteine adhesion (SCA) like LTPs present in the pistil are also proposed to provide competency to the growing pollen tube for perceiving further guidance signals released by the ovule in an unknown mechanism (J.,-C., Mollet *et al.*, 2000; Chae *et al.*, 2009). However, how LTPs are involved in the priming process is unknown. As previously reported, a gain-of-function mutant of *LTP5* (SALK_104674) leads to delayed *in-vitro* pollen tube growth and bulged pollen tube formation with low fertility and reduced seed set. The authors suggested that *LTP5* might be secreted from the pollen tube and function in maintaining pollen tube polarity. Pertaining to the known facts concerning the role of LTPs, our results point to a critical role of *LTP2* and *LTP5*, present

in the transmitting tract of the pistil, regulating or representing chemotropic cues, which play a crucial role in the gametophytic phase where the growing pollen tube changes its polarity and enters the funiculus sensing the guidance signal to enable precise targeting of the ovules. These findings opened up the possibility that presence of these small peptides in the transmitting tract might also act as a ligand for pollen tube receptors (e.g. PRK, pollen receptor-like kinases) and thus act in an autocrine manner, or may act as pollen-derived interaction partners of the synergid-localized receptor-like kinase FER (FERONIA) to induce male-female communication events. Very recently it has been shown that CRPs of the RALF peptide family represent the ligands for *Catharanthus roseus* RLK1 receptor-like kinases (CrRLK1L) such as FERONIA (FER) or ANXUR (ANX) and BUDDHA PAPER SEAL 2 (BUPS2) to regulate root growth and immunity or pollen tube growth and integrity, respectively. Interestingly, the interaction of FER with RALF23 peptides requires the LORELEI (LRE)-LIKE GLYCOSYLPHOSPHATIDYLINOSITOL (GPI)-ANCHORED PROTEIN 1/2/3 (LLG1/2/3). On the other hand, BUPS2, but not ANX1, binds a LLG3-RALF4-folded complex. Since RALFs, like LTPs, represent folded, disulfide bond-stabilized proteins, it is tempting to speculate that LTPs expressed in the transmitting tract of the pistil can also bind to receptors expressed on the pollen tube in a paracrine manner. Therefore, the identification of LTP interacting proteins including the possible receptors of these small cysteine rich signaling peptides would provide more insight into their potential role in pollen tube guidance.

6.6. How does LTPs connect to the callose homeostasis?

The abnormal deposition of callose in the *ltp2ltp5* ovules indicates that the loss of LTP2 and LTP5 function affect callose metabolism, disturbing the homeostasis between its synthesis and degradation. Callose deposition in the cell wall, in plasmodesmata or sieve tubes of the phloem is mediated by callose synthases (CalS), while hydrolytic enzymes β -1,3-glucanases (BGs) provide for callose degradation (De Storme and Geelen, 2014). Any alteration in the timing of BGs expression or failure to express BGs can lead to abnormal dissolution of callose wall, which has been shown to be a primary cause leading to male sterility in petunia and sorghum (Izhar and Frankel, 1971). There are numerous lines of evidence which suggest an important role for callose in multiple physiological and developmental processes (Chen and Kim, 2009). This includes the control of plant morphogenesis and organ formation, the regulation of information shuttling across symplastic connections (eg. plasmodesmata) or the reinforcement of the cell wall matrix upon pathogen invasion. Very few reports support its role in plant reproduction. Except for their role in microsporogenesis during anther and pollen development (Foote *et al.*, 1994b; Hird *et al.*, 1993; Lalanne *et al.*, 2004), or the self-incompatibility response

during pollination (Dumas and Knox, 1983), the function of callose during plant fertilization is rather limited. The high expression of BG4 and BG5 confined to the transmitting tissue of the style and the septum in the ovary of the bud in *Arabidopsis* was associated with a possible function in loosening the cell-wall in the transmitting tissue during the growth of the pollen tube through the pistil (Delp and Tapio Palva, 1999). In addition, the stigma-stylar-specific extracellular glucanase SP41 from tobacco, which is a glycosylated polypeptide comprising more than 12% of the total soluble transmitting tract protein, exhibits a proposed role in regulating the physiochemical properties of the transmitting tract matrix (Ori *et al.*, 1990). Of note, CalS proteins represent multi-span transmembrane protein and BGs, as most LTPs, represent extracellular proteins tethered to the plasma membrane via a GPI-anchor.

The *Arabidopsis* genome encodes twelve types of callose synthases (CalS), eleven type-I GPI-anchored endo-1,3-beta glucanases and 20 type-II endo-1,4-beta glucanases, suggesting that callose metabolism is highly complex (Wu *et al.*, 2018; Iswanto and Kim, 2017). Using public available microarray gene expression data Geneinvestigator (Hruz *et al.*, 2008), a differential expression pattern for all CalS, and Type I/ Type II glucanases was profiled across various tissue samples, in particular inflorescences and siliques (see Fig. 5.4). A heat map for the tissue-specific expression profiles shows that only few CalS and glucanases were predominantly expressed in ovules. Among the twelve CalS, only two, namely CalS3 and CalS8, were preferentially expressed in ovules (Fig. 5.4A). A previous report has demonstrated that a gain-of-function mutation in CalS3 displays callose hyper-accumulation which results in decreased plasmodesmal trafficking in root cells (Vatén *et al.*, 2011). On the contrary, the *calS3-1* knock-out mutant is neither affected in basal cell-to-cell movement in the root nor in overall plant growth and development. CalS8, however, together with CalS1, represent key genes in regulating callose accumulation at plasmodesmal channels during pathogen infection as well as mechanical wounding stress (Cui and Lee, 2016). The roles of CalS3 and CalS8 in gametophyte development and fertilization await further investigation. Among the type-II endo-1,4-beta glucanases, CEL1, CEL2, ATGH9B13/17/18 exhibit prominent expression in ovules (Fig. 5.4B). CEL1/2 have been shown to be involved in the formation of root syncytia induced by cyst nematodes (Wieczorek *et al.*, 2007), while AtGH9B17 was found to be highly expressed in ovules showing a proximal-distal pattern and high expression at the micropylar end of the inner integuments (Xie *et al.*, 2011). Finally, the so far uncharacterized type-II GPI-anchored endo-1,3-beta glucanases AT5G58480 and AT5G58090 (Fig. 5.4C) showed high expression in the ovule samples.

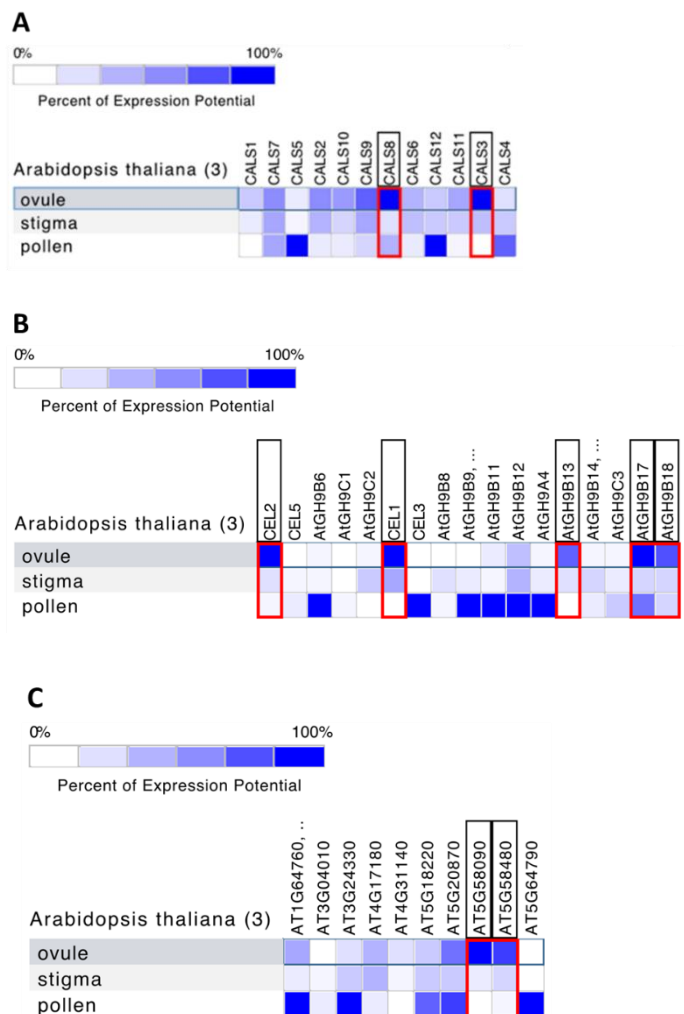


Fig. 5.4: Heatmap representing the expression patterns of the differentially regulated (A) 12 callose synthase (*AtCals*) (B) 11 type-I GPI-anchored endo-1,3-beta glucanase (C) 20 type-II endo-1,4-beta glucanase in inflorescence and silique sample in *A. thaliana* Columbia accession. The highlighted area represents the expression of highly expressed genes in the ovules.

Searching the STRING and ATTED databases, we found that the ovule expressed GPI-anchored endo-1,3-beta glucanase AT5G58480 was co-expressed with the plasmodesmata callose binding PDCB3 (AT1G18650) (Fig.4A). PDCB3, which is also highly expressed in the ovule and embryo, showed co-expression with two important female-derived fertilization factors *RALF-34* (Fig. 5.5A), and *LORELEI-LIKE-GPI ANCHORED PROTEIN 3 (LLG3)* (Fig. 5.5B), and also with the pollen receptor-kinase protein *PRK4*, the pollen-expressed guanine nucleotide exchange factor *ROPGEF1* and another GPI-anchored LTP, *LTPG1* (Fig. 5.5 A,B). Interestingly, one of our candidate genes *LTP5* which is expressed in both pollen tube and transmitting tract of the pistil was also predicted to interact with *LTPG1* and a pollen-receptor-kinase protein *PRK2A* (Fig. 5.5C). As noted above, LLGs form complexes with *RALF* peptides,

which in turn represent a ligand for the pollen RLK BUPS2 as well as the cell wall integrity sensory kinase FER (C., Li *et al.*, 2015). Whether secreted LTPs could also represent a scaffold for plasma membrane receptors and their ligands remains to be shown.

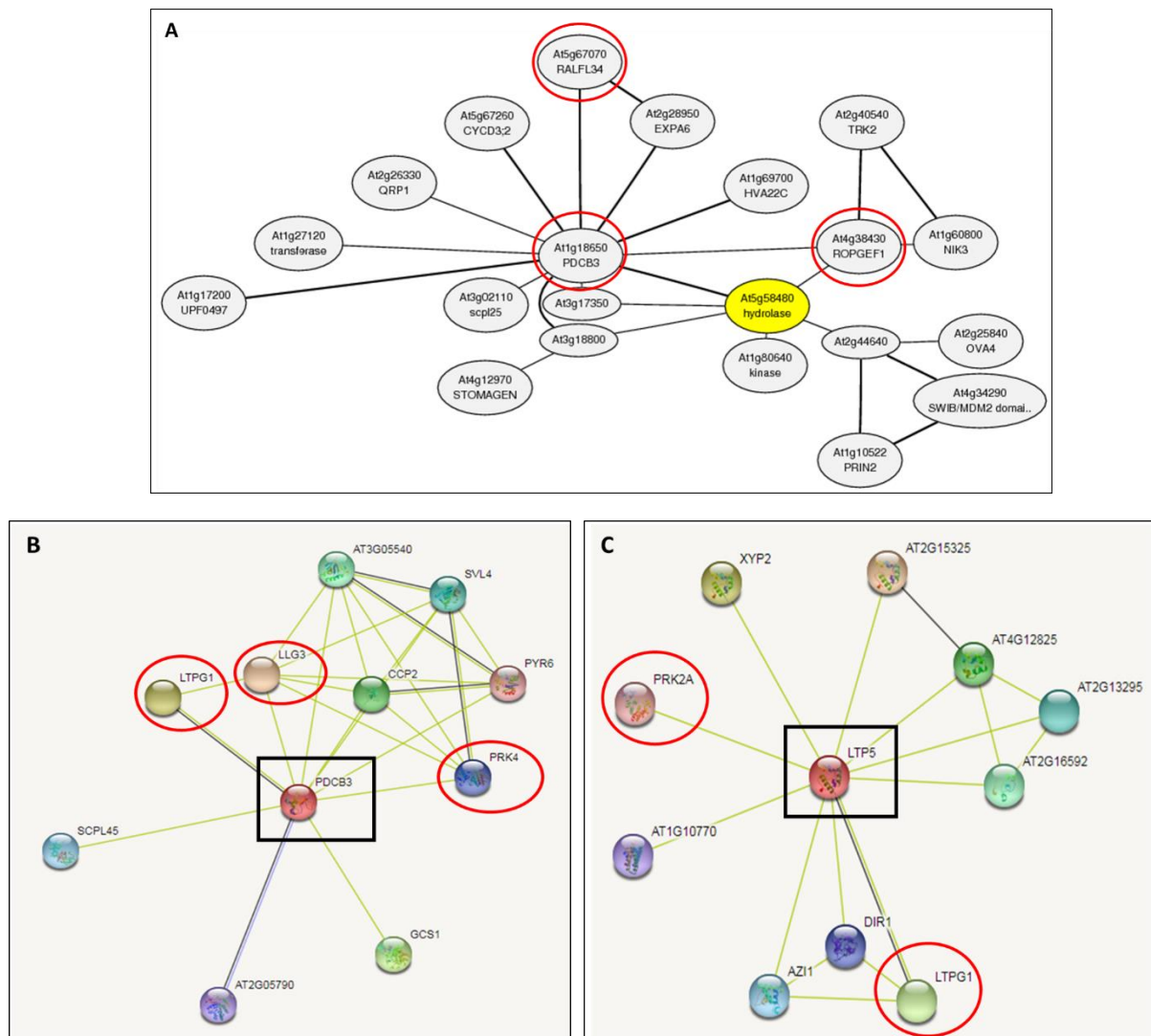


Fig. 5.5: Protein-protein interaction network analysis based on STRING and ATTED databases. (A) AT5G58480 (endo-1,3-beta glucanase) interacts with PDCB3 and PCDB3 displayed interaction with RALF-34 and RopGEF based on STRING analysis. (B) PCDB3 also interacts with LLG3, PRK4 and LTPG, (C) LTP showed interaction with LTPG1 and PRK2A based on ATTED analysis.

Previous reports suggested that, LePRK1 and LePRK2, two tomato pollen plasma membrane RLKs, bind to a variety of ligands, including a cysteine-rich extracellular protein (LAT52) (Tang *et al.*, 2002), a leucine-rich repeat protein (SHY) (Guyon *et al.*, 2004) from pollen, and two pistil/stigma expressed molecules STIL and STIG (Wengier *et al.*, 2010). Following activation, LePRK1 and LePRK2 interact with ROPGEF1 to activate the ROP pathway which mediates pollen tube growth. Reminiscent to the cysteine-rich extracellular proteins LAT52, and the stylar CRP STIG, the stylar expressed, secreted CRPs LTP2 and LTP5 may also act as ligands

for pollen PRK-like receptors. For this purpose, it has first to be proven that both LTPs are indeed secreted into the apoplast of stylar papillae cells. Furthermore, recombinant, properly folded LTP2/5 might be employed in pollen-tube growth assays for their capacity to regulate growth performance and guidance as well as activation of the ROGEFP-ROP pathway in an RLK-dependent manner. (Fig.5.6).

As shown above, the callose binding protein PDCB3 was predicted to interact with *RALF-34* and *LLG3*. The *LORELEI-LIKE-GPI ANCHORED PROTEIN-3 (LLG3)* which is expressed in the ovules acts as a chaperon and co-receptor of *FERONIA* (Liu *et al.*, 2016), providing a scaffold for RALF recognition. *LLG3* thus represents a key component in pollen reception and guidance mechanism and together with the cysteine-rich peptide *RAPID ALKALINIZATION FACTOR-34*, upon binding to *FERONIA*, induces pollen tube burst to release the sperm cells for gamete fusion (Ge *et al.*, 2017).

The RLK *FER* regulates various aspects of plant reproductive and vegetative growth, Previous findings have shown that a kinase-dead version of *FER* produces different phenotypes in roots and ovules, suggesting that signaling hubs related to cell-cell communication involve different interacting partners and/or downstream signaling events, in a cell type-specific manner (Haruta *et al.*, 2018). It is thus tempting to speculate that LTPs, together with CalS proteins and/or BGs, represent building blocks of RLK-controlled signalosomes in e.g. the female gametophyte. During the time course of this thesis we have generated stable transgenic *Arabidopsis* lines that express translational LTP2/5-YFP fusions under control of their respective promoters. In the first instance, these lines would allow to precisely identify the cell types that express our LTPs. Secondly, subsequent single-cell transcriptomic analyses employing FACS sorted protoplasts could provide an overview of RLKs co-expressed in this cell type. Together with the recently developed TurboID-based proximity labelling (PL) technique (Zhang *et al.*, 2019) followed by quantitative proteomic analysis, further genetic screening could reveal the interaction partners of LTPs and their underlying signaling pathways.

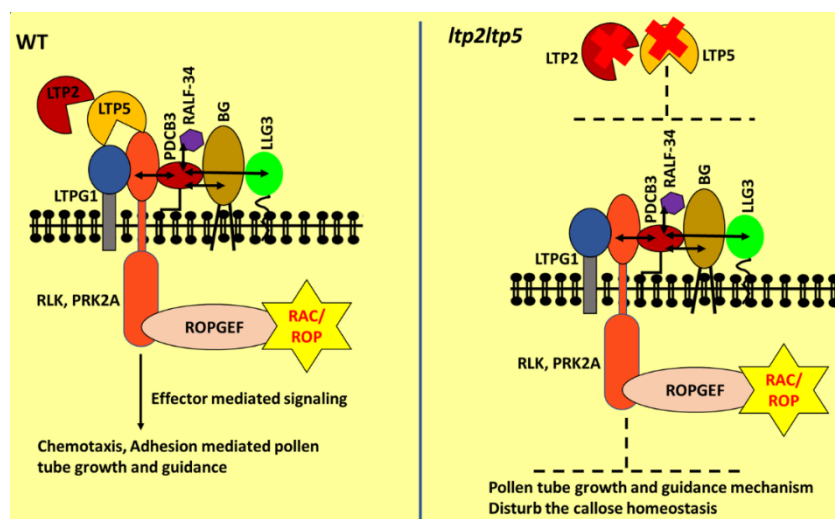


Fig. 5.6: Hypothetical model of LTP2/LTP5 mediated signaling during the growth and guidance of the pollen-tube. (A) In WT plants stilar expressed LTP2/LTP5 can act as a ligand which bind to pollen receptor like kinase PRK. Callose-binding protein, PDCB3 also interacts with PRK, endo-1,3-beta glucanase (BGs), RALF-34, LLG3 and ROPGEF. Binding of LTP2/LTP5 might stabilize the RLK and associated protein complex which further activates the ROPGEF signaling cascade mediating pollen tube growth and guidance. **(B)** In *ltp2ltp5* double knock-out plant, mutation in LTP2/LTP5 could destabilize the interaction between PRK and its associated partner inhibiting pollen-tube growth/guidance mechanism and causing perturbation in callose metabolism. Predicted protein-protein interaction are indicated by double headed arrow.

The second ovule expressed GPI-anchored endo-1,3-beta glucanase (AT5G58090) was predicted to interact with the two STEROL METHYLTRANSFERASE proteins SMT2 and SMT3 (Fig. 5.7A). Sterols and sphingolipids are synthesized at the endoplasmic reticulum (ER) and subsequently transported to the plasma membrane by both vesicular and non-vesicular pathway to form lipid rafts (Iswanto and Kim, 2017; Tong *et al.*, 2018).

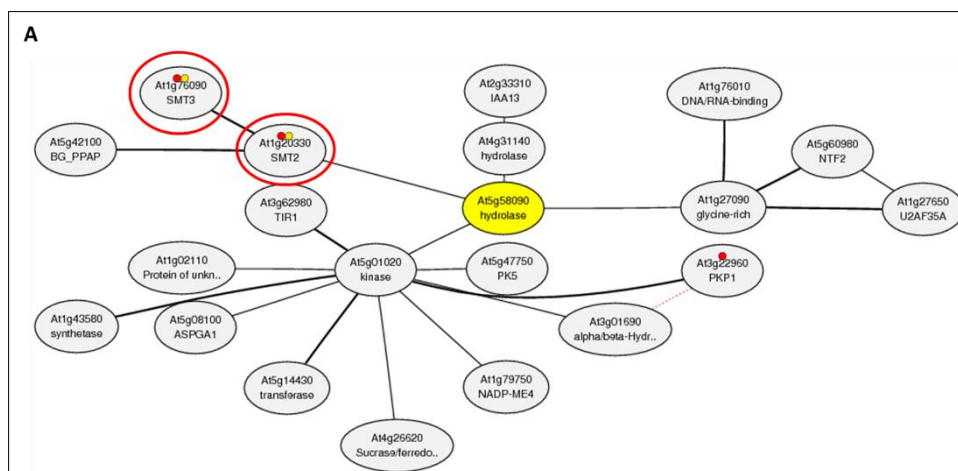


Fig. 5.7: Protein-protein interaction network analysis based on ATTED databases. (A) Interaction of GPI-anchored endo-1,3-beta glucanase (AT5G58090) with two STEROL METHYLTRANSFERASE SMT2 and SMT3.

Sterols play a crucial role in targeting GPI-anchored proteins and it has been shown, that the disruption of sterol biosynthesis causes a significant increase in callose deposition in the phloem but not at plasmodesmata (PD). Nevertheless, spectrometry-based analyses have shown that the lipid composition of PD membranes differed from that of the surrounding plasma membrane. PD membranes are particularly enriched in sterols and complex sphingolipids with very long saturated fatty acid tails. Interfering with sterol biosynthesis further resulted in mistargeting of GPI-anchored β -1,3-glucanases (PDBGs) (Farquharson, 2015). Another study proposed, that GLUCAN SYNTHASE-LIKE8 mediated callose deposition and STEROL METHYLTRANSFERASE2 mediated sterol synthesis, critically regulates the ploidy level in the

gametophytic meiotic cells, during both male and female sporogenesis. The data emphasized the role of callose and sterol biosynthesis in maintaining the ploidy consistency during the sexual polyploidization in *Arabidopsis* (De Storme et al. 2013). Mutations in STEROL METHYLTRANSFERASE SMT2 and SMT3 caused female sterility due to developmental defects of transmitting tract development in the pistil and impaired integument formation in the ovules. The *smt2smt3* plants exhibited low fertility with significant reduction in the seed set in comparison to WT (Nakamoto *et al.*, 2015).

It is already reported that, GPI-anchored callose binding (CBs) proteins and β -1,3-glucanases (BGs) are synthesized in the endoplasmic reticulum (ER) which are required to be transported to the plasma membrane as their target location. Thus, membrane composition appears critical for proper translocation of CBs and BGs and is mediated through lipid raft vesicle-mediated exocytosis process which regulate the callose homeostasis during plasmodesmata symplasmic movement (Iswanto and Kim, 2017). It is thus tempting to speculate, that the non-vesicular transport of sterols and complex shingolipids is also mediated by defined LTPs providing for the proper targeting of CBs and BGs, and possibly RLKs to plasma membrane micro domains, lipid rafts.

Lipid rafts entitled plasma membrane microdomains are enriched in sterols and sphingolipids. They have been shown to provide the structural basis and a regulatory role for the assembly and function of signaling hubs involved in cell-to-cell communication. In this context it was shown that the membrane-delimited ABA signal transduction pathway is regulated by lipid rafts (Demir *et al.*, 2013). Furthermore, lipid rafts play an important role in regulating the permeability of plasmodesmata in a callose dependent manner trafficking (Tilsner *et al.*, 2011; Iswanto and Kim, 2017). Sterol, sphingolipid enriched vesicles and sterol/sphingolipid-enriched membranes are not only required for the PD targeting of BGs and CalS, but it has recently been shown that also specific PM-located Leucine-Rich-Repeat Receptor-Like-Kinases (LRR-RLKs), QSK1 and IMK2, which under optimal growth conditions are absent from plasmodesmata, rapidly relocate and cluster to the pores in response to osmotic stress (Grison *et al.*, 2019).

It was further shown, that lipid transfer proteins anchored at membrane contact sites (LAMs) contain a pleckstrin homology (PH)-like domain or sterol-specific lipid transfer domains which facilitates the non-vesicular sterol transport at contact sites between the endoplasmic reticulum (ER) and other membranes (Tong *et al.*, 2018).

According to the current model (Fig. 5.8) LTPs could impinge on callose homeostasis in at least two ways. In the first scenario, vesicle-mediated exocytosis would provide for secretion of LTPs to the apoplast. Likewise, CalS/BGs and RLKs would be targeted to the plasma membrane. In this context, lipid-loaded LTPs might act as ligands and/or scaffolds (e.g. for

RALF peptides) to activate RLKs, which in turn would regulate callose homeostasis via their target CalS and BGs. In the second scenario, LTPs might act as mobile carriers shuttling the sterols/sphingolipids between the ER and the PM to generate plasma membrane micro domains (lipid rafts). This would provide the structural basis for the localized assembly of signalosomes, consisting of RLKs, CalS and BGs, that control callose dynamics. This role could be fulfilled by PM associated LTPs, acting at the inner leaflet of the PM, such as LTP3/4/12 (see results, Fig. 4.11, Fig. 4.13). Apart from their possible role as potential RLK ligands/scaffolding proteins, LTP2/5 (present in the apoplast) could act as sterol/sphingolipid carriers modulating lipid rafts at the extracellular leaflet of the PM.

On one hand, loss-of-function of LTP2/5 thus could result in a missing ligand/scaffold leading to the deregulation of RLK-controlled callose turnover. On the other hand, the lack of LTP2/5 could affect lipid raft composition and thus result in the improper targeting or assembly of signalosomes involved in the regulation of callose homeostasis. Currently, however, there is no evidence for either of these hypotheses. Still, the results obtained in this thesis are supportive for a prominent role of the enigmatic of LTP proteins in the sexual plant reproductive process. Our findings open doors for the study of specific LTPs in the context of new pathways. Considering the role of LTPs, either as signaling, scaffolding or transport proteins, together with their broad differential expression along male and female reproductive tissues, it is unquestionable that especially the LTP2/5 pair appears as a multifunctional protein moiety. Together they may thus act as a basal interactor along the crosstalk established between the germinating pollen tube and the female tissues, providing for a successful double fertilization. Future work is now required to elucidate the detailed molecular interaction between LTPs and their potential partners, including receptors expressed in pollen and synergid cells, which can provide some information regarding its plausible role as attractant molecule in pollen tube guidance mechanism.

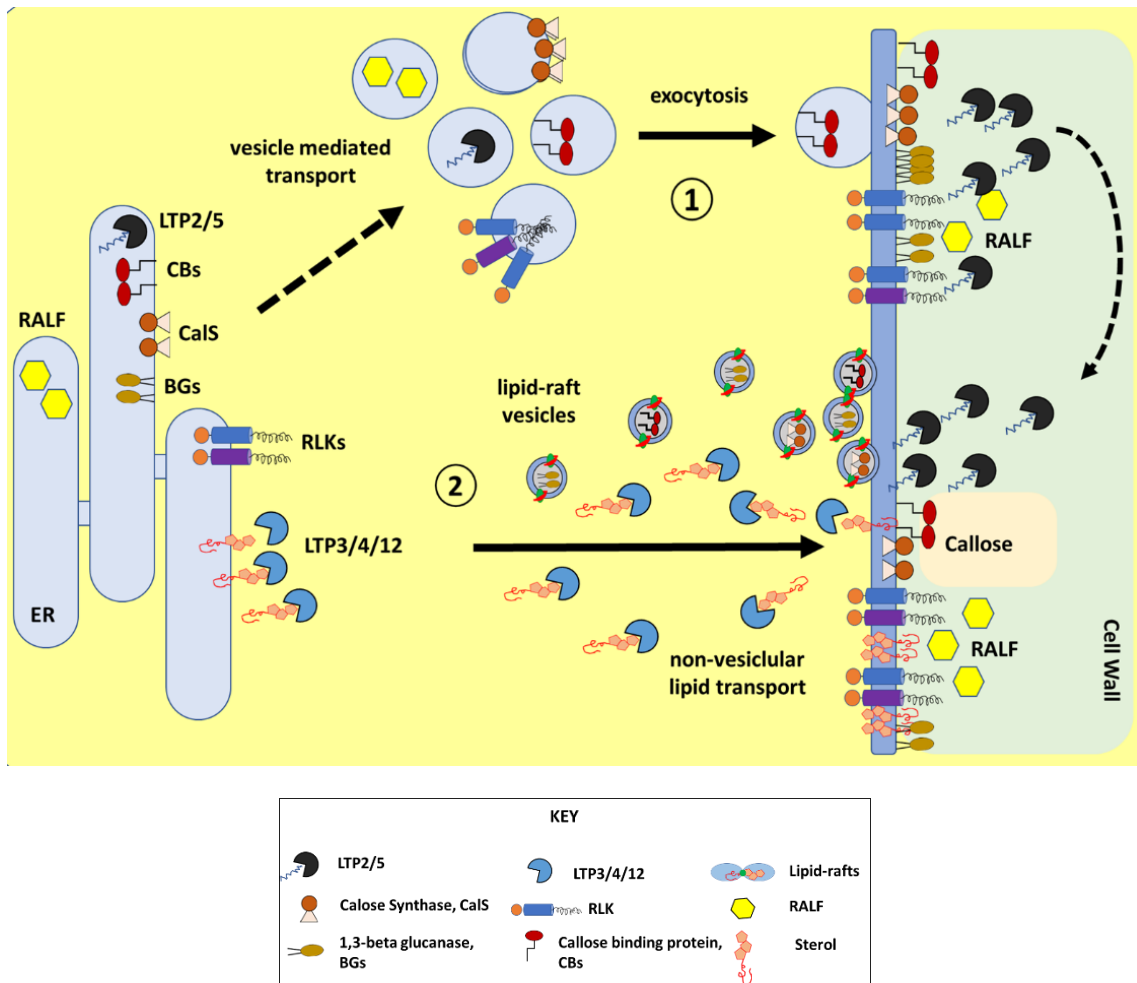


Fig. 5.8: Hypothetical role of LTPs in callose homeostasis: (1) Vesicle-mediated transport of CaS, CBs, BGs, RLKs and RALF to the plasma membrane. Apoplastic LTPs might act as ligands and/or scaffolds activating RLKs which in turn regulate callose homeostasis. **(2)** After sterol biosynthesis in ER, LTP mediated non-vesicular transport of sterols to plasma membrane facilitate the formation of lipid raft which help in proper targeting of GPI-anchored CBs and BGs to the plasma membrane, which maintains the callose turnover.

7. REFERENCES

- Alandete-Saez, M., Ron, M. and McCormick, S.** (2008) GEX3, Expressed in the Male Gametophyte and in the Egg Cell of *Arabidopsis thaliana* Is Essential for Micropylar Pollen Tube Guidance and Plays a Role during Early Embryogenesis. *Mol. Plant*, **1**, 586–598. Available at: <https://www.sciencedirect.com/science/article/pii/S167420521460366X> [Accessed January 25, 2019].
- Alonso, J.M., Stepanova, A.N., Leisse, T.J., et al.** (2003) Genome-wide insertional mutagenesis of *Arabidopsis thaliana*. *Science*, **301**, 653–7. Available at: <http://www.ncbi.nlm.nih.gov/pubmed/12893945> [Accessed March 31, 2019].
- Amien, S., Kliwer, I., Márton, M.L., Debener, T. and Geiger, D.** (2010) Defensin-Like ZmES4 Mediates Pollen Tube Burst in Maize via Opening of the Potassium Channel KZM1. *PLoS Biol*, **8**, 1000388. Available at: www.plosbiology.org [Accessed March 31, 2019].
- An, Y.Q., McDowell, J.M., Huang, S., McKinney, E.C., Chambliss, S. and Meagher, R.B.** (1996) Strong, constitutive expression of the *Arabidopsis* ACT2/ACT8 actin subclass in vegetative tissues. *Plant J.*, **10**, 107–21. Available at: <http://www.ncbi.nlm.nih.gov/pubmed/8758981> [Accessed June 15, 2019].
- Arondel, V., Vergnolle, C., Cantrel, C. and Kader, J.-C.** (2000) Lipid transfer proteins are encoded by a small multigene family in *Arabidopsis thaliana*. *Plant Sci.*, **157**, 1–12. Available at: <https://linkinghub.elsevier.com/retrieve/pii/S0168945200002326> [Accessed June 23, 2019].
- Berecz, B., Mills, E.N.C., Tamás, L., Láng, F., Shewry, P.R. and Mackie, A.R.** (2010) Structural Stability and Surface Activity of Sunflower 2S Albumins and Nonspecific Lipid Transfer Protein. *J. Agric. Food Chem.*, **58**, 6490–6497. Available at: <https://pubs.acs.org/doi/10.1021/jf100554d> [Accessed May 20, 2019].
- Berger, F., Haseloff, J., Schiefelbein, J. and Dolan, L.** (1998) Positional information in root epidermis is defined during embryogenesis and acts in domains with strict boundaries. *Curr. Biol.*, **8**, 421–430. Available at: <https://www.sciencedirect.com/science/article/pii/S0960982298701769?via%3Dihub> [Accessed July 12, 2019].
- Besser, K. von, Frank, A.C., Johnson, M.A. and Preuss, D.** (2006) *Arabidopsis* HAP2 (GCS1) is a sperm-specific gene required for pollen tube guidance and fertilization. *Development*, **133**, 4761–4769. Available at: <http://dev.biologists.org/cgi/doi/10.1242/dev.02683> [Accessed May 19, 2019].
- Biemelt, S., Tschiersch, H. and Sonnewald, U.** (2004) Impact of altered gibberellin metabolism on biomass accumulation, lignin biosynthesis, and photosynthesis in transgenic tobacco plants. *Plant Physiol.*, **135**, 254–65. Available at: <http://www.ncbi.nlm.nih.gov/pubmed/15122040> [Accessed July 25, 2019].
- Bircheneder, S. and Dresselhaus, T.** (2016) Why cellular communication during plant reproduction is particularly mediated by CRP signalling. *J. Exp. Bot.*, **67**.
- Boavida, L.C. and McCormick, S.** (2007) TECHNICAL ADVANCE: Temperature as a determinant factor for increased and reproducible in vitro pollen germination in *Arabidopsis thaliana*. *Plant J.*, **52**, 570–582. Available at: <http://doi.wiley.com/10.1111/j.1365-313X.2007.03248.x> [Accessed June 17, 2019].

- Boisson-Dernier, A., Franck, C.M., Lituiev, D.S. and Grossniklaus, U.** (2015) Receptor-like cytoplasmic kinase MARIS functions downstream of CrRLK1L-dependent signaling during tip growth. *Proc. Natl. Acad. Sci. U. S. A.*, **112**, 12211–6. Available at: <http://www.ncbi.nlm.nih.gov/pubmed/26378127> [Accessed June 3, 2019].
- Boisson-Dernier, A., Lituiev, D.S., Nestorova, A., Franck, C.M., Thirugnanarajah, S. and Grossniklaus, U.** (2013) ANXUR Receptor-Like Kinases Coordinate Cell Wall Integrity with Growth at the Pollen Tube Tip Via NADPH Oxidases J. B. Nasrallah, ed. *PLoS Biol.*, **11**, e1001719. Available at: <https://dx.plos.org/10.1371/journal.pbio.1001719> [Accessed May 18, 2019].
- BOLTE, S. and CORDELIÈRES, F.P.** (2006) A guided tour into subcellular colocalization analysis in light microscopy. *J. Microsc.*, **224**, 213–232. Available at: <http://www.ncbi.nlm.nih.gov/pubmed/17210054> [Accessed February 11, 2019].
- Boutrot, F., Chantret, N. and Gautier, M.-F.** (2008) Genome-wide analysis of the rice and arabidopsis non-specific lipid transfer protein (nsLtp) gene families and identification of wheat nsLtp genes by EST data mining. *BMC Genomics*, **9**, 86. Available at: <http://www.ncbi.nlm.nih.gov/pubmed/18291034> [Accessed April 3, 2019].
- Bozkurt, T.O., Richardson, A., Dagdas, Y.F., Mongrand, S., Kamoun, S. and Raffaele, S.** (2014) The Plant Membrane-Associated REMORIN1.3 Accumulates in Discrete Perihyphal Domains and Enhances Susceptibility to *Phytophthora infestans*. *Plant Physiol.*, **165**, 1005–1018. Available at: <http://www.ncbi.nlm.nih.gov/pubmed/24808104> [Accessed July 8, 2019].
- Brunaud, V., Balzergue, S., Dubreucq, B., et al.** (2002) T-DNA integration into the Arabidopsis genome depends on sequences of pre-insertion sites. *EMBO Rep.*, **3**, 1152–1157. Available at: <http://embor.embopress.org/content/3/12/1152> [Accessed June 17, 2019].
- Cai, S. and Lashbrook, C.C.** (2008) Stamen Abscission Zone Transcriptome Profiling Reveals New Candidates for Abscission Control: Enhanced Retention of Floral Organs in Transgenic Plants Overexpressing Arabidopsis *ZINC FINGER PROTEIN2*. *Plant Physiol.*, **146**, 1305–1321. Available at: <http://www.plantphysiol.org/lookup/doi/10.1104/pp.107.110908> [Accessed July 20, 2019].
- Cammue, B., Thevissen, K., Hendriks, M., et al.** (1995) A Potent Antimicrobial Protein from Onion Seeds Showing Sequence Homology to Plant Lipid Transfer Proteins. *Plant Physiol.*, **109**, 445–455. Available at: <http://www.plantphysiol.org/content/109/2/445> [Accessed June 11, 2019].
- Capron, A., Gourgues, M., Neiva, L.S., et al.** (2008) Maternal Control of Male-Gamete Delivery in Arabidopsis Involves a Putative GPI-Anchored Protein Encoded by the LORELEI Gene. *PLANT CELL ONLINE*, **20**, 3038–3049. Available at: <http://www.plantcell.org/cgi/doi/10.1105/tpc.108.061713> [Accessed January 4, 2019].
- Chae, K., Gonong, B.J., Kim, S.-C., Kieslich, C.A., Morikis, D., Balasubramanian, S. and Lord, E.M.** (2010) A multifaceted study of stigma/style cysteine-rich adhesin (SCA)-like Arabidopsis lipid transfer proteins (LTPs) suggests diversified roles for these LTPs in plant growth and reproduction. *J. Exp. Bot.*, **61**, 4277–4290. Available at: <https://academic.oup.com/jxb/article-lookup/doi/10.1093/jxb/erq228> [Accessed May 24, 2019].
- Chae, K., Kieslich, C.A., Morikis, D., Kim, S.-C. and Lord, E.M.** (2009) A Gain-of-Function Mutation of Arabidopsis Lipid Transfer Protein 5 Disturbs Pollen Tube Tip Growth and Fertilization. *Plant Cell*, **21**, 3902–3914. Available at:

- <http://www.plantcell.org/cgi/doi/10.1105/tpc.109.070854> [Accessed January 4, 2019].
- Chae, K. and Lord, E.M.** (2011) Pollen tube growth and guidance: Roles of small, secreted proteins. *Ann. Bot.*, **108**, 627–636. Available at: <https://academic.oup.com/aob/article-lookup/doi/10.1093/aob/mcr015> [Accessed May 24, 2019].
- Chae, K., Zhang, K., Zhang, L., Morikis, D., Kim, S.T., Mollet, J.-C., la Rosa, N. de, Tan, K. and Lord, E.M.** (2007) Two SCA (Stigma/Style Cysteine-rich Adhesin) Isoforms Show Structural Differences That Correlate with Their Levels of *in Vitro* Pollen Tube Adhesion Activity. *J. Biol. Chem.*, **282**, 33845–33858. Available at: <http://www.ncbi.nlm.nih.gov/pubmed/17878166> [Accessed March 30, 2019].
- Chapman, L.A. and Goring, D.R.** (2011) Misregulation of phosphoinositides in *Arabidopsis thaliana* decreases pollen hydration and maternal fertility. *Sex. Plant Reprod.*, **24**, 319–326. Available at: <http://link.springer.com/10.1007/s00497-011-0172-1> [Accessed June 1, 2019].
- Charvolin, D., Douliez, J.P., Marion, D., Cohen-Addad, C. and Pebay-Peyroula, E.** (1999) The crystal structure of a wheat nonspecific lipid transfer protein (ns-LTP1) complexed with two molecules of phospholipid at 2.1 Å resolution. *Eur. J. Biochem.*, **264**, 562–8. Available at: <http://www.ncbi.nlm.nih.gov/pubmed/10491104> [Accessed June 11, 2019].
- Chaudhury, A.M., Koltunow, A., Payne, T., Luo, M., Tucker, M.R., Dennis, E.S. and Peacock, W.J.** (2001) Control of Early Seed Development. *Annu. Rev. Cell Dev. Biol.*, **17**, 677–699. Available at: <http://www.annualreviews.org/doi/10.1146/annurev.cellbio.17.1.677> [Accessed April 1, 2019].
- Chen, C., Chen, G., Hao, X., Cao, B., Chen, Q., Liu, S. and Lei, J.** (2011) CaMF2, an anther-specific lipid transfer protein (LTP) gene, affects pollen development in *Capsicum annuum* L. *Plant Sci.*, **181**, 439–448. Available at: <http://www.ncbi.nlm.nih.gov/pubmed/21889050> [Accessed June 13, 2019].
- Chen, X.-Y. and Kim, J.-Y.** (2009) Callose synthesis in higher plants. *Plant Signal. Behav.*, **4**, 489–92. Available at: <http://www.ncbi.nlm.nih.gov/pubmed/19816126> [Accessed July 27, 2019].
- Chen, Y.-H., Li, H.-J., Shi, D.-Q., Yuan, L., Liu, J., Sreenivasan, R., Baskar, R., Grossniklaus, U. and Yang, W.-C.** (2007) The central cell plays a critical role in pollen tube guidance in *Arabidopsis*. *Plant Cell*, **19**, 3563–77. Available at: <http://www.ncbi.nlm.nih.gov/pubmed/18055609> [Accessed January 25, 2019].
- Cho, S.W., Kim, S., Kim, Y., Kweon, J., Kim, H.S., Bae, S. and Kim, J.-S.** (2014) Analysis of off-target effects of CRISPR/Cas-derived RNA-guided endonucleases and nickases. *Genome Res.*, **24**, 132–141. Available at: <http://genome.cshlp.org/cgi/doi/10.1101/gr.162339.113> [Accessed April 12, 2019].
- Cockcroft, S.** (1999) Mammalian phosphatidylinositol transfer proteins: emerging roles in signal transduction and vesicular traffic. *Chem. Phys. Lipids*, **98**, 23–33. Available at: <http://www.ncbi.nlm.nih.gov/pubmed/10358925> [Accessed June 11, 2019].
- Costa, L.M., Marshall, E., Tesfaye, M., et al.** (2014) Central cell-derived peptides regulate early embryo patterning in flowering plants. *Science*, **344**, 168–72. Available at: <http://www.ncbi.nlm.nih.gov/pubmed/24723605> [Accessed June 11, 2019].
- Costa, L.M., Yuan, J., Rouster, J., Paul, W., Dickinson, H. and Gutierrez-Marcos, J.F.** (2012) Maternal Control of Nutrient Allocation in Plant Seeds by Genomic Imprinting. *Curr. Biol.*, **22**, 160–165. Available at: <http://www.ncbi.nlm.nih.gov/pubmed/22245001> [Accessed May 18, 2019].

- Cresti, M., Keijzer, C.J., Tiezzi, A., Ciampolini, F. and Focardi, S.** (2006) Stigma of *Nicotiana*: Ultrastructural and Biochemical Studies. *Am. J. Bot.*, **73**, 1713. Available at: <http://doi.wiley.com/10.1002/j.1537-2197.1986.tb09702.x> [Accessed May 5, 2019].
- Cui, W. and Lee, J.-Y.** (2016) Arabidopsis callose synthases CalS1/8 regulate plasmodesmal permeability during stress. *Nat. Plants*, **2**, 16034. Available at: <http://www.nature.com/articles/nplants201634> [Accessed July 27, 2019].
- Dani, V., Simon, W.J., Duranti, M. and Croy, R.R.D.** (2005) Changes in the tobacco leaf apoplast proteome in response to salt stress. *Proteomics*, **5**, 737–745. Available at: <http://doi.wiley.com/10.1002/pmic.200401119> [Accessed May 23, 2019].
- Debono, A., Yeats, T.H., Rose, J.K.C., Bird, D., Jetter, R., Kunst, L. and Samuels, L.** (2009) Arabidopsis LTPG is a glycosylphosphatidylinositol-anchored lipid transfer protein required for export of lipids to the plant surface. *Plant Cell*, **21**, 1230–8. Available at: <http://www.ncbi.nlm.nih.gov/pubmed/19366900> [Accessed May 20, 2019].
- Deeken, R., Saupe, S., Klinkenberg, J., Riedel, M., Leide, J., Hedrich, R. and Mueller, T.D.** (2016) The Nonspecific Lipid Transfer Protein AtLtpI-4 Is Involved in Suberin Formation of Arabidopsis thaliana Crown Galls. *Plant Physiol.*, **172**, 1911–1927. Available at: <http://www.ncbi.nlm.nih.gov/pubmed/27688623> [Accessed June 19, 2019].
- Demir, F., Horntrich, C., Blachutzik, J.O., et al.** (2013) Arabidopsis nanodomain-delimited ABA signaling pathway regulates the anion channel SLAH3. *Proc. Natl. Acad. Sci.*, **110**, 8296–8301. Available at: <http://www.ncbi.nlm.nih.gov/pubmed/23630285> [Accessed July 28, 2019].
- Deng, T., Yao, H., Wang, Jin, Wang, Jun, Xue, H. and Zuo, K.** (2016) GhLTPG1, a cotton GPI-anchored lipid transfer protein, regulates the transport of phosphatidylinositol monophosphates and cotton fiber elongation. *Sci. Rep.*, **6**, 1–12. Available at: <http://dx.doi.org/10.1038/srep26829>.
- Denninger, P., Bleckmann, A., Lausser, A., et al.** (2014) Male–female communication triggers calcium signatures during fertilization in Arabidopsis. *Nat. Commun.*, **5**, 4645. Available at: <http://www.nature.com/articles/ncomms5645> [Accessed May 19, 2019].
- Diz, M.S., Carvalho, A.O., Ribeiro, S.F.F., Cunha, M. Da, Beltramini, L., Rodrigues, R., Nascimento, V. V., Machado, O.L.T. and Gomes, V.M.** (2011) Characterisation, immunolocalisation and antifungal activity of a lipid transfer protein from chili pepper (*Capsicum annuum*) seeds with novel α -amylase inhibitory properties. *Physiol. Plant.*, **142**, 233–246. Available at: <http://www.ncbi.nlm.nih.gov/pubmed/21382036> [Accessed May 23, 2019].
- Doan, D.N.P., Linnestad, C. and Olsen, O.-A.** (1996) Isolation of molecular markers from the barley endosperm coenocyte and the surrounding nucellus cell layers. *Plant Mol. Biol.*, **31**, 877–886. Available at: <http://link.springer.com/10.1007/BF00019474> [Accessed May 25, 2019].
- Dong, J., Kim, S.T. and Lord, E.M.** (2005) Plantacyanin plays a role in reproduction in Arabidopsis. *Plant Physiol.*, **138**, 778–89. Available at: <http://www.ncbi.nlm.nih.gov/pubmed/15908590> [Accessed January 8, 2019].
- Doulliez, J.-P., Michon, T., Elmorjani, K. and Marion, D.** (2000) Mini Review: Structure, Biological and Technological Functions of Lipid Transfer Proteins and Indolines, the Major Lipid Binding Proteins from Cereal Kernels. *J. Cereal Sci.*, **32**, 1–20. Available at: <https://linkinghub.elsevier.com/retrieve/pii/S0733521000903151> [Accessed June 11, 2019].
- Dresselhaus, T., Lorz, H. and Kranz, E.** (1994) Representative cDNA libraries from few

- plant cells. *Plant J.*, **5**, 605–610. Available at: <http://doi.wiley.com/10.1046/j.1365-313X.1994.05040605.x> [Accessed May 18, 2019].
- Duan, Q., Kita, D., Johnson, E.A., Aggarwal, M., Gates, L., Wu, H.M. and Cheung, A.Y.** (2014) Reactive oxygen species mediate pollen tube rupture to release sperm for fertilization in *Arabidopsis*. *Nat. Commun.*, **5**, 3129. Available at: <http://www.nature.com/articles/ncomms4129> [Accessed May 18, 2019].
- Edstam, M.M. and Edqvist, J.** (2014) Involvement of GPI-anchored lipid transfer proteins in the development of seed coats and pollen in *Arabidopsis thaliana*. *Physiol. Plant.*, **152**, 32–42. Available at: <http://www.ncbi.nlm.nih.gov/pubmed/24460633> [Accessed June 13, 2019].
- Edstam, Monika M., Viitanen, L., Salminen, T.A. and Edqvist, J.** (2011) Evolutionary History of the Non-Specific Lipid Transfer Proteins. *Mol. Plant*, **4**, 947–964. Available at: <https://www.sciencedirect.com/science/article/pii/S1674205214606298?via%3Dihub#fig1> [Accessed May 20, 2019].
- Edstam, Monika M., Viitanen, L., Salminen, T.A. and Edqvist, J.** (2011) Evolutionary History of the Non-Specific Lipid Transfer Proteins. *Mol. Plant*, **4**, 947–964. Available at: www.ebi.ac.uk/Tools/InterProScan/ [Accessed May 24, 2019].
- Fairn, G.D. and McMaster, C.R.** (2008) Emerging roles of the oxysterol-binding protein family in metabolism, transport, and signaling. *Cell. Mol. Life Sci.*, **65**, 228–236. Available at: <http://www.ncbi.nlm.nih.gov/pubmed/17938859> [Accessed June 11, 2019].
- Feng, Z., Zhang, B., Ding, W., et al.** (2013) Efficient genome editing in plants using a CRISPR/Cas system. *Nat. Publ. Gr.*, **23**. Available at: www.cell-research.com [Accessed June 27, 2019].
- Finer, K.R. and Finer, J.J.** (2000) Use of *Agrobacterium* expressing green fluorescent protein to evaluate colonization of sonication-assisted *Agrobacterium*-mediated transformation- treated soybean cotyledons. *Lett. Appl. Microbiol.*, **30**, 406–410. Available at: <http://doi.wiley.com/10.1046/j.1472-765x.2000.00737.x> [Accessed May 17, 2019].
- Foote, H.C., Ride, J.P., Franklin-Tong, V.E., Walker, E.A., Lawrence, M.J. and Franklin, F.C.** (1994a) Cloning and expression of a distinctive class of self-incompatibility (S) gene from *Papaver rhoeas* L. *Proc. Natl. Acad. Sci. U. S. A.*, **91**, 2265–9. Available at: <http://www.ncbi.nlm.nih.gov/pubmed/8134385> [Accessed March 6, 2019].
- Foote, H.C., Ride, J.P., Franklin-Tong, V.E., Walker, E.A., Lawrence, M.J. and Franklin, F.C.** (1994b) Cloning and expression of a distinctive class of self-incompatibility (S) gene from *Papaver rhoeas* L. *Proc. Natl. Acad. Sci. U. S. A.*, **91**, 2265–9. Available at: <http://www.ncbi.nlm.nih.gov/pubmed/8134385> [Accessed March 6, 2019].
- Foster, G.D., Robinson, S.W., Blundell, R.P., Roberts, M.R., Hodge, R., Draper, J. and Scott, R.J.** (1992) A *Brassica napus* mRNA encoding a protein homologous to phospholipid transfer proteins, is expressed specifically in the tapetum and developing microspores. *Plant Sci.*, **84**, 187–192. Available at: <https://www.sciencedirect.com/science/article/pii/0168945292901337> [Accessed April 4, 2019].
- Fritz-Laylin, L.K., Krishnamurthy, N., Tör, M., Sjölander, K. V and Jones, J.D.G.** (2005) Phylogenomic analysis of the receptor-like proteins of rice and *Arabidopsis*. *Plant Physiol.*, **138**, 611–23. Available at: <http://www.ncbi.nlm.nih.gov/pubmed/15955925> [Accessed May 28, 2019].
- Gao, Q.-F., Gu, L.-L., Wang, H.-Q., et al.** (2016) Cyclic nucleotide-gated channel 18 is an

- essential Ca²⁺ channel in pollen tube tips for pollen tube guidance to ovules in *Arabidopsis*. *Proc. Natl. Acad. Sci. U. S. A.*, **113**, 3096–101. Available at: <http://www.ncbi.nlm.nih.gov/pubmed/26929345> [Accessed June 10, 2019].
- García-Olmedo, F., Molina, A., Segura, A. and Moreno, M.** (1995) The defensive role of nonspecific lipid-transfer proteins in plants. *Trends Microbiol.*, **3**, 72–74. Available at: <https://www.sciencedirect.com/science/article/abs/pii/S0966842X00888794> [Accessed July 6, 2019].
- Gatta, A.T. and Levine, T.P.** (2017) Piecing Together the Patchwork of Contact Sites. *Trends Cell Biol.*, **27**, 214–229. Available at: <http://www.ncbi.nlm.nih.gov/pubmed/27717534> [Accessed May 22, 2019].
- Ge, Z., Bergonci, T., Zhao, Y., et al.** (2017) *Arabidopsis* pollen tube integrity and sperm release are regulated by RALF-mediated signaling. *Science (80-.)*, **358**, 1596–1600. Available at: <http://www.ncbi.nlm.nih.gov/pubmed/29242234> [Accessed June 3, 2019].
- Giulietti, A., Overbergh, L., Valckx, D., Decallonne, B., Bouillon, R. and Mathieu, C.** (2001) An Overview of Real-Time Quantitative PCR: Applications to Quantify Cytokine Gene Expression. *Methods*, **25**, 386–401. Available at: <https://www.sciencedirect.com/science/article/pii/S1046202301912617?via%3Dihub> [Accessed July 25, 2019].
- Gómez-Gómez, L. and Boller, T.** (2000) FLS2: an LRR receptor-like kinase involved in the perception of the bacterial elicitor flagellin in *Arabidopsis*. *Mol. Cell*, **5**, 1003–11. Available at: <http://www.ncbi.nlm.nih.gov/pubmed/10911994> [Accessed May 28, 2019].
- Goto, H., Okuda, S., Mizukami, A., Mori, H., Sasaki, N., Kurihara, D. and Higashiyama, T.** (2011) Chemical Visualization of an Attractant Peptide, LURE. *Plant Cell Physiol.*, **52**, 49–58. Available at: <http://www.ncbi.nlm.nih.gov/pubmed/21149297> [Accessed May 18, 2019].
- Grison, M.S., Kirk, P., Brault, M., Wu, X.N., Schulze, W.X., Benitez-Alfonso, Y., Immel, F. and Bayer, E.M.** (2019) Plasma membrane associated Receptor Like Kinases relocalise to plasmodesmata in response to osmotic stress. *bioRxiv*, 610881. Available at: <http://www.ncbi.nlm.nih.gov/pubmed/31300470> [Accessed July 28, 2019].
- Guan, Y., Lu, J., Xu, J., McClure, B. and Zhang, S.** (2014) Two Mitogen-Activated Protein Kinases, MPK3 and MPK6, Are Required for Funicular Guidance of Pollen Tubes in *Arabidopsis*. *Plant Physiol.*, **165**, 528–533. Available at: <http://www.plantphysiol.org/content/165/2/528> [Accessed January 26, 2019].
- Gui, C.-P., Dong, X., Liu, H.-K., et al.** (2014) Overexpression of the Tomato Pollen Receptor Kinase LePRK1 Rewires Pollen Tube Growth to a Blebbing Mode. *Plant Cell*, **26**, 3538–3555. Available at: <http://www.ncbi.nlm.nih.gov/pubmed/25194029> [Accessed June 1, 2019].
- Gutermuth, T., Herbell, S., Lassig, R., Brosché, M., Romeis, T., Feijó, J.A., Hedrich, R. and Konrad, K.R.** (2018) Tip-localized Ca²⁺-permeable channels control pollen tube growth via kinase-dependent R- and S-type anion channel regulation. *New Phytol.*, **218**, 1089–1105. Available at: <http://doi.wiley.com/10.1111/nph.15067> [Accessed July 11, 2019].
- Gutiérrez-Marcos, J.F., Costa, L.M., Biderre-Petit, C., Khbaya, B., O’Sullivan, D.M., Wormald, M., Perez, P. and Dickinson, H.G.** (2004) maternally expressed gene1 Is a novel maize endosperm transfer cell-specific gene with a maternal parent-of-origin pattern of expression. *Plant Cell*, **16**, 1288–301. Available at: <http://www.ncbi.nlm.nih.gov/pubmed/15105441> [Accessed May 18, 2019].

- Hamamura, Y., Nishimaki, M., Takeuchi, H., Geitmann, A., Kurihara, D. and Higashiyama, T.** (2014) Live imaging of calcium spikes during double fertilization in Arabidopsis. *Nat. Commun.*, **5**, 4722. Available at: <http://www.nature.com/articles/ncomms5722> [Accessed May 19, 2019].
- Hamilton, E.S. and Haswell, E.S.** The Tension-sensitive Ion Transport Activity of MSL8 is Critical for its Function in Pollen Hydration and Germination. Available at: www.pcp.oxfordjournals.org [Accessed June 3, 2019].
- Hamilton, E.S., Jensen, G.S., Maksaev, G., Katims, A., Sherp, A.M. and Haswell, E.S.** (2015) Mechanosensitive channel MSL8 regulates osmotic forces during pollen hydration and germination. *Science (80-.)*, **350**, 438–441. Available at: <http://www.sciencemag.org/cgi/doi/10.1126/science.aac6014> [Accessed June 10, 2019].
- Haruta, M., Gaddameedi, V., Burch, H., Fernandez, D. and Sussman, M.R.** (2018) Comparison of the effects of a kinase-dead mutation of FERONIA on ovule fertilization and root growth of Arabidopsis. *FEBS Lett.*, **592**, 2395–2402. Available at: <https://onlinelibrary.wiley.com/doi/abs/10.1002/1873-3468.13157> [Accessed July 27, 2019].
- Haruta, M., Sabat, G., Stecker, K., Minkoff, B.B. and Sussman, M.R.** (2014) A peptide hormone and its receptor protein kinase regulate plant cell expansion. *Science*, **343**, 408–11. Available at: <http://www.ncbi.nlm.nih.gov/pubmed/24458638> [Accessed May 18, 2019].
- Helle, S.C.J., Kanfer, G., Kolar, K., Lang, A., Michel, A.H. and Kornmann, B.** (2013) Organization and function of membrane contact sites. *Biochim. Biophys. Acta - Mol. Cell Res.*, **1833**, 2526–2541. Available at: <http://www.ncbi.nlm.nih.gov/pubmed/23380708> [Accessed May 22, 2019].
- Helmkamp, G.M., Harvey, M.S., Wirtz, K.W. and Deenen, L.L. Van** (1974) Phospholipid exchange between membranes. Purification of bovine brain proteins that preferentially catalyze the transfer of phosphatidylinositol. *J. Biol. Chem.*, **249**, 6382–9. Available at: <http://www.ncbi.nlm.nih.gov/pubmed/4371468> [Accessed June 11, 2019].
- HESLOP-HARRISON, Y. and SHIVANNA, K.R.** (2017) The Receptive Surface of the Angiosperm Stigma. *Ann. Bot.*, **41**, 1233–1258. Available at: <https://academic.oup.com/aob/article-abstract/41/6/1233/224171> [Accessed June 26, 2019].
- Higashiyama, T.** (2010) Peptide Signaling in Pollen-Pistil Interactions. *Plant Cell Physiol.*, **51**, 177–189. Available at: <https://academic.oup.com/pcp/article-lookup/doi/10.1093/pcp/pcq008> [Accessed March 29, 2019].
- Higashiyama, T. and Takeuchi, H.** (2015) The Mechanism and Key Molecules Involved in Pollen Tube Guidance. *Annu. Rev. Plant Biol.*, **66**, 393–413. Available at: <http://www.ncbi.nlm.nih.gov/pubmed/25621518> [Accessed June 9, 2019].
- Higashiyama, T., Yabe, S., Sasaki, N., Nishimura, Y., Miyagishima S, S., Kuroiwa, H. and Kuroiwa, T.** (2001) Pollen tube attraction by the synergid cell. *Science*, **293**, 1480–3. Available at: <http://www.ncbi.nlm.nih.gov/pubmed/11520985> [Accessed March 31, 2019].
- Hird, D.L., Worrall, D., Hodge, R., Smartt, S., Paul, W. and Scott, R.** (1993) The anther-specific protein encoded by the Brassica napus and Arabidopsis thaliana A6 gene displays similarity to beta-1,3-glucanases. *Plant J.*, **4**, 1023–33. Available at: <http://www.ncbi.nlm.nih.gov/pubmed/8281185> [Accessed June 30, 2019].
- Hiscock, S.J. and Allen, A.M.** (2008) Diverse cell signalling pathways regulate pollen-

- stigma interactions: the search for consensus. *New Phytol.*, **179**, 286–317. Available at: <http://doi.wiley.com/10.1111/j.1469-8137.2008.02457.x> [Accessed January 4, 2019].
- Holthuis, J.C.M. and Menon, A.K.** (2014) Lipid landscapes and pipelines in membrane homeostasis. *Nature*, **510**, 48–57. Available at: <http://www.ncbi.nlm.nih.gov/pubmed/24899304> [Accessed May 22, 2019].
- Hou, Y., Guo, X., Cyprys, P., Dresselhaus, T., Dong, J. and Correspondence, L.-J.Q.** (2016) Maternal ENODLs Are Required for Pollen Tube Reception in Arabidopsis. *Curr. Biol.*, **26**, 2343–2350. Available at: <http://dx.doi.org/10.1016/j.cub.2016.06.053> [Accessed June 8, 2019].
- Hruz, T., Laule, O., Szabo, G., Wessendorp, F., Bleuler, S., Oertle, L., Widmayer, P., Gruissem, W. and Zimmermann, P.** (2008) Genevestigator v3: a reference expression database for the meta-analysis of transcriptomes. *Adv. Bioinformatics*, **2008**, 420747. Available at: <http://www.ncbi.nlm.nih.gov/pubmed/19956698> [Accessed July 27, 2019].
- Huang, M.-D., Chen, T.-L.L. and Huang, A.H.C.** (2013) Abundant type III lipid transfer proteins in Arabidopsis tapetum are secreted to the locule and become a constituent of the pollen exine. *Plant Physiol.*, **163**, 1218–29. Available at: <http://www.ncbi.nlm.nih.gov/pubmed/24096413> [Accessed June 13, 2019].
- Huang, Q., Dresselhaus, T., Gu, H. and Qu, L.-J.** (2015) Active role of small peptides in Arabidopsis reproduction: Expression evidence. *J. Integr. Plant Biol.*, **57**, 518–521. Available at: <http://doi.wiley.com/10.1111/jipb.12356> [Accessed April 9, 2019].
- Huang, Q., Dresselhaus, T., Gu, H. and Qu, L.J.** (2015) Active role of small peptides in Arabidopsis reproduction: Expression evidence. *J. Integr. Plant Biol.*, **57**, 518–521.
- Imin, N., Kerim, T., Weinman, J.J. and Rolfe, B.G.** (2006) Low temperature treatment at the young microspore stage induces protein changes in rice anthers. *Mol. Cell. Proteomics*, **5**, 274–92. Available at: <http://www.ncbi.nlm.nih.gov/pubmed/16263700> [Accessed May 23, 2019].
- Ingram, G. and Gutierrez-Marcos, J.** (2015) Peptide signalling during angiosperm seed development. *J. Exp. Bot.*, **66**, 5151–5159.
- Iswanto, A.B.B. and Kim, J.-Y.** (2017) Lipid Raft, Regulator of Plasmodesmal Callose Homeostasis. *Plants*, **6**, 15. Available at: <http://www.ncbi.nlm.nih.gov/pubmed/28368351> [Accessed June 30, 2019].
- Jefferson, R.A., Kavanagh, T.A. and Bevan, M.W.** (1987) GUS fusions: beta-glucuronidase as a sensitive and versatile gene fusion marker in higher plants. *EMBO J.*, **6**, 3901–7. Available at: <http://www.ncbi.nlm.nih.gov/pubmed/3327686> [Accessed June 17, 2019].
- Jiao, J., Mizukami, A.G., Sankaranarayanan, S., Yamguchi, J., Itami, K. and Higashiyama, T.** (2017) Structure-Activity Relation of AMOR Sugar Molecule That Activates Pollen-Tubes for Ovular Guidance. *Plant Physiol.*, **173**, 354–363. Available at: <http://www.plantphysiol.org/lookup/doi/10.1104/pp.16.01655> [Accessed June 10, 2019].
- Jones-Rhoades, M.W., Borevitz, J.O. and Preuss, D.** (2007) Genome-Wide Expression Profiling of the Arabidopsis Female Gametophyte Identifies Families of Small, Secreted Proteins. *PLoS Genet.*, **3**, e171. Available at: <https://dx.plos.org/10.1371/journal.pgen.0030171> [Accessed March 29, 2019].
- Jones, D.S., Yuan, J., Smith, B.E., Willoughby, A.C., Kumimoto, E.L. and Kessler, S.A.** (2017) MILDEW RESISTANCE LOCUS O Function in Pollen Tube Reception Is Linked to Its Oligomerization and Subcellular Distribution. *Plant Physiol.*, **175**, 172–185. Available at: <http://www.ncbi.nlm.nih.gov/pubmed/28724621> [Accessed May 18, 2019].

- Kader, J.-C.** (1996) *KADER LIPID-TRANSFER PROTEINS LIPID-TRANSFER PROTEINS IN PLANTS*, Available at: www.annualreviews.org [Accessed May 20, 2019].
- Kaku, H., Nishizawa, Y., Ishii-Minami, N., Akimoto-Tomiyama, C., Dohmae, N., Takio, K., Minami, E. and Shibuya, N.** (2006) Plant cells recognize chitin fragments for defense signaling through a plasma membrane receptor. *Proc. Natl. Acad. Sci.*, **103**, 11086–11091. Available at: <http://www.ncbi.nlm.nih.gov/pubmed/16829581> [Accessed May 28, 2019].
- Kalla, R., Shimamoto, K., Potter, R., Nielsen, P.S., Linnestad, C. and Olsen, O.-A.** (1994) The promoter of the barley aleurone-specific gene encoding a putative 7 kDa lipid transfer protein confers aleurone cell-specific expression in transgenic rice. *Plant J.*, **6**, 849–860. Available at: <http://doi.wiley.com/10.1046/j.1365-313X.1994.6060849.x> [Accessed May 20, 2019].
- Kanaoka, M.M., Kawano, N., Matsubara, Y., Susaki, D., Okuda, S., Sasaki, N. and Higashiyama, T.** (2011) Identification and characterization of TcCRP1, a pollen tube attractant from *Torenia concolor*. *Ann. Bot.*, **108**, 739–747. Available at: <http://www.ncbi.nlm.nih.gov/pubmed/21546430> [Accessed May 26, 2019].
- Kandasamy, M.K., Nasrallah, J.B. and Nasrallah, M.E.** (1994) Pollen-pistil interactions and developmental regulation of pollen tube growth in *Arabidopsis*. *Development*, **120**. Available at: <http://dev.biologists.org/content/120/12/3405> [Accessed May 19, 2019].
- Kasahara, R.D., Portereiko, M.F., Sandaklie-Nikolova, L., Rabiger, D.S. and Drews, G.N.** (2005) MYB98 Is Required for Pollen Tube Guidance and Synergid Cell Differentiation in *Arabidopsis*. *PLANT CELL ONLINE*, **17**, 2981–2992. Available at: <http://www.ncbi.nlm.nih.gov/pubmed/16214903> [Accessed January 25, 2019].
- Kay Schneitz†,*, Martin Hülskamp‡, S.D.K. and R.E.P.** (1997) Dissection of sexual organ ontogenesis: a genetic analysis of ovule development in *Arabidopsis thaliana*. *Dev.* **124**, 1367–1376 *1367 Print. Gt. Britain © Co. Biol. Ltd. 1997, DEV0100*. Available at: <http://dev.biologists.org/content/develop/124/7/1367.full.pdf> [Accessed May 8, 2019].
- Kessler, S.A. and Grossniklaus, U.** (2011) She's the boss: signaling in pollen tube reception. *Curr. Opin. Plant Biol.*, **14**, 622–627. Available at: <https://www.sciencedirect.com/science/article/pii/S1369526611001191?via%3Dihub> [Accessed May 18, 2019].
- Kessler, S.A., Lindner, H., Jones, D.S. and Grossniklaus, U.** (2015) Functional analysis of related CrRLK1L receptor-like kinases in pollen tube reception. *EMBO Rep.*, **16**, 107–115. Available at: <http://embor.embopress.org/cgi/doi/10.15252/embr.201438801> [Accessed July 22, 2019].
- Konar, R.N. and Linskens, H.F.** (1966) The morphology and anatomy of the stigma of *Petunia hybrida*. *Planta*, **71**, 356–371. Available at: <http://link.springer.com/10.1007/BF00396321> [Accessed May 5, 2019].
- Koncz, C. and Schell, J.** (1986) The promoter of TL-DNA gene 5 controls the tissue-specific expression of chimaeric genes carried by a novel type of *Agrobacterium* binary vector. *MGG Mol. Gen. Genet.*, **204**, 383–396. Available at: <http://link.springer.com/10.1007/BF00331014> [Accessed June 19, 2019].
- Kouzai, Y., Nakajima, K., Hayafune, M., Ozawa, K., Kaku, H., Shibuya, N., Minami, E. and Nishizawa, Y.** (2014) CEBiP is the major chitin oligomer-binding protein in rice and plays a main role in the perception of chitin oligomers. *Plant Mol. Biol.*, **84**, 519–528. Available at: <http://www.ncbi.nlm.nih.gov/pubmed/24173912> [Accessed May 28, 2019].
- Kovalchuk, N., Smith, J., Pallotta, M., et al.** (2009) Characterization of the wheat

- endosperm transfer cell-specific protein TaPR60. *Plant Mol. Biol.*, **71**, 81–98. Available at: <http://www.ncbi.nlm.nih.gov/pubmed/19513805> [Accessed May 25, 2019].
- Kreis, M., Forde, B.G., Rahman, S., Mifflin, B.J. and Shewry, P.R.** (1985) Molecular evolution of the seed storage proteins of barley, rye and wheat. *J. Mol. Biol.*, **183**, 499–502. Available at: <https://www.sciencedirect.com/science/article/pii/0022283685900178> [Accessed May 20, 2019].
- Krohn, N.G., Lausser, A., Juranić, M. and Dresselhaus, T.** (2012) Egg Cell Signaling by the Secreted Peptide ZmEAL1 Controls Antipodal Cell Fate. *Dev. Cell*, **23**, 219–225. Available at: <https://linkinghub.elsevier.com/retrieve/pii/S1534580712002456> [Accessed May 18, 2019].
- Kusumawati, L., Imin, N. and Djordjevic, M.A.** (2008) Characterization of the Secretome of Suspension Cultures of Medicago Species Reveals Proteins Important for Defense and Development. *J. Proteome Res.*, **7**, 4508–4520. Available at: <http://pubs.acs.org/doi/abs/10.1021/pr800291z> [Accessed May 23, 2019].
- Lalanne, E., Honys, D., Johnson, A., Borner, G.H.H., Lilley, K.S., Dupree, P., Grossniklaus, U. and Twell, D.** (2004) SETH1 and SETH2, two components of the glycosylphosphatidylinositol anchor biosynthetic pathway, are required for pollen germination and tube growth in Arabidopsis. *Plant Cell*, **16**, 229–40. Available at: <http://www.ncbi.nlm.nih.gov/pubmed/14671020> [Accessed July 27, 2019].
- Lauga, B., Charbonnel-Campaa, L. and Combes, D.** (2000) Characterization of MZm3-3, a Zea mays tapetum-specific transcript. *Plant Sci.*, **157**, 65–75. Available at: <https://www.sciencedirect.com/science/article/pii/S0168945200002673?via%3Dihub> [Accessed May 23, 2019].
- Lee, S.B., Go, Y.S., Bae, H.-J., et al.** (2009) Disruption of Glycosylphosphatidylinositol-Anchored Lipid Transfer Protein Gene Altered Cuticular Lipid Composition, Increased Plastoglobules, and Enhanced Susceptibility to Infection by the Fungal Pathogen *Alternaria brassicicola*. *Plant Physiol.*, **150**, 42–54. Available at: <http://www.plantphysiol.org/content/150/1/42> [Accessed May 20, 2019].
- Lerche, M.H., Kragelund, B.B., Bech, L.M. and Poulsen, F.M.** (1997) Barley lipid-transfer protein complexed with palmitoyl CoA: the structure reveals a hydrophobic binding site that can expand to fit both large and small lipid-like ligands. *Structure*, **5**, 291–306. Available at: <https://www.sciencedirect.com/science/article/pii/S096921269700186X> [Accessed June 11, 2019].
- Leydon, A.R., Beale, K.M., Woroniecka, K., Castner, E., Chen, J., Horgan, C., Palanivelu, R. and Johnson, M.A.** (2013) Three MYB transcription factors control pollen tube differentiation required for sperm release. *Curr. Biol.*, **23**, 1209–14. Available at: <http://www.ncbi.nlm.nih.gov/pubmed/23791732> [Accessed March 29, 2019].
- Leydon, A.R., Chaibang, A. and Johnson, M.A.** (2014) Interactions between pollen tube and pistil control pollen tube identity and sperm release in the Arabidopsis female gametophyte. *Biochem. Soc. Trans.*, **42**, 340–5. Available at: <http://www.ncbi.nlm.nih.gov/pubmed/24646241> [Accessed May 18, 2019].
- Li, C., Yeh, F.-L., Cheung, A.Y., et al.** (2015) Glycosylphosphatidylinositol-anchored proteins as chaperones and co-receptors for FERONIA receptor kinase signaling in Arabidopsis. *Elife*, **4**. Available at: <http://www.ncbi.nlm.nih.gov/pubmed/26052747> [Accessed July 28, 2019].
- Li, H.-J., Zhu, S.-S., Zhang, M.-X., Wang, T., Liang, L., Xue, Y., Shi, D.-Q., Liu, J. and Yang, W.-C.** (2015) Arabidopsis CBP1 Is a Novel Regulator of Transcription Initiation in Central Cell-Mediated Pollen Tube Guidance. *Plant Cell*, **27**, 2880–93. Available at:

- <http://www.ncbi.nlm.nih.gov/pubmed/26462908> [Accessed January 25, 2019].
- Li, J., Gao, G., Xu, K., Chen, B., Yan, G., Li, F., Qiao, J., Zhang, Tianyao and Wu, X.** (2014) Genome-Wide Survey and Expression Analysis of the Putative Non-Specific Lipid Transfer Proteins in *Brassica rapa* L Tianzhen Zhang, ed. *PLoS One*, **9**, e84556. Available at: <http://www.ncbi.nlm.nih.gov/pubmed/24497919> [Accessed May 20, 2019].
- Li, M., Singh, R., Bazanova, N., Milligan, A.S., Shirley, N., Langridge, P. and Lopato, S.** (2008) Spatial and temporal expression of endosperm transfer cell-specific promoters in transgenic rice and barley. *Plant Biotechnol. J.*, **6**, 465–476. Available at: <http://www.ncbi.nlm.nih.gov/pubmed/18422887> [Accessed May 25, 2019].
- Li, S., Ge, F.-R., Xu, M., et al.** (2013) Arabidopsis COBRA-LIKE 10, a GPI-anchored protein, mediates directional growth of pollen tubes. *Plant J.*, **74**, 486–497. Available at: <http://doi.wiley.com/10.1111/tpj.12139> [Accessed January 24, 2019].
- Lindner, H., Kessler, S.A., Müller, L.M., Shimosato-Asano, H., Boisson-Dernier, A. and Grossniklaus, U.** (2015) TURAN and EVAN Mediate Pollen Tube Reception in Arabidopsis Synergids through Protein Glycosylation Z. Yang, ed. *PLOS Biol.*, **13**, e1002139. Available at: <http://dx.plos.org/10.1371/journal.pbio.1002139> [Accessed June 10, 2019].
- Lindner, H., Raissig, M.T., Sailer, C., Shimosato-Asano, H., Bruggmann, R. and Grossniklaus, U.** (2012) SNP-Ratio Mapping (SRM): identifying lethal alleles and mutations in complex genetic backgrounds by next-generation sequencing. *Genetics*, **191**, 1381–6. Available at: <http://www.ncbi.nlm.nih.gov/pubmed/22649081> [Accessed May 18, 2019].
- Lindorff-Larsen, K. and Winther, J.R.** (2001) Surprisingly high stability of barley lipid transfer protein, LTP1, towards denaturant, heat and proteases. *FEBS Lett.*, **488**, 145–8. Available at: <http://www.ncbi.nlm.nih.gov/pubmed/11163761> [Accessed May 20, 2019].
- Ling, Y., Zhang, C., Chen, T., Hao, H., Liu, P., Bressan, R.A., Hasegawa, P.M., Jin, J.B. and Lin, J.** (2012) Mutation in SUMO E3 ligase, SIZ1, Disrupts the Mature Female Gametophyte in Arabidopsis E. Newbigin, ed. *PLoS One*, **7**, e29470. Available at: <https://dx.plos.org/10.1371/journal.pone.0029470> [Accessed January 25, 2019].
- Liu, J., Zhong, S., Guo, X., et al.** (2013) Membrane-Bound RLCKs LIP1 and LIP2 Are Essential Male Factors Controlling Male-Female Attraction in Arabidopsis. *Curr. Biol.*, **23**, 993–998. Available at: <http://www.ncbi.nlm.nih.gov/pubmed/23684977> [Accessed June 6, 2019].
- Lopato, S., Borisjuk, N., Langridge, P. and Hrmova, M.** (2014) Endosperm transfer cell-specific genes and proteins: structure, function and applications in biotechnology. *Front. Plant Sci.*, **5**, 64. Available at: <http://www.ncbi.nlm.nih.gov/pubmed/24578704> [Accessed May 25, 2019].
- Lu, Y., Chanroj, S., Zulkifli, L., Johnson, M.A., Uozumi, N., Cheung, A. and Sze, H.** (2011) Pollen tubes lacking a pair of K⁺ transporters fail to target ovules in Arabidopsis. *Plant Cell*, **23**, 81–93. Available at: <http://www.ncbi.nlm.nih.gov/pubmed/21239645> [Accessed January 26, 2019].
- Maldonado, A.M., Doerner, P., Dixon, R.A., Lamb, C.J. and Cameron, R.K.** (2002) A putative lipid transfer protein involved in systemic resistance signalling in Arabidopsis. *Nature*, **419**, 399–403. Available at: <http://www.nature.com/articles/nature00962> [Accessed May 23, 2019].
- Mao, Y., Zhang, H., Xu, N., Zhang, B., Gou, F. and Zhu, J.-K.** (2013) Application of the

- CRISPR–Cas System for Efficient Genome Engineering in Plants. *Mol. Plant*, **6**, 2008–2011. Available at: <https://www.sciencedirect.com/science/article/pii/S1674205214602847> [Accessed June 27, 2019].
- Markert, S.M., Bauer, V., Muenz, T.S., et al.** (2017) 3D subcellular localization with superresolution array tomography on ultrathin sections of various species. *Methods Cell Biol.*, **140**, 21–47. Available at: <https://www.sciencedirect.com/science/article/pii/S0091679X17300481?via%3Dihub> [Accessed June 18, 2019].
- Márton, M.L., Cordts, S., Broadhvest, J. and Dresselhaus, T.** (2005) Micropylar pollen tube guidance by egg apparatus 1 of maize. *Science*, **307**, 573–6. Available at: <http://www.ncbi.nlm.nih.gov/pubmed/15681383> [Accessed May 18, 2019].
- Márton, M.L., Fastner, A., Uebler, S. and Dresselhaus, T.** (2012) Overcoming Hybridization Barriers by the Secretion of the Maize Pollen Tube Attractant ZmEA1 from Arabidopsis Ovules. *Curr. Biol.*, **22**, 1194–1198. Available at: <https://www.sciencedirect.com/science/article/pii/S0960982212005179?via%3Dihub> [Accessed May 18, 2019].
- Maruyama, D., Hamamura, Y., Takeuchi, H., Susaki, D., Nishimaki, M., Kurihara, D., Kasahara, R.D. and Higashiyama, T.** (2013) Independent Control by Each Female Gamete Prevents the Attraction of Multiple Pollen Tubes. *Dev. Cell*, **25**, 317–323. Available at: <https://www.sciencedirect.com/science/article/pii/S1534580713001846> [Accessed May 19, 2019].
- Matteis, M.A. De, Campli, A. Di and D'Angelo, G.** (2007) Lipid-transfer proteins in membrane trafficking at the Golgi complex. *Biochim. Biophys. Acta - Mol. Cell Biol. Lipids*, **1771**, 761–768. Available at: <https://www.sciencedirect.com/science/article/pii/S1388198107000790> [Accessed June 11, 2019].
- Mecchia, M.A., Santos-Fernandez, G., Duss, N.N., et al.** (2017) RALF4/19 peptides interact with LRX proteins to control pollen tube growth in *Arabidopsis*. *Science (80-.)*, **358**, 1600–1603. Available at: <http://www.ncbi.nlm.nih.gov/pubmed/29242232> [Accessed June 3, 2019].
- Michard, E., Lima, P.T., Borges, F., et al.** (2011) Glutamate Receptor-Like Genes Form Ca²⁺ Channels in Pollen Tubes and Are Regulated by Pistil D-Serine. *Science (80-.)*, **332**, 434–437. Available at: <http://www.ncbi.nlm.nih.gov/pubmed/21415319> [Accessed January 25, 2019].
- Micheva, K.D. and Smith, S.J.** (2007) Array Tomography: A New Tool for Imaging the Molecular Architecture and Ultrastructure of Neural Circuits. *Neuron*, **55**, 25–36. Available at: <http://www.ncbi.nlm.nih.gov/pubmed/17610815> [Accessed May 17, 2019].
- Miya, A., Albert, P., Shinya, T., et al.** (2007) CERK1, a LysM receptor kinase, is essential for chitin elicitor signaling in *Arabidopsis*. *Proc. Natl. Acad. Sci.*, **104**, 19613–19618. Available at: <http://www.ncbi.nlm.nih.gov/pubmed/18042724> [Accessed May 28, 2019].
- Miyazaki, S., Murata, T., Sakurai-Ozato, N., Kubo, M., Demura, T., Fukuda, H. and Hasebe, M.** (2009) ANXUR1 and 2, sister genes to FERONIA/SIRENE, are male factors for coordinated fertilization. *Curr. Biol.*, **19**, 1327–31. Available at: <http://www.ncbi.nlm.nih.gov/pubmed/19646876> [Accessed May 18, 2019].
- Mizukami, A.G., Inatsugi, R., Jiao, J., et al.** (2016) The AMOR Arabinogalactan Sugar Chain Induces Pollen-Tube Competency to Respond to Ovular Guidance. *Curr. Biol.*, **26**, 1091–1097. Available at:

- <https://www.sciencedirect.com/science/article/pii/S0960982216301221?via%3Dihub> [Accessed May 18, 2019].
- Mollet, J.-C., Park, S.-Y., Nothnagel, E.A. and Lord, E.M.** (2000) A Lily Stylar Pectin Is Necessary for Pollen Tube Adhesion to an in Vitro Stylar Matrix. *Plant Cell*, **12**, 1737–1749.
- Mollet, J.C., Park, S.Y., Nothnagel, E.A. and Lord, E.M.** (2000) A lily styлар pectin is necessary for pollen tube adhesion to an in vitro styлар matrix. *Plant Cell*, **12**, 1737–50. Available at: <http://www.ncbi.nlm.nih.gov/pubmed/11006344> [Accessed January 4, 2019].
- Mori, T., Kuroiwa, H., Higashiyama, T. and Kuroiwa, T.** (2006) GENERATIVE CELL SPECIFIC 1 is essential for angiosperm fertilization. *Nat. Cell Biol.*, **8**, 64–71. Available at: <http://www.nature.com/articles/ncb1345> [Accessed May 19, 2019].
- Mundy, J. and Rogers, J.C.** (1986) Selective expression of a probable amylase/protease inhibitor in barley aleurone cells: Comparison to the barley amylase/subtilisin inhibitor. *Planta*, **169**, 51–63. Available at: <http://link.springer.com/10.1007/BF01369775> [Accessed May 23, 2019].
- Muschietti, J., Dircks, L., Vancanneyt, G. and McCormick, S.** (1994) LAT52 protein is essential for tomato pollen development: pollen expressing antisense LAT52 RNA hydrates and germinates abnormally and cannot achieve fertilization. *Plant J.*, **6**, 321–338. Available at: <http://doi.wiley.com/10.1046/j.1365-313X.1994.06030321.x> [Accessed July 26, 2019].
- Nacken, W.K.F., Huijser, P., Beltran, J.P., Saedler, H. and Sommer, H.** (1991) Molecular characterization of two stamen-specific genes, tap1 and fil1, that are expressed in the wild type, but not in the deficiens mutant of *Antirrhinum majus*. *MGG Mol. Gen. Genet.*, **229**, 129–136. Available at: <http://link.springer.com/10.1007/BF00264221> [Accessed May 23, 2019].
- Nagahara, S., Takeuchi, H. and Higashiyama, T.** (2015) Generation of a homozygous fertilization-defective gcs1 mutant by heat-inducible removal of a rescue gene. *Plant Reprod.*, **28**, 33–46. Available at: <http://link.springer.com/10.1007/s00497-015-0256-4> [Accessed May 18, 2019].
- NAKAGAWA, T., SUZUKI, T., MURATA, S., et al.** (2007) Improved Gateway Binary Vectors: High-Performance Vectors for Creation of Fusion Constructs in Transgenic Analysis of Plants. *Biosci. Biotechnol. Biochem.*, **71**, 2095–2100. Available at: <http://www.ncbi.nlm.nih.gov/pubmed/17690442> [Accessed June 19, 2019].
- Newbiggin, E. and Read, S.** (2009) Callose and its Role in Pollen and Embryo Sac Development in Flowering Plants. *Chem. Biochem. Biol. 1-3 Beta Glucans Relat. Polysaccharides*, 465–498. Available at: <https://www.sciencedirect.com/science/article/pii/B9780123739711000145> [Accessed May 8, 2019].
- Ngo, Q.A., Vogler, H., Lituiev, D.S., Nestorova, A. and Grossniklaus, U.** (2014) A calcium dialog mediated by the FERONIA signal transduction pathway controls plant sperm delivery. *Dev. Cell*, **29**, 491–500. Available at: <http://www.ncbi.nlm.nih.gov/pubmed/24814317> [Accessed May 19, 2019].
- O. Carvalho, A. de, S. Teodoro, C.E. de, Cunha, M. Da, Okorokova-Facanha, A.L., Okorokov, L.A., Fernandes, K.V.S. and Gomes, V.M.** (2004) Intracellular localization of a lipid transfer protein in *Vigna unguiculata* seeds. *Physiol. Plant.*, **122**, 328–336. Available at: <http://doi.wiley.com/10.1111/j.1399-3054.2004.00413.x> [Accessed May 23, 2019].

- Okuda, S., Suzuki, T., Kanaoka, M.M., Mori, H., Sasaki, N. and Higashiyama, T.** (2013) Acquisition of LURE-Binding Activity at the Pollen Tube Tip of *Torenia fournieri*. *Mol. Plant*, **6**, 1074–1090. Available at: <http://www.ncbi.nlm.nih.gov/pubmed/23482369> [Accessed May 26, 2019].
- Okuda, S., Tsutsui, H., Shiina, K., et al.** (2009) Defensin-like polypeptide LUREs are pollen tube attractants secreted from synergid cells. *Nature*, **458**, 357–361. Available at: <http://www.nature.com/articles/nature07882> [Accessed March 29, 2019].
- Pagnussat, L., Burbach, C., Baluška, F. and la Canal, L. de** (2012) An extracellular lipid transfer protein is relocalized intracellularly during seed germination. *J. Exp. Bot.*, **63**, 6555–6563. Available at: <https://academic.oup.com/jxb/article-lookup/doi/10.1093/jxb/ers311> [Accessed May 23, 2019].
- Palanivelu, R., Brass, L., Edlund, A.F. and Preuss, D.** (2003) Pollen Tube Growth and Guidance Is Regulated by POP2, an Arabidopsis Gene that Controls GABA Levels. *Cell*, **114**, 47–59. Available at: <http://linkinghub.elsevier.com/retrieve/pii/S0092867403004793> [Accessed January 8, 2019].
- Park, S.-Y. and Lord, E.M.** (2003) Expression studies of SCA in lily and confirmation of its role in pollen tube adhesion. *Plant Mol. Biol.*, **51**, 183–189. Available at: <http://link.springer.com/10.1023/A:1021139502947> [Accessed May 24, 2019].
- Park, S.Y., Jauh, G.Y., Mollet, J.C., Eckard, K.J., Nothnagel, E.A., Walling, L.L. and Lord, E.M.** (2000) A lipid transfer-like protein is necessary for lily pollen tube adhesion to an in vitro stylar matrix. *Plant Cell*, **12**, 151–64. Available at: <http://www.ncbi.nlm.nih.gov/pubmed/10634914> [Accessed January 4, 2019].
- Pereira, A.M., Lopes, A.L. and Coimbra, S.** (2016) Arabinogalactan Proteins as Interactors along the Crosstalk between the Pollen Tube and the Female Tissues. *Front. Plant Sci.*, **7**. Available at: <http://journal.frontiersin.org/article/10.3389/fpls.2016.01895/full> [Accessed June 1, 2019].
- Prado, A.M., Colaço, R., Moreno, N., Silva, A.C. and Feijó, J.A.** (2008) Targeting of Pollen Tubes to Ovules Is Dependent on Nitric Oxide (NO) Signaling. *Mol. Plant*, **1**, 703–714. Available at: <http://www.ncbi.nlm.nih.gov/pubmed/19825574> [Accessed January 25, 2019].
- Qu, L.-J., Li, L., Lan, Z. and Dresselhaus, T.** (2015) Peptide signalling during the pollen tube journey and double fertilization. *J. Exp. Bot.*, **66**, 5139–5150. Available at: <http://www.ncbi.nlm.nih.gov/pubmed/26068467> [Accessed July 29, 2019].
- Quilichini, T.D., Friedmann, M.C., Samuels, A.L. and Douglas, C.J.** (2010) ATP-binding cassette transporter G26 is required for male fertility and pollen exine formation in Arabidopsis. *Plant Physiol.*, **154**, 678–90. Available at: <http://www.ncbi.nlm.nih.gov/pubmed/20732973> [Accessed June 14, 2019].
- Radauer, C. and Breiteneder, H.** (2007) Evolutionary biology of plant food allergens. *J. Allergy Clin. Immunol.*, **120**, 518–525. Available at: <https://www.sciencedirect.com/science/article/pii/S0091674907014224> [Accessed May 20, 2019].
- Ramesh, S.A., Tyerman, S.D., Xu, B., et al.** (2015) GABA signalling modulates plant growth by directly regulating the activity of plant-specific anion transporters. *Nat. Commun.*, **6**, 7879. Available at: <http://www.ncbi.nlm.nih.gov/pubmed/26219411> [Accessed July 11, 2019].
- Ran, F.A., Cong, L., Yan, W.X., et al.** (2015) In vivo genome editing using *Staphylococcus*

- aureus Cas9. *Nature*, **520**, 186–191. Available at: <http://www.ncbi.nlm.nih.gov/pubmed/25830891> [Accessed April 12, 2019].
- Salminen, T.A., Blomqvist, K. and Edqvist, J.** (2016) Lipid transfer proteins: classification, nomenclature, structure, and function. *Planta*, **244**, 971–997. Available at: <http://www.ncbi.nlm.nih.gov/pubmed/27562524> [Accessed June 14, 2019].
- Samuel, M.A., Chong, Y.T., Haasen, K.E., Aldea-Brydges, M.G., Stone, S.L. and Goring, D.R.** (2009) Cellular Pathways Regulating Responses to Compatible and Self-Incompatible Pollen in Brassica and Arabidopsis Stigmas Intersect at Exo70A1, a Putative Component of the Exocyst Complex. *PLANT CELL ONLINE*, **21**, 2655–2671. Available at: <http://www.ncbi.nlm.nih.gov/pubmed/19789280> [Accessed March 6, 2019].
- Sanchez, A.M.** (2004) Pistil Factors Controlling Pollination. *PLANT CELL ONLINE*, **16**, S98–S106. Available at: www.plantcell.org/cgi/doi/10.1105/tpc.017806. [Accessed March 2, 2019].
- Schiøtt, M., Romanowsky, S.M., Baekgaard, L., Jakobsen, M.K., Palmgren, M.G. and Harper, J.F.** (2004) A plant plasma membrane Ca²⁺ pump is required for normal pollen tube growth and fertilization. *Proc. Natl. Acad. Sci. U. S. A.*, **101**, 9502–7. Available at: <http://www.ncbi.nlm.nih.gov/pubmed/15197266> [Accessed May 19, 2019].
- Schneitz, K., Hülskamp, M., Kopczak, S.D. and Pruitt, R.E.** (1997) Dissection of sexual organ ontogenesis: a genetic analysis of ovule development in *Arabidopsis thaliana*. *Development*, **124**, 1367–76. Available at: <http://www.ncbi.nlm.nih.gov/pubmed/9118807> [Accessed July 1, 2019].
- Schneitz, K., Hülskamp, M. and Pruitt, R.E.** (1995) Wild-type ovule development in *Arabidopsis thaliana*: a light microscope study of cleared whole-mount tissue. *Plant J.*, **7**, 731–749. Available at: <http://doi.wiley.com/10.1046/j.1365-313X.1995.07050731.x> [Accessed May 12, 2019].
- Schoenaers, S., Balcerowicz, D., Breen, G., et al.** (2018) The Auxin-Regulated CrRLK1L Kinase ERULUS Controls Cell Wall Composition during Root Hair Tip Growth. *Curr. Biol.*, **28**, 722–732.e6. Available at: <https://www.sciencedirect.com/science/article/pii/S0960982218300836?via%3Dihub> [Accessed June 7, 2019].
- Schoenaers, S., Balcerowicz, D., Costa, A. and Vissenberg, K.** (2017) The Kinase ERULUS Controls Pollen Tube Targeting and Growth in *Arabidopsis thaliana*. *Front. Plant Sci.*, **8**, 1942. Available at: <http://journal.frontiersin.org/article/10.3389/fpls.2017.01942/full> [Accessed June 7, 2019].
- Schopfer, C.R., Nasrallah, M.E. and Nasrallah, J.B.** (1999) The male determinant of self-incompatibility in Brassica. *Science*, **286**, 1697–700. Available at: <http://www.ncbi.nlm.nih.gov/pubmed/10576728> [Accessed March 6, 2019].
- Sels, J., Mathys, J., Coninck, B.M.A. De, Cammue, B.P.A. and Bolle, M.F.C. De** (2008) Plant pathogenesis-related (PR) proteins: A focus on PR peptides. *Plant Physiol. Biochem.*, **46**, 941–950. Available at: <https://www.sciencedirect.com/science/article/abs/pii/S0981942808001137?via%3Dihub> [Accessed May 24, 2019].
- Sessions, A., Burke, E., Presting, G., et al.** (2002) A High-Throughput Arabidopsis Reverse Genetics System. *PLANT CELL ONLINE*, **14**, 2985–2994. Available at: <http://www.ncbi.nlm.nih.gov/pubmed/12468722> [Accessed June 17, 2019].
- Shewry, P.R., Beaudoin, F., Jenkins, J., Griffiths-Jones, S. and Mills, E.N.** (2002) Plant

- protein families and their relationships to food allergy. *Biochem. Soc. Trans.*, **30**, 906–10. Available at: <http://www.ncbi.nlm.nih.gov/pubmed/12440943> [Accessed May 20, 2019].
- Shiba, H., Takayama, S., Iwano, M., et al.** (2001) A pollen coat protein, SP11/SCR, determines the pollen S-specificity in the self-incompatibility of Brassica species. *Plant Physiol.*, **125**, 2095–103. Available at: <http://www.ncbi.nlm.nih.gov/pubmed/11299389> [Accessed May 25, 2019].
- Shimizu, K.K. and Okada, K.** (2000) Attractive and repulsive interactions between female and male gametophytes in Arabidopsis pollen tube guidance. *Development*, **127**.
- Shiu, S.-H. and Bleecker, A.B.** (2003) Expansion of the Receptor-Like Kinase/Pelle Gene Family and Receptor-Like Proteins in Arabidopsis. *Plant Physiol.*, **132**, 530–543. Available at: <http://www.ncbi.nlm.nih.gov/pubmed/12805585> [Accessed May 27, 2019].
- Shiu, S.-H. and Bleecker, A.B.** (2001) Receptor-like kinases from Arabidopsis form a monophyletic gene family related to animal receptor kinases. *Proc. Natl. Acad. Sci.*, **98**, 10763–10768.
- Shiu, S.-H., Karlowski, W.M., Pan, R., Tzeng, Y.-H., Mayer, K.F.X. and Li, W.-H.** (2004) Comparative Analysis of the Receptor-Like Kinase Family in Arabidopsis and Rice. *Plant Cell*, **16**, 1220–1234. Available at: <http://www.ncbi.nlm.nih.gov/pubmed/15105442> [Accessed May 28, 2019].
- Shiu, S.H. and Bleecker, A.B.** (2003) Expansion of the receptor-like kinase/Pelle gene family and receptor-like proteins in Arabidopsis. *Plant Physiol.*, **132**, 530–43. Available at: <http://www.ncbi.nlm.nih.gov/pubmed/12805585> [Accessed May 28, 2019].
- Silva, P. Da, Landon, C., Industri, B., Marais, A., Marion, D., Ponchet, M. and Vovelle, F.** (2005) Solution structure of a tobacco lipid transfer protein exhibiting new biophysical and biological features. *Proteins Struct. Funct. Bioinforma.*, **59**, 356–367. Available at: <http://www.ncbi.nlm.nih.gov/pubmed/15726627> [Accessed June 11, 2019].
- Simon, R. and Dresselhaus, T.** (2015) Peptides take centre stage in plant signalling. *J. Exp. Bot.*, **66**, 5135–5138.
- Smith, D.K., Jones, D.M., Lau, J.B.R., Cruz, E.R., Brown, E., Harper, J.F. and Wallace, I.S.** (2018) A Putative Protein O-Fucosyltransferase Facilitates Pollen Tube Penetration through the Stigma-Style Interface. *Plant Physiol.*, **176**, 2804–2818. Available at: <http://www.ncbi.nlm.nih.gov/pubmed/29467178> [Accessed June 1, 2019].
- Smyth, D.R., Bowman, J.L. and Meyerowitz, E.M.** (1990) *Early Flower Development in Arabidopsis*, American Society of Plant Physiologists. Available at: <http://www.plantcell.org/content/plantcell/2/8/755.full.pdf> [Accessed May 5, 2019].
- Sodano, P., Caille, A., Sy, D., Person, G. de, Marion, D. and Ptak, M.** (1997) ¹H NMR and fluorescence studies of the complexation of DMPG by wheat non-specific lipid transfer protein. Global fold of the complex. *FEBS Lett.*, **416**, 130–4. Available at: <http://www.ncbi.nlm.nih.gov/pubmed/9369197> [Accessed June 11, 2019].
- Sprunck, S., Rademacher, S., Vogler, F., Gheyselinck, J., Grossniklaus, U. and Dresselhaus, T.** (2012) Egg cell - Secreted EC1 triggers sperm cell activation during double fertilization. *Science (80-.)*, **338**, 1093–1097. Available at: <http://www.ncbi.nlm.nih.gov/pubmed/23180860> [Accessed March 31, 2019].
- Stone, S.L., Anderson, E.M., Mullen, R.T. and Goring, D.R.** (2003) ARC1 Is an E3 Ubiquitin Ligase and Promotes the Ubiquitination of Proteins during the Rejection of Self-Incompatible Brassica Pollen. *Plant Cell*, **15**, 885–898. Available at:

- <http://www.ncbi.nlm.nih.gov/pubmed/12671085> [Accessed March 6, 2019].
- Storme, N. De and Geelen, D.** (2014) Callose homeostasis at plasmodesmata: molecular regulators and developmental relevance. *Front. Plant Sci.*, **5**. Available at: <http://journal.frontiersin.org/article/10.3389/fpls.2014.00138/abstract> [Accessed July 27, 2019].
- Stührwohldt, N., Dahlke, R.I., Kutschmar, A., Peng, X., Sun, M.-X. and Sauter, M.** (2015) Phytosulfokine peptide signaling controls pollen tube growth and funicular pollen tube guidance in *Arabidopsis thaliana*. *Physiol. Plant.*, **153**, 643–653. Available at: <http://www.ncbi.nlm.nih.gov/pubmed/25174442> [Accessed January 27, 2019].
- Suelves, M. and Puigdomènech, P.** (1997) Different lipid transfer protein mRNA accumulate in distinct parts of *Prunus amygdalus* flower. *Plant Sci.*, **129**, 49–56. Available at: <https://www.sciencedirect.com/science/article/pii/S0168945297001039?via%3Dihub> [Accessed May 23, 2019].
- Szyroki, A., Ivashikina, N., Dietrich, P., et al.** (2001) KAT1 is not essential for stomatal opening. *Proc. Natl. Acad. Sci. U. S. A.*, **98**, 2917–21. Available at: <http://www.ncbi.nlm.nih.gov/pubmed/11226341> [Accessed July 10, 2019].
- Takayama, S., Shiba, H., Iwano, M., Asano, K., Hara, M., Che, F.-S., Watanabe, M., Hinata, K. and Isogai, A.** (2000) Isolation and characterization of pollen coat proteins of *Brassica campestris* that interact with S locus-related glycoprotein 1 involved in pollen-stigma adhesion. *Proc. Natl. Acad. Sci.*, **97**, 3765–3770. Available at: <http://www.pnas.org/cgi/doi/10.1073/pnas.97.7.3765> [Accessed May 26, 2019].
- Takeuchi, H. and Higashiyama, T.** (2012) A Species-Specific Cluster of Defensin-Like Genes Encodes Diffusible Pollen Tube Attractants in *Arabidopsis* U. Grossniklaus, ed. *PLoS Biol.*, **10**, e1001449. Available at: <https://dx.plos.org/10.1371/journal.pbio.1001449> [Accessed May 18, 2019].
- Takeuchi, H. and Higashiyama, T.** (2016) Tip-localized receptors control pollen tube growth and LURE sensing in *Arabidopsis*. *Nature*, **531**, 245–248. Available at: <http://www.nature.com/articles/nature17413> [Accessed May 18, 2019].
- Tang, W., Ezcurra, I., Muschietti, J. and McCormick, S.** (2002) A Cysteine-Rich Extracellular Protein, LAT52, Interacts with the Extracellular Domain of the Pollen Receptor Kinase LePRK2. *Plant Cell*, **14**, 2277–2287. Available at: <http://www.ncbi.nlm.nih.gov/pubmed/12215520> [Accessed January 26, 2019].
- Tang, W., Kelley, D., Ezcurra, I., Cotter, R. and McCormick, S.** (2004) LeSTIG1, an extracellular binding partner for the pollen receptor kinases LePRK1 and LePRK2, promotes pollen tube growth *in vitro*. *Plant J.*, **39**, 343–353. Available at: <http://www.ncbi.nlm.nih.gov/pubmed/15255864> [Accessed March 30, 2019].
- Tassin, S., Broekaert, W.F., Marion, D., Acland, D.P., Ptak, M., Vovelle, F. and Sodano, P.** (1998) Solution Structure of Ace-AMP1, a Potent Antimicrobial Protein Extracted from Onion Seeds. Structural Analogies with Plant Nonspecific Lipid Transfer Proteins †. *Biochemistry*, **37**, 3623–3637. Available at: <http://www.ncbi.nlm.nih.gov/pubmed/9521681> [Accessed June 11, 2019].
- Thoma, S., Kaneko, Y. and Somerville, C.** (1993) A non-specific lipid transfer protein from *Arabidopsis* is a cell wall protein. *Plant J.*, **3**, 427–36. Available at: <http://www.ncbi.nlm.nih.gov/pubmed/8220451> [Accessed May 23, 2019].
- Tilsner, J., Amari, K. and Torrance, L.** (2011) Plasmodesmata viewed as specialised membrane adhesion sites. *Protoplasma*, **248**, 39–60. Available at:

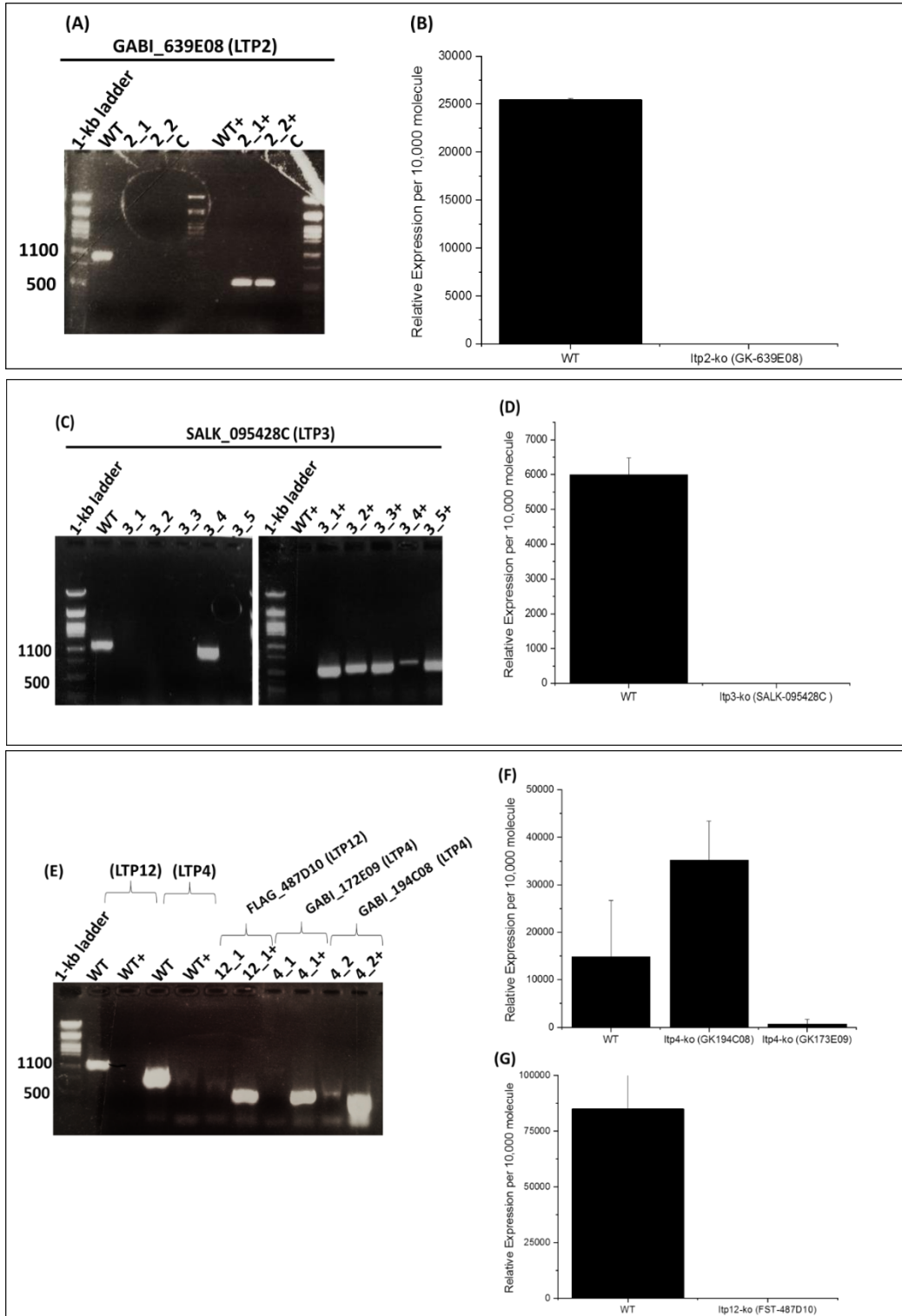
- <http://www.ncbi.nlm.nih.gov/pubmed/20938697> [Accessed July 27, 2019].
- Tong, J., Manik, M.K. and Im, Y.J.** (2018) Structural basis of sterol recognition and nonvesicular transport by lipid transfer proteins anchored at membrane contact sites. *Proc. Natl. Acad. Sci. U. S. A.*, **115**, E856–E865. Available at: <http://www.ncbi.nlm.nih.gov/pubmed/29339490> [Accessed June 30, 2019].
- Tsai, S.Q., Zheng, Z., Nguyen, N.T., et al.** (2015) GUIDE-seq enables genome-wide profiling of off-target cleavage by CRISPR-Cas nucleases. *Nat. Biotechnol.*, **33**, 187–197. Available at: <http://www.ncbi.nlm.nih.gov/pubmed/25513782> [Accessed April 12, 2019].
- Tsuboi, S., Osafune, T., Tsugeki, R., Nishimura, M. and Yamada, M.** (1992) Nonspecific Lipid Transfer Protein in Castor Bean Cotyledon Cells: Subcellular Localization and a Possible Role in Lipid Metabolism1. *J. Biochem.*, **111**, 500–508. Available at: <http://www.ncbi.nlm.nih.gov/pubmed/1618741> [Accessed June 27, 2019].
- Tung, C.-W., Dwyer, K.G., Nasrallah, M.E. and Nasrallah, J.B.** (2005) Genome-wide identification of genes expressed in Arabidopsis pistils specifically along the path of pollen tube growth. *Plant Physiol.*, **138**, 977–89. Available at: <http://www.ncbi.nlm.nih.gov/pubmed/15894741> [Accessed June 23, 2019].
- Vatén, A., Dettmer, J., Wu, S., et al.** (2011) Callose Biosynthesis Regulates Symplastic Trafficking during Root Development. *Dev. Cell*, **21**, 1144–1155. Available at: <http://www.ncbi.nlm.nih.gov/pubmed/22172675> [Accessed July 27, 2019].
- Verhoeven, T., Feron, R., Wolters-Arts, M., Edqvist, J., Gerats, T., Derksen, J. and Mariani, C.** (2005) STIG1 controls exudate secretion in the pistil of petunia and tobacco. *Plant Physiol.*, **138**, 153–60. Available at: <http://www.ncbi.nlm.nih.gov/pubmed/15821148> [Accessed May 5, 2019].
- Wang, H., Boavida, L.C., Ron, M. and McCormick, S.** (2008) Truncation of a protein disulfide isomerase, PDIL2-1, delays embryo sac maturation and disrupts pollen tube guidance in Arabidopsis thaliana. *Plant Cell*, **20**, 3300–11. Available at: <http://www.ncbi.nlm.nih.gov/pubmed/19050167> [Accessed January 25, 2019].
- Wang, H.W., Hwang, S.G., Karuppanapandian, T., Liu, A., Kim, W. and Jang, C.S.** (2012) Insight into the molecular evolution of non-specific lipid transfer proteins via comparative analysis between rice and sorghum. *DNA Res.*, **19**, 179–194. Available at: <https://academic.oup.com/dna/research/article-lookup/doi/10.1093/dnares/dss003> [Accessed April 25, 2019].
- Wang, T., Liang, L., Xue, Y., Jia, P.-F., Chen, W., Zhang, M.-X., Wang, Y.-C., Li, H.-J. and Yang, W.-C.** (2016) A receptor heteromer mediates the male perception of female attractants in plants. *Nature*, **531**, 241–244. Available at: <http://www.nature.com/articles/nature16975> [Accessed May 18, 2019].
- Wang, Z.P., Xing, H.L., Dong, L., Zhang, H.Y., Han, C.Y., Wang, X.C. and Chen, Q.J.** (2015) Egg cell-specific promoter-controlled CRISPR/Cas9 efficiently generates homozygous mutants for multiple target genes in Arabidopsis in a single generation. *Genome Biol.*, **16**.
- Webb, Mary C, Gunning, Brian E S, Webb, M C, Gunning,) B E S and Gunning, B E S** (1994) *Embryo sac development in Arabidopsis thaliana*, Springer-Verlag. Available at: <https://link.springer.com/content/pdf/10.1007%2FBF00228488.pdf> [Accessed May 8, 2019].
- Wengier, D.L., Mazzella, M.A., Salem, T.M., McCormick, S. and Muschietti, J.P.** (2010) STIL, a peculiar molecule from styles, specifically dephosphorylates the pollen receptor

- kinase LePRK2 and stimulates pollen tube growth in vitro. *BMC Plant Biol.*, **10**, 33. Available at: <http://bmcplantbiol.biomedcentral.com/articles/10.1186/1471-2229-10-33> [Accessed July 5, 2019].
- Wheeler, M.J., Vatovec, S. and Franklin-Tong, V.E.** (2010) The pollen S-determinant in Papaver: comparisons with known plant receptors and protein ligand partners. *J. Exp. Bot.*, **61**, 2015–2025. Available at: <https://academic.oup.com/jxb/article-lookup/doi/10.1093/jxb/erp383> [Accessed March 6, 2019].
- Wieczorek, K., Hofmann, J., Blöchl, A., Szakasits, D., Bohlmann, H. and Grundler, F.M.W.** (2007) Arabidopsis endo-1,4- β -glucanases are involved in the formation of root syncytia induced by *Heterodera schachtii*. *Plant J.*, **53**, 336–351. Available at: <http://doi.wiley.com/10.1111/j.1365-313X.2007.03340.x> [Accessed July 27, 2019].
- Wirtz, K.W. and Zilversmit, D.B.** (1968) Exchange of phospholipids between liver mitochondria and microsomes in vitro. *J. Biol. Chem.*, **243**, 3596–602. Available at: <http://www.ncbi.nlm.nih.gov/pubmed/4968799> [Accessed July 19, 2019].
- Wolf, S. and Höfte, H.** (2014) Growth Control: A Saga of Cell Walls, ROS, and Peptide Receptors. *Plant Cell*, **26**, 1848–1856. Available at: <http://www.ncbi.nlm.nih.gov/pubmed/24808052> [Accessed May 18, 2019].
- Wong, L.H., Gatta, A.T. and Levine, T.P.** (2019) Lipid transfer proteins: the lipid commute via shuttles, bridges and tubes. *Nat. Rev. Mol. Cell Biol.*, **20**, 85–101. Available at: <http://www.ncbi.nlm.nih.gov/pubmed/30337668> [Accessed June 11, 2019].
- Woriedh, M., Wolf, S., Márton, M.L., Hinze, A., Gahrtz, M., Becker, D. and Dresselhaus, T.** (2013) External application of gametophyte-specific ZmPMEI1 induces pollen tube burst in maize. *Plant Reprod.*, **26**, 255–266. Available at: <http://link.springer.com/10.1007/s00497-013-0221-z> [Accessed March 29, 2019].
- Wu, S.-W., Kumar, R., Iswanto, A.B.B. and Kim, J.-Y.** (2018) Callose balancing at plasmodesmata. *J. Exp. Bot.*, **69**, 5325–5339. Available at: <https://academic.oup.com/jxb/advance-article/doi/10.1093/jxb/ery317/5085387> [Accessed July 27, 2019].
- Xie, X.-J., Huang, J.-J., Gao, H.-H. and Guo, G.-Q.** (2011) Expression patterns of two Arabidopsis endo- β -1,4-glucanase genes (At3g43860, At4g39000) in reproductive development. *Mol. Biol.*, **45**, 458–465. Available at: <http://www.ncbi.nlm.nih.gov/pubmed/21790012> [Accessed July 27, 2019].
- Xing, H.-L., Dong, L., Wang, Z.-P., Zhang, H.-Y., Han, C.-Y., Liu, B., Wang, X.-C. and Chen, Q.-J.** (2014) A CRISPR/Cas9 toolkit for multiplex genome editing in plants. *BMC Plant Biol.*, **14**, 327. Available at: <http://bmcplantbiol.biomedcentral.com/articles/10.1186/s12870-014-0327-y> [Accessed June 19, 2019].
- Xiong, Y., Mei, W., Kim, E.-D., Mukherjee, K., Hassanein, H., Barbazuk, W.B., Sung, S., Kolaczowski, B. and Kang, B.-H.** (2014) Adaptive expansion of the maize maternally expressed gene (Meg) family involves changes in expression patterns and protein secondary structures of its members. *BMC Plant Biol.*, **14**, 204. Available at: <http://www.ncbi.nlm.nih.gov/pubmed/25084677> [Accessed May 25, 2019].
- Yeats, T.H. and Rose, J.K.C.** (2008) The biochemistry and biology of extracellular plant lipid-transfer proteins (LTPs). *Protein Sci.*, **17**, 191. Available at: <https://www.ncbi.nlm.nih.gov/pmc/articles/PMC2222726/> [Accessed July 26, 2019].
- Yu, G.-H. and Sun, M.-X.** (2007) Deciphering the Possible Mechanism of GABA in Tobacco Pollen Tube Growth and Guidance. *Plant Signal. Behav.*, **2**, 393–5. Available at:

- <http://www.ncbi.nlm.nih.gov/pubmed/19704611> [Accessed January 25, 2019].
- Yu, G.-H., Zou, J., Feng, J., Peng, X.-B., Wu, J.-Y., Wu, Y.-L., Palanivelu, R. and Sun, M.-X.** (2014) Exogenous γ -aminobutyric acid (GABA) affects pollen tube growth via modulating putative Ca^{2+} -permeable membrane channels and is coupled to negative regulation on glutamate decarboxylase. *J. Exp. Bot.*, **65**, 3235–48. Available at: <http://www.ncbi.nlm.nih.gov/pubmed/24799560> [Accessed July 11, 2019].
- Zhang, D., Wengier, D., Shuai, B., Gui, C.-P., Muschietti, J., McCormick, S. and Tang, W.-H.** (2008) The Pollen Receptor Kinase LePRK2 Mediates Growth-Promoting Signals and Positively Regulates Pollen Germination and Tube Growth. *PLANT Physiol.*, **148**, 1368–1379. Available at: <http://www.ncbi.nlm.nih.gov/pubmed/18799662> [Accessed June 1, 2019].
- Zhang, D. and Wilson, Z.A.** (2009) Stamen specification and anther development in rice. *Chinese Sci. Bull.*, **54**, 2342–2353. Available at: <http://link.springer.com/10.1007/s11434-009-0348-3> [Accessed June 13, 2019].
- Zhang, Dasheng, Liang, W., Yin, C., Zong, J., Gu, F. and Zhang, Dabing** (2010a) OsC6, encoding a lipid transfer protein, is required for postmeiotic anther development in rice. *Plant Physiol.*, **154**, 149–62. Available at: <http://www.ncbi.nlm.nih.gov/pubmed/20610705> [Accessed May 23, 2019].
- Zhang, Dasheng, Liang, W., Yin, C., Zong, J., Gu, F. and Zhang, Dabing** (2010b) OsC6, Encoding a Lipid Transfer Protein, Is Required for Postmeiotic Anther Development In Rice. *Plant Physiol.*, **154**, 149–162. Available at: <http://www.ncbi.nlm.nih.gov/pubmed/20610705> [Accessed June 13, 2019].
- Zhang, Y., Song, G., Lal, N.K., et al.** (2019) TurboID-based proximity labeling reveals that UBR7 is a regulator of N NLR immune receptor-mediated immunity. *Nat. Commun.*, **10**, 3252. Available at: <http://www.nature.com/articles/s41467-019-11202-z> [Accessed July 27, 2019].
- Zhong, S., Liu, M., Wang, Z., et al.** Cysteine-rich peptides promote interspecific genetic isolation in Arabidopsis. Available at: <http://science.sciencemag.org/> [Accessed June 4, 2019].
- Zhu, L., Chu, L.C., Liang, Y., Zhang, X.Q., Chen, L.Q. and Ye, D.** (2018) The arabidopsis CrRLK1L protein kinases BUP1 and BUP2 are required for normal growth of pollen tubes in the pistil. *Plant J.*, **95**, 474–486.

8. APPENDIX

8.1. Supplementary Data



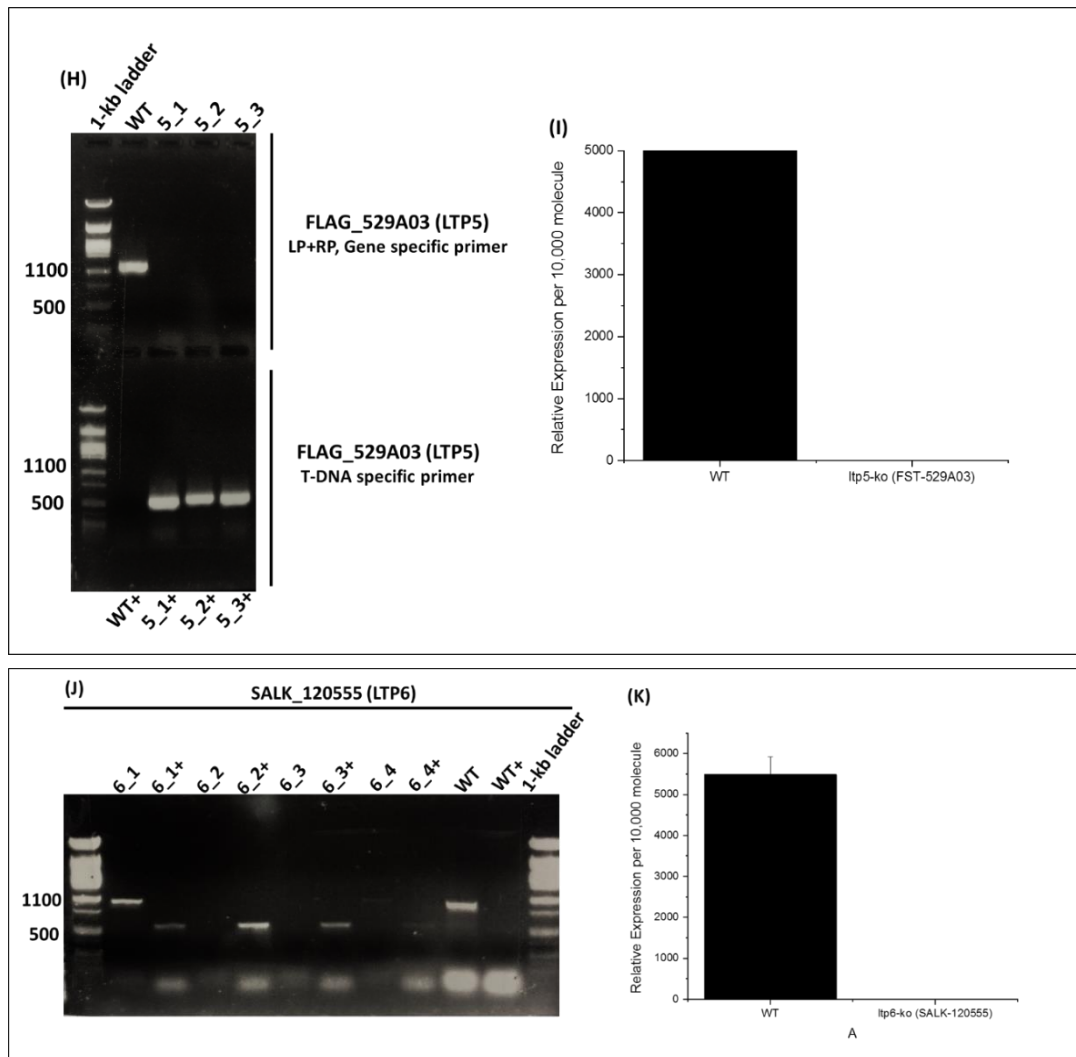


Fig. S.1: Genotyping of LTP T-DNA insertion mutants. (A, C, E, H, J) PCR based genotyping, amplification of wild-type allele using gene-specific primers (LP,RP) and T-DNA using (LP, T-DNA locus specific primers (for GABI-KAT), Lb1.3 (for SALK), Tag3/Rb4 (for FLAG). PCR using gene specific primers are denoted without (+) and using LP and T-DNA-locus specific primer are denoted with (+) (**B, D, F, G, I, K**) Relative expression levels of respective LTP in different homozygous T-DNA insertion mutants. All primers used for PCR-based genotyping and qPCR are listed in Table 1.4, 1.5 and 1.6.

8.2. Vector maps

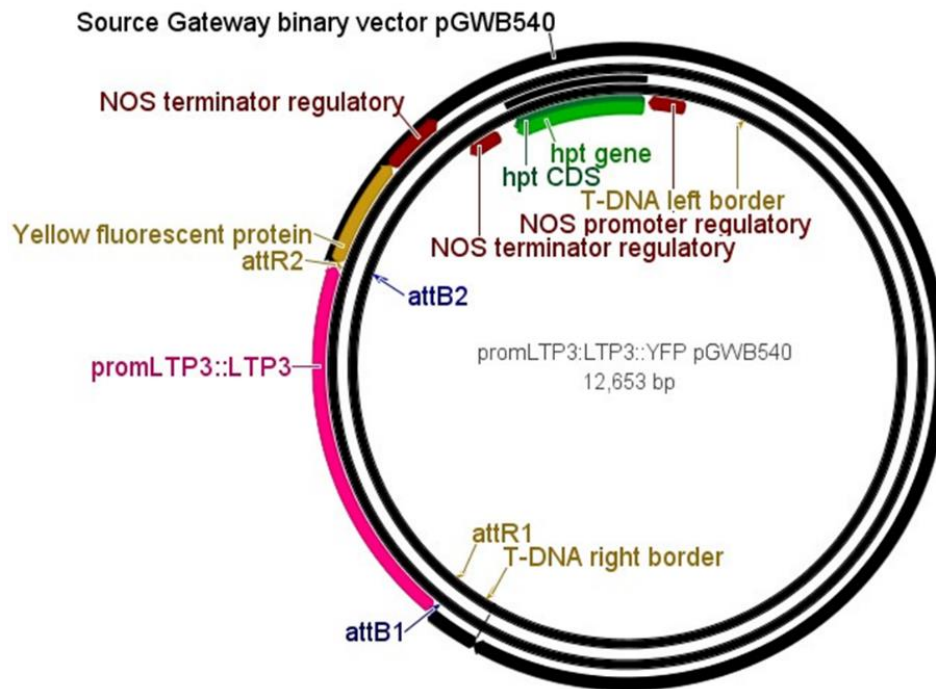


Fig. 8.1: Gateway destination vector pGWB540: Exemplary vector map of the plasmid constructs for the respective lipid transfer proteins LTP3 C-terminal fused with mVenus in pGWB540 vector. The vector was used for generating stable plants to study the localization of LTP protein and for transient expression in the *Nicotiana benthamina* leaves to locate LTP subcellularly. The vector map is the representative image of all the 6 LTPs which were selected for this study. hpt gene: resistance against hypoxanthine phosphoribosyl transferase (hygromycin). LB: left border of the T-DNA insertion; RB: right border of the T-DNA insertion.

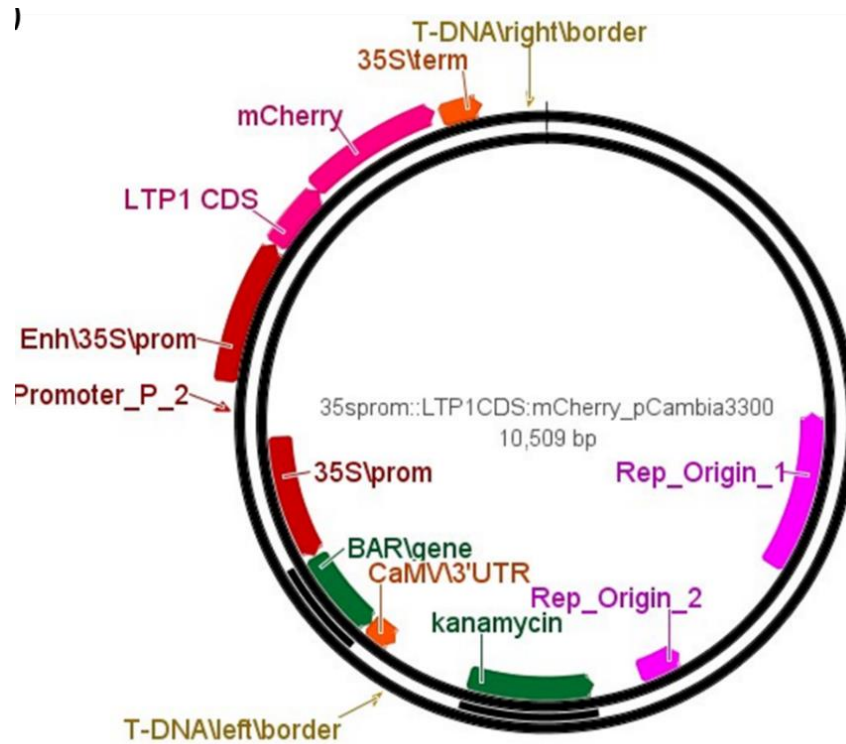


Fig. 8.2: Binary vector pCambia3300: Vector map of the plasmid constructs LTP1-mCherry for localization in the cell wall, with the coding sequence (coding) sequence"; CDS of At2g38540 (LTP1) and the C-terminal mCherry fusion (pCambia3300-35SProm::LTP1:mCherry). The vector was used for transient expression of the LTP1:mCherry- fusion protein, in *Nicotiana benthamina*. Bar: resistance gene against glufosinate (basta); KanR: kanamycin resistance gene; LB: left border of the T-DNA insertion; RB: right border of the T-DNA insertion

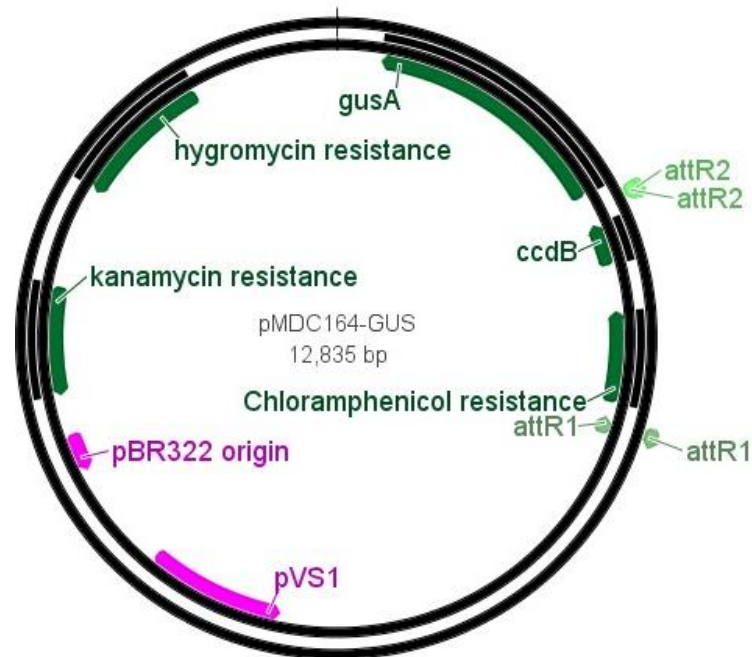


Fig. 8.3: Gateway vector pmdc164 including the β glucuronidase gene. The vector was used to clone the promoter sequences of selected LTPs, to analyze the tissue specific expression patterns of LTPs in stable transgenic plants. AttR1 & AttR2: recombination sites; HygR: hygromycin resistance gene; KanR: kanamycin resistance gene.

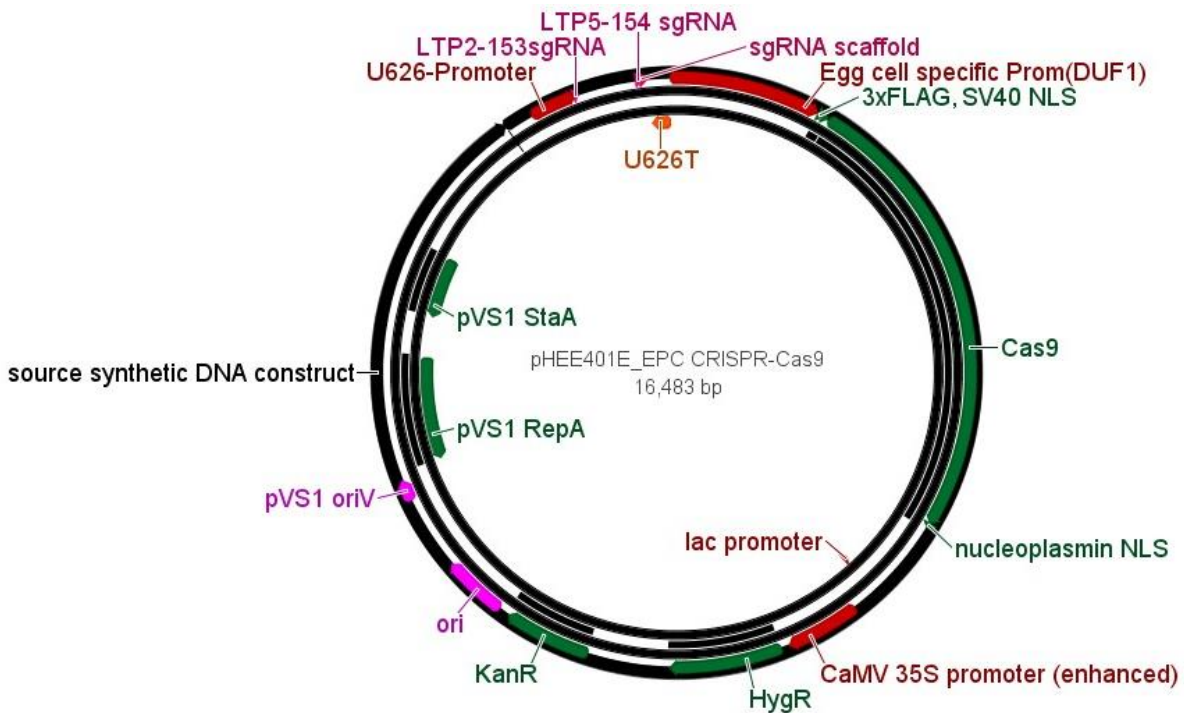


Fig. 8.4: Egg cell-specific promoter-controlled CRISPR/Cas9 binary vector pHEE401E: Two sgRNA expression cassettes pHEE401E vector was used to create LTP2/LTP5 double knock-out mutant. HygR: resistance against hygromycin, KanR: kanamycin resistance gene, sgRNA: two sgRNA expression cassettes; zCas9, *Zea mays* codon-optimized Cas9; U6-26p and U6-29p, two *Arabidopsis* U6 gene promoter; U6-26t, U6-26 terminator with downstream sequence; Hyg, hygromycin-resistance gene, LB: left border of the T-DNA insertion; RB: right border of the T-DNA insertion.

8.3. List of Figures

Page

| | |
|---|-----|
| Fig. 1.1: Double fertilization mechanism in angiosperms..... | 7 |
| Fig. 1.2: Different phases of pollen-stigma interaction | 8 |
| Fig. 1.3: Multiple guidance cues for pollen tubes. | 10 |
| Fig. 1.4: Model of RLK signaling in different steps of pollen-pistil interaction. | 16 |
| Fig. 1.5: Model of RLK signaling during pollen tube reception..... | 20 |
| Fig. 1.6: Cystine-rich peptides (CRPs) and their putative role in plant reproduction. | 21 |
| Fig. 1.7: Evolution and distribution of nsLTPs across different plant species | 25 |
| Fig. 1.8: Structural feature of plant nsLTPs..... | 27 |
| Fig. 1.9: A schematic illustration describing the proposed role of LTPs. | 29 |
| | |
| Fig. 3.1: Different developmental stage of flower development. | 47 |
| Fig. 3. 2: Illustrates a guide to identifying T-DNA insertion localization and map | 55 |
| Fig. 3.3: Assembly of DTIT2-PCR. | 64 |
| Fig. 3. 4: Schematic representation of two sgRNA expression cassette (DT1DT2-PCR + pHEE401) . | 65 |
| | |
| Fig. 4.1: A comprehensive analysis of LTP in <i>Arabidopsis</i> flower..... | 69 |
| Fig. 4.2: Schematic representation depicting sample preparation and harvest of the pollinated and non-pollinated pistils from the flowers of <i>Arabidopsis thaliana</i> | 70 |
| Fig. 4.3: Transcriptional regulation of LTPs upon pollination. | 71 |
| Fig. 4.4: GUS expression of 6 LTPs in the floral and reproductive tissue of <i>A.thaliana</i> | 74 |
| Fig. 4.5: GUS expression of LTP2, LTP3, LTP4, LTP5, LTP6 and LTP12 in 10 days old <i>Arabidopsis</i> seedling.. | 76 |
| Fig. 4.6: Sub-cellular localization of LTP2, LTP3, LTP4, LTP5 and LTP6 protein in <i>Arabidopsis</i> ovule and seedling. | 78 |
| Fig. 4.7: Schematic representation of fusion constructs. | 79 |
| Fig. 4.8: Sub-cellular localization of LTP2 fused to YFP in <i>N. benthamiana</i> epidermal cells imaged 4 days post infiltration | 81 |
| Fig. 4.9: Sub-cellular localization of LTP5 fused to YFP in <i>N. benthamiana</i> epidermal cells imaged 4 days post infiltration | 82 |
| Fig. 4.10: Sub-cellular localization of LTP6 fused to YFP in <i>N. benthamiana</i> epidermal cells imaged 4 days post infiltration..... | 83 |
| Fig. 4.11: Sub-cellular localization of LTP3 fused to YFP in <i>N. benthamiana</i> epidermal cells imaged 4 days post infiltration..... | 85 |
| Fig. 4.12: Sub-cellular localization of LTP4 fused to YFP in <i>N. benthamiana</i> epidermal cells imaged 4 days post infiltration | 86 |
| Fig. 4.13: Sub-cellular localization of LTP12 fused to YFP in <i>N. benthamiana</i> epidermal cells imaged 4 days post infiltration | 87 |
| Fig. 4.14: CLEM of 35S::LTP5-YFP in <i>N. benthamiana</i> agro-infiltrated epidermal cells embedded in LR White..... | 89 |
| Fig. 4.15:Schematic diagram of T-DNA insertions mutants. | 90 |
| Fig. 4.16: q-PCR gene expression analysis of <i>AtLTPs</i> T-DNA insertion mutants..... | 91 |
| Fig. 4.17: Characterization of <i>ltp2-ko</i> plants..... | 94 |
| Fig. 4.18: Characterization of <i>ltp3-ko</i> plants..... | 95 |
| Fig. 4.19: Characterization of <i>ltp5-ko</i> plants..... | 96 |
| Fig. 4.20: Evaluation of potential off-target using different algorithm | 98 |
| Fig. 4.21: Generation of <i>ltp2/ltp5</i> knockout lines by CRISPR/Cas9-mediated mutagenesis. | 99 |
| Fig. 4.22: CRISPR workflow. | 101 |
| Fig. 4.23: Alignment of T3 homozygous double mutants obtained via EPC CRISPR/cas9 mutagenesis. | 101 |
| Fig. 4.24: Analysis of mutagenesis profile from deep sequencing data using CRISPResso2 analysis tool. | 103 |

| | |
|---|-----|
| Fig. 4.25: Genotypic and phenotypic analyses of <i>ltp2ltp5</i> -ko mutant lines #P9-P2-P3 and #P9- P3-P3 | 105 |
| Fig. 4.26: Characterization of the EPC-CRISPR/Cas9 edited mutants #P31-P1, #P31-P2 | 106 |
| Fig. 4.27: Loss of function mutant <i>ltp2ltp5</i> confers aberrant pollen grain morphology and germination. | 107 |
| Fig. 4.28: Aberrant callose deposition in <i>ltp2ltp5</i> -ko mutant #P31-P2and #P31-P3 | 108 |
| Fig. 4.29: Defective pollen tube guidance and decreased ovule-targeting ability observed in the <i>ltp2ltp5</i> mutant line #P31-P2 and #P31-P3. | 109 |
| Fig. 4.30: The <i>ltp2ltp5</i> mutant #P31-P2 and #P31-P3 are semi-sterile and showed reduce seed set due to defect in the female gametophyte | 110 |
| Fig. 4.31: Detection of abnormal pollen tube guidance in self and cross-pollination between <i>ltp2ltp5</i> and Wt plants. | 112 |
| Fig. 4.32: Analysis of callose deposition pattern in wild-type and <i>ltp2ltp5</i> mutant ovules. | 114 |
| Fig. 4.33: Callose deposition during embryo sac development in wild-type and <i>ltp2ltp5</i> plants of <i>Arabidopsis thaliana</i> | 114 |
| | |
| Fig. 5.1: A schematic representation of the LTP-GUS expression in the reproductive tissues of <i>A. thaliana</i> | 116 |
| Fig. 5.2: Schematic diagram representing the subcellular localization of six Type-I nsLTP based on the transient expression in <i>Nicotiana Benthamian</i> | 118 |
| Fig. 5.3: Phylogenetic analysis of <i>Arabidopsis thaliana</i> type I and type II LTPs. | 119 |
| Fig. 5.4: Heatmap representing the expression patterns of the differentially regulated CalS and BGs in <i>A. thaliana</i> | 125 |
| Fig. 5.5: Protein-protein interaction network analysis based on STRING and ATTED databases. | 126 |
| Fig. 5.6: Hypothetical model of LTP2/LTP5 mediated signaling during the growth and guidance of the pollen-tube | 128 |
| Fig. 5.7: Protein-protein interaction network analysis based on ATTED databases | 129 |
| Fig. 5.8: Hypothetical role of LTPs in callose homeostasis | 131 |
| | |
| Fig. 8.1: Gateway destination vector pGWB540 | 154 |
| Fig. 8.2: Binary vector pCambia3300 | 155 |
| Fig. 8.3: Gateway vector pmdc164 including the β glucuronidase gene | 156 |
| Fig. 8.4: Egg cell-specific promoter-controlled CRISPR/Cas9 binary vector pHEE401E | 157 |
| | |
| Fig. S.1: Genotyping of LTP T-DNA insertion mutants. | 153 |

8.4. List of Tables

Page

| | |
|---|----|
| Table 1.1: <i>Arabidopsis thaliana</i> T-DNA mutant lines used in this work | 34 |
| Table 1.2: Transgenic <i>Arabidopsis thaliana</i> lines used in this work..... | 35 |
| Table 1.3: List of the vectors used in this study | 36 |
| Table 1.4: List of gene-specific primers used for genotyping T-DNA insertion mutants | 37 |
| Table 1.5: T-DNA primer/Locus specific primers list used for genotyping T-DNA insertion mutants... | 37 |
| Table 1.6: List of primer pair used for qPCR..... | 38 |
| Table 1.7: List of primers used for amplifying LTP promoters..... | 38 |
| Table 1.8: List of primers used for amplifying promLTP::LTP | 39 |
| Table 1.9: List of primers used for amplifying LTP cDNA | 39 |
| Table 1.10: List of primers used for generating LTP2sgRNA and LTP5sgRNA | 40 |
| Table 1.11: List of primers used for sequencing | 40 |
| Table 1.12: List of antibiotics | 41 |
| | |
| Table 2.1: Arabidopsis pollen germination media | 48 |
| | |
| Table 3.1: GUS staining solution..... | 49 |
| Table 3.2: Protocol for freeze substitution and LR-white embedding | 50 |
| Table 3.3: Protocol for immunolabelling | 51 |
| Table 3.4: Fixation FAA solution..... | 53 |
| Table 3. 5: Dehydration | 53 |
| Table 3.6: Resin Infiltration..... | 53 |
| | |
| Table 4.1: Primer pair to screen different T-DNA insertion mutants | 55 |
| Table 4.2: PCR reaction mix..... | 55 |
| Table 4.3: Settings used in thermocycler for genotyping | 55 |
| Table 4.4: Settings used in thermocycler for gradient PCR amplification | 56 |
| Table 4.5: Protocol for isolation of plasmid DNA..... | 57 |
| Table 4.6: Protocol for isolation of RNA | 58 |
| Table 4.7: Settings used in thermocycler for qPCR | 61 |
| | |
| Table 5.1: Set-up for BP recombination reaction | 61 |
| Table 5.2: Set up for LR recombination reaction..... | 62 |
| | |
| Table 6.1: Primer design for two target DT1T2-PCR | 64 |
| Table 6.2: Set up for creating two sgRNA construct pCBC-DT1T2 | 65 |
| | |
| Table 7.1: Comparative analysis of tissue-specific expression of nsLTPs using different gene expression databases. | 68 |

8.5. Abbreviations

| | |
|--------------------------------------|--|
| A. tumefaciens | Agrobacterium tumefaciens |
| A. thaliana | Arabidopsis thaliana |
| AGPs | Arabinogalactan glycoproteins |
| BETL | Basal endosperm transfer layer |
| BGs | β-1,3-Glucanases |
| bp | Base pairs |
| CaLS | Callose synthase |
| CaMV | Cauliflower Mosaic Virus |
| CBs | Callose binding protein |
| cDNA | Complementary deoxyribonucleic acid |
| CDS | Coding sequence |
| CLEM | Correlative Light and Electron Microscopy |
| CLSM | Confocal Laser Scanning Microscopy |
| CNGC18 | Cyclic nucleotide gated channel18 |
| Col0 | Columbia-0 |
| CRISPR | Clustered Regularly Interspaced Short Palindromic Repeats |
| CRP | Cysteine rich peptide |
| CrRLKs | Catharanthus roseus RLK1 |
| Ca²⁺_{cyt} | Cytosolic free calcium ion concentration |
| ddH₂O | Double-distilled water |
| DNA | Deoxyribonucleic acid |
| DEFL | Defensin-like |
| dNTP | deoxyribonucleotide triphosphate |
| DsRed | Dicosomia Red |
| E. coli | Escherichia coli |
| ECM | Extracellular matrix |
| ECP | Egg-cell specific promoter |
| EM | Electron Microscopy |
| ENODLs | Early nodulin-like proteins |
| ER | Endoplasmic reticulum |
| ESF1 | EMBRYO SURROUNDING FACTOR1 |
| ETC | Endosperm-transfer cells |
| EtOH | Ethanol |
| FD | Fast Digest |
| FER | Feronia |
| GABA | Gamma-aminobutyric acid |
| GLRs | Glutamate receptor |
| GPI | Glycosylphosphatidylinositol |
| GUS | β-glucuronidase |
| HAP | Hours after pollination |
| Hyg | Hygromycin |
| Kan | Kanamycin |
| kDa | Kilo Dalton |
| KO | Knock-out |
| LAS | Leica Application Suite |
| LB | Lysogeny broth |
| LCM | Laser-capture microdissection |
| LLG | Lorelei (Ire)-like glycosylphosphatidylinositol (gpi)-anchored protein |
| LRE | Lorelei |
| LRR | Leucine-rich repeat |
| LTPGs | Glycosylphosphatidylinositol-anchored lipid transfer proteins |
| MCSs | Membrane contact sites |
| MLO | Mildew Locus O |
| MPK | Mitogen-activated protein kinase |
| MS | Murashige and Skoog medium |
| N. benthamiana | Nicotiana benthamiana |
| NASC | Nottingham Arabidopsis Stock Centre |

| | |
|------------------------|---|
| nsLTP | Non-specific Lipid transfer protein |
| nt | Nucleotide |
| OD | Optical density |
| PAM | Protospacer adjacent motif |
| PcG | Polycomb-group |
| PCP | Pollen coat proteins |
| PCR | Polymerase chain reaction |
| PDCBs | Plasmodesmata callose binding |
| PGM | Pollen growth medium |
| pl | Isoelectric point |
| PIP4 | Phosphatidylinositol-4-phosphate |
| PM | Plasma membrane |
| PRRs | Pathogen related proteins |
| Prom | Promoter |
| PT | Pollen tube |
| qRT-PCR | Quantitative real time PCR |
| RLKs | Receptor like kinases |
| RALF | Rapid alkalization factor |
| RbohH and RbohJ | Respiratory burst oxidase homolog H and J |
| Rem | Remorin 1.3 |
| RNA | Ribonucleic acid |
| ROS | Reactive oxygen species |
| rpm | Revolutions per minute |
| RT | Room temperature |
| SCA | Stigma/stylar cysteine-rich adhesin |
| SCR | S-locus cysteine-rich protein |
| SEM | Scanning Electron Microscopy |
| sgRNA | Sing guide RNA |
| SLR-BP1 | S-locus-related glycoprotein, SLR-BINDING PROTEIN |
| SOC | Super Optimal broth with Catabolite repression |
| Spec | Spectinomycin |
| SRK | S-locus receptor kinase |
| TAE | Tris-acetate-EDTA |
| TCEP | Tris(2-carboxyethyl) phosphine |
| T-DNA | Transfer-DNA |
| TE | Tris-EDTA |
| TT | Transmitting tract |
| TTS | Transmitting tract specific |
| Ws | Wassilewskija |
| YEB | Yeast Extract Peptone |
| YEP | Yeast Extract Peptone |
| YFP | Yellow fluorescence protein |
| ZmES4 | Zea mays embryo sac 4 |

8.6. Curriculum Vitae

KHUSHBU KUMARI

Department of Molecular Plant Physiology and Biophysics
 cell phone: +49 174 9084288
 email: khushbu.kumari@stud-mail.uni-wuerzburg.de
 Contact number: +491749084288
 Skype Id: khushbu1115

Education

- | | |
|---|---|
| March 2016 - October 2019 (Expected) | University of Wuerzburg, Germany Department of Molecular Plant Physiology and Biophysics, PhD (Dr. rer. nat.) |
| April 2009- April 2014 | Integrated MSc in Life Sciences at National Institute of Science Education and Research, (INSPIRE Scholarship), Master Thesis: Production of mammalian cytokine (novel Interleukins <i>IL-33</i>) using <i>Physcomitrella patens</i> as model system. |
| January 2015 -July 2015 | Project Fellow at National Institute of Science Education and Research (NISER), Biotechnology Department (DBT funded), Bhubaneswar, India. |
| August 2015 -December 2015 | Industrial BIOCON-KGI Certification in Bioscience, Bangalore, India. |

Research Experience

- | | |
|---------------------|---|
| Oct 2014 – Nov 2014 | Internship at National Institute of Basic Biology (NIBB), Okazaki, Japan. Correlation between state transition and photo inhibition mechanism in <i>C.reinhardtii</i> using state-transition (qT) and quenching (qE) mutants. Supervisor: Prof. Jun Minagawa. |
| May 2013 – Aug 2013 | Internship at Albert-Ludwig's-Universität, Freiburg, Germany, (DAAD, A new passage to India Scholarship). Sub-cellular localization of PIN6 an auxin transporter protein in the nectary cells of <i>Arabidopsis thaliana</i> . Supervisor: Prof. Klaus Palme, Dr. Frank Ditengou. |

- May 2012 – July 2012 **Internship at National Institute of Plant Genome Research, Delhi, India, (INSPIRE Scholarship).**
 Cloning and expression of recombinant *IL-33* cytokine in *Oryza Sativa* through rice callus transformation. Supervisor: Prof. J. P. Khurana.
- May 2011 – July 2011 **Internship at National Institute of Science Education and Research (NISER), Bhubaneswar, India, (INSPIRE Scholarship).**
 Effect of single and multi-walled carbon nanotubes on the flowering time of *Arabidopsis thaliana*.
- May 2010 – July 2010 **Internship at National Institute of Science Education and Research (NISER), Bhubaneswar, India, (INSPIRE Scholarship).**
 Effect of Calcium on the post-transcriptional modification and stability of tubulin in the moss, *Physcomitrella patens*.

Achievements & Awards

- March 2016 – March 2019 **Doctoral Fellowship awarded by the Graduate School of Life Sciences (German Excellence Initiative), University of Wuerzburg, Germany.**
- April 2019 – June 2019 **DAAD STIBET Abschlussbeihilfe, University of Wuerzburg, Germany.**
 June 2019 – January 2019 **Career Development Fellowship, DFG, University of Wuerzburg, Germany.**
- May 2013 - August 2013 **DAAD Scholarship-A new Passage to India, Albert-Ludwig's-Universität, Freiburg, Germany.**
- April 2009- April 2014 **INSPIRE Scholarship of DST, Government. of India.**
- August 2015 -December 2015 **Gold Medalist- BIOCON-KGI Certification Program, BIOCON, Bangalore, India.**
- Oct 2014 – Nov 2014 **Selected for NIBB Internship Program, Japan**
 National Institute of Basic Biology, Okazaki, Japan.
- Jan 2012 **Best Poster Award in Plant Science, 99th Indian Science Congress, Bhubaneswar, India.**

Publication & Poster

Publication

Khushbu Kumari¹, Meng Zhao², Rosalia Deeken¹, Dirk Becker¹ (2019), Female gametophyte expressed *Arabidopsis* lipid transfer proteins LTP2/5 provide an unprecedented link between callose homeostasis, pollen tube guidance and fertilization success (2019). Manuscript to be submitted.

Aaram A.Kumar, Priyanka Mishra, **Khushbu Kumari**, K.C.Panigrahi (2012), Environmental Stress Influencing Plant Development and Flowering, *Frontiers in Biosciences*, **S4**, pp. **1315-1324**.

Aaram A.Kumar, **Khushbu Kumari**, Priyanka Mishra, K.C.Panigrahi (2012), Photoperiodic Flowering-A tale of Protein cross talk, **Proceedings at International Conference in Plant science** in post genomic era, pp 64-72,2011.

Posters

- | | |
|----------------|--|
| June 2018 | 25th International Congress on Sexual Plant Reproduction, Nagaragawa Convention Center, Gifu, Japan . |
| August 2018 | 12TH CONGRESS OF THE INTERNATIONAL PLANT MOLECULAR BIOLOGY, Montpellier, France . |
| Octobre 2017 | EUREKA-International Conference, University of Würzburg, Germany . |
| Septembre 2017 | Botanikertagung - Plant Research in a Changing World, Kiel, Germany . |
| October 2016 | EUREKA-International Conference, University of Würzburg, Germany . |